The Development of Candidate Therapeutic and Diagnostic Ligands for Prion Diseases

By

Robert Workman, BSc (Hons)

Thesis submitted to the University of Nottingham for the Degree of Doctor of Philosophy

September 2017

School of Veterinary Medicine and Science

Sutton Bonington Campus

Loughborough

Leicestershire

LE12 5RD

Author's Declaration

I declare that, except where reference is made to the contribution of others, that this thesis is the product of my own work and has not been submitted for any other degree at the University of Nottingham or any other institution.

Signature: _____

Robert George Workman

Abstract

To date there are no effective treatments for prion diseases, and these diseases are always fatal in both humans and animals. Additionally, the gold standard for diagnosis of these disease remains to be the analysis of biopsied brain tissue obtained post mortem. Consequently, there is a continued demand for therapeutics and ante-mortem diagnostics for prion diseases. This project addresses these demands by investigating candidate therapeutic and diagnostic ligands for prion diseases.

This study investigated recombinant prion proteins (rPrPs) as inhibitors in scrapie and bovine spongiform encephalopathy (BSE) *in vitro* amplification by protein misfolding cyclic amplification (PMCA). Three ovine rPrPs with the polymorphisms VRQ, ARQ and ARR and hamster rPrP were tested against scrapie PMCA in dilution series to calculate IC50 values. The two most potent inhibitors, VRQ and ARQ, were then similarly tested against bovine spongiform encephalopathy (BSE) amplification. The most potent inhibitor of both disease types, the ovine rPrP VRQ, was then observed to inhibit a range of different scrapie and BSE strains at a fixed concentration. It is recommended that further investigation into rPrP inhibitors is performed.

Strain characterisation of scrapie was investigated using rPrP inhibitors, following observations that the rPrP inhibitors generate a pattern of inhibition at a set concentration. Although this pattern of inhibition was repeatable in scrapie amplification by PMCA, this was limited to a single round of PMCA. Ultimately, this limited the application of this method to only amplification efficient prion strains and isolates. It is recommended that this method be investigated further in combination with the amplification of different isolates in substrates of different genotypes over multiple rounds of PMCA, as well as the analysis of glycoform ratios by western blotting. Here it was also identified that the imidazole used in the elution buffer for immobilised metal affinity chromatography (IMAC) can inhibit prion amplification in a strain dependent manner. This inhibition could be used in combination with the proposed method as a multi-faceted assay of prion strain characterisation.

The use of next generation phage display (NGPD) to map the epitopes of autoantibodies in the sera of scrapie infected sheep was also investigated. This was performed to identify peptides that were immunoreactive to autoantibodies

specific to the disease state. The identification of diagnostic peptides would then enable the development of an ante-mortem serological diagnostic test for scrapie. NGPD successfully selected immunoreactive peptides, of which 39 were selected for validation by peptide enzyme-linked immunosorbent assays (ELISAs). Although none of the peptides demonstrated diagnostic specificity by peptide ELISA, an optimised ELISA methodology was developed for future use in the validation of NGPD selected peptides. Further variations in the NGPD method, as well as validation by immunoassay, can be investigated to identify diagnostic peptides immunoreactive to scrapie specific autoantibodies.

Publications

The following publications contain work performed for the thesis:

Rob G. Workman, Ben C. Maddison & Kevin C. Gough (2017): Ovine recombinant PrP as an inhibitor of ruminant prion propagation in vitro, Prion, DOI:10.1080/19336896.2017.1342919.

Matthew J. O'Connor, Keith Bishop, Robert G. Workman, Ben C. Maddison & Kevin C. Gough (2017): In vitro amplification of H-type atypical bovine spongiform encephalopathy by protein misfolding cyclic amplification, Prion, DOI: 10.1080/19336896.2016.1259051.

Acknowledgements

"There's no use crying over every mistake, you just keep on trying until you run out of cake." – GLaDOS, Portal.

First and foremost, I would like to dedicate this work to my family for their unwavering support, help and love over the years. Without them, I would be not here today.

I also extend my greatest gratitude and appreciation to Dr Kevin Gough (School of Veterinary Medicine and Science, University of Nottingham) and Dr Ben Maddison (RSK-ADAS) for their work as my supervisors over the past 4 years. Their patience, support and encouragement have made this work possible, and made me a better researcher.

All my thanks and wishes go to Grazieli Maboni for her support and kindness. You have made my life a happy one.

Thanks also to those who have been with me through the years: Charlie Ducker, Harriet Day, Tom Wilding-Steele, Simon Shephard, Thomas Alanine, Natalie Healey, Andy Powell, Menna Milosevic, Owen Vickery, Megan Gollings, George Blundell-Hunter, Juliet Hucheson, Leah Goulding, Tessa Slater, Ryan Cardenas, Aouatif Belkhiri, Ramzi Al-Agele and many others.

My thanks go to the members of the RSK-ADAS team, as well as those in the research group: Keith Bishop, Claire Baker, Jon Owen, Helen Rees, Rose Reader, Mary Angani, Ali Gray and Katarzyna Zolnierczyk for their help and making these years so enjoyable. Matthew O'Connor has my uttermost appreciation for his company and music taste.

Finally, I extend my thanks to you – the reader, for your patience. I hope this work will be interesting and helpful to you.

Contents

Table of Contents

List of Figures

Chapter 1

Chapter 3

Chapter 4

Chapter 5

Chapter 6

List of Tables

Chapter 1

Chapter 2

Chapter 5

Chapter 6

Abbreviations

°C	degrees Celsius
ΔCq	quantification cycle
Aβ	amyloid beta
$A\beta_{42}$	amyloid beta 1-42
AD	Alzheimer's disease
ADAC	advanced data analysis centre
ANOVA	analysis of variance
AP	alkaline phosphatase
APHA	animal and plant health agency
APP	amyloid precursor protein
AUC	area under the curve
BDB	biopanning data bank
BSA	bovine serum albumin
BSE	bovine spongiform encephalopathy
CDI	conformation-dependent immunoassay
CFU	colony forming unit
CI	confidence interval
CJD	Creutzfeldt-Jakob disease
CNS	central nervous system
CSA	conformational stability assay
CSF	cerebrospinal fluid
CSSA	conformational solubility and stability assay
CWD	chronic wasting disease
Da	Dalton
DELFIA	dissociation-enhanced lanthanide fluorescence immunoassay
DIVA	differentiate vaccinated from infected animals
DLB	dementia with lewy bodies
Dpl	doppel protein gene
DNA	deoxyribonucleic acid
dNTP	deoxynucleotide
EC	European commission
EC50	the concentration of an effector at which the response is 50%
EDTA	ethylene diamine tetra-acetic acid
ELISA	enzyme-linked immunosorbent assay
Fabs	recombinant antibody fragments
fCJD	familial Creutzfeldt-Jakob disease

FACTT	fluorescent amplification catalyzed by T7 polymerase technique
FFI	fatal familial insomnia
FPLC	fast protein liquid chromatography
g	gram
GdnHCl	guanidinium hydrochloride
GdnHCl ½ values	the concentration of GdnHCl able to solubilise 50% of PrP^{Sc}
GFAP	glial fibrillary acidic Protein
GPI	glycosylphosphatidylinositol
GSS	Gerstmann-Sträussler-Scheinker syndrome
HD	Huntington's disease
HRP	horseradish peroxidase
iaCJD	iatrogenic Creutzfeldt-Jakob disease
IC50	the concentration of an inhibitor at which the response is 50%
IgG	immunoglobulin G
IgM	immunoglobulin M
IHC	immunohistochemistry
IMAC	immobilised metal affinity chromatography
IPCR	immuno polymerase chain reaction
IPTG	isopropyl β-D-1-thiogalactopyranoside
kDa	kilo Dalton
KO	knock out
LDS	lithium dodecyl sulphate
LOD	limit of detection
LRS	lymphoreticular system
M	molar
mAb	monoclonal antibody
MCI	mild cognitive impairment
mg	milligram
mL	millilitre
MLV	displaying murine leukemia virus
mM	millimolar
MOPS	3(N-morpholino) propanesulfonic acid
MRI	magnetic resonance imaging
MS	multiple sclerosis
MWCO	molecular weight cut off
NaPTA	sodium phosphotungstic acid

NEB	New England biolabs
ng	nanogram
NGPD	next generation phage display
NGS	next generation sequencing
NMR	nuclear magnetic resonance
NSP	national scrapie programme
OD	optical density
QuIC	quake induced conversion
PBS	phosphate buffered saline
PBST	tween supplemented phosphate buffered saline
PC12	pheochromocytoma cells
PCA	peptide competition assay
PCR	polymerase chain reaction
PD	Parkinson's disease
PE	phosphatidyletholamine
PFU	plaque forming units
PK	proteinase K
PMCA	protein misfolding cyclic amplification
pNPP	p-nitrophenyl phosphate
PNS	peripheral nervous system
POPG	phosphatidylglycerol
ppm	parts per million
PPS	pentosane polysulfate
PRNP	human prion protein gene
Prnp	animal prion protein gene
PrP^{C}	cellular prion protein
PrP^{res}	PK resistant form of PrP
PrP^{Sc}	the pathogenic isoform of the prion
PS	phosphatidylserine
PVDF	polyvinylidine difluoride
rARQ	recombinant ovine PrP with the polymorphisms ARQ
rARR	recombinant ovine PrP with the polymorphisms ARR
rHam	recombinant hamster PrP
rHum	recombinant human PrP
RNA	ribonucleic acid
ROC	receiver operating characteristic
rpm	revolutions per minute
rPrP	recombinant PrP

rNTP	ribonucleotide
RT-IPCR	real-time immuno polymerase chain reaction
RT-QuIC	real-time quake induced conversion
RT-PCR	real-time polymerase chain reaction
rVRQ	recombinant ovine PrP with the polymorphisms VRQ
SBV	Schmallenberg virus
sCJD	sporadic Creutzfeldt-Jakob Disease
scFvs	single chain antibodies
ScN_2A	scrapie infected neuroblastoma
SD	standard deviation
SDS	sodium dodecyl sulphate
SDS-PAGE	sodium dodecyl sulphate polyacrylamide electrophoresis
SMA	powdered milk baby formula
sPMCA	serial protein misfolding cyclic amplification
TAE	tris-acetate-EDTA
TBS	tris buffered saline
TBST	tween supplemented tris buffered saline
TGF-α	tumour growth factor-α
Tht	thioflavin T
TMB	tetramethylbenzidine
TME	transmissible mink encephalopathy
Tir	translocated intimin receptor
Tris	tris (hydroxymethyl) aminomethane
TSE	transmissible spongiform encephalopathy
µg	microgram
µL	microliter
µM	micromolar
vCJD	variant Creutzfeldt-Jakob disease
v/v	volume per volume
w/v	weight per volume
xg	gravitational force
yEGFP	yeast-enhanced green fluorescent protein

Chapter 1: Introduction

1.1. Prion Diseases

Prion diseases are fatal neurodegenerative conditions that affect both humans and livestock. They are characterized as part of a protein conformation disease group alongside Alzheimer's disease (AD) and Parkinson's disease (PD), where the central mechanism of disease is the misfolding of cellular proteins into pathogenic isoforms. Amongst these diseases prions are unique in that it is fully established that they are both naturally and experimentally transmissible between individuals and species (Gilch & Schätzl 2009). Recently the possibility of AD transmission was hypothesised. This followed the identification of amyloid beta (Aβ) deposition and pathology in 4 patients diagnosed with iatrogenic Creutzfeldt Jakob disease (CJD) after receiving treatment with contaminated growth hormone (Jaunmuktane et al. 2015). Experimental Aβ transmission has also been reported in primates and mice, but natural transmission remains to be confirmed (Baker et al. 1994; Heilbronner et al. 2013).

Prion diseases are classified as either sporadic, inherited or transmitted. The human prion disease sporadic CJD (sCJD) for example occurs with a frequency of $1/10^6$ people per year. CJD may be transmitted horizontally between humans (iatrogenic, iaCJD), inherited (familial, fCJD) or acquired by transfer of bovine spongiform encephalopathy (BSE) from contaminated meat products (variant, vCJD) (Hill et al. 1997; Hall et al. 2014). Other human forms of prion disease include kuru, fatal familial insomnia (FFI) and Gerstmann-Sträussler syndrome (GSS). Animal prion diseases include scrapie (first identified in 1732) which affects sheep and goats, BSE that affects cattle and chronic wasting disease (CWD) that affects elk and deer (Lee et al. 2013).

Initially the cause of prion diseases was enigmatic. Many causative agents were proposed including "slow viruses" due to the delayed onset of symptoms (Prusiner 1998). However it was first suggested by John Griffith in 1967 that the infectious agent may be protein in nature (Caughey 2001). These infectious protein agents have since been termed proteinaceous infectious particles (Prions), the main infectious constituent being a misfolded isoform of the cellular prion protein (PrP^C) (Prusiner 1998). This pathogenic isoform has been termed PrP^{Sc} after its discovery in scrapie infected sheep in 1982 (Prusiner 1982). As PrP^{Sc} is readily detected in the brain tissue of animals and humans suffering from prion diseases is considered to be the major/or sole component involved in infection and neurotoxicity (Prusiner 1998). In disease, PrP^{Sc} is believed to act as an infectious "seed" which converts PrP^C into further replicating copies (Prusiner 1982; Prusiner, 1998). This

is known as the "prion paradigm" where PrP^{Sc} initiates a cascade of PrP^{C} misfolding, spreading throughout the central nervous system (CNS) and peripheral nervous system (PNS) resulting in cognitive decline and death (Jucker & Walker 2013). Disease progression in prion diseases is classically associated with neuropathy of the CNS involving gliosis, spongiform degeneration, neurone loss, cognitive decline and inevitable death (Allroggen et al. 2000; Nicoll & Collinge 2009; Aguzzi & Falsig 2012). Clinical symptoms like cognitive decline are characterised by a significantly delayed onset following the advent of PrP^{Sc} accumulation. The mean incubation period of iaCJD is 28 years, 15 years for vCJD and between 34-56 or more years for kuru, leaving a prolonged window for asymptomatic transmission between patients (Collinge et al. 2006; Budka & Will 2015). However, by the onset of symptoms the mean survival time of patients is low, with a mean disease duration of 6 months for patients with sCJD (Zerr 2013). Prion diseases are difficult to diagnose prior to the later disease stages when clinical symptoms become manifest. Also, the short survival time after diagnosis provides a limited window for any therapeutic intervention.

The Prion Protein

PrP^{C} is a cell surface glycoprotein which is attached to the plasma membrane via a glycosylphosophoinositol (GPI) anchor. Human PrP^{C} is encoded by the gene *PRNP* on chromosome 20 and contains 3 exons. The open reading frame (ORF) exists within exon 3, and produces an mRNA transcript of 2.1-2.5 kb in length (Acevedo-Morantes & Wille 2014). Over 30 different mutations in this gene result in prion diseases of different clinical phenotypes including CJD, GSS and FFI (Acevedo-Morantes & Wille 2014). Following *PRNP* translation an N-terminal signal peptide and C-terminal peptide are removed, allowing for glycosylation and the addition of a GPI-anchor (Roucou 2014). The end product is a mature protein of 208 amino acids in length, consisting of a largely flexible N-terminus, a conserved hydrophobic region and a stable C-terminus comprising of three alpha helices and a small beta sheet domain (**Figure 1.1.**) (Riek et al. 1996; Rivera-milla et al. 2005; Kong et al. 2013). Approximately 43% of this structure is α-helical and 3% β-sheeted as determined by circular dichroism and nuclear magnetic resonance studies (**Figure 1.1.**) (Riek et al. 1996; Caughey 2001; DeMarco & Daggett 2004; Rivera-milla et al. 2005).

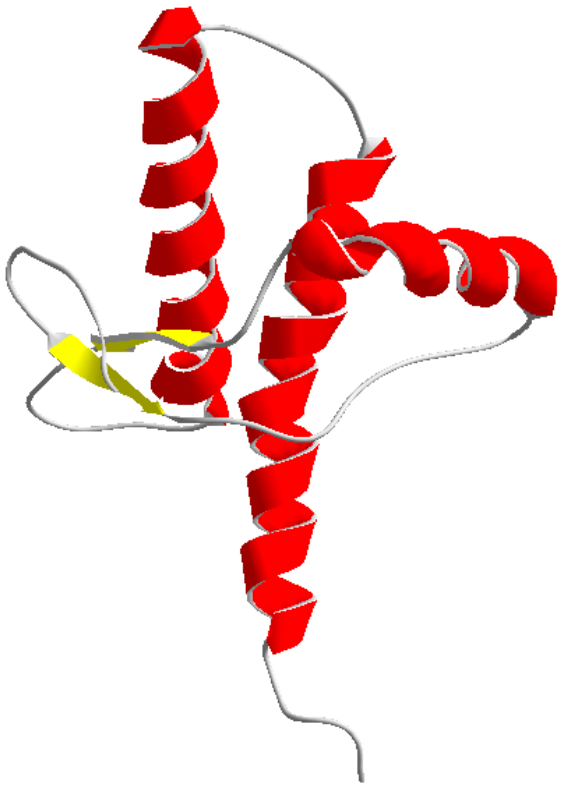

Figure 1.1. An in-solution nuclear magnetic resonance (NMR) structure of the C-terminal globular domain of human PrP^{C}, residues 90-231. This sequence of PrP^{C} adopts a predominantly alpha helical structure (red) with two beta sheets (yellow). The N-terminal region is flexible and unstructured (Kong et al. 2013). This image was produced using the Swiss-PDB Viewer, PDB number 2M8T.

PrP^{C} is expressed in all mammals and widely across distinct cell types with a greater abundance in neurons, neuroendocrine cells and in the lymphoreticular system (LRS) (Wadia et al. 2008). This widespread expression of PrP^{C} aids in the dissemination of infectious PrP^{Sc} in disease. Infection likely occurs orally (Hadlow et al. 1982). After infection, infectious PrP^{Sc} is believed to spread through the LRS, followed by the invasion of the nervous system through the enteric nervous system and entry into the CNS (Gough & Maddison 2010; Bradford & Mabbott 2012). That PrP^{C} is so widely expressed implies an important cellular role. Although no definitive function has been concluded, studies implicate PrP^{C} in performing a variety of roles that could contribute to the disease state if lost. Indeed, the *Prnp* gene is widely conserved in animals, again, suggesting an important biological role (Rivera-milla et al. 2005).

An important model in the investigation of PrP^C function and its role in disease are *Prnp* knockout (KO) mice. Initially *Prnp* KO mice (named the Edinburgh and Zurich I lines) were reported to exhibit normal growth and development for up to seven months, suggesting that a loss of PrP^C function does not contribute or cause the disease state (Büeler et al. 1992; Manson et al. 1994). However, other lines of KO mice produced since have displayed abnormal phenotypes in growth, synaptic function, interrupted sleep patterns, motor coordination and others (Collinge et al. 1994; Priola 1999; Steele et al. 2007; Schmitz et al. 2014). These abnormalities may in part be artefacts of technical issues in the production of *Prnp* KO mice. The Zurich II KO line for example exhibited a loss of motor coordination and death by cerebellar ataxia, later identified to be resultant from the *Prnp* promoter driving the expression of an adjacent gene encoding the protein Doppel (Dpl) (Moore et al. 1999; Li et al. 2000). Additionally, the use of mice with mixed genetic backgrounds for gene deletion can have the effect of increasing phenotypic variability, masking subtle phenotypes or affecting alleles linked to the deleted gene as demonstrated with the Zurich II line (Steele et al. 2007). It is therefore difficult to elucidate whether the observed phenotypes in KO mice are directly resultant from *Prnp* deletion. Furthermore, despite the reports of phenotypes in *Prnp* KO mice, PrP^C function does not appear to be vital for survival and its absence does not appear to contribute to disease pathogenesis. An established phenotype is that *Prnp* KO mice are resistant to prion infection (Büeler et al. 1993). This further supports the hypothesis that it is the presence and/or replication of PrP^{Sc} itself that is the cause of disease pathogenesis, and that the presence and expression of PrP^C is required for disease development (Büeler et al. 1993; Steele et al. 2007; Rambold et al. 2008).

PrP^{Sc} Structure

The key event in prion disease is the misfolding of PrP^C to the isotype PrP^{Sc}. Although PrP^C and PrP^{Sc} share the same primary amino acid sequence, it is important to stress that they are both biochemically distinct. Such differences include the insolubility of PrP^{Sc} in detergents, resistance of PrP^{Sc} to protease digestion and a change in secondary structure from the 43% alpha-helix in PrP^C to 40% beta sheet in PrP^{Sc} (**Figure 1.2.**) (Zhu et al. 2008; Wang et al. 2015). The structural differences between PrP^C and PrP^{Sc} were initially demonstrated by studies using circular dichroism (CD) and Fourier-transform infrared (FTIR) spectroscopy. These studies determined that PrP^{Sc} consists of a greater amount of beta sheet secondary structure than PrP^C (**Figure 1.2.**) (Caughey et al. 1991; Pan et al. 1993; Safar et al. 1993). These findings in themselves indicated that PrP^C

and PrP^{Sc} are fundamentally different at the structural level, providing a hypothesis for pathology and propagation. As a consequence, understanding PrP^{Sc} structure could yield potential avenues to develop novel therapeutic strategies.

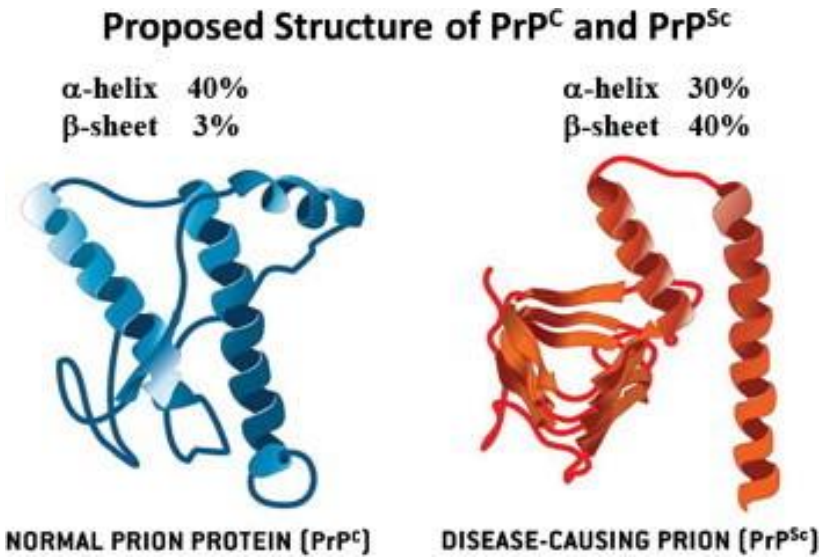

Figure 1.2. Proposed PrP^{C} and PrP^{Sc} secondary structure (Lee et al. 2013).

Determining the structure of PrP^{Sc} has proven difficult in spite of comprehensive efforts. This challenge arises in part from the difficulty of obtaining PrP^{Sc} crystal or NMR structures due to its aggregated state, heterogeneity, low quantity in tissue and insolubility in detergents (Wille et al. 2004). As a consequence, it has not been possible to crystallize PrP^{Sc} for study by X-ray crystallography. In spite of this a number of different structural models have been proposed based on experimental observations and simulations. The first of these models is based on the observation from transmission election microscopy that truncated PrP^{Sc} (PrP^{27-30}) can trimerically stack into β-helical prion rods in 2D crystal structures (**Figure 1.3. A**) (Merz et al, 1981; Prusiner 1998; Supattapone et al. 2002; Govaerts et al. 2004). PrP^{27-30} is the protease resistant core of PrP^{Sc}, formed after the N-terminus (residues 23-89) is removed by digestion with proteinase K (PK) (Wille et al. 2004). Digestion with PK removes protein impurities as well as PrP^{C} which may otherwise contribute to difficulties in structural studies. X-ray diffraction on PrP^{27-30} samples later suggested that the β-structure of PrP^{27-30} amyloid has a β-solenoid structure, an observation corroborated by similar studies on the fungal prion HET-s (Wille et al. 2009; Wan et al. 2012; Silva et al. 2015). The structure of PrP^{Sc} in this model is stable, allowing for up to 60 hydrogen bonds between four β-strands

and accounting for the known biochemical properties of prion particles (Silva et al 2015). Recently it was reported that PrP^{27-30} fibrils form four rung β-solenoid structures, determined by electron cryomicroscopy (Vazquez-Fernandez et al. 2016). This β-solenoid model allows for a hypothesised mode of prion propagation, where solenoid rungs actively template unstructured PrP^{C} (Vazquez-Fernandez et al. 2016). Although PrP^{27-30} retains infectivity and hence is biologically relevant for study, its use to generate a model of PrP^{Sc} folding is questionable as not all structural information is present (Govaerts et al. 2004).

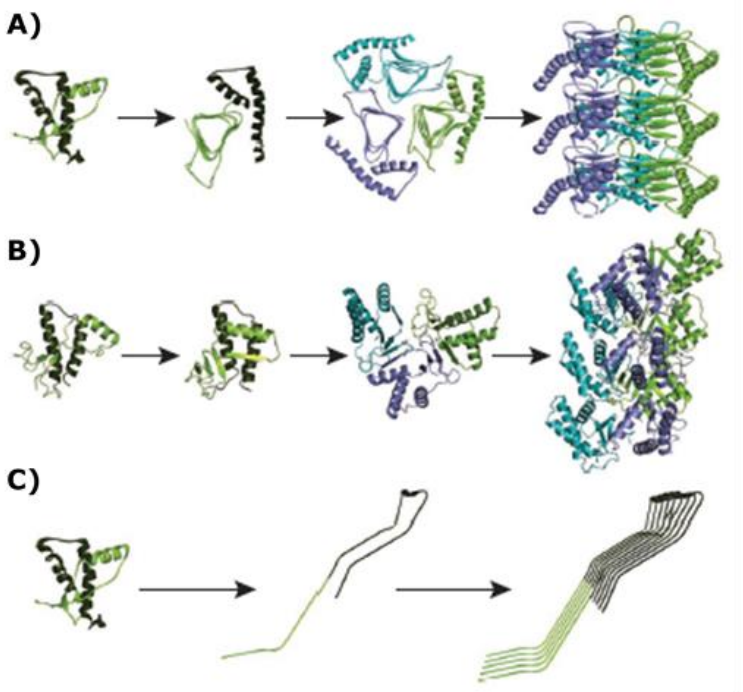

Figure 1.3. Models proposed for the misfolding of PrP^{C} to form PrP^{Sc}. **A**) The β-helical model, where PrP^{27-30} forms a β-helix motif (green) with residues 90-177 while residues 178-230 maintain the α-helical structure of PrP^{C}. **B**) The β-spiral model, where residues 109-29 of PrP form spiralling β-sheet cores with the α-helices of PrP maintaining their native conformation. **C**) The parallel β-sheet stacking model, where PrP refolds to form in-register parallel β-sheets (Diaz-Espinoza & Soto 2012).

Another model was constructed using molecular dynamics simulations of mutant Syrian hamster PrP in changing pH conditions (DeMarco & Daggett 2004). These simulations observed the spiralling of β-sheeted cores are similar to structures observed by low resolution structural studies (**Figure 1.3. B**) (DeMarco & Daggett 2004). However, this model only used residues 109-219 of the PrP sequence, including a mutation at D147N that directed the model towards misfolding. Yet its strength is the unbiased prediction of the ordered β-structure from folded PrP^{C}

(Diaz-Espinoza & Soto 2012). Another model proposes that PrP^C completely unfolds, then refolds to form parallel in register β-sheets (**Figure 1.3. C**) (Cobb et al. 2007). This is supported by model simulations of amyloid fibril formation by recombinant PrP (Groveman et al. 2014). However, this work utilised recombinant PrP from Syrian hamster with an amino acid sequence 90–231, and not the complete PrP sequence. In addition, molecular simulations may not completely include all physiological conditions including cofactor and water molecules (Groveman et al. 2014). Consequently, it may be questioned how representative the model is of native PrP^{Sc} structure.

Although these models provide useful insights into PrP^{Sc} structure, their differences and ultimately theoretical basis highlights the limits of our current knowledge on PrP^{Sc} structure (Diaz-Espinoza & Soto 2012). The heterogeneity between structural models further limits the capacity to develop effective diagnostics and therapeutics for prion diseases (DeMarco & Daggett 2004). It may also be noted that the structure of PrP^{Sc} is not necessarily restricted to amyloid alone. An increasingly recognised hypothesis is that PrP^{Sc} forms populations of different tertiary structures. Smaller prion oligomers in fact may be the cause of neurotoxicity rather than the amyloid aggregates (Colby & Prusiner 2011; Wang et al. 2015).

Prion Conversion and Propagation

The conversion of PrP^C to PrP^{Sc} is a key event in prion diseases due to its association with disease progression and pathogenesis. Although the accumulation of PrP^{Sc} was initially hypothesised to be the major pathological event, this pathology may in fact be related to the conversion mechanism itself (Trevitt & Collinge 2006). However, limited knowledge into the mechanisms behind prion replication hinders these research efforts. Greater understanding of the fundamental mechanisms of prion propagation could allow for the design of more effective inhibitors of this process. The current paradigm of PrP^{Sc} propagation, the "prion paradigm", is the protein only model. In this model PrP^{Sc} replicates using PrP^C as "substrate" without any requirement for nucleic acids (Prusiner 1998). That PrP knockout mice are resistant to PrP^{Sc} replication and associated pathogenesis indicates the necessity of PrP^C as a substrate (Büeler et al. 1993). *De novo* infectious prions have also been produced *in vitro* through serial rounds of protein misfolding cyclic amplification (PMCA), confirming that this protein conversion is a central event in prion disease (Castilla et al. 2005; Weber et al. 2007). PrP^{Sc} propagation itself can also be competitively inhibited by recombinant or

heterogeneous prion proteins, confirming the requirement of both PrP^{Sc} and PrP^{C} for prion propagation (Meier et al. 2003; Masel et al. 2005; Hizume et al. 2009; Kobayashi et al. 2009; Yuan et al. 2013). Although these studies provide strong evidence for the protein only model, the underlying mechanism behind conversion is unknown. To counter this limitation, several models of prion propagation have been proposed. These models include the template-directed refolding model, the nucleation-seeding model and the involvement of folding intermediates (**Figure 1.4.**) (Prusiner 1998; Pan et al. 2005; Rigter et al. 2010; Zhou et al. 2016). Each model is a proposed mechanism of prion propagation, and they are not necessarily mutually exclusive. In the template-directed refolding model PrP^{Sc} replicates by enforcing its conformation on PrP^{C} to generate more copies of PrP^{Sc}, a trait shared by the protein tau in AD (**Figure 1.4. A**) (Prusiner 1998; Sanders et al. 2014; Kaufman et al. 2016). That the stability of disease phenotypes can be maintained between hosts and species indicates a faithful propagation of the PrP^{Sc} conformation onto PrP^{C} substrate, and supports such a model as template-directed refolding (Makarava & Baskakov 2012). Template-directed refolding posits that there is a rate limiting step in conversion, the refolding of PrP^{C} to PrP^{Sc} (Zhou et al. 2016). The PrP^{C}-PrP^{Sc} interaction is central to this model, with homology between host and pathogenic PrP sequences acting as a predisposition to prion diseases such as sCJD (Palmer et al. 1991). This led to the hypothesis that heterozygous PrP^{C} may provide a protective role against prion infection, later demonstrated by studies of prion propagation *in vitro* and *in vivo* (Kobayashi et al. 2009). Another hypothesis postulates that amyloid fibrils like prions form in a mechanism named as nucleation-seeding (**Figure 1.4. B**) (Come et al. 1993; Gilch & Schätzl 2009). In this nucleation-seeding model, as part of template-induced conversion PrP^{Sc} polymers recruit PrP^{C} substrate at nucleation sites (Aguzzi & Falsig 2012). Over time this leads to the polymerisation of PrP^{Sc} fibrils that then break to seed the polymerisation of new aggregate seeds (**Figure 1.4. B**). Indeed similar mechanisms have been proposed with Aβ and α-synuclein fibrillization, due to the propensity of these proteins to form nucleating seeds *in vitro* (Lomakin et al. 1996; Necula et al. 2003). Evidence for the nucleation-seeding model is provided by *in vitro* methods of prion replication, including PMCA pioneered by Saborio and colleagues in 2001 (**Figure 1.5.**) (Saborio et al. 2001).

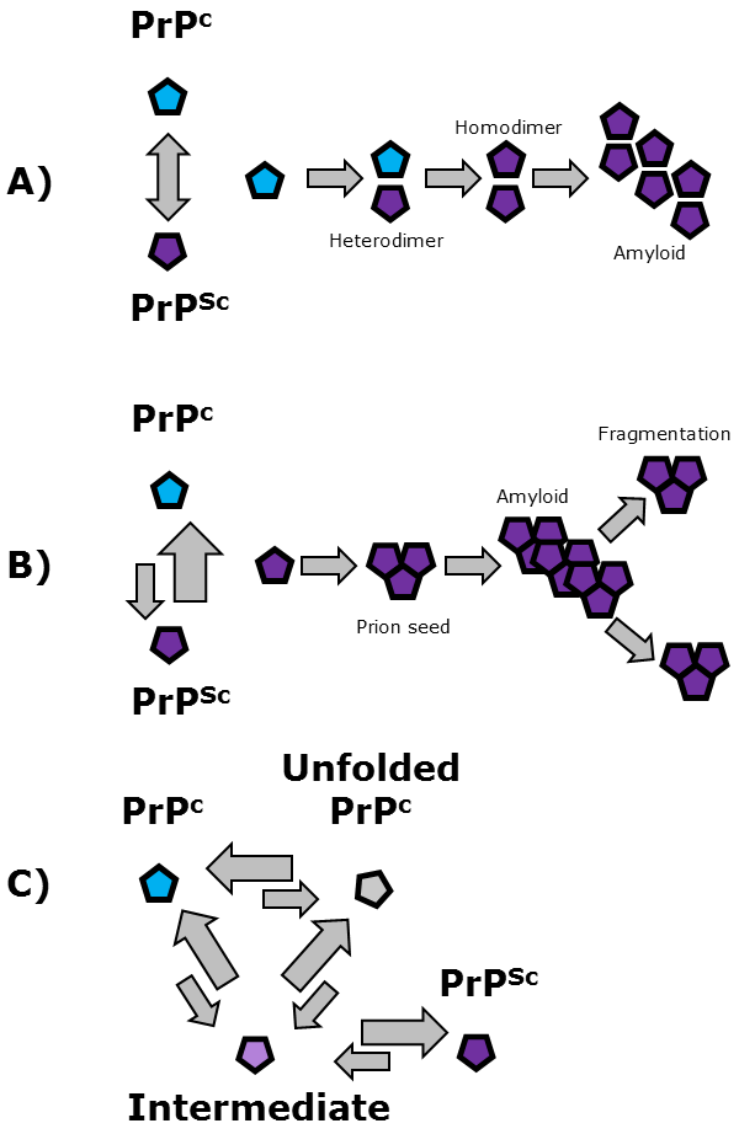

Figure 1.4. Models of prion conversion. **A**) The template-directed refolding model hypothesises the induced conversion of endogenous PrP^{C} into disease associated PrP^{Sc} by the pathogenic protein. The energy required to unfold PrP^{C} may act as a threshold that prevents spontaneous conversion. **B**) The nucleation-seeding model posits that PrP^{C}-PrP^{Sc} conversion is in a thermodynamic equilibrium. PrP^{Sc} monomers aggregate to form amyloid seeds, which may then fragment to form further nucleating seeds. **C**) Folding by intermediates has also been hypothesised, where PrP^{C} can misfold to form an unfolded or partially unfolded intermediate which can then fold into PrP^{Sc}. This figure was adapted from (Aguzzi et al. 2001 and Gerber et al. 2007).

This technique utilises cycles of growth and sonication to grow and break PrP^{Sc} aggregates in the mechanism described by nucleation and seeding (**Figure 1.5.**). The success of this method for amplifying PrP^{Sc} supports the validity of the

nucleation seeding model and allows for the exponential amplification of prions *in vitro* (**Figure 1.5.**) (Zou & Gambetti 2005). This technique has also been adapted for *in vitro* amplification of α-synuclein, Aβ and tau, again indicating that a similar mechanism of propagation occurs between protein agents in different misfolding diseases (Herva et al. 2014; Meyer et al. 2014). In addition, PMCA has been used to demonstrate the *de novo* generation of infectious prions from brain homogenate and recombinant PrP through multiple rounds of sonication and incubation (Castilla et al. 2005; Weber et al. 2007; Zhang et al. 2013).

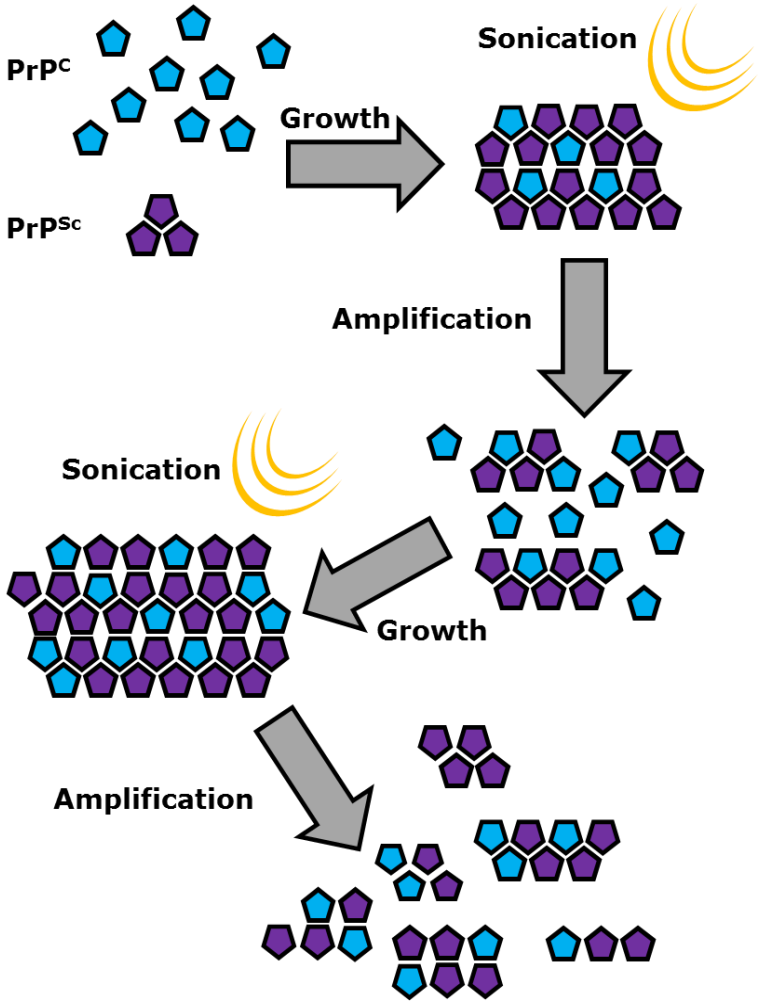

Figure 1.5. An illustration of PMCA. In this method, healthy brain homogenate containing PrP^{C} is incubated with PrP^{Sc} or "spike" (e.g. in an infected brain homogenate). Incubation allows for PrP^{C} to be misfolded and incorporated into PrP^{Sc} aggregates. Sonication then fragments PrP^{Sc} aggregates into further nucleation centres. Cycling these rounds of incubation and sonication enables the exponential propagation of PrP^{Sc} over time. This diagram was adapted from (Saborio et al. 2001).

PMCA may therefore provide a close approximation to *in vivo* replication as these *de novo* prions share similar biochemical characteristics to PrP^{Sc} from infected brains, and caused disease in inoculated rodent models (Castilla et al. 2005; Weber et al. 2007). The nucleation-seeding model accounts for *in vitro* experimental data of prion replication, yet it is still limited in describing the complexity of the mechanism itself (Rigter et al. 2010).

Kinetics studies indicate the role of a folding intermediate in the nucleation-seeding mechanism (**Figure 1.4. C**). Initially it was believed that the kinetics of PrP^{Sc} propagation occurred in two steps of elongation and breakage, akin to the proposed mechanism of nucleation–seeding (Caughey 2001; Masel et al. 2005). More recently a study simulating the folding of two mutant PrP^{27-30} proteins observed three step kinetics in conversion, suggesting the requirement of a folding intermediate (**Figure 1.4. C**) (Jenkins et al. 2008). Previous folding studies have also implicated the role of an intermediate precursor in PrP^{Sc} formation, and models of fibril formation and solution-state NMR indicate that a PrP intermediate can exist as part of the folding pathway (**Figure 1.4. C**) (DeMarco & Daggett 2004; Govaerts et al. 2004; Apetri et al. 2006; Gerber et al. 2007). It has been demonstrated that this intermediate may play a role in the nucleation model of prion propagation. By measuring PrP^{C} unfolding by fluorescence at pH 5.5 and pH 7, it was reported that the folding intermediate has a near-native structure resembling a molten-globule state (Jenkins et al. 2008). This observation is consistent with the nucleation-seeding model of prion folding, where the secondary and tertiary structures are proposed to form simultaneously (Jenkins et al. 2008). Indeed, observations by NMR support that a persistent structure remains in spite of the major structural remodelling as part of conversion, indicating that the molten globule intermediate may be more conducive to PrP^{Sc} fibrillation (Hosszu et al. 2005). The precise mechanism of this folding pathway remains elusive. However, inhibiting the folding mechanism should prevent PrP^{Sc} propagation and accumulation as a potential therapeutic strategy.

Cofactors and Prion Replication

A matter of debate is whether cofactors are required for the PrP^{Sc} conversion mechanism. Even though infectious prions can be generated *de novo* they cannot be generated from PrP^{C} alone, indicating that cofactors may be necessary for propagation (Zurawel et al. 2014). Due to the heterogeneity of the brain substrate used in PMCA identifying these cofactors is challenging, although studies implicate the involvement of a "Protein X", lipids or RNA (Prusiner 1998; Saa et al. 2012;

Yuan et al. 2013; Zurawel et al. 2014). The requirement of a cofactor was proposed following studies investigating the transmission of prions into mice transgenic for human *PRNP*, where species-specific variants of cofactors were proposed to be contributing to prion propagation (Telling et al. 1995). Although the identity of such a cofactor was unknown, it was assumed to be protein in nature and was named "Protein X" (Telling et al. 1995). It was later reported that Protein X may bind a specific epitope on PrP^{C}, as mutating residues at 214, 218 and others had an inhibitory effect on PrP^{Sc} propagation (Kaneko et al. 1997). It was proposed that these mutants were binding Protein X as dominant negative inhibitors, thereby preventing PrP^{Sc} propagation (Kaneko et al. 1997). Co-transfection of these mutants with wild type mouse PrP^{C} into scrapie infected neuroblastoma (ScN_2A) cell culture also resulted in the inhibition PrP^{Sc} formation, but only for specific mutations (Kaneko et al. 1997). It was hypothesised that this dominant negative inhibition was caused by the mutations affecting the affinity of PrP^{C} for Protein X. However, the authors were unable to directly measure the effect of the mutations on PrP^{C} conversion. Because of this it is possible that these mutations reduced the efficacy of PrP as a conversion substrate, similar to that observed with heterologous PrP^{C} (Priola et al. 1994). Subsequent studies centred on Protein X as a potential therapeutic target, and demonstrated that compounds designed to block Protein X binding to PrP successfully inhibited scrapie propagation in neuroblastoma cells *in vitro* (Perrier et al. 2000). Despite the accumulated evidence for Protein X, the identity of such a cofactor remains enigmatic. More recent reports even throw the necessity of Protein X into scrutiny, including observations that the dominant negative effect of mutant PrP occurs in cofactor free polymerisation of purified PrP^{Sc} *in vitro* (Lee et al. 2007; Geoghegan et al. 2009). Instead of protein X, the cause of this dominant negative activity could be due to the generation of PrP^{Sc} populations with increased or decreased conversion efficiencies (Hizume et al. 2009). Indeed, this decreased conversion efficiency can account for the inhibition observed with heterologous PrP^{C}, as well as with prion strain interference (Priola et al. 1994; Bartz et al. 2007; Geoghegan et al. 2009; Hizume et al. 2009; Kobayashi et al. 2009).

Alternatively, lipids and RNA are also considered cofactors for PrP^{Sc} propagation, and have been determined necessary for conversion *in vitro* and for *in vivo* infectivity (Edgeworth et al. 2010; Wickner et al. 2010). Indeed, poly (A) RNA has been previously identified as a necessary cofactor for conversion *in vitro*, and can induce *de novo* formation of hamster PrP^{Sc} (Telling et al. 1995; Geoghegan et al. 2007; Deleault et al. 2007; Suttappone 2014). Treatment of amplification

substrate with nucleases removes the capacity of prions to replicate in PMCA, supporting the role of RNA polyanions as replication cofactors (Deleault et al. 2007). Heparin and heparin sulphate have been reported to maintain prion strain characteristics and infectivity in PMCA even after RNA removal (Imamura et al. 2016). 1-palmitoyl-2-oleoyl phosphatidylglycerol (POPG), a phospholipid and membrane constituent, also demonstrably supports the production of *de novo* infectious prions when used in tandem with RNA (Wang et al. 2010). Another study using rPrP with preparations of different phospholipids reported that removal of these lipids in serial PMCA did not completely prevent PrP^{Sc} amplification, but it did result in the loss of prion infectivity (Deleault et al. 2012). Through reintroduction of these cofactors it was elucidated that phospholipids such as phosphatidyletholamine (PE) were required for the maintenance of infectivity, while anionic RNA molecules were not (Deleault et al. 2012). Therefore, both RNA and lipids aid prion propagation and lipids may be necessary for the maintenance of infectivity.

A similar relationship can be observed in other protein misfolding diseases. Both prion and Aβ neuropathology are dependent on membrane binding, implicating a shared mechanism of propagation and disease pathology (Florent-Béchard et al. 2009; Fluharty et al. 2013). Lipids in particular have been determined to be important for Aβ binding to membranes and fibril formation (Chi et al. 2008). Lipids including phosphatidylserine (PS) can induce amyloid formation in a number of different proteins including amyloid beta 1-42 ($A\beta_{42}$) (Yip et al. 2002; Zhao et al. 2004). Furthermore, a combination of molecular dynamics (MD) simulation, circular dichroism, NMR and liposome binding studies have implicated Aβ in binding preferentially to membranes with constituents including POPG (Terzi et al. 1997; Wong et al. 2009; Yu et al. 2013). The protein tau is similarly stimulated to polymerise by cofactors. Ligands such as heparin, sulphated glycosaminoglycan and RNA can induce tau polymerisation *in vitro* over the course of a few days (Friedhoff et al. 2000; Mandelkow 2012). α-synuclein can likewise be induced to aggregate using lipid cofactors, with polymerisation efficiency dependent on lipid to protein ratios (De Franceschi et al. 2011; Dikiy & Eliezer 2012). Cofactors implicated in α-synuclein aggregation include but are not limited to fatty acids like arachidonic acid, heterogenous micelles and docoshexanoic acid, as well as the polysaccharide heparin (Necula et al. 2003; De Franceschi et al. 2011). The commonality of cofactors between these diseases ultimately indicates a similar misfolding pathway, yet the details of any common folding mechanism for these proteins compared to PrP^{Sc} remains unknown (Ma 2012). With increasing insights

into the cofactors required in protein misfolding diseases, new light may be shed into the mechanisms of prion replication and pathology. Identifying the cofactors pivotal to prion replication may aid our current understanding of the process, and reveal novel targets for developing effective therapeutics (Ferreira et al. 2014).

Prion Strains

Following prion conversion, PrP^{Sc} aggregates can form different conformations with differing biochemical properties and associated pathologies, termed prion strains (Stein & True 2014). These differences in biochemical properties result in strains exhibiting classifiable symptomology, transmission between hosts, sensitivity to PK digestion, PrP^{Sc} deposition, spongiform degeneration and glycosylation ratios (Bruce 2003; Owen et al. 2007). A definitive property of strains is the maintenance of biochemical and pathological characteristics upon serial passage, after the species transmission barrier is overcome (Aguzzi & Calella 2009). Exploitation of these characteristics has enabled the identification of up to 30 prion strains (Stein & True 2014). Prion strains initially presented a contradiction to the protein only hypothesis, as an alternative mode of inheritance to genetics is necessary to explain such a phenomenon (Caughey 2001; Diaz-Espinoza & Soto 2012; Berry et al. 2013). A possible explanation for strain heterogeneity is the prion cloud hypothesis (**Figure 1.6.**). This asserts that PrP^{Sc} strains exist as a heterogeneous pool of variants arising from variation in PrP^{Sc} tertiary structure (**Figure 1.6. A**) (Li et al. 2010; Makarava & Baskakov 2013). Upon transmission to a new host those variants most fit for the new environment hold an advantage for replication and become dominant (Baskakov 2014). This hypothesis arose following the observation that extracts from FFI and sCJD patients both produced two forms of PrP^{Sc} (with protease-resistant fragments of 19kDa or 21kDa) after inoculation in transgenic mice (Telling et al. 1996). These biochemical differences were hypothesised to be resultant from differences in the conformation of PrP^{Sc} (Telling et al. 1996; Peretz et al. 2001). Studies using growth selective conditions have observed that a change in conditions induces change in prion variants, both in mice and in yeast (Bateman & Wickner 2013). It has been argued that the [PSI^{+}] prion protein of *S. cerevisiae* exists in an array of amyloid structures, as [PSI^{+}] replication generates new variants in non-selective growth *in vivo* (Bateman & Wickner 2013). Such observations of Darwinian selection of prions have also been reported by numerous cell culture studies and in transgenic mice, as well as in response to treatment with prion therapeutics such as quinacrine (Li et al. 2010; Giles et al. 2011; Berry et al 2013; Bian et al 2013; Berry et al. 2015). The cloud hypothesis could therefore account for the observed resistance of prions to drug

treatment. Strain adaptation during repeat passage in a new host species can itself be characterized by a decrease in incubation period before the development of symptoms, an increase in attack rate, and alteration of PrP^{Sc} physical properties, changes in PrP^{Sc} deposition, and a change in clinical symptoms (Baskakov 2014). The population of available cofactors may also affect strain infectivity and propagation, as strain properties can be altered through changing the cofactor composition in PMCA (Deleault et al. 2012).

The characteristics of prion strains may be dictated by both the 3D structure of PrP^{Sc} and the local host environment (Gonzalez-Montalban et al. 2013). This is hypothesised in the deformed templating model, where the replication environment acts to affect prion replication (**Figure 1.6. B**) (Makarava & Baskakov 2013). This model suggests that daughter fibrils can adopt different structural properties to the seed depending on the environment, resulting in a population of *de novo* variants over time (**Figure 1.6.**) (Makarava & Baskakov 2012). Indeed, altering the RNA and PE content during PMCA can affect strain characteristics such as sensitivity to PK and amplification rates (Deleault et al. 2012; Gonzalez-Montalban et al. 2013). The generation of de novo PrP^{Sc} from non-infectious rPrP fibrils is proposed to occur in a two-step mechanism. In the first step, atypical PrP^{res} (from PrP^{C}) can be seeded by rPrP amyloid fibrils. From the self-propagating atypical PrP^{res}, rare deformed templating events then produce PrP^{Sc} with distinct biochemical characteristics and with greater replication efficiency (Makarava et al. 2016). In transgenic mice overexpressing PrP^{C}, the rate of atypical PrP^{res} is increased but not the rate of PrP^{Sc} formation, suggesting that the rate of PrP^{Sc} formation is limited by the frequency of rare deformed templating events rather than PrP^{C} expression (Makarava et al. 2016). Although deformed templating does not directly contradict with the cloud hypothesis, it offers an explanation for the origin of PrP^{Sc} populations whereas the cloud hypothesis assumes their existence prior to selection. Together, deformed templating and the cloud hypothesis may account for the mechanism by which prions adapt to new hosts/conditions and how they develop drug resistance (Makarava & Baskakov 2013). The combination of strain characteristics, host genotypes and phenotypes may thereby change the efficacy of different therapeutics or diagnostics (Trevitt & Collinge 2006).

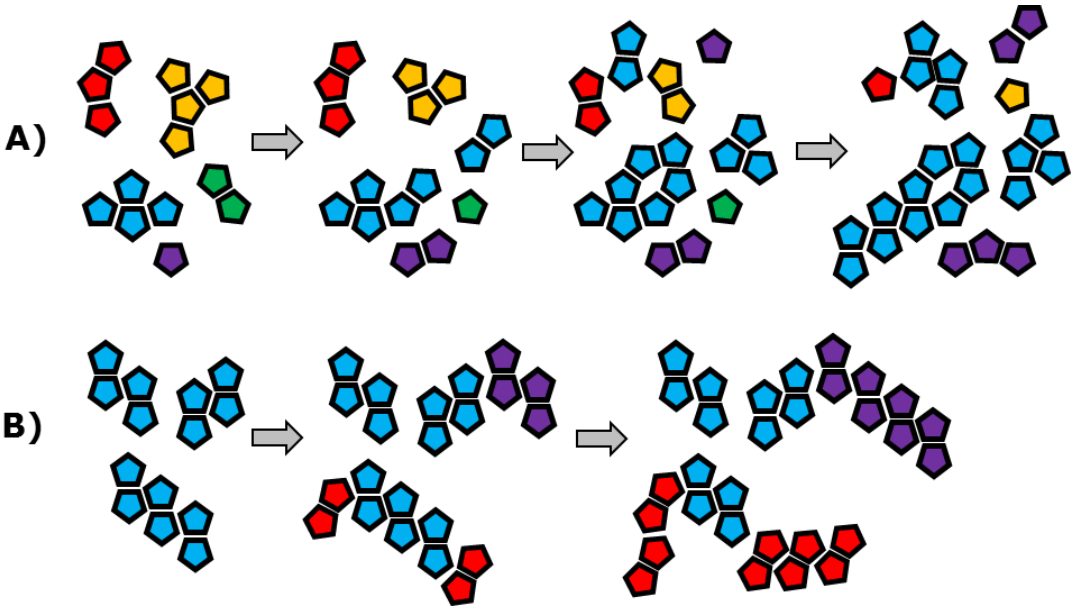

Figure 1.6. The cloud hypothesis and deformed templating hypothesis. **A**) The cloud hypothesis posits that a prion strain consists of a population of different PrP^{Sc} structural variants, represented by different colours. Environmental changes apply selective pressure, leading to the dominance of a particular variant. **B**) In deformed templating, it is hypothesised that prion variants arise from rare conversion events, and can compete with and even replace the original variant. Adapted from (Makarava & Baskakov 2013).

Genetics and Susceptibility

Although prion diseases may be primarily considered disorders of protein misfolding, the host genotype can significantly influence disease susceptibility and inheritance. Transmission of a prion isolate across species or between hosts can be met with reduced efficacy. This is known as the species transmission barrier, where the efficacy of prion transmission is determined by the infectious prion and host environment, including the PrP^{C} amino acid sequence (Scott et al. 1993). In human prion diseases, mutations in the *PRNP* sequence are thought to be responsible for inherited diseases such as familial CJD (fCJD), GSS and FFI (Caughey 2001). Within the human *PRNP* gene there are two major polymorphic codons: 129 for methionine (M) or valine (V) and 219 for glutamate (E) or lysine (K) (Kobayashi et al. 2009). These polymorphisms have been recognised as potential markers for susceptibility and resistance in CJD. vCJD victim cases who have been genetically tested are predominantly 129 M/M homozygous, with the exception of a recent case which was 129 M/V heterozygous (Ironside 2012; Mok & Jaunmuktane 2017). Those heterozygous for 129 M/V or 219 E/K are also

underrepresented in cases of sCJD (Kobayashi et al. 2015). Additionally, cases of sCJD are more numerous in patients homozygous for 129 M/M over patients homozygous for V/V (Brown et al. 2012). This in turn implicates 129 V/V and 129 M/V polymorphs in some level of resistance to vCJD transmission and sCJD development, but does not guarantee protection. In addition, the 219 E/K polymorphism appears to confer sCJD resistance, corroborated by *in vivo* and *in vitro* studies where 219 E/K confers resistance to prion infection in mice (Kobayashi et al. 2009). Recent studies have also identified that the polymorphism at V127G in human *PRNP* acts as a preventative of Kuru disease development (Mead et al. 2009; Asante et al. 2015; Zhou et al. 2016). It has since been reported that in molecular dynamics simulations this polymorphism is unfavourable for forming stable fibril and dimer interactions (Zhou et al. 2016).

Analogous observations have been made in sheep, where polymorphisms occur at codons 136 (Alanine/Valine), 154 (Arginine/Histidine) and 171 (Glutamine/Histidine/Arginine) that can confer disease resistance/susceptibility (Gough et al. 2014). Sheep genotypes and ovine PrP proteins are named according to these polymorphisms i.e. ARR, VRQ, and AHQ etc. Flock and genome studies have determined that polymorphisms such as VRQ and ARQ are associated with increased susceptibility to classical scrapie, while ARR/ARR homozygous sheep are the most resistant (Bossers et al. 1996; Hunter 1997; Tranulis et al. 2002; Baylis et al. 2004). However, as in humans the resistant genotype does not guarantee protection, and rare cases of scrapie have been identified in sheep homozygous for ARR/ARR (Groschup et al. 2007). This observation of relatively resistant sheep polymorphs has led to a scrapie eradication programme in the United Kingdom known as the National Scrapie Programme (NSP). The NSP was launched in 2001 in the aim of eradicating TSEs in sheep, primarily to prevent any possible zoonotic BSE transmission via sheep meat and to control the spread of scrapie in the sheep population (Ortiz-Pelaez et al. 2014). This was followed by other European states in 2003 implementing similar eradication programmes (Melchior et al. 2010). The aim of the NSP is to maximise the scrapie resistant genotype ARR/ARR and to minimise the frequency of VRQ in the sheep population as a means of limiting the occurrence of classical scrapie (Truscott & Ferguson 2009). In 2016 no cases of classical scrapie were reported in sheep in the UK, from 568 confirmed cases in 2000, although this is subject to the number of animals tested by active surveillance (TSE surveillance statistics, Animal and Plant Health Agency). The NSP has thereby contributed to a large reduction in the number classical scrapie cases.

Prions as an Insight into Other Protein Misfolding Diseases

Prion diseases form part of a group of conditions called protein conformation diseases (or protein misfolding diseases) that include AD, PD and Huntington's disease (HD) (Saa et al. 2012). It is being increasingly recognized that the "prion paradigm", the conversion of a cellular protein to a pathogenic isotype, is a contributing mechanism behind these diseases (Jucker & Walker 2013). In AD for instance the aggregation of Aβ, a proteolytic product of the amyloid protein precursor (APP), is associated with disease pathology and clinical symptoms (Fluharty et al. 2013). As in prion diseases, this mechanism involves the misfolding and accumulation of normal Aβ into fibrils with a predominant β-sheet structure, a process later associated with neuropathy and loss of cognitive function (Soto 2003). This process is shared with other disease associated proteins such as α-synuclein in PD and tau in AD (Soto 2003; Bousset et al. 2013). Like prions, Aβ aggregates may be found in varying sizes from small, soluble oligomers to large, insoluble fibrils (Jucker & Walker 2013). However, only the PrP^{Sc} protein is considered a proteinaceous infectious particle due to its transmissibility (Aguzzi & Rajendran 2009). This is a position that may soon change, as recently it has been suggested that the tau protein involved in AD should in fact be considered to be a prion protein itself (Sanders et al. 2014; Kaufman et al. 2016). This follows from observations that mutant tau proteins can maintain specific biochemical characteristics such as different molecular weights after digestion with pronase, and can maintain these characteristics *in vitro* and in mouse bioassays (Sanders et al. 2014). 18 tau strains were later characterized from recombinant, mouse and human sources which produce characteristic pathology in transgenic mice (Kaufman et al. 2016). Amyloid in AD has also been reported to exhibit strain like lesions in humanised mice models, and transmission can be achieved via inoculation with diseased brain homogenate (Aguzzi et al. 2007; Diaz-Espinoza & Soto 2012; Heilbronner et al. 2013). Purified Aβ has been demonstrated to produce AD-like disease in transgenic mice, where it was a necessity to disease development much like PrP^{Sc} (Stöhr et al. 2012). Evidence for α-synuclein strains has been reported, including different biochemical properties that are propagated faithfully *in vivo* (Bousset et al. 2013). Tau, Aβ and α-synuclein may well then be considered as prions themselves, were it not for undemonstrated natural transmission (Aguzzi & Rajendran 2009). Together these studies indicate that there is an underlying similarity in protein misfolding and pathogenesis between these diseases, in spite of the heterogeneity between the protein agents. As prion propagation can be effectively modelled *in vitro*, it could act as a platform for high

throughput screening of therapeutics that may have a broader application across protein misfolding diseases (Panegyres & Armari 2013).

Prion Disease Zoonosis

To date the only known zoonotic prion disease is BSE. The first case of BSE in the United Kingdom was identified in 1986, after brain homogenate from suspected animals was transmitted into wild type mice resulting in consistent profiles of vacuolation in the dorsal medulla, hypothalamus and septum (Diack et al. 2014). What followed was a major epidemic of BSE in cattle during the ensuing years resulting in the slaughter of millions of cattle to prevent transmission to humans, yet transmission is believed to have eventually occurred via the consumption of infected beef (Hill et al. 1997). This led to the identification of a new form of CJD bearing biochemical similarities to BSE, termed variant CJD (Will et al. 1997). Reported cases of vCJD have since resulted in 231 deaths worldwide as of December 2016 with no surviving victims (The National CJD Research and Surveillance Unit). Although the number of vCJD cases have been lower than feared, concerns have been raised over secondary transmission from contaminated blood, growth hormones and neurosurgical instruments (Aguzzi et al. 2007; Hall et al. 2014). A recent study screening patient appendixes for PrP^{Sc} estimated there to be 493 carriers of abnormal PrP per million of the UK population (1/2028), a figure higher than previous estimates (Frosh et al. 2004; Hilton et al. 2004; Clewley et al. 2009; De Marco et al. 2010; Gill et al. 2013). This prevalence of the pathogenic prion protein in the UK population presents a potential hazard to human health as the long-term consequences are unknown, including the increased risk of secondary transmission (Gill et al. 2013). Additionally, there remains the possibility that other strains of animal prions may exist that have a greater transmission efficiency to humans compared to BSE.

The risk of CWD zoonosis has been investigated both environmentally and experimentally. CWD is transmissible to a number of mammals including cervids, sheep, goat, cattle, transgenic mice expressing cervid PrP^{C}, bank voles, ferrets and squirrel monkeys (Benestad et al. 2016). However, transgenic mice expressing human PrP^{C} and primates display resistance to disease development (Saunders et al. 2012; Kurt & Sigurdson 2016). This implies that the species barrier for CWD transmission to humans could be sufficient to prevent zoonosis, and there is currently no epistemological evidence of transmission to humans, although concerns of transmission remains (Kurt & Sigurdson 2016). Scrapie has been known to exist for hundreds of years, and although once endemic in the UK,

cases of classical scrapie have been reduced to 0 as of 2016 through the National Scrapie Plan (Tranulis 2002; Truscott & Ferguson 2009; Wickner et al. 2010; Ortiz-Pelaez et al. 2014). Scrapie is classically considered to be non-infectious to humans due to epistemological evidence, and that countries free from scrapie have similar frequency of sCJD cases to countries with scrapie (Comoy et al. 2015). However, a more recent study reported the transmission of scrapie to a primate host, raising the possibility of transmission to humans (Comoy et al. 2015).

Prion Disease Prevalence and the Need for Continued Vigilance

At its height, the BSE epidemic caused widespread panic as rising cases of vCJD were confirmed to be caused by the consumption of infected beef (Hill et al. 1997). However, in recent years cases of vCJD have fallen from their height of 28 deaths in the UK in 2000 to 1 in 2016 (The National CJD Research and Surveillance Unit). The number of cattle known to have carried BSE and were resultantly slaughtered has also fallen from a height of 43194 in 1992 to 0 as of 2016 (TSE surveillance statistics, Animal and Plant Health Agency). Likewise, the numbers of cases of scrapie have fallen to no cases of classical scrapie in sheep reported in 2016 (TSE surveillance statistics, Animal and Plant Health Agency). These observations raise the question of whether TSE diagnosis and surveillance remains essential to the protection of public health.

Despite the fall in cases of vCJD, the number of sCJD cases have remained consistent with the highest number of deaths each year (1-2/million people), resulting in 1786 reported deaths in the UK since recordings began in 1990 (The National CJD Research and Surveillance Unit). The total number of deaths caused by vCJD in the UK during this time has been 178, with 80 cases of iaCJD and 178 cases of fCJD (The National CJD Research and Surveillance Unit). These data illustrate a continued risk of iatrogenic CJD as the numbers of sCJD and fCJD cases remain consistent (Hall et al. 2014). The full extent of the impact of vCJD on the population is also unknown. As discussed earlier, a recent study screening PrP in lymphoreticular tissue of the UK population estimated there to be a larger percentage of the population as asymptomatic carriers of the vCJD prion than previously reported in analogous studies (Frosh et al. 2004; Hilton et al. 2004; Clewley et al. 2009; De Marco et al. 2010; Gill et al. 2013). Additionally, it was recently reported that a patient with an asymptomatic infection could readily transmit disease into mice (Diack et al 2014). Together this indicates that the presence of asymptomatic vCJD carriers in the UK population may continue to pose a risk to public health. These individuals may never develop full clinical

symptomology, but the potential for secondary infection remains. Furthermore, it is reported that the mean incubation period for the development of symptoms for vCJD is 15 years (Budka & Will 2015). The prolonged incubation periods for these diseases raises concerns as to the long-term consequences of the BSE outbreak and vCJD transmission. Cases of vCJD reached a peak in 2000, of which all were definite or likely M/M 129 homozygous (Ironside 2012; Diack et al. 2014; TSE Surveillance and Research Unit). However, recently the first M/V 129 heterozygous case of vCJD was identified in the UK (Mok & Jaunmuktane 2017). With this recent case of vCJD, the possibility remains that further cases of vCJD may emerge in M/V 129 heterozygous individuals with longer incubation periods. This in turn raises concerns as to the transmission of vCJD by blood donors. As the distribution of UK blood donors are 42% M/M, 47% M/V and 11% V/V, the recent case of M/V vCJD raises the possibility that a greater number of the UK population are at risk to iatrogenic CJD than previously thought (Nurmi et al. 2003).

Out of animal prion diseases, CWD remains endemic in North America with cases reported in South Korea after the importation of infected animals (Saunders et al. 2012). Due to the presence of CWD in free roaming deer herds the prevalence of CWD is difficult to survey, and as of October 2016, 164 American counties in 21 states, as well as 2 Canadian provinces reported CWD in free roaming herds (Centres for Disease Control and Prevention; Canadian Food Inspection Agency). Due to the spread of CWD it is unlikely that reducing the number of cases in North America is currently feasible, although the emergence of CWD in New York was successfully contained (Miller & Fischer 2016). As of 2016 two cases of CWD have been identified in Norway (Benestad et al. 2016; Ricci et al. 2017). The origin of these new cases is unknown, but the threat of CWD to the deer population in Norway means intensive surveillance is required to contain the spread of the disease (Benestad et al. 2016). This is especially poignant as control or elimination of CWD is considered infeasible once the disease becomes endemic in the cervid population (Ricci et al. 2017).

Although scrapie was once an endemic prion disease in the UK, cases of classical scrapie have dropped to 0 as of 2016 (Animal Plant and Health Agency). Nevertheless, scrapie prions can remain present in the environment for days to years, acting as a reservoir of infectious scrapie prions (Georgsson et al. 2006; Maddison et al. 2010). Additionally, the established method of decontamination by 20000 parts per million (ppm) sodium hypochlorite is insufficient in controlling environmental infectivity (Hawkins et al. 2014). Although scrapie is no longer

endemic, the risk remains of classical scrapie reoccurring through environmental reservoirs. Given the potential zoonosis of these diseases, continued surveillance of prion diseases in both humans and animals can be argued to be necessary in order to monitor and contain the spread of CWD, to monitor any resurgence in classical scrapie cases, to monitor for the emergence of novel strains and to fully understand the long-term consequences of asymptomatic carriers of vCJD on the UK population.

1.2. Research into Prion Therapeutics

Pharmaceutical Therapeutics

Compounds targeting PrP^{Sc} have been developed by screening in animal models, cell culture and cell free *in vitro* replication assays (Trevitt & Collinge 2006; Ferreira et al. 2014). An early study investigating 2000 drugs and natural products identified a number of compounds with high Inhibitor Concentration 50% (IC50) values for PrP^{res} formation in ScN_2A cell culture (Kocisko et al. 2003). The compounds identified were then tested in scrapie infected mice, although the inhibitory efficacy of these compounds was insignificant (Kocisko et al. 2004). Numerous compounds have also been screened and investigated for their anti-PrP^{Sc} activity including heparin sulphate mimetics, tetrapyrollic compounds, congo red dye, suramin, branched polyamines, thioflavin, dendramers and copper (Trevitt & Collinge 2006; Rigter et al. 2010; McCarthy et al. 2013; Panegyres & Armari 2013). However, few have been as successful in *in vivo* models as in *in vitro* models either due to toxicity, poor pharmokinetic profiles or the inability to cross the blood brain barrier (Féraudet et al. 2005; Ferreira et al. 2014). Furthermore, when applied in the clinical phase of disease none are effective at preventing disease progression (Barret et al. 2003). Despite these drawbacks some pharmaceuticals have been assessed in clinical trials, a key example being pentosane polysulfate (PPS). PPS is a sulphated, semi synthetic polyanion with a heparin like structure that has been implicated in decreasing PrP^{Sc} deposition and neuropathy in animals (Doh-ura et al. 2004). Clinical studies using PPS have shown mild therapeutic potential. An initial study treating a single patient with PPS reported a survival period of 30 months after treatment (Todd et al. 2005). A following clinical study with four patients in the UK with iatrogenic CJD and inherited GSS suggested that PPS treatment enhanced the mean survival of the study group (Bone et al. 2008). This suggestion arose from the observation that patients with iatrogenic CJD had survival periods of up to 29 and 32 months after diagnosis, towards the maximum 39 month survival rate of CJD patients reported

in natural history surveys (Bone et al. 2008; Stewart et al. 2012). However, a more recent study of 11 patients treated with PPS since 2004 reported no significant effect on disease progression, and it may be concluded that PPS has little therapeutic potential in future treatment strategies (Tsuboi et al. 2009). Another pharmaceutical that has been utilised in clinical trials is quinacrine, first identified to have an anti-PrP^{Sc} activity in ScN_2A cell culture (Barret et al. 2003). Although quinacrine could inhibit PrP^{res} formation, it is unable to break or facilitate the destruction of prion aggregates (Barret et al. 2003). Ultimately this limits the capacity of quinacrine for therapeutic intervention, but clinical trials have been attempted. However, no individual trial has identified any therapeutic benefit of quinacrine treatment following clinical trials in over 100 patients between the UK and US (Collinge et al. 2009; Geschwind et al. 2013). In addition, it was recently reported that quinacrine can promote PrP^{Sc} propagation in deer, elk and moose to form an altered strain type, called Q-CWD (Bian et al. 2014). That quinacrine has reportedly different affects between species raises queries as to the current drug discovery methodology for prion diseases (Bian et al. 2014). The antibiotic tetracycline was initially observed to bind to PrP peptides, preventing the formation of amyloid fibrils, reverting the protease insensitivity of PrP^{Sc} aggregates and preventing cytotoxicity *in vitro* (Tagliavini et al. 2000). Further studies elucidated that tetracycline as well as doxycycline and minocycline can delay the onset of 263K scrapie in hamsters when treatment is administered from the date of infection as well as in advanced stages of infection (Forloni et al. 2002; De Luigi et al. 2008). Positive effects of doxycycline were demonstrated in a trial with 21 patients with suspected CJD who were treated with doxycycline from diagnosis to death, reporting a mean survival time of 13 months of treated patients relative to 6 months for untreated patients (Tagliavini 2008). A following double blind study investigated the efficacy of doxycycline in 121 patients with suspected or definite CJD (Haïk et al. 2014). Although there were no adverse effects from the treatment, there was no significant differences in survival between treated and placebo groups (Haïk et al. 2014). Doxycycline is again to be tested in a double blind clinical trial of 10 patients with FFI, with the efficacy of treatment to be determined over a course of 10 years (Forloni et al. 2015). Flupirtine maleate was first identified to protect neuronal cells from toxic beta-amyloid peptides (Müller et al. 1997). Following these observations, a double-blind study with flupirtine was attempted with 26 patients with sCJD and 2 with iatrogenic CJD (Otto et al. 2004). Treated patients demonstrated less deterioration in dementia tests, indicating beneficial effects on cognitive function, although there was no significant increase in survival time (Otto et al. 2004). Further clinical trials have yet to be attempted.

No clinical studies to date have reported the reversal of prion disease progression or associated symptomology. The development of pharmaceuticals has been limited by *in vivo* toxicity, a lack of *in vivo* activity and the difficulty of implementing clinical trials with limited patient numbers (Panegyres & Armari 2013; Ferreira et al. 2014). Large numbers of patients are required for drug testing, but the rare occurrence of CJD cases makes such large scale testing difficult (Panegyres & Amari 2013). Progress may also be limited by the potential development of prion drug resistance, as well as the rapidity of disease onset and progression (Berry et al. 2013). With the current diagnostic methods, a patient may not even be suspected of CJD until mid to late stages of disease. As the determination of survival rate is relative to the disease stage at the diagnosis of disease, this can make discerning the therapeutic efficacy of a compound difficult (Thompson et al. 2013).

Immunotherapeutic Approaches

Other therapeutic candidates for prion diseases are antibodies and their derivatives (Rovis & Legname 2014). Research into immunotherapeutics has focused predominantly on the use of anti-PrP antibodies, or to promote immune responses to prion infection. Anti-PrP antibodies have been successful in inhibiting prion replication *in vitro* and *in vivo*, yet they are limited by neurotoxicity, insolubility to the blood brain barrier and poor pharmokinetic profiles (Rovis & Legname 2014). An example of these efforts was the development of anti-PrP^{C} antibodies that could inhibit PrP^{Sc} propagation *in vitro*. One such study identified recombinant antibody fragments (Fabs) that reduced prion titres in ScN_2a cells by binding PrP^{C} (Peretz et al. 2001). It was reported that the antibody Fab D18 (recognises residues 132-156) cleared PrP^{Sc} formation with an IC50 of 9 nM (Peretz et al. 2001). Other examples include the antibodies 6H4, Sha31 and the SAF antibodies 15 to 37 which were reported to reduce cellular PrP^{Sc} by up to 70% *in vitro* (Enari et al. 2001; Féraudet et al. 2005). *In vivo* mice models also demonstrated that scrapie onset in mice was delayed following treatment with monoclonal antibodies (mAbs) (White et al. 2003). Though promising from *in vitro* experiments, the decrease in prion titre may be resultant from the dilution of PrP^{Sc} in cell culture after numerous cell divisions (Peretz et al. 2001). Furthermore, PrP^{C} crosslinking caused by antibodies has been discovered to cause neuronal apoptosis, and further difficulties with immunotherapy of other amyloidosis have further limited the potential for antibody-based therapeutics (Aguzzi et al. 2007). Immunotherapy methods are also limited by the inability of antibodies to cross

the blood brain barrier, limiting the use of anti-PrP^{Sc} antibodies as therapeutic ligands (Féraudet et al. 2005; Rigter et al. 2010; Rovis & Legname 2014). Although these factors act to rule out the majority of these antibodies for therapeutic intervention, many have become invaluable in prion research for the immunodetection of PrP^{Sc}.

An alternative to using antibodies as a direct therapeutic is the stimulation of an active immune response against prion infection. Indeed, immunisation of mice with rPrP has been observed to delay the onset of disease (Sigurdsson et al. 2002). Triggering an immune response against PrP^{Sc} is difficult however due the prion protein being seen as "self", and the immune system is unlikely to recognise the structural changes in PrP^{Sc} as a foreign antigen (Rovis & Legname 2014). A number of methods have been attempted to overcome this problem. One tactic is to use immunopotentiators to increase the response of the immune system to PrP^{Sc}. Indeed this has been used to identify unique antibody ligands for PrP^{Sc} by using the immunopotentiator Freund's adjuvant in mice inoculated with scrapie (Masujin et al. 2013). This is an effective method for identifying anti-PrP antibodies, but agents like Freund's adjuvant are toxic and this strategy does not facilitate PrP^{Sc} clearance from infected animals (Masujin et al. 2013). Another strategy is to present part of the PrP sequence on virus particles. Immunising mice with PrP-displaying murine leukemia virus (MLV) for instance has been reported to establish an anti-PrP^{Sc} immune response upon infection, although this did not completely overcome PrP tolerance (Nikles et al. 2005; Aguzzi et al. 2007). Alternative strategies include the use of recombinantly expressed antibodies, intrabodies, that bind targets intracellularly (Cardinale & Biocca 2008). This method has been reported to inhibit prion propagation *in vitro*, in one instance by retaining PrP^{C} in the endoplasmic reticulum of rat pheochromocytoma cells (PC12) (Cardinale & Biocca 2008). These developments make immunotherapeutic treatments an important and potentially rewarding pursuit. In recent years a therapeutic strategy has emerged to therapeutically target Aβ binding to PrP^{C} with antibodies. Following this rationale, the murine anti-PrP antibodies ICSM-18 and ICSM-32 were reported to prevent Aβ toxicity by preventing inhibition of long term potentiation (LTP) *in vivo* (Freir et al. 2011). An antibody PRN100, a human derivative of ICSM-18, has also been reported to prevent Aβ toxicity *in vivo* (Klyubin et al. 2014). PSN100 is currently awaiting testing in human clinical trials. Despite these advances the antibody treatments produced so far have only been able to prolong the onset of disease symptoms, and are still limited in their capacity to reverse symptomology (Rigter et al. 2010).

The Use of Peptides and Recombinant Proteins

Although the majority of effort into prion therapeutics has arguably been carried out on pharmaceuticals and immunotherapeutics, there is potential for the investigation into peptide and protein inhibitors of prion replication. This approach is made even more attractive through the role that protein self-interactions contribute to prion propagation, and that investigation into protein inhibitors may allow exploitation of this underlying mechanism (Rigter et al. 2010). In the late 1990s for instance it was demonstrated that synthetic peptides of the PrP protein inhibited prion propagation in *in vitro* cell free conversion assays (Chabry 1998). This study highlighted that peptides matching the sequence of PrP residues 109-141 could inhibit PrP^{Sc} replication in a dose dependent manner. This work was furthered by the same group in 1999, where peptides of the same sequences were studied in different *in vitro* cell free assays expressing mouse or hamster PrP^{C} (Chabry et al. 1999). These peptides were found to cross inhibit prion replication in each system, but did not inhibit replication in scrapie infected murine neuroblastoma cell cultures (Chabry et al. 1999). This was shortly followed by the development of β-sheet breakers, peptides with complementary sequences to the target prion protein which had been previously demonstrated to inhibit fibrillogenesis in rat models of Alzheimer's disease (Soto et al. 1998; Soto et al. 2000). These peptides also prevented PrP^{res} formation *in vitro* and *in vivo* (Soto et al. 2000). Although these findings demonstrated the potential of peptide inhibitors for therapeutic applications, they are limited by their sensitivity to proteolysis, their inability to cross the blood brain barrier and toxicity (Chabry et al. 1999; Féraudet et al. 2005). Potential methods of overcoming these limitations may include the use of virus constructs to transduce and express peptides *in vivo*, the use of cationic liposomes to carry the peptides through the blood brain barrier or direct cerebroventricular infusion similar to that used for PPS (Todd et al. 2005; Cardinale & Biocca 2008; Bone et al. 2008). Although no clinical therapeutics have been produced using synthetic peptides, it has since been reported that prion peptides can selectively recognise PrP^{Sc} over PrP^{C}, highlighting a potential use for such peptides in prion diagnostics (Lau et al. 2007).

Heterologous PrP^{C} has been demonstrated across a number of studies to have potential anti-prion properties (Michael Scott et al. 1993; Priola et al. 1994; Horiuchi et al. 2000; Geoghegan et al. 2009; Kobayashi et al. 2009; Kobayashi et al. 2015; Asante et al. 2015; Seelig et al. 2015). These studies identified that heterologous or mutant PrP can actively suppress prion propagation when used at

ratios that rival or exceed the stoichiometric concentration of PrP^{C} (Horiuchi et al. 2000). Indeed, recombinant and fragmented PrP can also act as potent inhibitors of PrP^{Sc} conversion *in vitro* (Meier et al. 2003; Masel et al. 2005; Campbell et al. 2013; Yuan et al. 2013; Altmeppen et al. 2015). This includes that recombinant PrP can inhibit prion propagation in PMCA (Yuan et al. 2013). Both human and hamster rPrP inhibited prion amplification in PMCA and replication within scrapie infected hamster cells in a dose dependent manner (Yuan et al. 2013). More recently recombinant hamster PrP^{C} was demonstrated to slow scrapie progression in transgenic mice in a dose dependent manner (Skinner et al. 2015). It is uncertain what the inhibitory mechanism of rPrPs is in prion amplification, but it has been previously demonstrated that homology between PrP^{Sc} and substrate PrP^{C} is required for interaction and propagation (Chabry et al. 1998; Caughey 2001). That the stoichiometry between host PrP^{C} and rPrP affects scrapie propagation *in vivo* raises the possibility that rPrPs inhibit prion replication through either competing for binding to either PrP^{Sc} or PrP^{C}, by destabilizing PrP^{Sc} aggregates or preventing the binding of cofactors (Yuan et al. 2013; Skinner et al. 2015). This may occur in a similar mechanism to that proposed for inhibition by anti-prion peptides, whereby peptides can prevent PrP^{Sc} conversion by either competing for binding sites to PrP^{C}, sequestering PrP^{C} to subcellular locations or stabilizing PrP^{C} (Gilch & Schatzl 2009). At present, although matters of *in vivo* transportation and diffusion may limit the application of peptide and protein inhibitors, they provide a potential for the development of therapeutics directly and indirectly by elucidating the underlying mechanisms of prion propagation.

1.3. The Development and Limitations of Prion Diagnostics

Exploiting the Physiochemical Properties of Prions

Efforts to produce diagnostic tests for prion diseases have predominantly focused on PrP^{Sc} as a disease biomarker, and PrP^{Sc} is the only validated marker of the disease state (Properzi & Pocchiari, 2013). However, as PrP^{C} and PrP^{Sc} share the same amino acid sequence it is difficult to produce ligands that specifically distinguish between these isoforms. Anti-PrP antibodies may be generated in animals, but then cannot differentiate between PrP^{C} and PrP^{Sc} experimentally (Gilch & Shatzl 2009). Immunoglobulin G (IgG) and scFv antibodies have been produced in efforts to distinguish between the isoforms, although their limited application is apparent as no validated or commercial tests have been developed with their use (Korth et al. 1997; Piccardo et al. 1998). Immunoglobulin M (IgM) antibodies have also been produced that reportedly bind to and immunoprecipitate

PrP^{Sc} amyloid fibrils, but this recognition is non-specific due to paratope-independent interactions (Morel et al. 2004). Alternatively, a number of IgM and IgG antibodies targeting a conserved tyrosine-tyrosine-arginine motif in PrP appeared to selectively precipitate PrP^{Sc}, but their specificity was questioned by their ability to immunoprecipitate partially misfolded and protease sensitive PrP^{C} (Caughey 2003). As a consequence, the specific detection of PrP^{Sc} involves the exploitation of physiochemical differences between the prion isotypes by proteinase digestion, facilitated by differential precipitation and/or *in vitro* replication to concentrate or amplify PrP^{Sc} before detection.

Digestion of infected tissue with proteinase K produces a truncated version of PrP^{Sc}, PrP^{res} (PrP^{27-30}) while completely digesting PrP^{C} (Saborio et al. 2001; Stanker et al. 2010). As PrP^{Sc} is resistant to PK digestion, the presence of PrP^{res} in samples has become a diagnostic hallmark of prion infection (Wang et al. 2015). The use of PK treatment significantly aided the diagnosis of BSE during the epidemic of the 1980s-1990s and served as the basis for diagnostic tests for prion diseases in the following years (Silva et al. 2015). However, a limiting characteristic of PK is the sensitivity of specific prion species to proteases, which may in turn affect the sensitivity of these tests (Benestad et al. 2008). This also facilitates the differentiation of TSE strains by protease sensitivity (Bruce 2003; Safar et al. 2005). Alternative proteolytic enzymes have been investigated, including trypsin or thermolysin which leave the N-terminus of PrP^{Sc} intact upon digestion (Owen et al. 2007; Yam et al. 2010). Advantages in leaving the N-terminus intact include the use of N-terminus recognizing monoclonal antibodies for PrP^{Sc} detection to aid discrimination between different prion strains, or for capture by immobilised metal affinity chromatography (IMAC) for concentration and purification (Owen et al. 2007). Indeed this technique can be used to characterise scrapie isolates and distinguish between scrapie and experimental ovine BSE (Owen et al. 2007). One of these studies went as far as to establish a novel sandwich Enzyme-Linked Immunosorbent Assay (ELISA) using trypsin digestion, although this technique has not reached widespread use (Yam et al. 2010). An alternative method involves the denaturation of PrP^{Sc} with guanidinium hydrochloride (GdnHCl) in combination with immunoassays. Progressive denaturation by GdnHCl reveals buried epitopes within PrP^{Sc} that are seen in both native and denatured versions of PrP^{C} allowing for discrimination between PrP^{Sc} infected and non-infected samples (Safar et al. 1998). Further development of this method by pre-treatment with PK increased the sensitivity of conformation-dependent immunoassay (CDI) 30 to 100-fold for

the detection of vCJD prions, and rivalled the sensitivity of mouse bioassays for the detection of sCJD, fCJD and iaCJD prions (Bellon et al. 2003; Safar et al. 2005).

Assay sensitivity can also be limited by the low concentration of PrP^{Sc} in preclinical or peripheral tissue samples, requiring enrichment or concentration of PrP^{Sc} to detectable levels (Nicoll & Collinge 2009). Selective precipitation with sodium phosphotungstic acid (NaPTA) can be utilised to selectively precipitate and concentrate PrP^{Sc} due to its insolubility in detergents (Kramer & Bartz 2009). NaPTA precipitation has become a widely used technique in prion research due to its simplicity and rapidity (Yuan et al. 2006). Selective precipitation can also be achieved through the use of steel beads, yet the use of precipitation can be limited by the amount of tissue sample available and the very low concentration of PrP^{Sc} in some tissues (Edgeworth et al. 2011). Alternatively, the relative concentration of PrP^{Sc} can be increased by amplification *in vitro.* Just as PMCA serves as an *in vitro* model of prion replication it also exponentially amplifies the concentration of PrP^{Sc} from samples (**Figure 1.5.**) (Saborio et al. 2001). Success of amplification is determined by PK digestion and detection of amplification products by western or dot blotting (Properzi & Pocchiari 2013; Saá & Cervenakova 2015). However, PMCA can be subject to spontaneous PrP^{Sc} formation during amplification, a complication that could result in false positive disease diagnosis (Saá & Cervenakova 2015).

By utilizing automated tube shaking in place of sonication, and recombinant PrP as substrate instead of brain homogenate, the method of Quaking Induced Conversion (QuIC) was produced (Atarashi et al. 2008). Similarly to PMCA, reaction products were initially analysed by western blotting which is time consuming and labour intensive. This method has since been further developed by replacing blotting with the use of thioflavin T (ThT) (Atarashi et al. 2011). ThT is a fluorescent dye sensitive to amyloid fibrils and enables the quantification of PrP^{Sc} amplification in real time (RT-QuIC) (Peden et al. 2012). In recent years, RT-QuIC has been adapted for the detection of multiple human and animal disease types in a variety of tissue types (Cramm et al. 2014; Orrú et al. 2015). Both PMCA and RT-QuIC are highly sensitive methods, able to detect infectious prions at low titres in varying tissues. This makes these methods promising candidates for the development of ante-mortem diagnostic tests.

PrP^{Sc} Detection by Immunoassay and Immunohistochemistry

Disease symptoms in human and animal prion diseases are not considered specific enough for definite diagnosis of clinical disease (Gough et al. 2015). Consequently, the gold standard for definitive disease diagnosis in humans and animals is post mortem immunoassay detection of PrP^{Sc} in brain tissue (Lee et al. 2013). Other conventional methods of diagnosis include mouse bioassays, although these methods are time consuming and expensive (Grassi et al. 2008). A range of rapid high throughput diagnostics have been developed to aid diagnosis of prion diseases in animals (Wang et al. 2015). A number of these developments have led to rapid commercial tests for the detection of PrP^{Sc} in post mortem brain biopsy tissue. Out of these tests, 9 have been approved by the European Commission (EC) for TSE surveillance in sheep, goats and cattle (**Table 1.1.**). Initially diagnosis of diseases relied on passive surveillance of clinical symptoms, but in 2001 the use of these tests was made mandatory in order to monitor TSEs in food producing animals (Meloni et al. 2012). With the identification of CWD cases in Europe, rapid screening methods will also be required for the surveillance and containment of CWD (Ricci et al. 2017). The first case of CWD in Norway was analysed by TeSeE ELISA and western blotting (Bio-Rad), demonstrating that commercial tests may be readily adapted for CWD surveillance (Benestad et al. 2016). Thousands of cervids in Norway are scheduled to be sampled for screening as part of the CWD surveillance program, and commercial screening tests will be heavily used (Ricci et al. 2017). Despite the development of rapid tests for ruminant prion diseases, there remains no commercial rapid immunoassay for human prion diseases as biochemical diagnosis is made by western blotting (Ugnon-Café et al. 2011).

Protease digestion, commonly by PK, is used to pre-treat tissue in most of these rapid immunoassay methods (**Table 1.1.**). Protease digestion is used to degrade PrP^{C} that may compete for antibody binding. However, prion strains can vary in their resistance to proteases (Tzaban et al. 2002; Safar et al. 2005a; Thackray et al. 2007; Gambetti et al. 2008). For example, atypical scrapie/Nor98 is less resistant to PK than classical scrapie, a characteristic which initially resulted in contrasting results between commercial immunoassays (Benestad et al. 2008). Because of this, several commercial immunoassays previously approved by the EC for the detection of classical scrapie were identified to be not sensitive for the routine detection of atypical scrapie (Webster et al. 2009).

Table 1.1. EC approved commercial PrP^{Sc} rapid tests for BSE and scrapie surveillance.

Test Name	Producer	Method	Disease	Reference
Prionics-Check Western test	Prionics AG	Western blot	BSE	McKinley et al. 1983
Prionics-Check LIA test	Prionics AG	ELISA	BSE	Barry et al. 1986
Prionics Check PrioSTRIP	Prionics AG	Immuno chromatographic	BSE Scrapie	Prionics AG 2001
Bio-Rad TeSeE SAP rapid test	Bio-Rad	ELISA	BSE Scrapie	Barry et al. 1986
Bio-Rad TeSeE Sheep/Goad rapid test	Bio-Rad	ELISA	Scrapie	Barry et al. 1986
Enfer TSE Version 3	Abbott Labs	ELISA	BSE	Barry et al. 1986
IDEXX HerdChek BSE Antigen Test Kit	IDEXX Laboratories	ELISA	BSE	Barry et al. 1986
IDEXX HerdChek BSE-Scrapie Antigen Test Kit	IDEXX Laboratories	ELISA	BSE scrapie	Barry et al. 1986
AJ Roboscreen Beta Prion BSE EIA Test	AJ Roboscreen	ELISA	BSE	Barry et al. 1986

The detection of atypical scrapie in sheep was also reported to be dependent on the tissue used for immunoassay. In surveillance, these rapid tests commonly rely on the use of brainstem tissue, but this source proved unreliable for the detection of atypical scrapie PrP^{Sc} (Benestad et al. 2003; Benestad et al. 2008; Kittelberger et al. 2010; Beringue & Andreoletti 2014). In cases of Swiss goat atypical scrapie, brainstem tissue was negative for PrP^{Sc} but positive in the midbrain and thalamus (Seuberlich et al. 2007). These studies imply that surveillance statistics for

atypical scrapie could have been underrepresented due to the predominant use of brainstem tissue and PK treatment in immunohistochemistry and immunoassays (Seuberlich et al. 2007; Benestad et al. 2008). Furthermore, these studies highlighted that the source of tissue for detection as well as the common use of PK treatment could affect TSE surveillance for other diseases. Because of this, the recommended rapid immunoassays for scrapie surveillance were reviewed to include only those that could detect atypical and classical scrapie (Webster et al. 2009).

Although the sensitivity of prion strains to protease digestion can affect the sensitivity of immunoassays, it can also be exploited for the differential identification of strains. For example, BSE and scrapie can be differentiated by PK sensitivity in an immunoassay format (Simon et al. 2008). Western blotting can distinguish between prion strains based on the size of PK-resistant PrP^{Sc} fragment sizes or glycosylation ratios (Nicoll & Collinge 2009). Immunoassays have also been developed that enable prion strain identification. One such method is CDI (Safar et al. 1998; Safar et al. 2002). In CDI PrP^{Sc} is incubated in a singular or increasing concentration of GdnHCl. Epitope availability in a subsequent ELISA is measured for both treated and untreated samples. A main strength of this method is the correction of background signals by measuring antibody binding to exposed epitopes on PrP^{C} (within the untreated sample) which can be subtracted from the increasing availability of the epitope upon PrP^{Sc} denaturation (within the denatured sample; Bellon 2003). With the addition of PK treatment CDI can discriminate PrP^{Sc} from PrP^{C} with greater sensitivity than immunohistochemistry (IHC) in the brains of CJD patients (Safar et al. 2005). Because CDI measures the stability of PrP^{Sc} conformers in a given population, this method allows for discrimination between prion strains with different stabilities (Safar et al. 1998). Further to this, CDI does not necessitate the use of PK digestion, allowing a full characterization of prion strains, particularly where they produce a relatively high proportion of PK-sensitive PrP^{Sc} (Safar et al. 2005; Kramer & Bartz 2009). Despite the promise of CDI, further diagnostic applications have yet to be investigated. Another method is the Conformation Stability Assay (CSA) that measures proteinase sensitivity upon PrP^{Sc} denaturation (Safar et al. 1998; Peretz et al. 2001). This method uses a gradient of denaturing conditions with GdnHCl followed by PK digestion to measure the increase in protease sensitivity of a sample. Using the half maximal concentration of GdnHCl as a value of stability ($GdnHCl_{½}$) this method is able to reproducibly distinguish between scrapie strains (Peretz et al. 2001). The CSA was later developed to assess the detergent solubility of PrP^{Sc} during denaturation

with GdnHCl, called the conformational solubility and stability assay (CSSA) (Pirisinu et al. 2010). This method enabled the characterization of classical and atypical scrapie, BSE, as well as MM1 and MM2 sCJD (Pirisinu et al. 2010; Pirisinu et al. 2011). CSSA has also been demonstrated to successfully discriminate between bank vole strains of scrapie and CJD (Pirisinu et al. 2011; Pirisinu et al. 2013). These methods demonstrate the effective use of protease resistance and epitope availability in denaturing conditions to characterize prion strains.

Other immunoassays have been developed to enhance the sensitivity of rapid screening tests. The dissociation-enhanced lanthanide fluorescence immunoassay (DELFIA) measures the solubilisation of PrP^{Sc} in increasing concentrations of GdnHCl (Barnard et al. 2000). Soluble PrP^{C} is removed in lower concentrations of GdnHCl, with PrP^{Sc} only being solubilised in higher concentrations of denaturant. The calculation of percent PrP^{Sc} in the homogenate can then be determined by immunoassay (Barnard et al. 2000; Barnard et al. 2007). This method has been used to detect a range of diseases in various tissue types, including CJD in brain, spleen and blood, BSE in brain and scrapie in brain with a sensitivity of up to 10 pg of PrP (Barnard et al. 2000; Dabaghian et al. 2006; Barnard et al. 2007; Lukan et al. 2013). Fluorescent amplification catalyzed by T7 polymerase technique (FACTT) is a method similar to that of ELISA but instead, quantifies RNA synthesis by T7 RNA Polymerase from a secondary antibody conjugated to a DNA template (Zhang et al. 2006; Chang et al. 2007; Freudenberg et al. 2008). With inclusion of a prion amplification step by QuIC before detection of PrP^{Sc}, this assay was reported to detect prion aggregates from the blood of late stage infected mice with 100% sensitivity and specificity (Chang et al 2007). Despite promising reports, the lack in any further development or application of the assay brings its original efficacy into question. FACTT itself is an adaptation of immuno-PCR (IPCR), which has widely been reported as a sensitive diagnostic assay (Niemeyer et al. 2007). In this method, the secondary antibody used is similarly conjugated to a DNA template. However, in IPCR the template is eluted by digestion with a restriction enzyme and then PCR amplified to be detected and quantified by gel electrophoresis or within a Real Time PCR system (RT IPCR) (Niemeyer et al. 2007). This method has been applied to the detection of scrapie prions from brain homogenate (Barletta et al. 2005). It has since been tailored to increase the sensitivity of RT IPCR for scrapie over the BioRad TeSeE method by 1000-fold, but remains to be developed into a practical assay for routine testing (Reuter et al. 2009). Although these tests have enabled faster and more sensitive detection of prion diseases, their routine use in diagnosis is still limited by their requirement

for post-mortem tissue. As neuropathy occurs towards later stages of disease, these diagnostics are also limited in their capacity to work in tandem with therapeutic treatments (Rigter et al. 2010). The development of sensitive ante-mortem tests that can identify PrP^{Sc} in early stages of disease are therefore still a key area of interest, in particular as there remains no routine immunoassay for the detection of human prion diseases pre-mortem.

The Development of Ante-Mortem Diagnostic Tests

The current lack of effective ante-mortem tests for prion diseases is in part due to clinical signs only being present very late in disease development, and the lack of any immune responses in the host (Zou & Gambetti 2005). Brain biopsied tissue obtained post mortem is predominantly used in the diagnosis and surveillance of human and animal prion diseases. Yet in many prion diseases PrP^{Sc} accumulation in the CNS occurs later in the disease state after spreading through the LRS and enteric nervous system (Gough & Maddison 2010). Therefore, sources other than brain tissue must be considered for use in early ante-mortem diagnostic tests. However, tissue involvement in prion dissemination can be affected by the host and prion strain type. In scrapie and CWD there is detectable PrP^{Sc} involvement in the LRS (Garza et al. 2014). On the other hand, PrP^{Sc} in BSE is largely infectious in the CNS, with little involvement in the LRS (Gough et al. 2010). Because of this difference in PrP^{Sc} dissemination between diseases, different tissue sources may be exploited for ante-mortem diagnosis. For example, because of the involvement of scrapie PrP^{Sc} in the LRS, sheep tonsil, rectal mucosa and third eyelid lymphoid tissue can be used in ante-mortem IHC tests for scrapie, while PMCA has been demonstrated to detect PrP^{Sc} in milk, buccal swabs, urine and faeces (O'Rourke et al. 2000; Wells et al. 2000; Maddison et al. 2007; Gonzalez-Romero, et al. 2008; Maddison et al. 2009; Maddison et al. 2010; Terry et al. 2011; Gough et al. 2012; Moda et al. 2014). However, the presence of PrP^{Sc} in lymph tissue can be dependent on host genotype, with less involvement in ARR/ARR sheep than VRQ/VRQ sheep (van Keulen et al. 2002). In humans ante-mortem, though not definite, diagnosis of CJD is made through the assessment of clinical symptoms, magnetic resonance imaging (MRI), electroencephalography as well as the detection of surrogate markers such as 14-3-3 protein in CSF (Zerr et al. 2009; Puoti et al. 2012). These diagnostics are not completely reliable and the presence of 14-3-3 protein is inconsistent between patients (Allroggen et al. 2000). Alternatively, tonsil or appendix tissue are used for IHC tests, with diagnostics being developed for use with blood and cerebrospinal fluid (CSF) (Hill et al. 1999; Joiner et al. 2002; Atarashi et al. 2011; Gill et al. 2013; Orrú et al. 2015). Tests

using these sources are becoming increasingly essential due to concerns over iatrogenic transmission of CJD in humans (Gill et al. 2013; Hall et al. 2014). Because of this a blood based detection system would be preferable to allow screening of blood and plasma stocks (Lacroux et al. 2014). However, the main challenge in developing methods to screen blood and other sources are the very high sensitivity and specificity required to detect the low concentration of infectious prions or PrP^{Sc} in low occurrence rates in these sources (Edgeworth et al. 2011).

It is because of these low concentrations of PrP^{Sc} that samples require additional enrichment/amplification steps by PMCA, QuIC, precipitation or matrix capture (Yuan et al. 2006; Terry et al. 2011; Edgeworth et al. 2011; Properzi & Pocchiari 2013). As an example, PrP^{Sc} detection in blood has been demonstrated through matrix-capture on stainless steel beads coupled with an ELISA immunoassay (Edgeworth et al. 2011). This study reported the detection of 10% (w/v) vCJD brain homogenate diluted in whole blood to a maximum dilution of 10^{-10}, with 71.4% sensitivity and 100% specificity (Edgeworth et al. 2011). More recently this method was used to screen 5000 samples from the American Red Cross with a specificity of 100%, confirmed in a healthy UK group (Jackson et al. 2014). The method was also tested against 10 vCJD cases with a sensitivity of 70% and a 95% confidence interval of 47.8%-88.7% (Jackson et al. 2014). This method certainly has a strong potential for use in vCJD diagnosis, with a potential application in screening blood and plasma stores.

Rather than concentrate PrP^{Sc} in a given sample, PMCA is utilised to amplify PrP^{Sc} for detection by immunoassay. To date PMCA has been experimentally proven to enable the detection of PrP^{Sc} from sheep milk, faeces, saliva and human urine (Gough et al. 2009; Terry et al. 2011; Gough et al. 2012; Moda et al. 2014). Progress was defined with the detection of PrP^{Sc} in blood leukocyte fractions of scrapie infected sheep and mice, demonstrating a clear potential for PMCA to act in tandem with diagnostics (Thorne & Terry 2008; Tattum et al. 2010). Interestingly this method utilised the polyanion polyadenylic acid to stimulate amplification (Thorne & Terry 2008; Tattum et al. 2010). Since then this PMCA method has been used to successfully diagnose experimentally infected sheep in field studies, but with use on brain rather than blood samples (Thorne et al. 2012). Another study amplified vCJD and BSE using serial PMCA to detect preclinical concentrations of PrP^{Sc} from sheep and primate blood (Lacroux et al. 2014). This has also been achieved in human urine with a sensitivity of 92.9% and specificity

of 100% (Moda et al. 2014). Recently, using a combination of PrP^{Sc} capture by plasminogen beads and amplification by PMCA, all 18 clinical vCJD patients were identified from the sera of 256 patients with a sensitivity of 100% and specificity of 99.2% (Bougard et al. 2016). The 99.2% specificity was due to two patients who went on to develop clinical vCJD between 1-3 years later, demonstrating the potential of PMCA to act as a presymptomatic diagnostic test (Bougard et al. 2016). In a separate study PMCA was used for the detection vCJD in the blood of 14 clinical patients with 100% sensitivity and specificity (Concha-Marambio et al. 2016). Yet PMCA comes with its own limitations, including the possibility of false positive results through spontaneous prion generation or cross contamination (Saá & Cervenakova 2015). In spite of these concerns PrP^{Sc} detection in human tissues by PMCA has only been recorded in infected individuals and not in negative controls, leading to a specificity of 100% (Castilla et al. 2005; Castilla et al. 2008; Thorne & Terry 2008; Lacroux et al. 2014; Moda et al. 2014; Saá & Cervenakova 2014; Bougard et al. 2016). However, PMCA requires up to 5 or more days to amplify PrP^{Sc} for sufficient detection, hindering its capacity for rapid diagnosis. A microplate based PMCA method was reported to amplify scrapie as well as vCJD prions over a single 48h round, although this relied on the use of mouse brain lysate as substrate and has yet to be developed for use in non-brain tissue (Moudjou et al. 2014). As a consequence, a diagnostic test which can be performed faster and safer would be more broadly applicable for prion disease diagnosis.

RT-QuIC has been demonstrated to amplify PrP^{Sc} from multiple disease types of both humans and animals. In humans, RT-QuIC has been demonstrated to detect sCJD (including strains Type 1 and 2), iaCJD, vCJD, genetic CJD (gCJD) and FFI (Atarashi et al. 2011; McGuire et al. 2012; Cramm et al. 2014; Christina D. Orrú et al. 2015; Schmitz et al. 2016). Animal diseases detected by RT-QuIC include CWD (from Elk and Deer), hamster 263K, sheep and goat classical scrapie, atypical scrapie, mouse strains (chandler, ME7, 87V and 22L), transmissible mink encephalopathy (TME, Drowsy and Hyper strains), classical BSE (C-BSE), and atypical H-type and L-type BSE (Wilham et al. 2010; Atarashi et al. 2011; Peden et al. 2012; Orrú et al. 2015; Masujin et al. 2016; Dassanayake et al. 2016; Hwang et al. 2017). Several of these studies used RT-QuIC to discriminate between sCJD and non-CJD patients from CSF samples with 98-100% specificity (Atarashi et al. 2011; Peden et al. 2012). However, at the time this method required up to five days to perform with a chance of up to 23% of false negative results (Orrú et al. 2015). More recently the methodology has been improved with an increased temperature, the use of SDS within the amplification buffer and recombinant

hamster PrP substrate, achieving diagnosis within 14 hours and with a sensitivity of 95.8% and specificity of 100% (Orrú et al. 2015; Orrú et al. 2016). Indeed, this method is over 10^4-fold more sensitive for C-BSE or L-type BSE than the IDEXX HerdCheck BSE-scrapie short assay (Orrú et al. 2015). RT-QuIC has also been applied to human and deer nasal brushings for the detection of sCJD and CWD, although with a lower sensitivity of 70% for human and 69.8% for deer (Orrú et al. 2014; Haley et al. 2016). Although this allows for a highly practical and efficient method of prion diagnosis RT-QuIC has not been applied for use in blood. Attempts have been made towards this end however. RT-QuIC has been coupled with immunoprecipitation (termed eQuIC) to detect 10% (w/v) vCJD brain homogenate in a -10^4 dilution in spiked sera (Orrú et al. 2011). eQuIC may then be effective for screening human sera, although its sensitivity is currently six orders of magnitude lower than matrix-capture (Edgeworth et al. 2011). Until recently it remained to be established how reproducible the sensitivity and specificity of RT-QuIC is between laboratories, an essential step towards its development as an ante-mortem diagnostic test. One study screened 54 CSF samples from sCJD patients and 37 non-prion disease control samples across two laboratories, as well as 1 sCJD CSF sample and 5 non-prion disease controls across four laboratories in a two-ring trial (Cramm et al. 2015). In parallel to this 110 CSF samples positive for sCJD, gCJD and FFI were screened with 400 non-prion disease CSF samples. Overall, the study reported a sensitivity of 85% and specificity of 99% (Cramm et al. 2015). Another two-ring trial testing 25 CSF samples between 11 laboratories achieved a combined sensitivity of 85.6%-100% and a combined specificity of 100% (McGuire et al. 2016). These studies highlight a clear potential for the use of RT-QuIC as a sensitive pre-clinical diagnostic test. Recently RT-QuIC was adapted for the detection of α-synuclein in CSF (Fairfoul et al. 2016). This test was reported to detect disease associated α-synuclein in patients with PD or dementia with lewy bodies (DLB) with sensitivities of 92% and 95%, respectively, and specificity of 100% (Fairfoul et al. 2016). This development demonstrates the potential of RT-QuIC to act as a powerful and sensitive ante-mortem diagnostic test for multiple protein misfolding disorders. The remaining absence of validated ante-mortem tests for PrP^{Sc} however suggests that the methods described here require improvement or further validation (Wilham et al. 2010; Nicoll & Collinge 2009; Properzi & Pocchiari 2013).

It has been proposed that the use of rPrPs as substrate in QuIC could limit the determination of strain-dependent characteristics, as rPrPs lack secondary modifications. However, in recent years the identification of different strains by

RT-QuIC has been made possible for a number of human and animal prion strains. The use of bank vole rPrP RT-QuIC allowed the identification of up to 28 different prion strains and disease types, of which 5 had not been successfully amplified previously (Orrú et al. 2015). This development removed the need for strain-specific amplification conditions, making RT-QuIC potentially a broad platform diagnostic test for multiple prion diseases (Orrú et al. 2015). However, differentiation between strains can be lost at lower concentrations of PrP^{Sc} seed (Masujin et al. 2016). PMCA is also effective for amplifying different strains including L-BSE and H-BSE, and maintains strain properties and infectivity, although each strain requires specific amplification conditions (Murayama et al. 2016; O'Connor et al. 2017). This gives RT-QuIC the advantage that a single set of conditions can be used to identify multiple disease and strain types. However, RT-QuIC is limited in its capacity to generate infectious prions (Saá & Cervenakova 2015). RT-QuIC was demonstrated to maintain strain like secondary structure properties of Chandler and 22L strains, but these properties and infectivity were lost after the initial round of amplification (Sano et al. 2015). As PMCA is the only technology that can successfully amplify infectious prions *in vitro* it may remain a preferential method of investigating prion biology, while RT-QuIC can possibly be utilized more easily as an ante-mortem diagnostic test (Saá & Cervenakova 2014). The reported consistency of sensitivity and specificity of RT-QuIC for the identification of CJD between laboratories, combined with potential application for the identification of other protein misfolding diseases supports the application of RT-QuIC to aid clinical diagnosis (Cramm et al. 2015; McGuire et al. 2016; Fairfoul et al. 2016).

1.4. Autoantibody Detection as a Means of Disease Diagnosis: An Application for Next Generation Phage Display

Autoantibodies are Candidate Serological Biomarkers for Neurodegenerative Diseases

Many of the diagnostics discussed so far involve the direct detection of PrP^{Sc}, with or without methods of enrichment or amplification. An alternative diagnostic approach is the use of biomarkers other than PrP^{Sc} for prion disease diagnosis. One such approach could involve the autoantibody response to prion diseases. Autoantibodies are produced by autoreactive B cells that recognize self-antigens, such as cellular proteins and nucleic acids, which can be released in disease (Tan 2001). Autoantibodies offer an attractive target for diagnostics due to their high antigen specificity, availability and half-life in sera (Ydens et al. 2017). As such

they have been a strategic target in the development of diagnostics for diseases including cancer and rheumatoid arthritis (Cho-Chung 2006). Autoantibody responses to prion diseases have also been reported. For example, Anti-PrP autoantibodies can be generated against recombinant PrP which display anti-PrP^{Sc} activity in ScN2a cell culture models (Gilch et al. 2003). Additionally, anti-PrP autoantibodies can be detected in human CSF by peptide-based ELISA, and can inhibit prion fibril formation *in vitro* as well as PrP peptide mediated toxicity (Wei et al. 2012; Roettger et al. 2013). Autoantibodies have been identified which are immunoreactive to potential disease biomarkers. Examples include axonial neurofilaments, NMDR receptor and glial fibrillary acidic Protein (GFAP) (Sotelo et al. 1980; Tiwana et al. 1999; Nomura et al. 2009; Mackay et al. 2012). However, no diagnostic assay has been produced using autoantibody biomarkers for prion diseases.

Autoantibodies have been identified against proteins involved in other neurodegenerative diseases, including Aβ, tau and α-synuclein (Nath et al. 2003; Bartos et al. 2012; Heinzel et al. 2014). Importantly, the presence of autoantibodies in these diseases have been exploited for the development of diagnostics. Autoantibodies identified in the sera of patients with AD have been used in the development of diagnostic ELISAs, although the propensity of these autoantibodies to form complexes with Aβ in sera has led to conflicting results (Maftei et al. 2012). In spite of this, autoantibodies present in the sera of patients with AD, PD and Multiple Sclerosis (MS) can be used to discriminate between healthy and diseased sera by human protein microarray (Nagele et al. 2011; Han et al. 2012; Ayoglu et al. 2013). Autoantibodies in the sera of patients with AD and PD were used to differentiate between a control disease (breast cancer) and AD/PD sera, indicating that these autoantibodies were disease specific (Nagele et al. 2011; Han et al. 2012). Recently the same technology was applied to the sera of 236 patients with AD and mild cognitive impairment (MCI) (DeMarshall et al. 2016). Compared to a control group the sensitivity and specificity of disease diagnosis was 100%, demonstrating that autoantibodies can be selectively targeted and exploited for diagnosis of AD (DeMarshall et al. 2016). This approach remains to be validated for other neurological diseases, yet these studies indicate that there may be diagnostic biomarkers in pre-clinical CSF or sera specific to prion infection that could be exploited for prion disease diagnosis.

Next Generation Phage Display as a High Throughput Method for Diagnostic Ligand Identification

Identifying autoantibodies from sera as a means of disease diagnosis is a difficult task. Different methods may be employed, including protein microarray which has already been utilized to identify autoantibodies in AD, PD as well as other diseases, such as breast cancer (Nagele et al. 2011; Anderson et al. 2011; Han et al. 2012; Ayoglu et al. 2013; DeMarshall et al. 2016). High throughput approaches like microarrays allow for a large-scale screening of potential ligands from a population like a peptide library. They may also be used to map interactomes of a protein, which has been performed with PrP^C using protein microarrays previously (Satoh et al. 2009). Protein microarray offers a powerful high throughput screening method for autoantibody detection. Yet the efficacy of protein microarrays can be limited by a number of factors, including the quality of genetic information available for the organism being screened, the use of single splice variants as constructs for protein arrays and disease heterogeneity (e.g. in cancer) (Phizicky et al. 2003; Jaluria et al. 2007; Chen & Snyder 2010; Ng et al. 2015). Protein arrays can also be limited by protein functionality. For instance, the printing of proteins onto microarrays can decrease the efficacy of biomarker capture due to denaturation or the burial of epitopes (Ramachandran et al. 2008). Epitope burial is particularly a risk with arrays using linear epitopes, such as peptide arrays (Ramachandran et al. 2008). The most used method for producing proteins for microarray is through recombinant expression in *E. coli*. The lack of secondary modifications in these proteins, as well as incorrect folding, may also affect protein activity and epitope binding (Zhu & Snyder 2003). Therefore, even quality microarrays may be limited in their capacity for identifying disease related antigens. An alternative for the high throughput screening of disease biomarkers is provided by phage display.

In phage display a library of random peptide, cDNA or antibody sequences are displayed on the surface of bacteriophage typically fused to the phage coat proteins PIII or PVIII, the bacteriophage themselves containing phagemids that encode the sequence of the displayed ligand (Pande et al. 2010). This way phage display couples a phenotypic library of ligands to their respective genotypes in a population of bacteriophage (Chan et al. 2014). Phage display libraries are usually highly diverse (10^7-10^{11} ligand sequences for example) resulting in the individual frequency of ligands being extremely low (Ravn et al. 2013). From this originating library, the aim of a panning experiment is to isolate specific ligands displayed on the phage that recognise a target of interest. As the frequency of individual ligands

in the library are initially so low, specific binders are commonly enriched and identified through a process called biopanning, where the bacteriophage library is exposed to target fixed to a matrix, followed by washing to remove nonspecific ligands (**Figure 1.7.**). The bacteriophages encoding the specific binders are then eluted and used to infect bacterial culture for further growth to produce a sub library of ligands (**Figure 1.7.**). Further rounds of panning and infection can then concentrate these specific binders, usually over 3-5 panning rounds (**Figure 1.7.**). Specific binders are then identified traditionally by screening on microtiter plates by ELISA or western blotting, but these methods are particularly labour intensive and have a limited access to the repertoire of ligands within the enriched phage display sub library (Díez et al. 2015). Ligand identification can also be achieved by deep sequencing of the resultant sub libraries, allowing a more in depth analysis (Dias-neto et al. 2009; Matochko et al. 2012; D'Angelo et al. 2014). Phage display is a powerful method for identifying ligands with therapeutic or diagnostic applications (Pande et al. 2010). As an example, phage display has been successful in identifying now commercially utilised medicines such as adalimumab, a mAb targeting tumour growth factor-α (TGF-α), for treatment of rheumatic arthritis and Crohn's disease (Chan et al. 2014). Phage display has also been successfully utilised to produce PrP-binding mAbs or single chain antibodies (scFvs) to probe the conformational structure of PrP^{Sc} or to identify diagnostic and therapeutic ligands for prion diseases (Williamson et al. 1996; Adamson et al. 2007; Flego et al. 2007; Zuber et al. 2008; Wuertzer et al. 2008). Peptide phage display has been successfully applied to detect autoantibodies for disease diagnosis including cancer, rheumatoid arthritis, traumatic brain injury and MS (Cortese 1996; Govarts et al. 2007; Ran et al. 2008; Tong et al. 2008; Somers et al. 2011; Yao et al. 2012; Ghoshal et al. 2016). Phage display thereby presents a method of ligand discovery that could potentially be used to identify sera based autoantibodies specific to prion diseases. However, there are several concerns that affect peptide identification and validation by phage display, including the loss of important binders and enrichment of non-specific peptides. These issues arises from i) the presence of non-target specific peptides which are nonetheless enriched by the biopanning process due to binding to solid supports, blockers or, in the case of panning against antibodies, to non-paratope regions of the antibodies, ii) the selective advantage of some peptides during library amplification due to low toxicity to their bacterial host during propagation or less energy demands during transcription and translation and iii) inefficiency of the washing procedure (**Figure 1.7.**). The first two scenarios result in the enrichment of what are known as "parasitic peptides" (Derda et al. 2011; Matochko et al.

2012; Matochko et al. 2014). Another limitation is that the ligands selected for may not necessarily be the most desirable. For example, if the target was in an impure environment such as a cell surface, phage display would most likely select for ligands of more common receptors or moieties like glycosyl groups than the target of interest (Zhang et al. 2011; Derda et al. 2011). Therefore, there would be no guarantee that the ligands being selected are specific for the target of interest (Derda et al. 2011; D'Angelo et al. 2014).

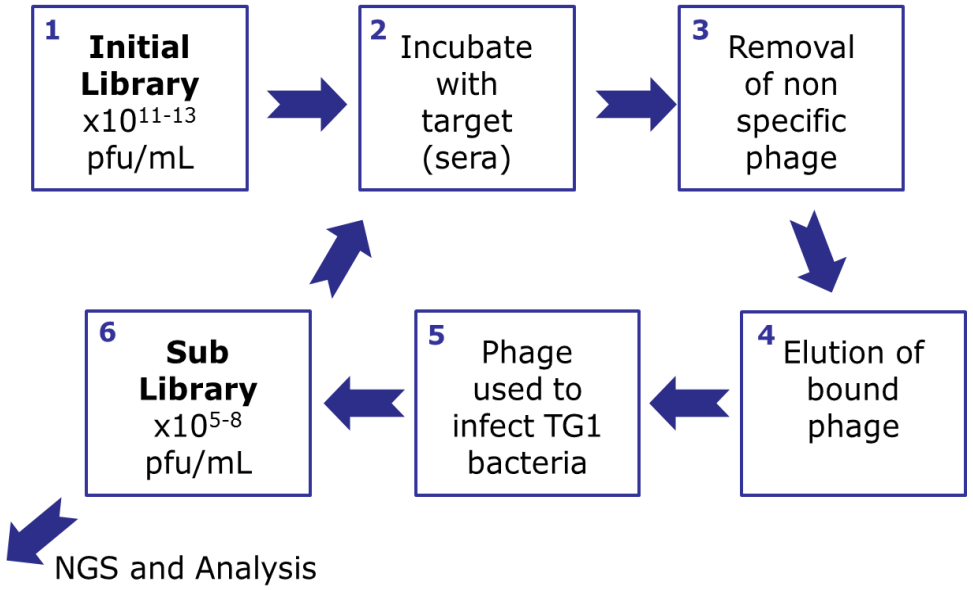

Figure 1.7. The method of biopanning in phage display. 1) The random library of ligands is amplified by growth in TG1 *E. coli* to generate a library with 100s-1000s of copies of each individual peptide. 2) This library is incubated with the target of interest, immobilised on an appropriate solid support. 3) Once binding has occurred non-binders are removed by washing. 4) Bound phage are then eluted by pH-shift or competitive elution. 5) The eluted phage are used to infect bacterial cell culture. 6) The infected bacteria are then either grown to amplify the sub library of phage for further rounds of biopanning or they are analysed by sequencing, ELISA, western blotting or microarray.

This limitation may be overcome by subtractive screening, where biopanning may be performed in environments with and without the target to identify desirable ligands that are only selected to the target (Gnanasekar et al. 2004). Examples of this could include a subtractive screen against sera from patients either without disease or with an unrelated disease. This method is commonly used and strongly recommended to reduce the enrichment of nonspecific ligands (Molek et al. 2011; Liu et al. 2015). There are also a number of databases such as MOTIF or MimoDB,

which detail ligands and peptides identified from multiple studies (Huang et al. 2011). More recently the MimoDB database was updated to the biopanning data bank (BDB) with 2904 sets of biopanning data from 1322 papers (He et al. 2016). Using these databases researchers can remove commonly found nonspecific peptides and antibodies during analysis. For example, sequences such as SVSVGMKPSPRP and HAIYPRH have been proved to be nonspecific peptides and can be removed during analysis (Kolb & Boiziau 2005; Brammer et al. 2008). As more nonspecific sequences are identified and incorporated into databases the task of selecting specific ligands will become more efficacious.

Enhancing the depth of library analysis can also aid the identification and removal of non-specific ligands by making more of the sub libraries available for analysis. In recent years this has been done by the analysis of phage display libraries with next generation sequencing (NGS), a method recognised as next generation phage display (NGPD) (Dias-neto et al. 2009; Zhang et al. 2011; Ravn et al. 2013; Matochko et al. 2014; Brinton 2016; Naqid et al. 2016). This method uses the NGS data to quantify the frequency of clones in a given sub library (D'Angelo et al. 2014). By doing so it is possible to screen thousands to millions of sequences to assess sub library diversity, whereas Sanger sequencing or ELISAs can screen only hundreds of clones (Ravn et al. 2013). NGPD has already been utilised to demonstrate the enrichment of non-specific peptides during biopanning. By using specific primers to probe a phage library through rounds of biopanning, it was revealed that parasitic peptides can constitute up to 20% of a 10^6 PFU/mL sub library (Matochko et al. 2012). This evidenced that parasitic peptides are indeed enriched in phage display, and can result in the loss of rare peptide binders which are outcompeted (Matochko et al. 2012). It was also reported that the diversity of binders against a given target is reduced considerably though multiple rounds of panning (Matochko et al. 2012). However, with a much higher capacity for the screening of specific ligands, NGPD can be carried out to screen sub libraries at earlier biopanning stages prior to this loss of diversity. Indeed even one round of panning has been reported as sufficient for ligand discovery (Zhang et al. 2011; 'T Hoen et al. 2012). Importantly this allows for the identification of rare binders which would otherwise be lost in later biopanning rounds. This is especially relevant to the characterization of complex heterogeneous interactions of phage ligands with complex targets, for example when libraries of phage-peptides are bound by polyclonal antibodies (Ravn et al. 2013). The screening of earlier rounds of panning will facilitate the identification of more comprehensive sets of peptides that interact with polyclonal antibodies. The application of NGPD to mapping

polyclonal antibodies may hold potential for identifying specific autoimmune epitopes that mark pre-symptomatic stages of prion diseases, where there is a characteristically low to minimal immune response. As an example, the "antibodyome" in HIV-1 infected, healthy and vaccinated patients has been characterised in response to treatment with the therapeutic antibody VRC01 (Wu et al. 2012). Although not specifically a NGPD method, this study highlights that even in a disease which classically evades immune responses NGS can be used to characterise the epitopes present in infected individuals (Wu et al. 2012). Since NGPD has been demonstrated to be able to enrich and identify antibody binders against defined antigens, this technique has a potential to screen the changes in the antibodyome in response to infection (Ravn et al. 2013). This is especially poignant as in prion diseases there is little immune response to infection, yet there may be changes within the antibodies presented in serum that may be identified by NGPD to be markers of a pre-clinical disease state. NGPD can also be applied to detect serum antibodies for disease diagnostics. As an example, NGPD has been successfully applied to identify immunoreactive peptides that are recognised by antibodies produced by pigs and chickens in response to infection by *Salmonella enterica* serovar Typhimurium (Naqid et al. 2016). These peptides could then be utilised in diagnostic ELISAs to discriminate against infected versus control animals (Naqid et al. 2016). The epitopes of IgGs in the sera of HIV patients have also been mapped using peptide NGPD (Ryvkin et al. 2012). Although a relatively new technique, these studies demonstrate the potential of NGPD for the screening of sera for disease specific antibodies. In addition, this method outputs diagnostic ligands that can then be used to establish rapid and cost-effective diagnostics. Phage display has already been reported to identify sera based autoantibodies specific to different diseases. With the increased depth of analysis provided by NGS allowing the more effective recognition of candidate target-specific peptides, NGPD could be effectively applied to the detection of autoantibodies in the sera of patients with neurodegenerative diseases.

1.5. Aims of the Study

1. Investigation into recombinant PrP as an inhibitor of prion amplification *in vitro*

It was recently demonstrated that within a PMCA model of human and mouse PrP^{Sc} replication, the addition of rPrPs inhibited prion amplification in a dose dependent manner (Yuan et al. 2013). Hamster rPrP also slowed disease progression in a mouse model (Skinner et al. 2015). This project aims to investigate the inhibitory effect of three ovine rPrPs (VRQ, ARQ, ARR) and hamster rPrP on scrapie PMCA *in vitro*. From this data, the efficacy of each inhibitor will be compared by the determination of IC50 values. The most potent inhibitors will then be tested in PMCA with a range of ruminant prion strains and amplification substrates to determine the effects of heterologous and homologous rPrP inhibition efficacy. The efficacy of these inhibitors may give insight into their potential use as a therapeutic for prion diseases, as well as elucidating further into prion conversion.

2. The use of rPrP inhibition to characterise prion strains

To date the gold standard for prion strain characterization is through multiple transmissions of strain characteristics in mouse bioassay (Aguzzi et al. 2007). Although effective this method is time consuming and labour intensive. Other methods are available to discriminate between the biochemical characteristics of prion strains including immunohistochemistry of PrP^{Sc} deposition, protease sensitivity, glycoform ratios, structural stability and propagation in cell culture (Gough et al. 2015). Here, the study will determine whether different rPrP inhibitors have different inhibitory efficacies in inhibition of the replication of distinct strains in PMCA. This will determine whether the pattern of inhibition produced by these different inhibitors can be exploited to act as a characteristic of prion strains defining them *in vitro*.

3. Identification of Immunoreactive peptides that recognise scrapie specific autoantibodies by Next Generation Phage Display

Phage display has been used elsewhere to identify autoantibody biomarkers in cancer, rheumatoid arthritis, traumatic brain injury and MS (Zhong et al. 2008; Somers et al. 2008; Somers et al. 2011; Ghoshal et al. 2016). The recent development of NGPD allows in depth analysis of phage ligands with lower risks of

library bias ('T Hoen et al. 2012). NGPD has already been applied to identify immunoreactive peptides that can be used in diagnostic assays for antibodies produced against *Salmonella enterica* (Naqid et al. 2016). Other studies have reported that sera based autoantibodies can be successfully used to differentiate between healthy patients and patients with AD, PD or MS (Nagele et al. 2011; Han et al. 2012; Ayoglu et al. 2013; DeMarshall et al. 2016). It was hypothesised that NGPD could be applied to map the epitopes of sera based autoantibodies in scrapie infected sheep. In doing so, immunoreactive peptides could be identified that selectively bind autoantibodies specific to the disease state. If successful this would act as a proof of principle for NGPD in detecting autoantibodies to neurodegenerative protein misfolding diseases, and potentially serve as the basis for future sera based diagnostic assays.

Chapter 2: Materials and Methods

2. 1. Recombinant PrPs as Diagnostic and Therapeutic Ligands

2. 1.1. Source of Tissue Samples

Healthy and diseased brain tissue was, unless otherwise stated, sourced from the Animal and Plant Health Agency Biological Archive (APHA, Addlestone, Surrey, UK). Infected material was obtained from confirmed TSE-infected ruminants submitted to the APHA for diagnosis. Healthy ovine brain tissue was obtained from a scrapie-free, New Zealand derived flock (ARSU, APHA), and bovine brain tissue from a confirmed BSE negative Fresian cow. Ovine BSE samples originated from ovine BSE challenges of sheep carried out by the APHA. CH1641 scrapie isolates were donated kindly by Professor N. Hunter, The Roslin Institute (Neuropathogenesis Division, University of Edinburgh). Infected bovine brain tissue was from 71 pooled BSE positive cases (SE12929/0749 and SE1945/0035) or from 4 isolates (SE1762/0013) sourced from APHA. Apl_{338ii} and G_{338} scrapie brain tissue were obtained from mouse bioassay by other members of the research group as described by (Gough et al. 2012; Maddison et al. 2015).

2. 1.2. Preparation of 10% (w/v) Diseased Brain Homogenates

Brain tissue was segmented using a scalpel. Pre-weighed 2 mL centrifuge tubes (Stratech) were then prepared with up to 1 mL of glass beads (1 mm diameter, Stratech). Segmented brain tissue was added to each tube, which were then re-weighed. To each tube a corresponding volume of brain lysis buffer (0.5% (v/v) Nonidet P-40 (Fluka Analytical) and 0.5% (w/v) sodium deoxycholate (Fisher Scientific) in phosphate buffer saline (PBS) (137 mM NaCl, 2.7 mM KCl, 10 mM Na_2HPO_4, 1.8 mM KH_2PO_4, pH 7.4) was added to produce a 10% (w/v) homogenate. Homogenisation of the brain tissue was carried out at 4800 oscillations/minute for 60 seconds using a mini bead beater (Stratech). Homogenate was then separated into aliquots for storage at -80°C.

Alternatively, homogenates were prepared by syringe. Segmented brain tissue was weighed in bijous and reconstituted to 10% (w/v) with brain lysis buffer. Homogenisation was carried out by passing sample five times through syringes with blunt (19G, 21G and then 23G) monojet needles of decreasing gauge. Homogenate was then centrifuged at 2000 xg for five minutes and the supernatant was removed and separated into aliquots for storage at -80ºC. All steps were carried out in a microbiological safety cabinet (MSC), category I/III. Infected isolates used in this study are shown in (**Table 2. 1.9.**).

2. 1.3. Preparation of 10% (w/v) Healthy Brain Homogenates

Healthy brain tissue was washed and deveined prior to homogenisation. Brain tissue was then segmented via scalpel, and then further segmented using a blender. This tissue was homogenised in conversion buffer (50 mM NaCl (Fisher Scientific), 4 mM ethylene diamine tetra-acetic acid (EDTA) (Fisher Scientific), pH 8, 1% (v/v) Triton X-100 (Fisher Scientific) and miniprotease inhibitor (Roche) in phosphate buffer saline (PBS), pH 7.4) using a bead beater and glass beads (1 mm diameter) to a 10% (w/v) final concentration. Following homogenisation, the tissue was centrifuged for 10 minutes at 600 xg to pellet cellular debris. Supernatant was carefully removed and separated into aliquots and stored at -80ºC. All steps were carried out at 4ºC or on ice. The healthy brain homogenates used in this study can be observed in (**Table 2. 1.3.**). Brains 17, 21 and Bovine were prepared by other members of the research team.

Table 2. 1.3. Details of the healthy brain tissue homogenate used throughout this investigation.

Brain Number*	Isolate Number	Genotype
17	PG0648/09	VRQ/VRQ
21	PG1562/10	ARQ/ARQ
51	PG0211/12	AHQ/AHQ
Bovine	Bovine	Bovine

*All homogenates were prepared at 10% (w/v).

2. 1.4. Expression and Purification of Ovine and Hamster Recombinant Prion Proteins

Glycerol stocks of rPrP expressing bacteria were available for the study and, unless otherwise stated, were previously produced within the research group. VRQ, ARR and Hamster recombinant proteins were expressed in Novablue (DE3) *E. coli* in the plasmid pET22b. ARQ recombinant protein (IDEXX Laboratories) was expressed in Top10 *E. coli* in the plasmid pET41(a+). The expression in either plasmid is controlled by a lac operon with a T7 promoter, induced by the addition of isopropyl β-D-1-thiogalactopyranoside (IPTG). Each clone expressed the amino acid sequence of 23-231 of PrP, with no vector derived tags or amino acids. Glycerol stocks of each expressing clone were streaked out onto 2x YT agar (2YT medium containing 16 g tryptone (Sigma Aldrich), 10 g Yeast Extract (Merck), 5 g NaCl and 15 g of bioagar (Sigma Aldrich), made to 1 L with dH_2O) plates

containing 100 µg/mL ampicillin (Sigma Aldrich) (VRQ, ARR, Hamster) or 50 µg/ml kanamycin (Life Technologies) (ARQ) and 1% (w/v) glucose (Fisher Scientific). Plates were incubated at 37°C overnight.

Single colonies of *E. coli* were picked with sterile pipette tips and inoculated into 5 mL of 2YT medium containing 100 µg/mL ampicillin (VRQ, ARR, Hamster) or 50 µg/mL kanamycin (ARQ) and 1% (w/v) glucose in sterile universals. These cultures were grown at 37°C, 180 rpm in a shaking incubator overnight. 5 mL of each medium was incubated as a contamination control. 2.5 mL of overnight culture was used to inoculate 500 mL of 2YT with 3% (w/v) glucose and 100 µg/mL ampicillin (VRQ, ARR, Hamster) or 50 µg/mL kanamycin (ARQ) in a sterile 1 L baffled flasks. These were incubated at 37°C, 200 rpm until an optical density 610 nm (OD_{610}) of 0.4. Cultures were centrifuged at 2800 xg for 30 minutes. Cell pellets were resuspended into 500 mL of 2YT with 100 µg/mL ampicillin (VRQ, ARR, Hamster) or 50 µg/ml kanamycin (ARQ) and 1 mM IPTG (Calbiochem). Cultures were incubated shaking at 37°C overnight.

Cells were then harvested by centrifugation at 2800 xg for 30 minutes and stored at -20°C prior to lysis. Cell pellets were resuspended in 2.5 mL of lysis buffer (50 mM NaH_2PO_4 (Fisher Scientific), 300 mM NaCl (pH 8.0), 0.1% (v/v) Nonidet P-40, 10 mg/mL lysozyme (Sigma Aldrich), and Roche complete protease inhibitor without EDTA). Cell suspensions were then incubated at 37°C for 1 hour. DNase I (Bio-Rad) (1 mg/mL, 240 µL) and 120 µL $MgCl_2$ (Fisher Scientific) (1 M) were added and incubated at room temperature for 15 minutes. Lysate was centrifuged at 12000 xg for 20 minutes at 4°C. The pellets were resuspended in 25 mL of wash buffer (10 mM Tris Base (Merck), pH 8, 0.1% (v/v) Nonidet P-40) and incubated on ice for 20 minutes. Cell pellets were recovered by centrifugation as described above. Washing was repeated 3 times until the pellets were white in colour. Pellets were then gently solubilised in 2.5 mL of solubilisation buffer (8 M urea (GPR Rectapur), 50 mM NaH_2PO_4, 300 mM NaCl, pH 7.5) by pipetting. Solubilisation was performed overnight at room temperature with rotation. Debris was pelleted by centrifugation at 10000 rpm for 20 minutes using a Beckman-Coulter centrifuge. Supernatant for each clone was pooled and the volume was increased to 30 mL with solubilisation buffer for purification through Fast Protein Liquid Chromatography (FPLC) (AKTA prime, GE Healthcare).

rPrPs were purified by immobilised affinity chromatography (IMAC). An IMAC Hi-Trap chelating column (5 mL) (GE healthcare) was pre-charged with 50 mM $CuSO_4$

(Sigma Aldrich) using the FPLC machine. The column was washed with solubilisation buffer, then loaded with solubilised rPrP at a flow rate of 0.2 mL/minute. Protein was then refolded on the column as described previously, using a gradient of 8 M urea to 0 M over a course of 2.5 hours, with an initial flow rate of 0.5 mL/minute for 10 minutes followed by 1 mL/minute for 140 minutes (Zhan et al. 1997). rPrP was then eluted on a 0-0.5 M imidazole gradient in elution buffer (300 mM NaCl and 50 mM NaH_2PO_4) at a flow rate of 0.5 mL/minute for 110 minutes. 1 mL fractions were collected for 15 fractions, followed by 2 mL fractions using an automatic fraction collector and stored at 4°C. The elution peak and protein purity was assessed by SDS-PAGE (see **Section 2. 2.13.**). Gels were then stained with Instant Blue (Expedeon) overnight at room temperature with rotation. Gels were destained with dH_2O until protein bands were clearly visible. Fractions containing rPrP were pooled, protein concentrations were determined by Bradford assay against a bovine serum albumin (BSA) standard (Sigma Aldrich) (**Section 2. 1.8.**), and samples were aliquoted and stored at -80ºC with 20% (w/v) sucrose.

2. 1.5. Protein Misfolding Cyclic Amplification

PMCA reactions (see **Section 2. 1.6.**, **2. 1.9.**, **2. 1.10.** and **2. 1.16.**) were prepared in clear 0.2 mL polymerase chain reaction (PCR) tubes (Corning). These were transferred into a circular tube rack in an ultrasonicating water bath (model 3000; Misonix). Cycles of PMCA were carried out for 24 hours (1 PMCA round) at 37ºC using a wattage of 190-200 W. The sonication time used was 40 seconds, with incubation times of 29 minutes and 20 seconds for each cycle. For serial PMCA (sPMCA) experiments, after a PMCA round, 50 µL of reaction product was added to 100 µL of fresh substrate and 100 µL of this was used in the subsequent round of PMCA (up to 5 PMCA rounds were carried out). Remaining reaction products were stored at -20ºC for analysis.

2. 1.6. Determination of IC50 Values for Recombinant PrPs

Reactions were prepared with 88 µL of brain homogenate substrate (Brain 17, **Table 2. 1.3.**) mixed with 60% (w/v) sucrose (to a final concentration of 2% (w/v)), brain lysis buffer and recombinant PrP to a total volume of 95 µL. Recombinant PrP was added at final concentrations of 50 nM, 100 nM, 200 nM, 400 nM, 800 nM and 1200 nM. The details of the recombinant proteins used are shown in (**Table 2. 1.6.**). To these reactions 5 µL PrP^{Sc} "spike" (diluted 1:10 in brain lysis buffer) was added. The isolate of scrapie used was PG1361/05, and the isolate of BSE used was SE1762/0013 (**Table 1. 2.9.**). Reactions were amplified for a single 24h cycle of PMCA only. Controls included untreated (containing no

rPrP), substrate only controls (for PK digestion efficiency) and inhibition control reactions (1200 nM rVRQ, shown to cause 94% inhibition by western blotting). Reaction products were digested with proteinase K followed by analysis by dot blotting and densitometry.

Table 2. 1.6. Details of the recombinant PrPs used in this investigation.

Recombinant Protein	Species	Residues
VRQ	*Ovis aries*	23-231
ARR	*Ovis aries*	23-231
ARQ	*Ovis aries*	23-231
Hamster	*Aesocritus auratus*	23-231

2. 1.7. Dialysis of the rVRQ Protein to Remove Imidazole

A 0.5 mL G2 dialysis cassette (10000 Da molecular weight cut off (MWCO)) (Life Technologies) was hydrated with PBS or conversion buffer for 2 minutes at 4ºC. 400 µL of rVRQ stock (**Table 2. 1.6.**) was loaded into the dialysis cassette via pipetting. Dialysis was carried out in 400 mL of PBS or conversion buffer (cooled to 4°C) for one hour with mild agitation. The buffer was changed, and dialysis was performed for another hour. Optionally, a third round of dialysis was performed for 2 hours with fresh buffer. This was performed if the rVRQ protein was to be biotinylated (see **Section 2. 1.13**). All steps were carried out on ice. Following dialysis rVRQ was removed from the dialysis cassette by pipette and stored at -20°C. The protein concentration was determined by Bradford assay (**Section 2. 1.8.**).

2. 1.8. Determining Protein Concentration by Bradford Assay

Bradford assays were performed according to the manufacturer's instructions. Briefly, Nunc-Immuno Maxisorp ELISA plates (Thermo Scientific) were prepared with 5 µL of BSA standards at final concentrations of 2, 1, 0.75, 0.5, 0.25 and 0 mg/mL in buffer analogous to the protein being analysed. Each standard was loaded in triplicate. 5 µL of the unknown protein solution was loaded in triplicate and 250 µL of Bradford reagent (Sigma Aldrich) was added to each well. Plates were incubated for 10 minutes at room temperature before measurement on a Tecan GenIos plate reader at a wavelength of 620 nm. The values obtained from the standard curve were used to calculate the concentration of protein by the equation $y=mx+c$.

2. 1.9. Establishing rVRQ as an Inhibitor of Prion Amplification

Reactions were prepared in duplicate as outlined in **Section 2. 1.5.** using a final concentration of 400 nM of dialysed rVRQ per reaction without sucrose. rVRQ was tested on a number of isolates from classical ovine scrapie, G_{338} scrapie, Apl_{338ii} scrapie, CH1641 scrapie, ovine BSE and bovine BSE. These isolates are described in (**Table 2. 1.9.**). Reactions were spiked with 5 µL diluted (1:10 in brain lysis buffer) isolate, except in the instance of J2935, SE1929 and SE1945 which were spiked directly at 5 µL. Isolates were usually amplified in substrates corresponding to their genotype, e.g. PG1361/05 in VRQ/VRQ (Brain 17), SE1945/0035 in Bovine Substrate (**Tables 2. 1.3.** and **2. 1.9.**). Ovine BSE was amplified in VRQ/VRQ substrate. All reactions were performed for 5 cycles to allow comparison between strains and isolates. Additional controls included non-spiked PMCA reactions (negative amplification) and PG1361/05 (ARQ/VRQ) amplifications with no rPrP (positive amplification). Reaction products were digested with proteinase K and analysed by western and dot blotting, followed by densitometry.

Table 2. 1.9. Isolates analysed for rVRQ inhibition, including their strain type, genotype and source. All isolates were prepared as 10% (w/v) brain homogenates.

Strain Type	Isolate Number	Genotype	Source
Classical	PG1361/05	VRQ/ARQ	Ovine Cerebellum
Scrapie	PG1563/02	VRQ/VRQ	Ovine Spinal Cord
	PG0157/05	AHQ/VRQ	Ovine Cerebellum
	PG1499/02	AHQ/VRQ	Ovine Cerebellum
G_{338} Scrapie	MC136477	VRQ/VRQ	Mouse Bioassay
	MC136553	VRQ/VRQ	Mouse Bioassay
Apl_{338ii} Scrapie	MC141403	VRQ/VRQ	Mouse Bioassay
	MC141404	VRQ/VRQ	Mouse Bioassay
CH1641	J2916	AHQ/ARQ	Ovine Cerebellum
Scrapie	J2935	AHQ/ARQ	Ovine Cerebellum
Ovine BSE	PG0392/04	ARQ/ARQ	Bovine Cerebellum
	PG1693/03	ARQ/ARQ	Bovine Cerebellum
Bovine BSE	SE1929/0749	Bovine	Brain Pool of 71 BSE Cases
	SE1945/0035	Bovine	Brain Pool of 71 BSE Cases
	SE1762/0013	Bovine	Brain Pool of 4 BSE Isolates

2. 1.10. Characterization of Classical Scrapie by rPrP Inhibition

PMCA reactions were prepared as outlined in **Section 2. 1.5.** using either a final concentration of 400 nM or 200 nM of rPrP inhibitors (see **Table 2. 1.6**). Ten reactions were prepared per inhibitor and control, spiked with 5 µL (1:10 in brain lysis buffer) of PG1361/05 (ARQ/VRQ) scrapie (see **Table 2. 1.9.**). PMCA was run for a single 24-hour cycle only. Alternative reactions were attempted using 2.5 µL of undiluted spike or by carrying out two cycles of PMCA without transferring PMCA product into fresh substrate. Experiments testing 400 nM or 200 nM of rPrP inhibitors were run in triplicate. All reaction products were digested with proteinase K and analysed by dot blotting and densitometry.

2. 1.11. Determining Imidazole as a Select Inhibitor of Prion Strain Amplification

PMCA reactions were prepared as outlined in **Section 2. 1.5.** using final concentrations of 40, 20, 10, 5, 2, 1, 0.5 and 0 mM of imidazole (Sigma Aldrich). Reactions were prepared in duplicate, spiked with PG1361/05 or PG0392/04 in Brain 17 or Bovine brain homogenates (see **Tables 2. 1.3.** and **2. 1.9.**). sPMCA was performed for five days, with the brain substrate and imidazole added fresh each day. Reaction products were digested with proteinase K and analysed by dot blotting and densitometry.

2. 1.11. Treatment of PMCA Products with Proteinase K

PK digests of PMCA products were prepared to a final concentration of 100 µg/mL PK (Sigma Aldrich) and 0.1% (w/v) sodium dodecyl sulphate (SDS) (Sigma Aldrich) in PBS. Digestion was performed at 39°C for 1 hour. The reactions were stopped by storage at -80°C for 5 minutes. Samples were then diluted in LDS sample buffer (NuPAGE, Invitrogen) containing 5% (v/v) β-mercaptoethanol (Sigma Aldrich). Samples were heated to 100ºC for 10 minutes using a heat block.

2. 1.12. Analysis of PMCA Products by Dot Blotting

Nitrocellulose membranes (GE Healthcare) were marked with a 1 cm^2 pencil grid. 2.5 µL of PK digested sample (prepared with 4x LDS, 5% β-mercaptoethanol) was loaded into the centre of each square by pipette and dried for 15 minutes at room temperature. Membranes were then blocked overnight at 4ºC in 5% powdered milk formula (SMA) prepared in tris buffered saline (TBS) (50 mM Tris-Base, 150 mM NaCl, pH 8) with 0.05% (v/v) tween 20 (TBST). Blots were then incubated with the monoclonal antibody Sha31 at a concentration of 1:40000 in 0.5% (w/v) SMA/TBST for two hours at room temperature. Blots were incubated for a further

90 minutes with 1:2000 polyclonal goat anti-mouse secondary antibody in 0.5% (w/v) SMA/TBST. Blots were exposed to EZ-ECL chemiluminescent substrate (Geneflow), heat sealed in polyethylene tubing and visualised using a phototek photon counting camera. All incubation and wash steps were performed with mild agitation (50 rpm) on an orbital shaker.

2. 1.13. Analysis of PMCA Products by Sodium Dodecyl Sulphate-Polyacrylamide Gel Electrophoresis (SDS-PAGE) and Western Blotting

Pre-cast polyacrylamide gels (12% (w/v) acrylamide, Invitrogen) were loaded with 20 µL of PK digest (prepared with either 2x LDS or 4x LDS for a loading volume of 4 or 6 µL of PMCA product). SDS-PAGE was run for 90 minutes at 150 V using 1x MOPs buffer (Invitrogen). Proteins within the gel were transferred onto polyvinylidine difluoride (PVDF) membrane (Life Technologies) via transfer electrophoresis at 30 V for 75 minutes with transfer buffer (Invitrogen). Membranes were blocked overnight at 4°C in 5% (w/v) SMA/TBST. The membranes were then probed and developed as described for the dot blotting (**Section 2. 1.12**) with the exception that the Sha31 primary antibody was used at a 1:80000 dilution.

2. 1.14. Biotinylation of rVRQ

The kit used for biotinylation was the BioTag kit from Sigma Aldrich, and the method follows the manufacturer's instructions. Dialysed rVRQ was prepared in PBS as described in **Section 2. 1.7.** with three rounds of dialysis. The protein concentration was then determined by Bradford assay as described in **Section 2. 1.8.** 3-sulfo-N-hydroxysuccinimide ester (BAC-SulphoNHS) biotinylation reagent (Sigma Aldrich) was dissolved with 30 µL of DMSO (Sigma Aldrich) and 1 mL of 0.1 M Sodium Phosphate Buffer, pH 7.2 (Sigma Aldrich), 5 mg/mL final concentration. BAC-SulphoNHS was added to dialysed rVRQ at a 13:1 molar ratio and incubated at 4ºC for 2 hours. Biotinylated rVRQ was then stored at 4ºC for immediate use or at -20ºC for future use.

2. 1.15. Development of an ELISA to Measure the Binding of rVRQ for PrP^{Sc} and PrP^{C}

Nunc-Immuno Maxisorp ELISA plates were coated with 100 µL/well of 10 µg/mL rVRQ in elution buffer (50 mM NaH_2PO_4, 300 mM NaCl, 0.5 M imidazole, pH 7.5), 20% (w/v) sucrose. As a positive control wells were also coated with 100 µL/well of Sha31 antibody at a final concentration of 1:12000. Plates were incubated overnight at 4ºC. Plates were then blocked with 100 µL of 5% (w/v) SMA in PBS

with 0.05% (v/v) Tween 20 (Fisher Scientific) (PBST) for two hours at room temperature. 100 µL/well of 1% (w/v) healthy (Brain 17, see **Table 2. 1.3.**) or diseased (PG1361/05, see **Table 2. 1.9.**) brain homogenate was added to the plate and incubated at room temperature for one hour. Bound PrP^{Sc} and PrP^{C} were probed with 100 µL/well of 10 µg/mL biotinylated rVRQ in 0.5% (w/v) SMA/PBST for one hour at room temperature. The probe was then detected using 100 µL/well of streptavidin-HRP (Abcam) at a concentration of 1:15000 in 0.5% (w/v) SMA/PBST for one hour at room temperature. Wells were then exposed to 100 µL of tetramethylbenzidine (TMB) (Bio-Rad) for one hour at room temperature, and colour development was stopped by adding 100 µL/well of 2 M sulphuric acid (Fisher Scientific). Absorbance was then read using a Tecan GeneIos at 450 nm.

2. 1.16. Seeding of PMCA reactions with rVRQ-captured PrP^{Sc}

rVRQ was dialysed as described in **Section 2. 1.7.** Dynabeads™ M-280 Tosylactivated (Invitrogen) were resuspended by vortexing for 30 seconds. 335 µL of resuspended beads (10 mg) were transferred to sterile 1.5 mL Eppendorfs. Beads were magnetized and resuspended in 335 µL of 0.1 M boric acid (Fisher Scientific), pH 9.5 to wash. Beads were magnetized and resuspended in 200 µg of dialysed rVRQ in 0.1 M boric acid, pH 9.5, and incubated overnight at 37°C with gentle agitation. A background control of beads without rVRQ was also prepared to assess the extent of non-specific binding of PrP^{Sc} to the beads.

The beads were washed x3 with 1 mL TBS by magnetization and resuspension. Beads were blocked with 1 mL of 5% (w/v) SMA in TBS for 1 hour at room temperature with rotation. Beads were washed x3 with TBS as above and resuspended in 335 µL of 1% (w/v) isolate PG1361/05 (ARQ/VRQ) in 5% (w/v) SMA/TBS (**Table 2. 1.9.**). The isolate and beads were incubated at room temperature for 1 hour with rotation. Beads were transferred to fresh tubes and washed x5 with TBS, then resuspended in 335 µL of TBS. Resuspended beads were used as spikes in PMCA reactions with 10 µL (300 µg beads), 5 µL (150 µg beads), 2 (60 µg beads) and 1 µL (30 µg beads). These volumes were mixed with 90 µL of Brain 17 (**Table 2. 1.3.**) and made to 100 µL with conversion buffer. PMCA was performed as described in **Section 2.5.** Reaction products were analysed by western blotting as described in **Sections 2. 1.11.** and **2. 1.13.**

2. 1.17. Statistical Analysis of Dot and Western Blots

Dot and western blots were analysed using ImageJ software as monograph images (Schneider et al. 2012). Percent inhibition was calculated relative to the mean

intensity of untreated controls. Values were then plotted using GraphPad Prism (Version 7, San Diego, CA). IC50 values were determined by nonlinear regression, log inhibitor verses response (variable slope) model with constraints at 100% and 0%. This model calculates the IC50 value from the data and does not assume a sigmoidal relationship. Data generated in strain characterisation (**Section 2. 1.10.**) were analysed by a one-way analysis of variance (ANOVA) paired with a Tukey *post-hoc* test of data in GraphPad Prism 7.

2. 2. Selection of Diagnostic Peptides Reactive to Autoantibodies from the Sera of Scrapie Infected Sheep

2. 2.1. Source of Blood Samples

Blood from scrapie infected sheep was obtained from an experimentally infected sheep flock (APHA, Ripley). Blood was sourced post infection at ages 6, 9, 12, 15, 16, 18, 21, 22 months and post mortem. Blood from scrapie negative sheep was sourced from a New-Zealand-derived, classical scrapie free flock (APHA, ARSU). Blood was sourced at months 3, 6, 9, 12, 15, 16, 18, 19, 20, 21, 22, 23 and 24 after birth.

2. 2.2. Preparation of Sera from Sheep Blood

Sera from ARSU and Ripley flock sheep was prepared by members of RSK-ADAS. Blood from infected and non-infected sheep was heated to 37°C for one hour to clot. Blood clots were loosened from tube walls and were stored overnight at 4°C. Sera was decanted into fresh 50 mL falcon tubes (Corning) and centrifuged at 10000 xg for 30 minutes in a Thermoscientific X3R multifuge. Sera supernatant was stored at -80°C in fresh 50 mL falcon tubes.

2. 2.3. Determining Phage Titre

All cell culture work was performed in a laminar flow unit. Bacteria used in phage display were *Escherichia coli* TG1 supE thi-1Δ (lac-proAB) Δ (mcrB-hsdSM) 5 (rK-mK) (F traD36 proAB lacUqZΔM15), stored at -80ºC in 0.5 mL aliquots prior to use. For growth on solid media, TG1 bacteria were thawed at room temperature and used to inoculate 5 mL of 2YT media in a sterile universal. TG1 bacteria were grown overnight at 37ºC, 150 rpm in an orbital shaking incubator. The next day the TG1 bacteria were streaked onto m9 minimal media agar plates and incubated at 37ºC for 48 hours. M9 media consists of 1x m9 salts (6.4 g $Na_2HPO_4.7H_2O$ (Fisher Scientific), 15 g KH_2PO_4 (Fisher Scientific), 5 g NH_4Cl (Fisher Scientific) and 2.5 g NaCl in 250 mL dH_2O), 0.8% (w/v) MgCl, 0.4% (w/v) Thiamine HCl (Sigma

Aldrich), 2% (w/v) glucose (Fisher Scientific) and 2% bioagar. After 48 hours plates were stored at 4°C as a working source of TG1 cells. This was repeated weekly to maintain a fresh source of viable TG1 cells.

A colony of TG1 bacteria was picked and used to inoculate 5 mL of 2YT media. 5 mL of 2YT media containing 150 µg/mL ampicillin acted as a phage-contamination control. These cultures were incubated overnight at 37ºC, 150 rpm. The following day, providing no growth was observed in the control, 1 mL of the grown subculture was used to inoculate 100 mL of 2YT in a sterile conical glass flask. This was incubated at 37ºC, 200 rpm until an OD_{610} of 0.4-0.6. 1 µL of bacteriophage solution produced from library preparation (**Sections 2. 2.4., 2.6., 2.7.**) was diluted in 99 µL of TG1 culture, then serially diluted 10-fold 5 times in sterile 1.5 mL Eppendorfs. Infection was performed at 37ºC for 30 minutes static, with inversion every 10 minutes. Infected culture was spread onto 2YT agar plates containing 150 µg/mL ampicillin. An additional plate was spread with 100 µL of TG1 culture as a phage-contamination control. Plates were incubated overnight at 37ºC. The following day colonies on each plate were counted. The number of colonies combined with the dilution factor of the culture used to spread on each plate were used to determine colony forming units (CFU)/mL by the following equation:

Colony forming units per millilitre (CFU/mL) = Colonies counted/Volume of phage used to infect (mL) x Dilution factor (mL)

2. 2.4. Peptide Library Preparation

Two separate peptide phage libraries were used, donated by Professor Fanco Felici, University of Molise, Italy. These libraries consist of peptides inserted at the N-terminus of the phage coat protein pVIII, either displayed as linear peptides or constrained. Constrained peptides contain cysteine residues flanking the peptide sequence so that upon display they form a disulphide bond. Each library is designated as PC89-L (linear) or PC89-C (constrained) respectively. Each library has a diversity of 10^7 peptide sequences.

Each library was propagated in TG1 bacteria, stored as 1 mL aliquots at -80ºC. To prepare each library, a 1 mL aliquot of each library was used to inoculate 500 mL of 2YT media containing 1% (w/v) glucose and 150 µg/mL ampicillin in 2 L culture flasks. Cultures were grown at 37ºC for 2 hours, 220 rpm in an orbital shaker incubator until an OD_{610} of 0.4. TG1 bacteria were superinfected with 50 µL of

M13K08 helper phage ($1x10^{13}$ CFU/mL) (New England Bioloabs) with incubation at 37ºC for 1 hour static. Each culture was pelleted at 3000 xg for 20 minutes. 40 mL aliquots of supernatant were taken in 50 mL falcon tubes and placed on ice. The pH of each aliquot was lowered to 4.2 using HCl (Fisher Scientific) (diluted 2:1 in dH_2O) and stored on ice for 1 hour. Each tube was centrifuged at 8000 xg for 30 minutes. Pellets were resuspended in 10 mL of sterile PBS. 20 µL of 2 M NaOH was added with agitation to neutralize the pH. The phage were then separated into 1 mL aliquots in sterile 1.5 mL Eppendorfs and centrifuged at 12000 xg for 1 minute to remove remaining cellular debris. Supernatant was pooled in 50 mL Falcon tubes and stored at 4°C. Phage titre was then determined as described in **Section 2. 2.3.**

2. 2.5. Purification of IgG antibodies from sheep sera using Melon Gel

IgG antibodies were purified from sheep sera using a Melon Gel IgG Spin Purification Kit (Thermo Scientific) according to manufacturer's instructions. Spin Columns (Thermo Scientific) were prepared with 500 µL of resuspended Melon Gel IgG Purification Support Buffer (Thermo Scientific). These columns were centrifuged at 3000 xg for 1 minute. The columns were then washed with 300 µL of Purification Buffer (Thermo Scientific) by centrifugation as above. Each column was then incubated with 500 µL of 10% (v/v) sheep sera/Purification Buffer for 10 minutes at room temperature with rotation. Columns were centrifuged at 3000 xg for 1 minute. The flow through containing purified IgG was stored at 4ºC. The concentration was determined by Bradford assay as described in **Section 2. 2.8**, and purity was assessed by SDS-PAGE as described in **Section 2. 1.13.** IgGs were prepared immediately prior to use in phage display. Purified IgG antibodies from individual animals were pooled at a concentration of 1.5 mg/mL, with month 12 and month 21 pooled as separate groups.

2. 2.6. Purification of IgG antibodies from sheep sera using SureBeads™ Protein G Magnetic Beads

SureBeads™ Protein G Magnetic Beads (Bio-Rad) were resuspended by vortexing for 30 seconds. Resuspended beads were separated into 100 µL aliquots in sterile 1.5 mL Eppendorfs and were centrifuged at 3000 xg for 1 minute. The beads were resuspended in 1 mL of sterile PBST to wash, repeated three times. Beads were resuspended in 195 µL of PBS and 5 µL of sheep sera (**Table 2. 2.6.**). Sera and beads were incubated together at room temperature for 10 minutes with rotation. The beads were then washed three times as described. Elution was performed by resuspending the beads in 20 µL of 20 mM glycine (Fisher Scientific), pH 2, with

incubation at room temperature for 5 minutes at room temperature. Beads were pelleted by centrifugation at 12000 xg for 1 minute and the eluate was neutralized with 2 µL of 1 M phosphate buffer (Sigma Aldrich), pH 7.4. Eluate was stored at 4°C. Elution products were assessed for purity by SDS-PAGE (**Section 2. 1.13.**). Protein concentration was determined by Bradford assay (**Section 2. 1.8.**).

Table 2. 2.6. Sera isolates used for the purification of IgG antibodies. The sheep samples were obtained from the scrapie infected Ripley flock (APHA).

Sample Reference	Sheep Number	Month Post Challenge	Genotype
PG0950/07	06-1048	12, 21	VRQ/VRQ
PG0147/08	06-1049	12, 21	VRQ/VRQ
PG0889/07	06-1050	12, 21	VRQ/VRQ
PG0894/07	06-1051	12, 21	VRQ/VRQ
PG0764/07	06-1052	12, 21	VRQ/VRQ
PG0957/07	06-1053	12, 21	VRQ/VRQ

2. 2.7. Round 1 panning phage libraries against IgG antibodies from sheep sera

The sub library produced from this round of biopanning was used in the subsequent round 2 biopanning of all phage display experiments in this study. Equal amounts of phage from PC89-L and PC89-C libraries were pooled using the phage titre calculated as described in **Section 2. 2.3**. Superblock (Thermo Scientific) was added to the pooled phage with a final concentration of 10% (v/v) and incubated at room temperature for 1 hour with rotation. 12x 1 mL aliquots of blocked phage were transferred to sterile 1.5 mL eppendorfs. 5 µL of sheep sera (see **Table 2. 2.7.**) was added to each tube and incubated for 2 hours at room temperature with rotation.

SureBeads™ Protein G Magnetic Beads were resuspended by vortexing for 30 seconds. Resuspended beads were separated into 100 µL aliquots in sterile 1.5 mL Eppendorfs. The beads were centrifuged at 3000 xg for 1 minute. The beads were resuspended in 1 mL of sterile PBST to wash, repeated three times. Beads were then resuspended in 1 mL of 10% (v/v) superblock in PBS and incubated at room

temperature for one hour with rotation. Beads were pelleted by centrifugation as before. Blocked phage/sera was then used to resuspend the blocked magnetic beads, followed by incubation at room temperature for 2 hours with rotation. The beads were then washed by centrifugation and resuspension as described above x10 with PBST and x5 with PBS. Following this the beads were centrifuged at 3000 xg. Bound phage were then eluted by two separate methods.

In the first method bound phage were used to directly infect a culture of TG1 bacteria. The beads were resuspended in 100 µL of sterile PBS. 50 µL of this suspension was used to infect a 1 mL culture of TG1 bacteria at an OD_{610} of 0.4 at 37ºC for 30 minutes. The infected bacteria were then spread onto bioassay plates (Thermo Scientific) with 2YT agar, 150 µg/mL ampicillin and 1% (w/v) glucose and incubated overnight at 37ºC. Residual infected bacteria were titred as described in **Section 2. 2.3**. In the second method, bound phage were eluted competitively with purified IgG antibodies from distinct scrapie-infected animals, prepared as described in **Section 2. 2.5**. For information in regards to the sera samples used, see (**Table 2. 2.6.**). Beads with bound phage were resuspended in 100 µL of 1.5 mg/mL of pooled purified IgG antibodies. The binding capacity of SureBeads™ Protein G Magnetic Beads is ≥6 µg/mg, and 100 µL of bead solution should contain 1 mg of beads (Bio-Rad). Purified antibodies were therefore added at a >20x excess of the binding capacity of the beads. Bacteriophage were eluted separately for month 12 or month 21 time-points for each animal (**Table 2. 2.7.**). Elution was performed at room temperature for 1 hour with rotation. The beads were then centrifuged at 12000 xg for 1 minute. 50 µL of eluate was then used to infect 1 mL of TG1 culture at an OD_{610} of 0.4 for 30 minutes at 37ºC. The infected bacteria were spread onto bioassay plates (Thermo Scientific) with 2YT agar, 150 µg/mL ampicillin and incubated overnight at 37ºC. Residual eluted bacteriophage were used to determine the phage titre as described in **Section 2. 2.3**. Colonies were then harvested from each bioassay dish. To do so, 2 mL of sterile 2YT media 40% (v/v) glycerol was applied to each dish and cells were harvested using a sterile spreader. Harvested cells were stored as 250 µL aliquots at -80ºC.

Table 2 2.7. Sheep sera used in round 1 biopanning. The sheep samples were obtained from the scrapie infected Ripley flock (APHA).

Sample Reference	Sheep Number	Month Post Challenge	Genotype
PG0949/07	06-1026	12, 21	VRQ/VRQ
PG0093/08	06-1030	12, 21	VRQ/VRQ
PG0944/07	06-1032	12, 21	VRQ/VRQ
PG0078/08	06-1033	12, 21	VRQ/VRQ
PG0908/07	06-1038	12, 21	VRQ/VRQ
PG0905/07	06-1042	12, 21	VRQ/VRQ

2. 2.8. Round 2 Biopanning

The sub libraries produced in **Section 2. 2.7.** were used in round two panning. A 250 µL aliquot of each sub library produced in **Section 2. 2.7**. was used to inoculate 150 mL of sterile 2YT media, 150 µg/mL ampicillin, 1% (w/v) glucose in sterile 500 mL baffled flasks (Corning). Each culture was incubated at 37ºC for 90 minutes at 180 rpm in a rotating incubator or until an OD_{610} of 0.4. Cultures were superinfected with 60 µL of $1x10^{13}$ PFU/mL of M13K07 helper phage. Cultures were then incubated at 37ºC for 1 hour static. Cultures were partitioned into 50 mL aliquots in 50 mL Falcon tubes and pelleted at 2800 xg for 20 minutes using a Beckman-Coulter centrifuge. Cell pellets were resuspended in 50 mL of 2YT, 1% (w/v) glucose, 150 µg/mL ampicillin and 50 µg/mL kanamycin. The resuspended cells were then used to inoculate 100 mL 2YT, 1% glucose, 150 µg/mL ampicillin and 50 µg/mL kanamycin in 500 mL baffled flasks. The cultures (3 x 150 ml for each sub library) were incubated at 30ºC overnight, 200 rpm.

The following day each culture was partitioned into 40 mL aliquots in 50 mL Falcon tubes and centrifuged at 3000 xg for 20 minutes. 20 mL of supernatant was collected and titred as described in **Section 2. 2.3.** All supernatant samples from a single sub library were pooled, then equal amounts of phage from each of the sub libraries were pooled using the phage titre. The pooled phage was then aliquoted into 1 ml volumes in sterile Eppendorf's. 10x PBS was added to a final concentration of 1x, and superblock was added to a final concentration of 10% (v/v). The tubes were then incubated at room temperature for 1 hour with rotation. 5 µL of sera was then added to each tube, followed by incubation at room temperature for 2 hours with rotation. For details of sera used in round 2 panning, see (**Chapter 5**). SureBeads™ Protein G Magnetic Beads were prepared and blocked as described in **Section 2. 2.7**. The beads were resuspended in the

blocked phage/sera and incubated at room temperature for 2 hours with rotation. The beads were then washed, eluted and harvested by the methods described in **Section 2. 2.7**. The phage titre of each eluate was determined as described in **Section 2. 2.3**. Each phage eluate was used to infect TG1 bacteria and harvested cells were stored as 250 µL aliquots at -80ºC.

2. 2.9. DNA Extraction and Preparation for Next Generation Sequencing

Phagemid vectors within each sub library were isolated using Gene Elute Plasmid Miniprep Kits (Sigma Aldrich) according to manufacturer's instructions. 250 µL of cells harvested from round 2 biopanning (**Section 2. 2.8.**) were centrifuged at 12000 xg for 1 minute. Pellets were resuspended in 200 µL of Resuspension Solution (Sigma Aldrich). 200 µL of Lysis Solution (Sigma Aldrich) was added to each tube and mixed by inversion 8 times. After 4-5 minutes 350 µL of Neutralization/Binding Solution (Sigma Aldrich) was added and mixed by inversion 8 times. Cell debris was pelleted by centrifugation at 12000 xg for 10 minutes.

Gene Elute Binding Columns (Sigma Aldrich) were prepared by the addition of 500 µL Column Preparation Solution (Sigma Aldrich), followed by centrifugation at 12000 xg for 10 minutes. 750 µL of cell lysate was loaded to each column and DNA was bound by centrifugation at 12000 xg for 1 minute. This step was repeated if the sample volume was greater than 750 µL. Each column was loaded with 750 µL of Wash Solution (Sigma Aldrich) and centrifuged at 12000 xg for 1 minute. This was repeated for an additional wash, followed by an additional centrifugation at 12000 xg for 1 minute to remove excess ethanol. 25 µL of Buffer NE (Macherey-Nagel) was added to each column and incubated at room temperature for 1 minute. Eluted DNA was collected in sterile 1.5 mL Eppendorfs by centrifugation at 12000 xg for 1 minute.

DNA concentration was determined using a Nanodrop 8000 Spectrophotometer (Thermo Scientific) measuring absorbance at 260 nm. Each sample was diluted to a concentration of 10 ng/µL with deionised, DNase/RNase free water. This DNA was used as a template for PCR reactions, with PCR reaction mixes prepared as shown in (**Table 2. 2.9. 1.**).

Table 2. 2.9. 1. Reaction preparation for PCR.

Volume (µL)	Reagent	Concentration
5	Platinum Hi Fi Buffer	10X
1	dNTPs	10 mM
2	$MgSO_4$	50 mM
1	Forward Primer	10 µM
1	Reverse Primer	10 µM
1	Template	10 µM
0.2	Platinum Taq Polymerase High Fidelity	5 U/µL
38.8	dH_2O	N/A

PCR reactions were performed to amplify peptide coding region and to include a linking sequence in the PCR products. The primers used in these reactions were P8forward1 and P8reverse1 as displayed in (**Table 2. 2.9. 2.**). These primers are specific to PC89 vector sequences that flank the peptide coding region. PCR reactions were performed with an initial stage of 95°C for 3 minutes, followed by 18 cycles of 95°C for 30 seconds, followed by 60°C for 30 seconds and 68°C for 30 seconds. The final step was performed at 75°C for 5 minutes, and reaction products were stored at 4°C. Reactions were performed using a TC-512 (Techne).

Table 2. 2.9. 2. Primers used in multiplexing PCR reactions.

Primer	Sequence (5'->3')	Tm (°C)
P8forward1	GTAATCCTTGTGGTATCCGATGCTGCTTTTCGCTGC	71.6
P8reverse1	CTAGAACATTTCACTTACGGTTTTCCCAGTCACG	67.0
P1 c	CCTCTCTATGGGCAGTCGGTGATCTAGAACATTTC ACTTAC	70.5

Primers P8forward1 and P8reverse1 were sourced from Eurofins. P1 Prim-linker2 was sourced from Sigma Aldrich.

PCR products were analysed by agarose gel electrophoresis. 3% agarose gels were prepared by suspension of 4.5 g agarose in 150 µL of TAE buffer (40 mM Tris, pH 7.6, 20 mM acetic acid, 1 mM EDTA) followed by heating to boiling point using a laboratory microwave. Nancy-520 (Sigma Aldrich) was added to a final

concentration of 0.003% (v/v). 10 µL of PCR reaction products were mixed with 2 µL of 6x Orange Dye (Thermo Scientific), of which 10 µL was loaded into 3% agarose gels, immersed in TAE buffer. Gel electrophoresis was performed at 100 V for 1 hour. Gels were imaged using an ImageQuant300 (GE Healthcare).

PCR products (330 bp) were purified using a NucleoSpin® Gel and PCR Clean-up kit (Macherey-Nagel) according to manufacturer's instructions. PCR products were mixed with double the volume of NTI Buffer (diluted 1:5 in dH_2O, Macherey-Nagel). DNA was then bound to NucleoSpin® Gel and PCR Clean-up Columns (Macherey-Nagel) by centrifugation at 11000 xg for 30 seconds. Columns were washed twice with 700 µL of Buffer NT3 (Macherey-Nagel) by centrifugation at 11000 xg for 30 seconds. Excess ethanol was removed by centrifugation at 11000 xg for 1 minute. DNA was then eluted with 25 µL of Buffer NE by incubation at room temperature for 1 minute, followed by centrifugation at 11000 xg for 1 minute. PCR reactions were then performed using 1 µL of purified PCR products as template. The primers used in this reaction were the P1 Prim-linker2 (**Table 2. 2.9. 2.**) as well as unique barcode primers (**Appendix I**). PCR reactions were performed as described above.

Reaction products were quantified using a Qubit ds DNA BR Assay Kit (Invitrogen). 2 µL of product was mixed with 198 µL of Buffer A/B. 10 µL of standards, 0 ng/µL and 100 ng/µL respectively were prepared by diluting 10 µL of standard into 190 µL of Buffer A/B. Each mixture was mixed by pipetting and measured using a Qubit Fluoremeter (Invitrogen). 150 ng of each product was then pooled and the final sample quantified by the Qubit ds DNA BR Assay Kit. The pooled DNA was resolved by agarose gel electrophoresis. Gel bands (330 bp) were excised using a sterile scalpel and purified using a NucleoSpin® Gel and PCR Clean-up kit as described above. DNA was eluted with 50 µL of Buffer NE by incubation at room temperature for 1 minute, followed by centrifugation at 11000 xg for 1 minute.

The DNA amplicons were further purified using an Agencourt AMPure XP Purification Kit (Beckman Coulter, UK) as per manufacturer's instructions. 1.8 volumes of magnetic beads were added to DNA products and incubated at room temperature for 5 minutes. The beads were then magnetized for 2 minutes and resuspended in 70% (v/v) ethanol/dH_2O. Beads were magnetized for 2 minutes, and ethanol was removed by aspiration followed by evaporation for 5 minutes at room temperature. Beads were resuspended in 20 µL of Buffer NE and incubated at room temperature for 5 minutes. The beads were then magnetized for 2 minutes

and supernatant was transferred to sterile 1.5 mL Eppendorfs. Purified DNA was quantified by Qubit ds DNA BR Assay and analysed for purity by gel electrophoresis. Up to 200 ng of purified amplicon of size 330 bp (maximum volume 50 µL) was then sent for sequencing by van Ion Torrent PGM service (University of Pennsylvania, US).

2. 2.10. Analysis of Next Generation Sequencing Data and Peptide Synthesis

Perl scripts were used to process and analysed NGS data files. The scripts used in this study were also used by (Naqid et al. 2016), and are provided at https://figshare.com/articles/Mapping_B_cell_responses_to_bacterial_infection_using_next_generation_phage_display/1566818**.** Briefly, sequencing data was received from the University of Pennsylvania as tar.gz files and unpacked as FASTQ files. FASTQ files were converted to FASTA files using the script demultiplex.sh. Demultiplexed FASTA files were translated into 3 reading frames using the scripts translate.sh and translate.pl. During this step the stop codons TAG, TAA and TGA were replaced with the amino acid glutamine (Q). Frame files were conjoined using the script cat.sh. Each peptide sequence is flanked by the sequence motifs AEGEF and DPAKAA. These sequences were utilized to identify and quantify peptide sequences linked to individual bar codes using the script iterate.sh. A maximum of 2 mismatches were permitted for each barcode, with a minimum of 4 amino acids between flanking motifs required for the peptide sequence to be analysed. The frequency of peptide sequences in a given barcode compared to a set of pooled peptide sequences from barcodes of negative reference controls. The frequency and ratio of peptide sequences between these groups was compared using a two-proportion Z-test (Zhang et al. 2011; Naqid et al. 2016):

$$\left(z = \frac{p1 - p2}{\sqrt{\frac{p1(1-p1)}{n1} + \frac{p2(1-p2)}{n2}}} \right)$$

Z scores are calculated through the ratio and frequency of peptides between a target sample (n1) and control sample (n2) where p1 is the number of sequences of a specific peptide against the target sample/n1, and p2 is the number of sequences of a specific peptide against the control sample/n2. To increase test stringency peptides were selected with a specific Z-score cut off, such as 2. Different analyses were performed using different control samples or by pooling the data for scrapie or uninfected samples from each time point. Candidate peptides were synthesised with an amidated N-terminus and with flanking motifs

AEGEF and DPAKAA by Biomatik Corporation (Canada) at >75% purity, 5 mg each. Peptides were dissolved to a stock concentration of 10 mg/mL and stored at -20°C.

2. 2.11. Screening Peptides by Enzyme Linked Immunosorbent Assay

The following represents the original ELISA method used in the current study. 100 µL of peptides (100 µg/mL in 100 mM sodium carbonate-bicarbonate buffer, pH 9.6 (Sigma Aldrich)) were coated in triplicate in Nunc-Immuno MaxiSorp 96 well plates at 4°C overnight. As a negative control wells were coated with 100 µg/mL of the peptide PIF (sequence HVMDADQESVSQSDI) in 100 mM sodium carbonate buffer, pH 9.6. Wells were blocked with 100 µL of 3% (w/v) skimmed milk powder (Marvel) in PBS for 1 hour at 25°C with agitation. Wells were washed x6 with PBST and x6 with PBS. Bound peptides were probed with 100 µL sera diluted 1 in 50 in 3% (w/v) Marvel/PBS for 1 hour at 25°C with rotation. Bound antibodies were detected with anti-IgG secondary antibodies for 1 hour at 25°C with rotation. The wells were washed as above. Ovine antibodies were detected using a mouse anti-ovine IgG secondary antibody (alkaline phosphatase (AP) conjugate) (1:10000 in 3% (w/v) Marvel/PBS, 100 µL/well) (Thermo Scientific). Bound bovine antibodies were detected using a rabbit anti-bovine secondary antibody (AP conjugate) (1:15000 in 3% (w/v) Marvel/PBS, 100 µL/well) (Sigma Aldrich). The wells were washed again as above. Bound secondary antibody was detected with 100 µL of SIGMAFAST™ p-Nitrophenyl Phosphate substrate (pNPP) (Sigma Aldrich). Absorbance was measured at 405 nm after 4 hours (bovine) or overnight (ovine) using a Tecan GeneIos plate reader. Steps of this protocol were empirically optimised as follows:

2. 2.11.1. Incubation Temperature

Assay temperature during incubation steps was optimised by running parallel ELISAs with incubation steps performed at room temperature or at 25°C. Incubation at 25°C resulted in a stronger development of observable signals. All incubation steps for subsequent ELISAs were therefore performed at 25°C.

2. 2.11.2. Antibody Concentrations

Rabbit anti-bovine IgG secondary antibodies (AP conjugate) were sourced from Sigma Aldrich and Invitrogen. These were diluted in 3% (w/v) Marvel/PBS and tested at concentrations from 1:15000 to 1:30000 (Sigma antibody) and 1:2000 to 1:20000 (Invitrogen antibody). Rabbit anti-ovine IgG secondary antibodies (AP conjugate) were sourced from Sigma Aldrich and Invitrogen. These were diluted

in 3% (w/v) Marvel/PBS and tested at concentrations from 1:5000 to 1:50000 (Sigma antibody) and 1:5000 to 1:60000 (Invitrogen antibody).

2. 2.11.3. Shaking Conditions

With antibody concentrations optimised, it was determined whether the use of agitation during incubation steps would enhance signal production. Agitation in assay incubation steps was optimised by running parallel ELISAs with incubation steps performed either still or shaking at 200 rpm on a plate shaker. Assays performed under shaking conditions displayed greater absorbance.

2. 2.12. Peptide Competition Assay (PCA)

The use of PCAs is to confirm the reactivity of diagnostic peptides, in this instance for sera based IgG antibodies. This was used to confirm the reactivity of anti-SBV and anti-scrapie IgG peptides identified through ELISA screening. 100 µL/well of peptide or PIF (negative control) at 100 µg/mL in 100 mM sodium carbonate-bicarbonate buffer, pH 9.6 was coated in triplicate in Nunc-Immuno Maxisorp 96 well plates at 4°C overnight. Wells were blocked with 100 µL of 3% (w/v) Marvel/ PBS for 1 hour at 25°C with agitation. Wells were washed x6 with PBST and x6 with PBS. Free peptide was prepared in a dilution series from 100 µg/mL to 0 µg/mL in sera diluted 1 in 50 in 3% (w/v) Marvel/PBS. 100 µL of free peptide/sera was added to each well for 1 hour at 25°C with rotation. Wells were washed x6 with PBST and x6 with PBS. Bound antibodies were detected with anti-IgG secondary antibodies in 3% (w/v) Marvel/PBS, 100 µL/well for 1 hour at 25°C with rotation. Wells were washed x6 with PBST and x6 with PBS and bound secondary antibody was detected with 100 µL/well of pNPP. Absorbance was measured at 405 nm after 4 hours (bovine) or overnight (ovine) using a Tecan GeneIos plate reader.

2. 2.13. Sera Dilution Assay

The reactivity of peptides for sera based IgG antibodies was also determined by performing ELISAs with sera from infected animals diluted into sera from negative animals. This was to ascertain the extent of non-specific binding which occurs in the assay. Wells of Nunc-Immuno Maxisorp plates were coated in triplicate with 100 µL/well of specific peptide or PIF (negative control peptide) at 100 µg/mL in 100 mM sodium carbonate-bicarbonate buffer, pH 9.6 at 4°C overnight. Wells were washed x6 with PBST and x6 with PBS. Wells were then blocked with 100 µL of 3% (w/v) Marvel/ PBS for 1 hour at 25°C with agitation. Wells were then washed x6 with PBST and x6 with PBS. Bound peptide was probed with positive sera in a

dilution series in negative sera from 100% to 0% diluted 1 in 50 in 3% (w/v) Marvel/PBS for 1 hour at 25°C with agitation. Wells were washed x6 with PBST and x6 with PBS and bound antibody detected with secondary antibody and pNPP as described above. Absorbance was measured at 405 nm after 4 hours (bovine) or overnight (ovine) using a Tecan GeneIos plate reader.

2. 2.14. Preparation of Biotinylated DNA Probes for Fluorescent Amplification Catalyzed by T7 Polymerase Technique (FACTT)

PCR reactions were set up as described in **Table 2. 2.9.1.** using the plasmid Tir pET41$_a$ (+) as a reaction template. This is a pET41$_a$ (+) plasmid containing the gene for translocated intimin receptor (Tir) from *E. coli*. The primers used in each reaction are shown in **Table 2. 2.14.** PCR reactions were performed with an initial denaturation for 5 minutes at 95°C followed by 30 cycles of 95°C for 30 seconds, 57°C for 30 seconds and 72°C for 30 seconds. The final step was performed at 72°C for 10 minutes. Reaction products were assessed by gel electrophoresis and purified using a NucleoSpin® Gel and PCR Clean-up kit as described in **Section 2. 2.9.** DNA concentration was determined using a Nanodrop 8000 Spectrophotometer.

Table 2. 2.14. Primers used for FACTT preparation.

Primer	Sequence (5'->3')	Tm (°C)	Modification
Tir F1	AGATCTCGATCCCGCGAA	57	5'-Biotin
Tir R1	AGTTCCTCCTTTCAGCAA	52.5	None

2. 2.15. Antibody Detection by FACTT

This describes the attempt to establish FACTT as a working method, based on the method reported by (Zhang et al. 2006). This step aimed to develop the detection of bound secondary antibodies using the biotinylated DNA probe and T7 RNA Polymerase. 20 µL of rabbit anti-bovine IgG secondary antibody (biotin-conjugated) was added in triplicate to wells of a 96-well Nunc-Immuno Maxisorp plate (Thermo Scientific) at concentrations of 1:4000-1:2000 in 20 mM sodium carbonate-bicarbonate buffer, pH 9.6, overnight at 4°C. As a negative control 100 µL of 100 µg/mL BSA was added in triplicate 100 mM sodium carbonate-bicarbonate buffer, pH 9.6, overnight at 4°C. Wells were blocked with 20 µL of 3% (w/v) Marvel/ PBS for 1 hour at 25°C with agitation. Wells were washed x3 with PBST and x3 with PBS. 20 µL of 0.5 µg/mL of streptavidin (Sigma Aldrich) in 3% (w/v) Marvel/PBS was incubated in each well for 1 hour at room temperature.

Wells were washed 6x with PBST. 20 µL of 250 ng/mL biotinylated DNA probe (**Section 2. 2.15.**) was incubated in each well at room temperature for 1 hour. Wells were washed 6x with PBST. 20 µL of reaction mix was added to each well, consisting of 60 U T7 RNA Polymerase (New England Biolabs, NEB) and 1.25 µM rNTPs (NEB) in 1x T7 buffer (NEB). Plates were incubated at 37°C for 3 hours. 20 µL of 250 ng/µL biotinylated DNA probe was added in triplicate as a positive control. 20 µL of Quant-iT™ RiboGreen™ (Thermo Scientific) was added (diluted 1:200 in dH_2O) to each well. The plate was read at an excitation wavelength of 485 nm and an emission wavelength of 530 nm using a FLUOstar® Omega plate reader (BMG Labtech).

2. 2.16. Preparation of Biotinylated DNA Probes for Real Time Immuno PCR (RT-IPCR)

This method, including primers and probes, were adapted from the protocol described by (He and Patfield, 2015). PCR reactions were set up as described in **Table 2. 2.9. 1.** with the primers F1 and R1 (**Table 2. 2.16.**) and using the plasmid pUC19 as the reaction template (He and Patfield, 2015). PCR reactions were performed with an initial 95°C denaturation for 10 minutes followed by 40 cycles of 95°C for 15 seconds and 62°C for 1 minute. Reaction products were assessed and purified by gel electrophoresis using a NucleoSpin® Gel and PCR Clean-up kit as described in **Section 2. 2.9**. The concentration of products was determined using a Nanodrop 8000 Spectrophotometer.

Table 2. 2.16. Primers used for RT-PCR preparation and reactions.

Primer	Sequence (5'->3')	Tm (°C)	Modification
F1	CCCGGATCCCAGCAATAAACCAGCCAGCC	72.3	5'-Biotin
R1	TATGCAGTGCTGCCATAACCATGA	61	None
RTF	CCATAACCATGAGTGATAACACTGCT	61.6	None
RTR	CGATCAAGGCGAGTTACATGATC	60.6	None
RT IPCR Probe 1	ACCGAAGGAGCTAACCGCTTTTTTGCAC	66.6	5'-FAM 3'-BHQ1

These primer sequences were obtained from He and Patfield, 2015. BamHI restriction sites are underlined.

2. 2.17. RT-IPCR

This method is the typical RT-IPCR protocol developed in this study. 100 µL of peptides (100 µg/mL in 100 mM sodium carbonate-bicarbonate buffer, pH 9.6) were coated in triplicate in maleic anhydride activated 96 well plates (Thermo Scientific) at 37°C overnight. Wells were blocked with 100 µL of 3% (w/v) Marvel milk powder in PBS for 1 hour at 25°C with rotation. Wells were washed x6 with PBST and x6 with PBS. Bound peptides were probed with 100 µL of sera diluted 1:50 in 3% (w/v) skimmed milk powder/PBS for 1 hour at 25°C with rotation. Secondary anti-ovine antibody biotin-conjugate (Thermo Scientific) was incubated with streptavidin at a 1:2 molar ratio in 3% (w/v) Marvel/PBS for one hour at room temperature. Bound ovine antibodies were probed using the secondary-streptavidin conjugate for 1 hour at 25°C. Wells were washed 3x with PBST and 4x with sterile TETBS (TBS with 5 mM EDTA and 0.05% (v/v) tween20). Wells were incubated with 100 µL of biotinylated DNA probe (0.5 ng/µL in TETBS) for 1 hour at room temperature. The wells were then incubated with 100 µL of 1U BamHI in Buffer 3.1. (New England Biolabs) for 2 hours at 37°C. Digests were stored at 4°C overnight. 50 µL of digested product was transferred to a fresh 0.2 mL clear polystyrene PCR tube (Greiner Bio-One). 15 µL of product was used in RT-PCR as described in (**Table 2. 2.17.**). The primers and probe used in these reactions are displayed in (**Table 2. 2.16.**). PCR reactions were performed as described in **Section 2. 2.9.** on a CFX Real Time Detection System prepared in Hard Shell® 96 well PCR plates (Bio-Rad). Controls included 1 µL of biotinylated DNA probe at 0.5 ng/µL (positive control) or 15 µL of dH_2O (negative control). Wells treated with secondary antibody only acted as a background control. Results were analysed using CFX Manager Software (Bio-Rad).

Table 2. 2.17. The conditions used in RT-IPCR.

Volume (µL)	Reagent	Concentration
5	Platinum Hi Fi Buffer	10X
1	dNTPs	10 mM
2	$MgSO_4$	50 mM
1	RTF	10 µM
1	RTR	10 µM
15	Template	N/A
0.2	Platinum Taq Polymerase High Fidelity	5 U/µL
24.8	dH_2O	N/A
2.5	RT IPCR Probe 1	10 µM

ELISAs were performed in parallel to RT-IPCR assays, where secondary antibody biotin-conjugates were detected using streptavidin-HRP conjugate as described in **Section 2. 1.15.** This method was produced through optimisation of each protocol step. Steps were optimised empirically to produce this method. This was done using both SBV peptide 15 versus sera 726 and scrapie peptide 2 versus sera PG0350:

2. 2.17. 1. Antibody Concentration

Rabbit anti-bovine and anti-ovine IgG (H+L) secondary antibodies (biotin conjugated) were sourced from Sigma Aldrich and Thermo Scientific. These antibodies were diluted in 3% (w/v) Marvel/PBS and tested at concentrations from 1:4000 to 1:20000, detected with streptavidin-HRP conjugate as described in **Section 2. 1.15**.

2. 2.17. 2. Plate Immobilisation

With secondary antibody concentrations optimised, four types of plate were tested for their efficacy in peptide ELISAs: Nunc-Immuno Maxisorp plates, MicroWell™ Polysorp® Immobilizer plates (Sigma Aldrich), maleic anhydride activated 96 well plates (Thermo Fisher Scientific) and streptavidin coated plates (Alpha Diagnostic International). Maleic anhydride coated plates proved the most efficacious.

2. 2.17. 3. Biotin-Streptavidin Conjugate formation

With the plate type optimised, three methods of detecting peptide-captured IgGs were tested: sequential, modular or direct (Niemeyer et al., 2007). In the sequential method, anti-IgG secondary antibody, streptavidin and biotinylated DNA probe were added to the plate in sequential incubation steps of 1 hour at room temperature, separated by washing x3 with TETBS and x3 with TBS. In the modular method, biotinylated secondary antibody and streptavidin were preincubated together for 1 hour at room temperature before use. In the direct method biotinylated secondary, streptavidin and biotinylated DNA probe were all preincubated together for 1 hour at room temperature before use. None of the methods proved more effective. The modular method was chosen as the preferred method to limit the required volume of biotinylated DNA probe for each assay.

2. 2.17. 4. Comparing the Sensitivity of RT-IPCR with Peptide ELISA

To compare the sensitivity of peptide ELISAs and RT-IPCR, sera PG1409/08 was used to coat a Nunc-Immuno Maxisorp plate in increasing dilutions of 1:2500 to 1:15000. Bound antibodies were detected using anti-ovine IgG antibodies (AP

conjugated or biotin conjugated) for detection. RT-IPCR was not more sensitive than the peptide ELISAs.

2. 2.18. Screening Peptides by Optimised Enzyme Linked Immunosorbent Assay

The following method represents the optimised ELISA protocol developed in this study. 100 µL of peptides or PIF (negative control) (100 µg/mL in 100 mM sodium carbonate-bicarbonate buffer (pH 9.6) were coated in duplicate in maleic anhydride activated 96 well plates at 37°C overnight. Wells were blocked with 100 µL of 3% (w/v) Marvel/TBS for 1 hour at 25 °C with rotation. Wells were washed x6 with TBST and x6 with TBS. Bound peptides were probed with 100 µL sera diluted 1:50 in 3% (w/v) Marvel/TBS (pre-blocked for 1 hour at room temperature) for 1 hour at 25°C with rotation. Plates were washed as above. Bound ovine antibodies were detected using a rabbit anti-ovine IgG (H+L) secondary antibody (AP conjugate) (1:10000 in blocking buffer, 100 µL/well). Plates were washed as above. Bound bovine antibodies were detected using an anti-bovine IgG (H+L) secondary antibody (AP conjugate) (1:15000 in blocking buffer, 100 µL/well). Plates were washed as above. Bound secondary was detected with 100 µL of pNPP. Absorbance was measured at 405 nm after 1 hour (bovine) or 2 hours (ovine) using a Tecan GeneIos plate reader. This method was produced through empirical optimisation of each protocol step:

2. 2.18. 1. Plate Immobilisation

Four types of plate were tested for their efficacy in peptide ELISAs: Nunc-Immuno Maxisorp plates, 96 well Microwell™ Polysorp® Immobilizer plates, maleic anhydride activated 96 well plates and streptavidin coated plates. Maleic anhydride coated plates proved the most efficacious for assay development.

2. 2.18. 2. Sera Pre-Incubation

To investigate the possibility of minimising background readings, ELISAs were performed with sera diluted in 3% Marvel/PBS and incubated at room temperature for 1 hour before use. This demonstrated to decrease background signals, and was incorporated into the method.

2. 2.18. 3. Assay Buffer

ELISAs were typically performed using PBS and PBST as the buffers of choice. As an alternative, TBS and TBST were utilised as replacement buffers for PBS and

PBST, respectively. TBS and TBST were observed to marginally decrease background signals.

2. 2.19. 4. Purified Ovine IgG Capture

Purified IgG antibodies were prepared from sera by melon gel or Surebeads™ Protein G Coupled Magnetic Beads as described in **Section 2. 2.5.** and **2.6.** ELISAs were performed using a dilution series of purified IgGs from 50-0 µg/mL in 3% (w/v) Marvel/TBS at 100 µL/well. This was done in parallel with sera diluted 1:50 in 3% (w/v) Marvel/TBS as a comparison. Diluted sera continued to produce the greatest observable signal.

2. 2.19. Peptide ELISA Data Analysis

Mean absorption values were calculated for each sample. Mean values for each background control (treated with buffer only) were also calculated, plus 3x the standard deviation. These values acted as a cut off value, and were subtracted from each sample value. Alternatively, the mean values for the negative peptide control PIF were subtracted from each sample. Receiver Operator Characteristic (ROC) analysis was performed with Graphpad Prism 7 on the data. Area under the curve (AUC) and p values were produced using a confidence interval (CI) of 95%, with discriminatory peptides being determined as having a p value of <0.05.

Chapter 3: Characterisation of Recombinant PrPs as Therapeutic Ligands

3.1. Introduction

Research into prion therapeutics has predominantly focused on pharmaceutical or antibody based treatments to delay or prevent prion propagation and the onset of symptoms (Panegyres & Armari 2013). Potential therapeutics such as suramin, congo red, tetrapyrollic compounds, thioflavin, dendramers and copper have shown promising results in both cell-free and cell culture *in vitro* models (Trevitt & Collinge 2006; Rigter et al. 2010; Mccarthy et al. 2013; Panegyres & Armari 2013). Despite promising results *in vitro*, these therapeutics have not been as successful *in vivo* (Féraudet et al. 2005; Panegyres & Armari 2013). However, a small number of candidate therapeutics have been tested in clinical trials, following successful studies *in vitro* and in *in vivo* animal models. These therapeutics include PPS, quinacrine, tetracyclines and flurpirtine maleate (Otto et al. 2004; Tsuboi et al. 2009; Collinge et al. 2009; Geschwind et al. 2013; Haik et al. 2014; Forloni et al. 2015). However, none of these therapeutics have yet displayed any effective management or reversal of disease symptoms. Furthermore, their assessment can be limited by factors including their inability to cross the blood brain barrier and the limited number of patients in clinical trials (Pangyres & Armari 2013; Haik et al. 2014). To date there remains an imperative for the development of therapeutics that can effectively manage or reverse disease symptoms.

Candidate therapeutic ligands also include protein and peptide inhibitors. For example, the investigation into synthetic prion peptides as therapeutic ligands led to a group of anti-PrP^{Sc} peptides known as β-sheet breakers (Soto et al. 1998; Soto et al. 2000). These peptides developed by Soto and colleagues displayed inhibitory activity in *in vitro* cell free assays against both scrapie and amyloid β deposition, and reduced mouse adapted scrapie (139A) infectivity in transgenic mice (Soto et al. 1998; Soto et al. 2000). Despite these promising reports, the therapeutic potential of these peptides is limited by their size, toxicity, vulnerability to proteolysis and inability to cross the blood brain barrier (Chabry 1998; Chabry et al. 1999; Féreaudet et al. 2005). Prion peptides have since been utilized as inhibitors in PMCA, with limited success (Rigter et al. 2009). Consequently, no peptide-based therapeutics for prion diseases have yet been developed.

Protein based inhibitors include heterologous PrP^{C}, which has been reported to inhibit prion propagation *in vitro* and *in vivo* (Scott et al. 1993; Priola et al. 1994; Horiuchi et al. 2000; Geoghegan et al. 2009; Kobayoshi et al. 2009; Kobayoshi et al. 2015; Asante et al. 2015; Skinner et al. 2015; Seelig et al. 2015). Recently it

was identified that human and mouse rPrP can inhibit prion propagation in PMCA and ScN2a cell culture (Yuan et al. 2013). This followed previous reports that recombinant PrP can interfere in prion amplification by PMCA (Nishina et al. 2006; Gonzalez-Montalban et al. 2011). Recombinant hamster PrP has since been reported to prolong the propagation and development of symptoms of RML-Chandler scrapie in transgenic mice (Skinner et al. 2015). These studies highlight the potential therapeutic application of recombinant and heterologous PrPs.

In this study, the use of recombinant PrPs as therapeutic ligands was investigated in the *in vitro* model of prion propagation, PMCA. This tested three ovine rPrPs (rVRQ, rARR and rARQ) as well as hamster rPrP (rHam) as inhibitors of scrapie and bovine BSE amplification by PMCA. The protein rVRQ was further used as an inhibitor of distinct scrapie and BSE strains. The mechanism of inhibition was then investigated by testing the affinity of rVRQ for PrP^{Sc} and the role of rPrP secondary structure in the inhibitory mechanism.

3.2. Results

3.2.1. Expression and Purification of Recominant Ovine and Hamster PrPs

The recombinant prion proteins rVRQ, rARQ, rARR and rHam (residues 23-231) were expressed in *E. coli* and purified by IMAC to the level of single protein bands of approximately 24 kDa, assessed by SDS-PAGE (**Figure 3.2.1.**). The purified product for each protein was assessed by Bradford assay using a standard BSA curve, with a mean yield of 12 mg per litre of bacterial culture.

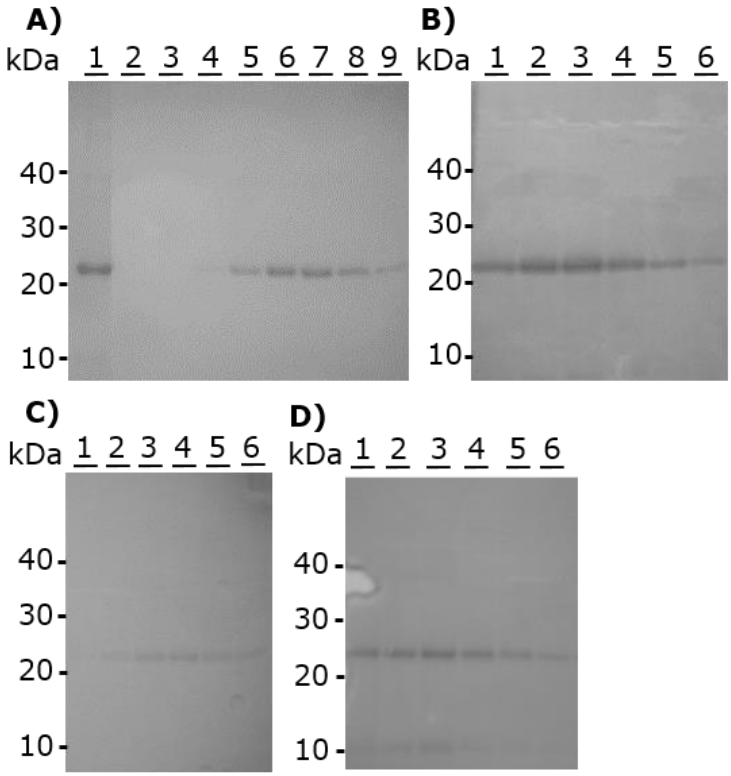

Figure 3.2.1. SDS-PAGE analysis of rPrPs expressed in E. coli followed by purification with IMAC. **A)** Analysis of rVRQ eluted fractions. Lane 1: rVRQ protein from inclusion bodies solubilised in urea, 4.5 µL was analysed from a total of 30 mL of solubilised rVRQ. Non-purified rPrP is shown for rVRQ only. Lanes 2-9: elution fractions after IMAC. **B)** Analysis of rARQ eluted fractions. Lanes 1-6: elution fractions. **C)** Analysis of rARR eluted fractions. Lanes 1-6: elution fractions. **D)** Analysis of rHam eluted fractions. Lanes 1-6: elution fractions. 4.5 µL of each elution fraction was analysed from a total of 2 mL. Molecular weight markers are shown.

3.3. Assessing the Efficacy of rPrP Inhibitors in Scrapie Amplification

To investigate the potential use of the recombinant proteins as inhibitors of prion propagation, rVRQ, rARQ, rARR and rHam were tested in a dilution series from 0 to 1200 nM in PMCA with classical scrapie (PG1361/05, ARQ/VRQ) (**Figure 3.3.1.**). 1200 nM rVRQ was used as an inhibition control confirmed by western blotting (**Figure 3.3.2.**). PrP^{C} substrate controls were included to assess the efficacy of PK digestion. The 100% inhibition control was used as a background reading for each blot. rPrPs were added prior to PMCA commencement, and inhibitory activity was determined by the PrP^{Sc} levels on blots measured by densitometry using ImageJ software. Decreases in signal intensities were then calculated as percent inhibition relative to untreated controls (no rPrP), from which mean inhibitor concentration 50% (IC50) values were calculated by plotting percent inhibition against log concentration (**Figure 3.3.4.**). From these data, it was determined that the protein rVRQ was the strongest overall inhibitor of scrapie amplification with a mean IC50 of 122 nM. This was followed by hamster (181 nM), rARQ (288 nM) and rARR (505 nM). These values were calculated from three independent experiments for each inhibitor. Reactions treated with rVRQ, rARR and rARQ were also analysed by western blotting to cross reference the values obtained by dot blotting (**Figure 3.3.3., 3.3.5.**), the method previously used to generate inhibition values following PMCA (Yuan et al. 2013). The IC50 values calculated from the western blots were 85 nM for rVRQ, 515 nM for rARR and 201 nM for rARQ. As these relative values were similar to those calculated by dot blotting, not all reactions were analysed and these data show that the dot blot is indeed detecting PrP^{Sc} identified as a triplet by western blot. PMCA reactions were also treated with an unrelated protein control (BSA) at a concentration of 1200 nM which had no statistically significant inhibitory effect on amplification ($p = 0.97$) whereas reactions treated with 1200 nM rVRQ were significantly different ($p = 0.03$), calculated by an unpaired Student's t-test (**Figure 3.3.6.**).

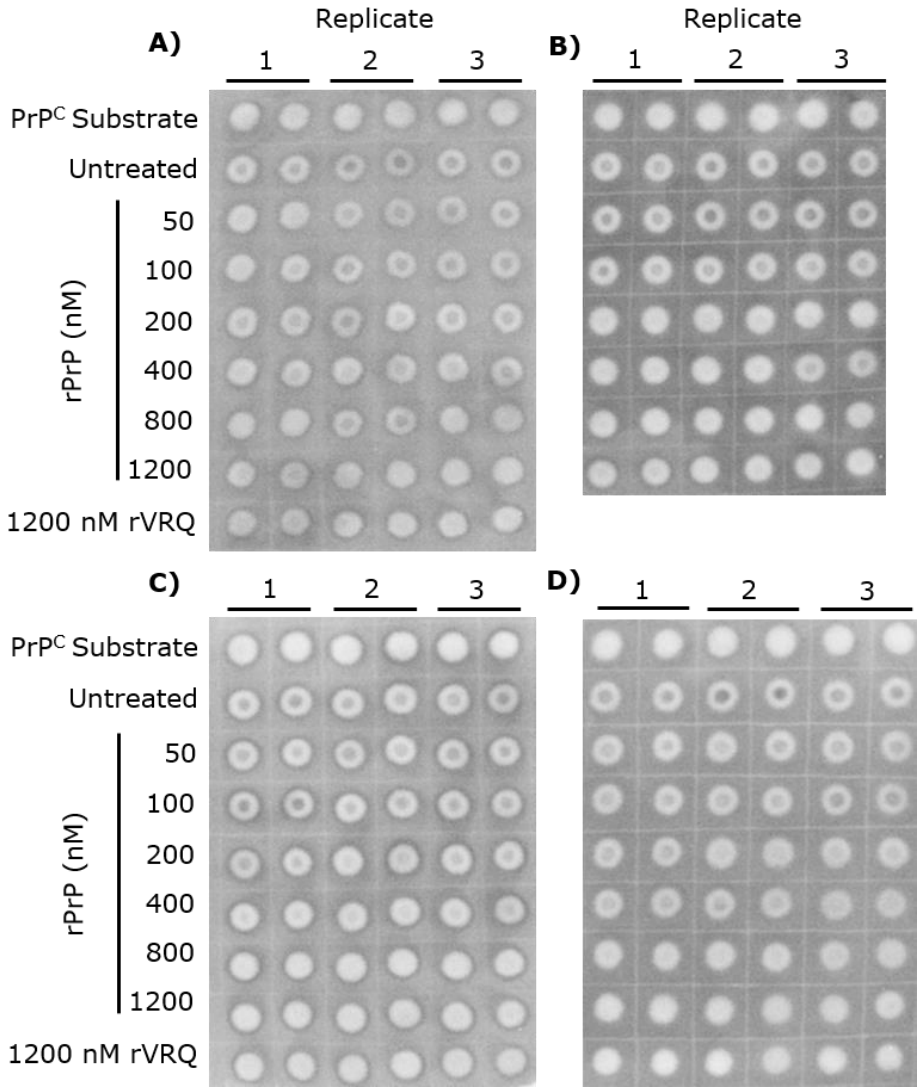

Figure 3.3.1. Representative dot blots of scrapie (PG1361/05) PMCA reaction products amplified in the presence or absence of **A)** rARR **B)** rVRQ **C)** rHam **D)** rARQ. The inhibitors were tested in a dilution series of 50-1200 nM. PrP^C substrate and uninhibited PMCA product controls are shown, with 1200 nM rVRQ reactions used as an inhibition background control. As a consequence, rVRQ inhibition was only measured up to 800 nM. PrP^C substrate controls are included to demonstrate the efficacy of PK digestion. Reactions were performed in triplicate, and blotted in duplicate to account for intra blot variation. 0.83 µL of PK digested PMCA product was analysed per reaction. The entire experiment was repeated 3 times to generate the mean IC50 values.

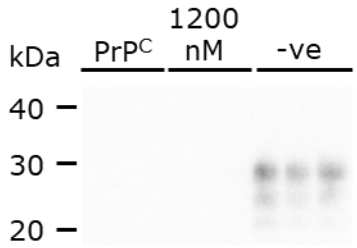

Figure 3.3.2. PMCA reactions treated with 1200 nM rVRQ, analysed by western blotting. PrP^C substrate and uninhibited PMCA product controls (-ve) are shown. PrP^C substrate controls are included to demonstrate the efficacy of PK digestion. Reactions were performed in triplicate, and 6.7 µL of PK digested PMCA product was analysed per reaction. Each blot included PrP^C and uninhibited (-ve) controls. Molecular weight markers are shown. The mean percent inhibition was calculated as 94% with a standard deviation of 1.9.

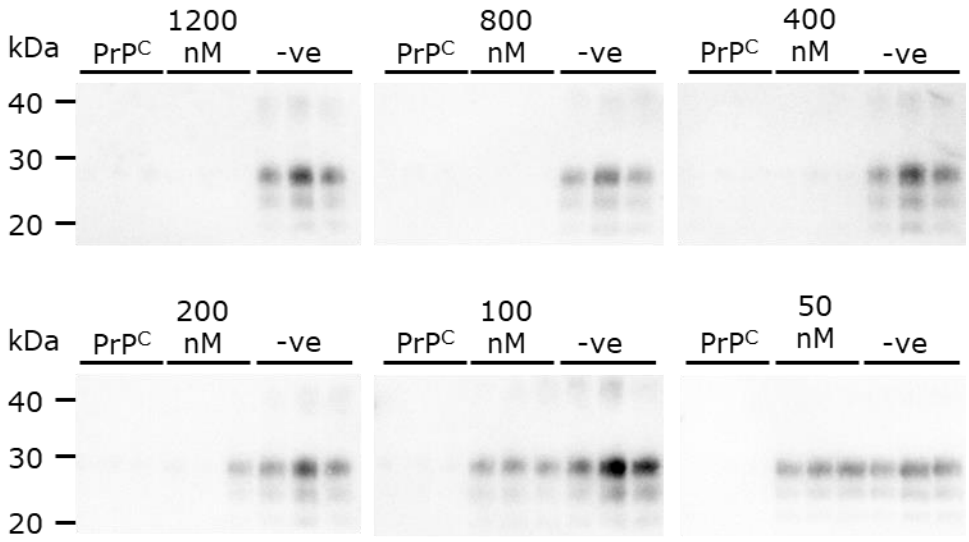

Figure 3.3.3. Representative western blots of rVRQ treated PMCA reactions. rARR and rARQ reactions were also analysed by western blot (data not shown) to cross reference the IC50 values calculated from dot blotting. 6.7 µL of PK digested PMCA product was analysed per reaction. Each blot included PrP^C and uninhibited (-ve) controls. Molecular weight markers are shown. The entire experiment was repeated 3 times to generate the mean IC50 values.

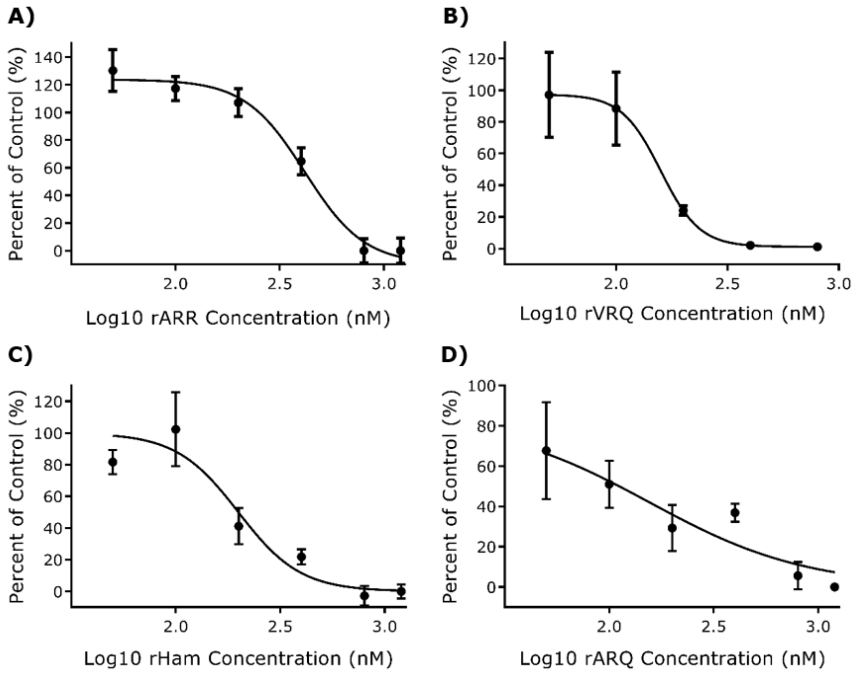

Figure 3.3.4. Representative plots displaying log concentration of rPrP inhibitors versus percent of control PrP^{Sc} levels for classical scrapie (ARQ/VRQ, PG1361/05) amplification. **A)** rARR **B)** rVRQ **C)** rHamster **D)** rARQ. These values were calculated from densitometry analysis of each dot blot. Mean IC50s for each protein were calculated as 505 nM for rARR, 122 nM for rVRQ, 228 nM for rARQ and 181 nM for rHamster. Each inhibitor was tested in a dilution series of 50, 100, 200, 400, 800 and 1200 nM. 1200 nM rVRQ was used as an inhibition background control. As a consequence, only data points for 50-800 nM are displayed for rVRQ treated reactions.

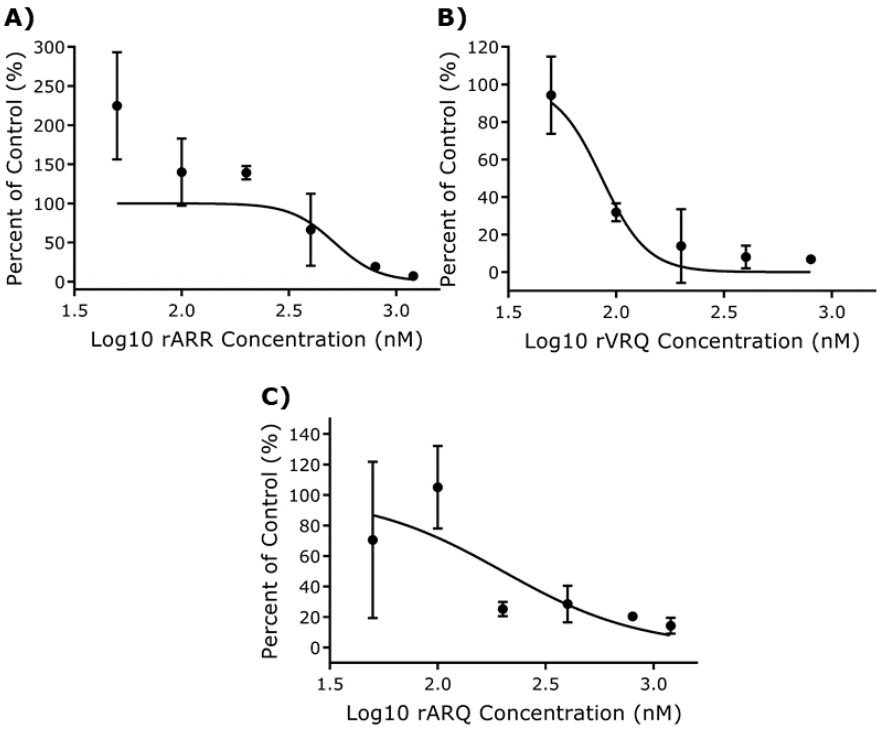

Figure 3.3.5. Representative plots displaying log concentration of rPrP inhibitors versus percent of control PrP^{Sc} levels for classical scrapie (ARQ/VRQ, PG1361/05) amplification. **A)** rARR **B)** rVRQ **C)** rARQ. Each inhibitor was tested in a dilution series of 50, 100, 200, 400, 800 and 1200 nM. IC50s calculated were 85 nM for rVRQ, 515 nM for rARR and 201 nM for rARQ. These values were calculated from densitometry analysis of each blot. 1200 nM rVRQ was used as an inhibition background control. Consequently, only data points for 50-800 nM are displayed for rVRQ treated reactions.

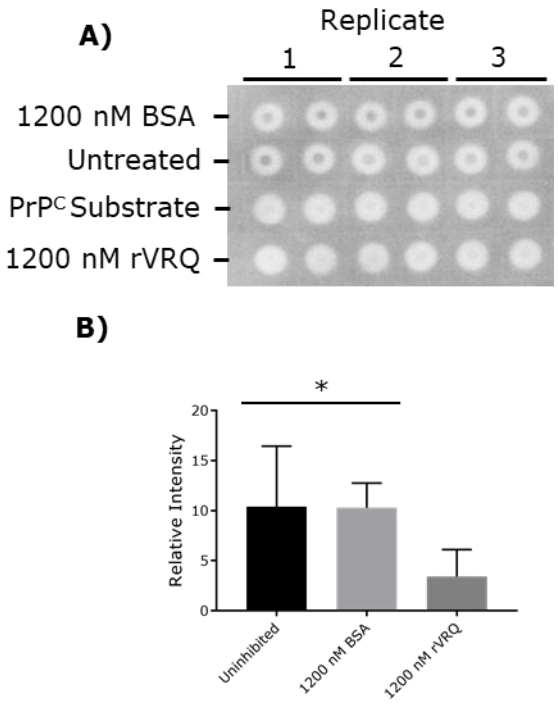

Figure 3.3.6. PMCA reactions were treated with 1200 nM BSA as an unrelated protein control. **A**) Dot blot analysis of PMCA reactions treated with 1200 nM BSA and 1200 nM rVRQ (postive inhibition control). Reactions were performed in triplicate and blotted in duplicate to account for intra-blot variation, and 0.83 µL of PK digested PMCA product was analysed per reaction. PrP^C substrate controls and untreated controls are shown. **B**) Dot blots were analysed by densitometry and plotted using Graphpad Prism 7. *: p values <0.05. The difference in amplification between uninhibited reactions and 1200 nM treated reactions was statistically significant as determined by an unpaired Student's t-test (p = 0.03).

3.4. Inhibition of Bovine BSE Amplification with rVRQ and rARQ

Out of the rPrP proteins tested in scrapie PMCA, rVRQ was observed to have the highest inhibitory activity with a mean IC50 of 122 nM. As the proteins rVRQ and rARQ share sequence homology to the scrapie seed and for rVRQ the substrate used for amplification (ARQ/VRQ and VRQ/VRQ, respectively), it was hypothesised that this sequence homology contributed to inhibitor efficacy.

Firstly, conditions for bovine BSE PMCA were optimised. It was observed that the elution buffer used for storing the rPrP proteins interfered with bovine BSE prion amplification. This activity was previously undetected as the scrapie strain utilised in initial experiments displayed no inhibition when amplified with elution buffer. This interference was investigated by performing PMCA with bovine BSE in the presence of the different buffer components. Bovine BSE amplification appeared to be inhibited in the presence of elution buffer over five rounds of PMCA, but inhibition was not observed in the presence of other reaction constituents (**Figure 3.4.1.**). Bovine BSE was then amplified in the presence of either elution buffer or conversion buffer (**Figure 3.4.2.**). Both bovine BSE isolates amplified over 5 rounds of PMCA with conversion buffer, but amplification was inhibited in the presence of elution buffer (**Figure 3.4.2.**). Therefore, rPrPs were dialysed with conversion buffer prior to use in all subsequent PMCA experiments. The bovine BSE isolate SE1762/0013 was found to amplify in bovine substrate sufficiently over 1 round of PMCA to allow for the determination of IC50 values. Therefore, SE1762/0013 was used in subsequent PMCA reactions. Using these conditions, rVRQ and rARQ were tested in a dilution series from 50 nM to 1200 nM using SE1762/0013 as PrP^{Sc} seed (**Figure 3.4.3.**). Inhibition controls consisted of the scrapie isolate PG1361/05 treated with 1200 nM rVRQ. Densitometry values were plotted in Graphpad Prism 7 and used to calculate mean IC50 values of 171 nM for rVRQ and 336 nM for rARQ (**Figure 3.4.4.**).

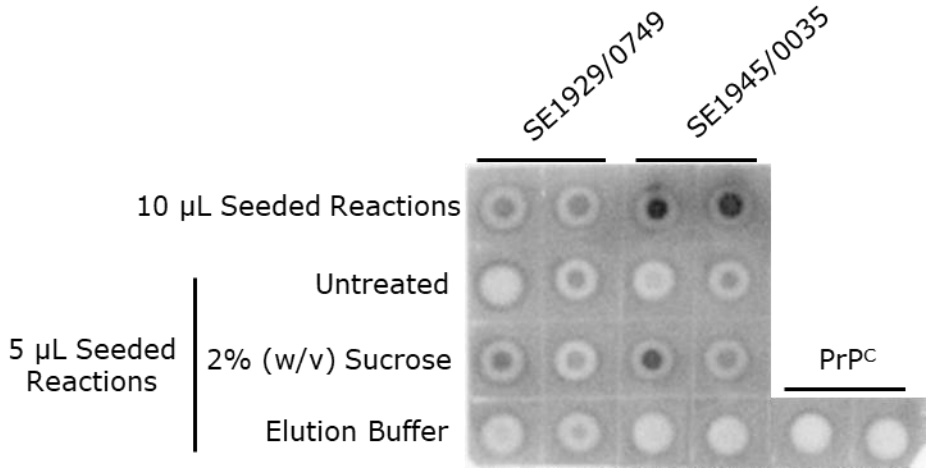

Figure 3.4.1. Determining optimum amplification conditions for bovine BSE. Bovine BSE isolates SE1929/0749 and SE1945/0035 were amplified for 5 rounds of PMCA in bovine substrate. Controls included reactions seeded with 10 µL bovine BSE as a positive amplification control and PrP^C substrate control. Reactions seeded with 5 µL of BSE isolate were either untreated, treated with 2% (w/v) sucrose in elution buffer without imidazole, or with elution buffer containing 500 mM imidazole.

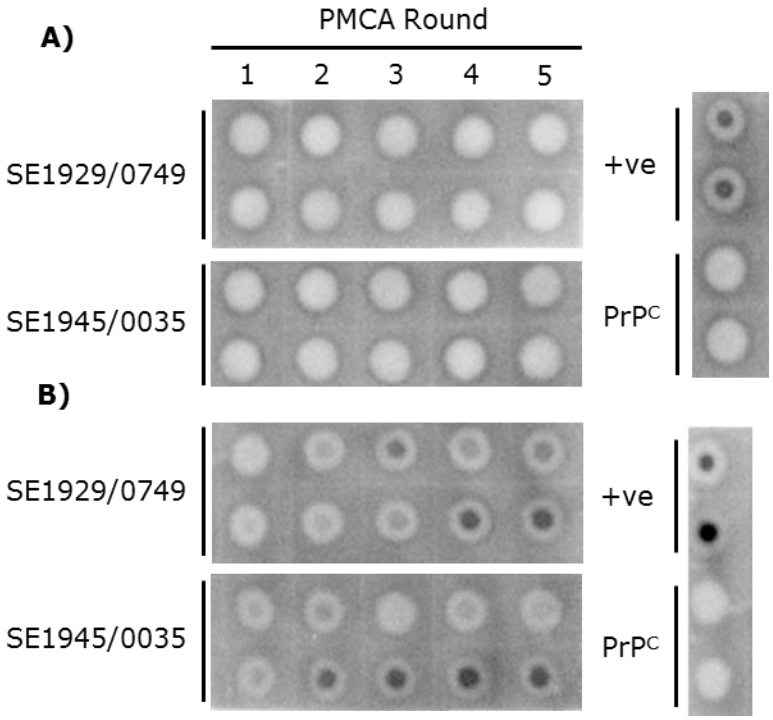

Figure 3.4.2. Amplification of bovine BSE with **A)** elution buffer or **B)** conversion buffer. Images were taken from the same blots, exposed for the same amount of time. Reactions were blotted in parallel with reactions treated with rVRQ which are not displayed. PMCA reactions were performed over 5 days in duplicate, and 0.83 µL of PK digested PMCA product was analysed per reaction. PrP^C substrate controls and PG1361/05 positive amplification (+ve) controls are shown. PG1361/05 was used as an amplification control due to the greater availability of brain homogenate.

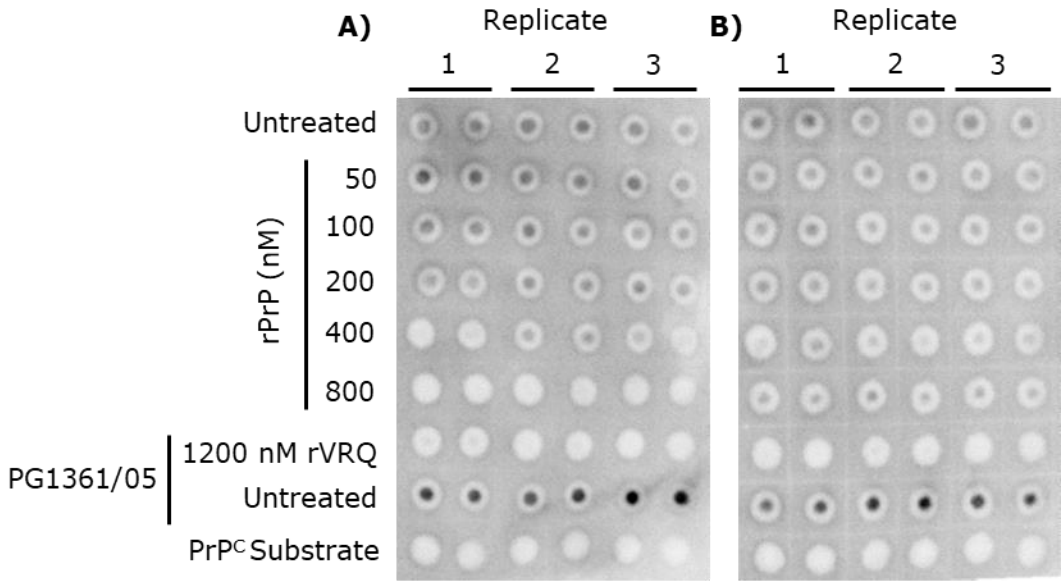

Figure 3.4.3. Representative dot blots of PMCA reaction products amplified in the presence of **A)** rVRQ **B)** rARQ in bovine BSE (SE1762/0013). The inhibitors were tested in a dilution series of 50-800 nM of rPrP. Controls included PrP^C substrate, untreated PMCA reactions, and reactions treated/untreated with 1200 nM rVRQ with the scrapie isolate PG1361/05. 1200 nM rVRQ reactions used as an inhibition background control. Reactions were performed in triplicate and blotted in duplicate to account for intra blot variation, with 0.83 µL of PK digested PMCA product was analysed per reaction. rVRQ and rARQ were dialysed against conversion buffer prior to use. All experiments were repeated 3 times to generate mean IC50 values.

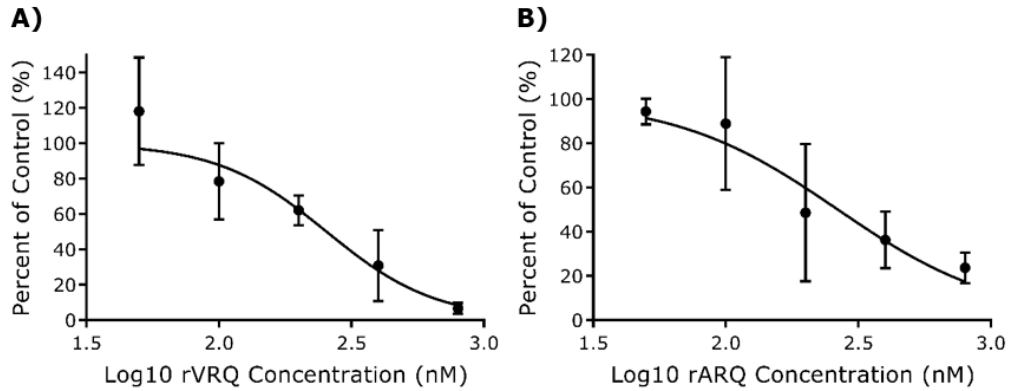

Figure 3.4.4. Representative plots displaying log concentration of rPrP inhibitors versus percent of control in bovine BSE (SE1762/0013). These values were calculated from densitometry analysis of each dot blot. **A)** rVRQ **B)** rARQ. Mean IC50s for each protein were calculated as 171 nM for rVRQ and 336 nM for rARQ. Each inhibitor was tested in a dilution series of 50, 100, 200, 400 and 800 nM. 1200 nM rVRQ in scrapie (PG1361/05) amplification was used as an inhibition background control.

3.5. Optimising Prion Strain Amplification by PMCA

The protein rVRQ was identified as the strongest inhibitor of both scrapie and BSE prion amplifications with mean IC50 values of 122 nM and 171 nM, respectively. Due to this activity, it was questioned whether rVRQ could be used as an inhibitor of different ruminant prion strains. Firstly, the amplification conditions for different prion strains were optimised. To optimise the amplification conditions for each strain, PMCA reactions were performed for up to five rounds of sPMCA, and isolates were initially amplified using substrate with a matching genotype. Classical scrapie (PG1361/05, with *Prnp* genotype ARQ/VRQ and PG1563/02, VRQ/VRQ), transgenic mouse passaged strain Apl_{338}ii scrapie (MC140403 and MC140404, both VRQ/VRQ), transgenic mouse passaged strain G_{338} scrapie (MC136477 and MC136553, both VRQ/VRQ) isolates were observed to amplify over 5 days in ovine VRQ/VRQ substrate with 0.5 µL of PrP^{Sc} seed (**Figure 3.5.1.**). The isolates MC140403, MC136477 and MC136553 required up to 5 days of sPMCA for successful amplification. Therefore, further PMCA reactions were analysed at round 5 only. Additional classical scrapie isolates PG0157/05 (AHQ/VRQ) and PG1499/02 (AHQ/VRQ) were investigated for amplification in VRQ/VRQ or AHQ/AHQ substrate in reactions seeded with 0.5 µL or 5 µL PrP^{Sc}, analysed by western blotting (**Figure 3.5.2. A**). Although both PG0151/05 and PG1499/02 were observed to amplify after 5 days in ovine VRQ/VRQ substrate and with 5 µL of PrP^{Sc} seed, the isolates PG1361/05 and PG1563/02 had already been identified to amplify in VRQ/VRQ substrate. Additionally, PG0157/05 and PG1499/02 could not be amplified consistently under these conditions. Therefore, PG1361/05 and PG1563/02 were selected for inhibition by rVRQ. The CH1641 scrapie isolate J2935 (AHQ/ARQ) had been previously reported to be amplified in AHQ/AHQ or ARQ/ARQ substrate (Taema 2012). Therefore, amplification of J2935 was investigated in these substrates with reactions seeded with 5 µL of PrP^{Sc}. It was observed that J2935 successfully amplified in ovine AHQ/AHQ substrate over 5 days, with 5 µL of PrP^{Sc} seed (**Figure 3.5.2. B**). Ovine BSE isolates PG0392/04 and PG1693/04 (ARQ/ARQ) were also previously reported to be amplified in VRQ/VRQ, ARQ/ARQ and AHQ/AHQ substrates. Both isolates were observed to amplify successfully over 5 days in ovine VRQ/VRQ substrate with 0.5 µL PrP^{Sc} seed (**Figure 3.5.2. B**). Amplification of bovine BSE had been previously optimised.

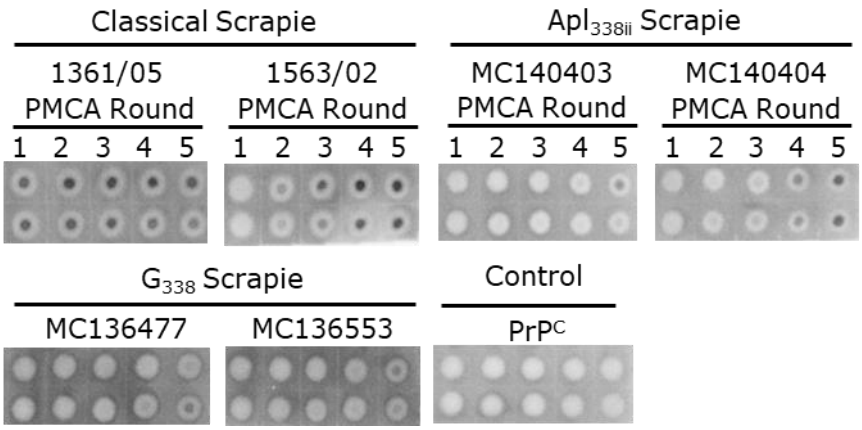

Figure 3.5.1. Scrapie prion isolates were identified that could amplify over 5 rounds of PMCA in ovine VRQ/VRQ substrate. Reactions were performed in duplicate, and PMCA products from cycles 1-5 were analysed by dot blotting to determine the optimal round for analysing rVRQ inhibition. The control included is PK digested PrP^C substrate. 0.83 µL of PK digested PMCA product was analysed per reaction.

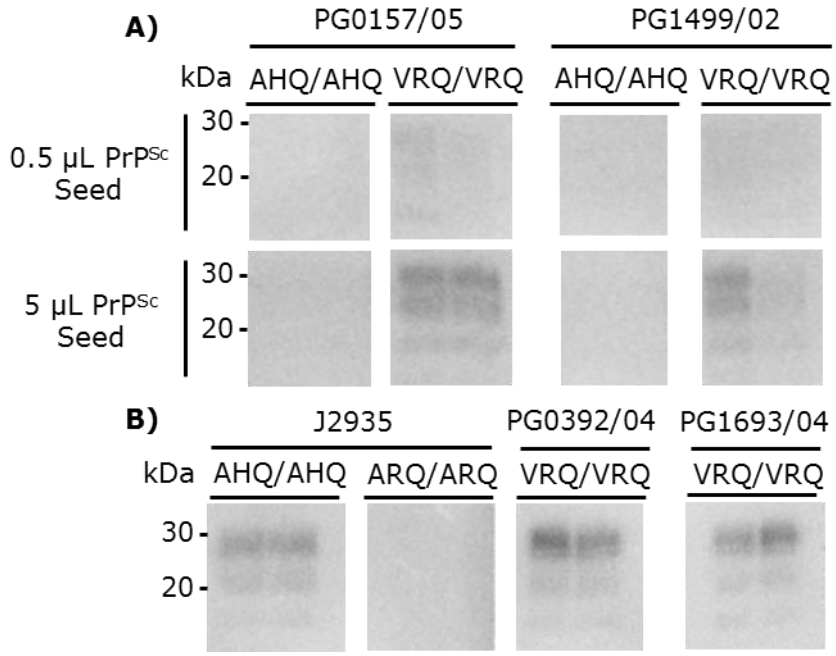

Figure 3.5.2. Western blot analysis of day 5 amplification products of classical scrapie, CH1641 scrapie and ovine BSE. **A**) Classical scrapie isolates PG0157/05 (AHQ/VRQ) and PG1499/02 (AHQ/VRQ) were amplified over 5 PMCA rounds in AHQ/AHQ or VRQ/VRQ ovine substrate, with either 0.5 µL or 5 µL of PrP^{Sc} seed. **B**) CH1641 scrapie isolate J2935 (AHQ/ARQ) was amplified over 5 PMCA rounds in AHQ/AHQ or ARQ/ARQ substrate with 5 µL of PrP^{Sc} seed. Additionally, ovine BSE isolates PG0392/04 and PG1693/04 (ARQ/ARQ) were amplified over 5 PMCA rounds in VRQ/VRQ substrate with 5 µL of PrP^{Sc} seed. Reactions were performed in duplicate. 6.7 µL of PK digested PMCA reaction was analysed per reaction. Molecular weight markers are shown.

3.6. Characterising the rVRQ Protein as an Inhibitor of Scrapie, Ovine BSE and Bovine BSE Amplification

Amplification conditions had been optimised for prion strains over 5 rounds of sPMCA. rVRQ was then tested as an inhibitor of a number of scrapie and BSE isolates over 5 rounds of sPMCA. The scrapie isolates included classical scrapie (PG1361/05, ARQ/VRQ and PG1563/02, VRQ/VRQ), transgenic mouse passaged strain Apl_{338}ii scrapie (MC140403 and MC140404, both VRQ/VRQ), transgenic mouse passaged strain G_{338} scrapie (MC136477 and MC136553, both VRQ/VRQ), CH1641 scrapie (J2935, ARQ/AHQ) ovine BSE (PG0392/04 and PG1693/04, both ARQ/ARQ) and bovine BSE strains (SE1929/0749 and SE1945/0035). For a full list of the TSE isolates used here, see (**Table 2. 1.9., Chapter 2**). Isolates were treated with 400 nM of rVRQ, analysed by western blotting (**Figure 3.6.1**). Each of these isolates were amplified in VRQ/VRQ substrate, with the exception of J2935 (AHQ/AHQ substrate), SE1929/0749 and SE1945/0035 (both bovine substrate). In each instance, it was observed that at a concentration of 400 nM, rVRQ consistently acted as a strong inhibitor of prion amplification regardless of prion strain or disease type with a mean inhibition of 83.6% (**Figure 3.6.2**).

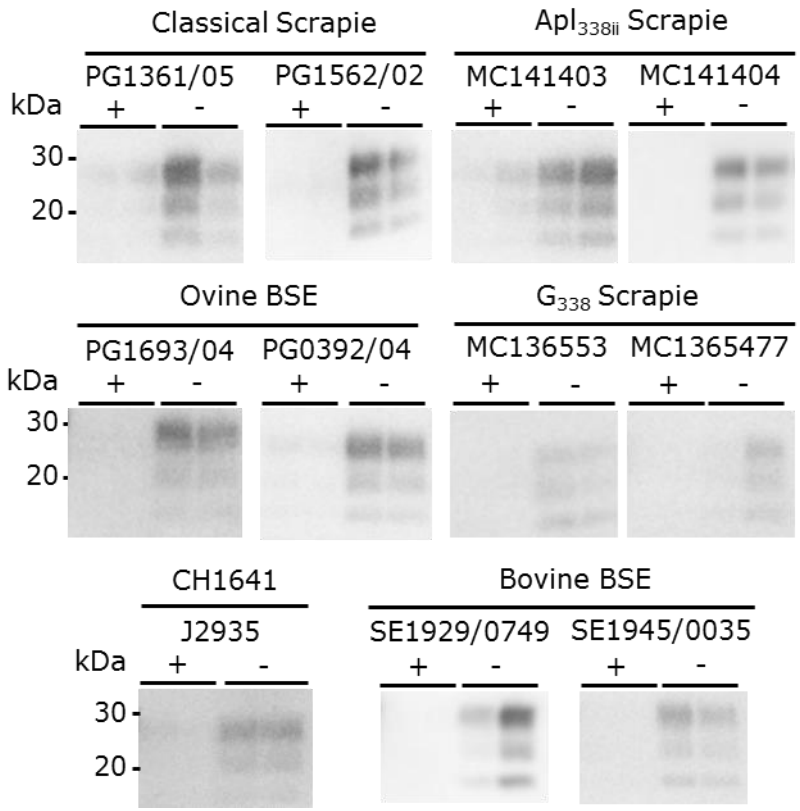

Figure 3.6.1. Representative western blots of scrapie and BSE strain amplification by PMCA for 5 rounds treated (+) or untreated (-) with 400 nM rVRQ. 6.7 µL of PK digested PMCA reaction was analysed per reaction. Reactions were performed in duplicate per experiment, and experiments were repeated twice. Classical scrapie, Apl_{338ii} scrapie, G_{338} scrapie and ovine BSE isolates were amplified with a VRQ/VRQ substrate. CH1641 scrapie was amplified with an AHQ/AHQ substrate. Bovine BSE was amplified in bovine substrate. All reactions were spiked with 0.5 µL of PrP^{Sc} seed, with the exception of bovine BSE and CH1641 scrapie which were spiked with 5 µL. rVRQ was dialysed against conversion buffer prior to use. Molecular weight markers are shown. For a full list of the TSE isolates used here, see **Table 2. 1.9., Chapter 2**.

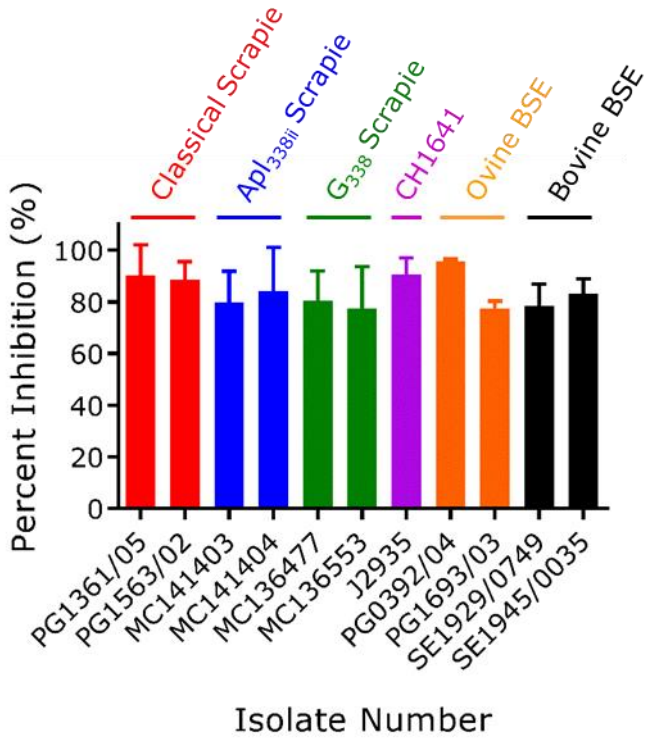

Figure 3.6.2. Percent inhibition of prion strains and isolates calculated from day 5 PMCA products by western blotting and densitometry. Values from densitometry were calculated as percent inhibition using untreated controls as 100% amplification. This data was collected from two separate experiments for each isolate.

3.7. Investigation into the Mechanism of rVRQ Inhibition

With rVRQ consistently identified as an inhibitor of ruminant prion amplification independent of prion strain or disease type, the mechanism of inhibition was investigated. In the study by (Yuan et al. 2013) it was determined that rPrP can bind specifically to PrP^{Sc} over PrP^{C}, and it was suggested that this may be important to the inhibitory mechanism. NaPTA precipitation has also been used to demonstrate that recombinant PrP-Fc binds specifically to PrP^{Sc} (Meier et al. 2003). Therefore, it was investigated whether rVRQ binds to PrP^{Sc}.

To determine whether rVRQ bound PrP^{Sc} and/or PrP^{C}, an ELISA was devised to test PrP^{Sc} binding to rPrP. NuncImmuno Maxisorp plates were coated with 10 µg/mL rVRQ and exposed to 1% (w/v) scrapie isolate (PG1361/05) or healthy brain (PG0648/09). PrP^{Sc} or PrP^{C} binding was then probed by biotinylated rVRQ and detected with streptavidin-HRP. As a positive control rVRQ was captured using SAF32 antibody coated at a concentration of 10 µg/mL. For the ELISA itself, the highest absorption values were observed for the non-brain homogenate controls (**Figure 3.7.1**). PrP^{Sc} capture appears to give higher absorbency values than PrP^{C}, but this is not statistically significant ($p = 0.39$) (**Figure 3.7.1.**). As the assay containing no brain homogenate gave the highest signal, it is likely that the rVRQ on the plate is interacting with the rVRQ in solution and that this interaction is actually blocked to some extent by the presence of brain homogenate, possibly PrP components.

As an alternative method to test whether rVRQ binds PrP^{Sc}, Dynabeads™ M-280 Tosylactivated were coated with rVRQ. These coated beads were used to capture PrP^{Sc} from a scrapie isolate (PG1361/05) and seed PMCA reactions at a volume of 5 µL or 1 µL (**Figure 3.7.2.**). This was performed with both rVRQ coated beads and non-coated beads (non-specific binding control). rVRQ coated beads were able to seed PMCA reactions, while bead only controls were not (**Figure 3.7.2.**). Reactions seeded with 5 µL of rVRQ-beads amplified to 32% of the positive amplification control (that contained seed equivalent to 100% capture of PrP^{Sc}), while beads without rVRQ seeded 6% (**Figure 3.7.2. A**). The difference in amplification between coated and uncoated beads was statistically significant as determined by an unpaired Student's t-test, with a p value of 0.03. Reactions seeded with 1 µL of rVRQ-beads amplified to 17%, while beads without rVRQ seeded 4.5% (**Figure 3.7.2. B**). However, this difference was not statistically significant ($p = 0.07$).

It was investigated whether the native conformation of rVRQ affects inhibition. rVRQ was heat denatured and used in amplification of scrapie (PG1361/05) at a concentration of 1200 nM, in parallel with non-denatured rVRQ (**Figure 3.7.3.**). Both forms of the rVRQ inhibited PrP^{Sc} replication (71.6 and 85% for native and denatured rVRQ, respectively). Whilst denatured rVRQ demonstrates marginally less inhibition, this was not statistically significant as analysed by an unpaired Student's t-test ($p = 0.08$) (**Figure 3.7.3.**).

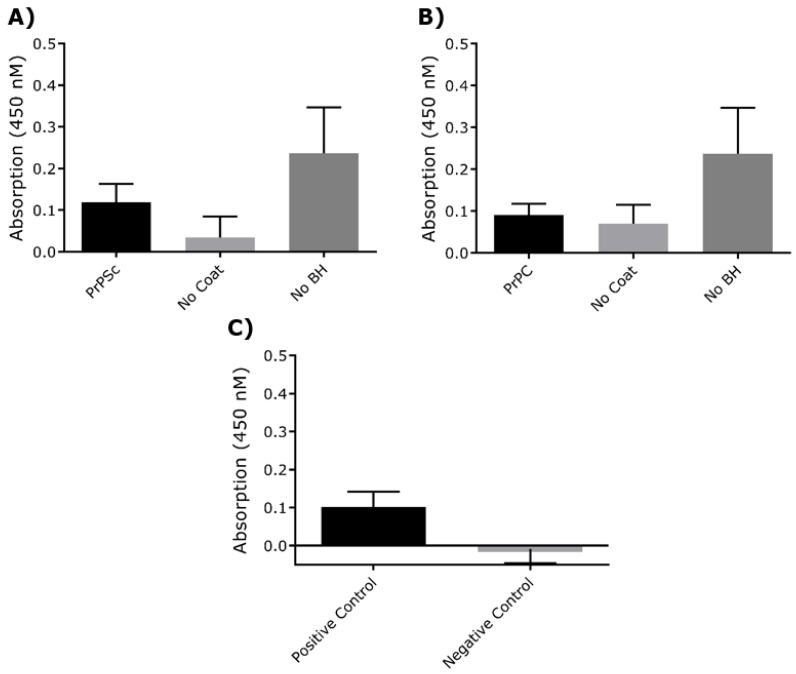

Figure 3.7.1. Bar plots displaying the capture of PrP^{Sc} or PrP^{C} by rVRQ, detected by a biotinylated rVRQ probe. Wells were coated with 10 µg/mL rVRQ and incubated with 1% (w/v) scrapie (ARQ/VRQ, PG1361/05) or healthy (VRQ/VRQ, PG0648/09) brain homogenate (BH). Wells were probed with biotinylated rVRQ and detected with a streptavidin-HRP conjugate. **A)** rVRQ capture and detection of PrP^{Sc}. **B)** rVRQ capture and detection of PrP^{C}. **C)** Positive and negative controls. There was no statistically significant difference between PrP^{Sc} and PrP^{C} binding as assessed by an unpaired Student's t-test ($p = 0.39$). The non-capture rVRQ (No Coat), and non-brain homogenate treated (No BH) controls for each group are displayed. The positive control was 10 µg/mL biotinylated rVRQ captured by SAF32, detected with streptavidin-HRP. The negative control was SAF32 antibody only. Wells treated with biotinylated rVRQ probe only were used as a background control.

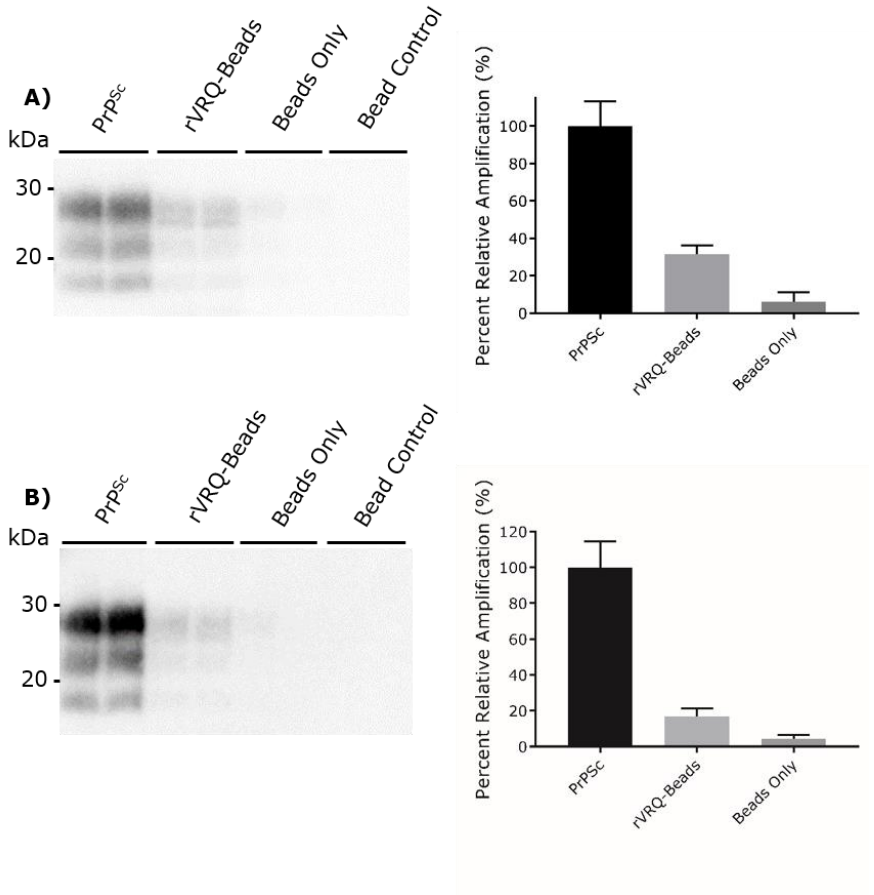

Figure 3.7.2. Dynabeads™ tosylactivated were coated with rVRQ (rVRQ-Beads) or untreated (Beads Only). These beads captured PrP^{Sc}, were washed and used to seed PMCA reactions in parallel beads which had not been incubated with brain homogenate (Bead Control). Bead Controls acted as a background for each western blot. **A)** Reactions seeded with 5 µL of beads, analysed by western blotting and densitometry. PMCA reactions seeded with rVRQ-Beads were statistically significantly different from reactions seeded with Beads Only ($p = 0.03$) determined by an unpaired Student's t-test. B) Reactions seeded with 1 µL of beads, analysed by western blotting and densitometry. Reactions seeded with rVRQ-Beads were not significantly different from Beads Only ($p = 0.07$). 6.7 µL of PK digested PMCA reaction was analysed by western blotting per reaction. Molecular weight markers are shown.

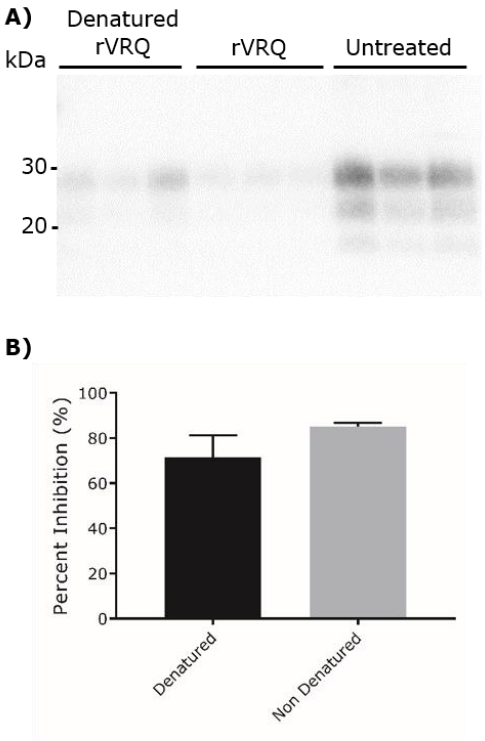

Figure 3.7.3. Inhibition of scrapie (PG1361/05) amplification with denatured and non-denatured rVRQ. **A)** PMCA reactions treated with 1200 nM denatured rVRQ or non-denatured rVRQ were analysed by western blotting. 6.7 µL of PK digested PMCA product was analysed per reaction. **B)** The blot was analysed by densitometry and values were calculated as percent inhibition using the untreated control. There was no significant difference in inhibition between denatured and non-denatured rVRQ as determined by an unpaired Student's t-test, with a p value of 0.08.

3.8. Discussion

Despite decades of research there remains no effective therapeutic strategy for treating prion diseases, and confirmatory diagnosis in humans remains to be made by the post mortem IHC of biopsy brain tissue (Lee et al. 2013). Research into therapeutics has encompassed multiple avenues including pharmaceutical, immunoprotectives, immunisation and peptides. Recombinant, heterogeneous or fragmented PrP have also been demonstrated as potent inhibitors of PrP^{Sc} conversion *in vitro*, highlighting these ligands as potential anti prion therapeutics (Priola 1999; Horiuchi et al. 2000; Meier et al. 2003; Masel et al. 2005; Nishina et al. 2006; Hizume et al. 2009; Kobayashi et al. 2009; Campbell et al. 2013; Yuan et al. 2013; Kobayashi et al. 2015; Altmeppen et al. 2015; Skinner et al. 2015; Seelig et al. 2015). Here, the recent identification that recombinant PrP can act as an inhibitor of prion replication has been further advanced using the model of *in vitro* amplification, PMCA.

This study focused on the application of ovine rPrPs and hamster rPrP as inhibitors of scrapie and BSE amplification by PMCA. Out of the four rPrPs tested (rVRQ, rARR, rARQ and rHam) the ovine rVRQ protein was consistently identified as the most potent inhibitor of ARQ/VRQ scrapie amplification with a mean IC50 of 122 nM in VRQ/VRQ substrate. Following the hypothesis that primary amino acid sequence homology between rPrPs and the seed/substrate could be important for inhibition, inhibitors rVRQ and rARQ were further tested in PMCA with bovine BSE using bovine brain substrate. IC50 values were calculated as 171 nM for rVRQ and 366 nM for rARQ. That rVRQ acts as the stronger inhibitor in both scrapie and bovine BSE PMCA indicates that it can consistently act as an inhibitor of prion amplification, independently of sequence homology with the seed/substrate. The IC50s calculated here are higher than the effective concentration (EC50) values reported previously by (Yuan et al. 2013), who also performed PMCAs with a homologous genotype between seed and substrate. In their study, an EC50 of 60 nM was reported for human rPrP (rHum) (Sequence 23-231, 129V) in PMCA seeded with iCJD (V/V 129) and transgenic mouse brain homogenate (human *Prnp* V/V 129) as substrate (Yuan et al. 2013). This study also reported an EC50 of 120 nM for mouse rPrP (23-231) in PMCA seeded with mouse PrP^{Sc} (139A) using mouse brain homogenate as substrate, which is closer to the 122 nM reported for rVRQ in scrapie amplification in this study. That these reported IC50/EC50 values vary between disease and host type could be resultant of internal experimental variation, for example within the amplification efficiency of individual isolates. Indeed, the efficacy of classical scrapie amplification in PMCA can vary between

isolates and genotypes (Thorne et al. 2012). Therefore, it could be expected that the efficacy of rPrP inhibition can vary with the isolates and substrates used in PMCA. Furthermore, the method of analysis can affect the calculation of IC50 values. Here, IC50 values were calculated from the densitometry of dot blots, confirmed by western blotting. Western blotting was observed to produce similar IC50 values to dot blotting, although lower. For example, rVRQ was calculated to have an IC50 of 122 nM from dot blotting, and 85 nM from western blotting. The EC50 values reported previously were calculated from western blotting, which may account for the difference to values reported here (Yuan et al. 2013). However, that the IC50 values calculated from western blotting (85 nM for rVRQ) are in a similar range to those reported previously (60 nM for rHum), indicates that the inhibitory efficacy between rVRQ and rHum are similar (Yuan et al. 2013). A means of investigating this further would be to screen additional scrapie and BSE isolates to ascertain the efficacy of rPrP inhibition between isolates, as well as performing analysis in parallel by dot blot and western blotting.

rVRQ was demonstrably the stronger inhibitor in both classical scrapie and bovine BSE PMCA, suggesting that rVRQ can consistently inhibit prion propagation in distinct disease types. To investigate this hypothesis, rVRQ was used as an inhibitor of distinct strains and disease types over 5 days of sPMCA. The strains included classical scrapie (from ARQ/VRQ and VRQ/VRQ hosts), Apl_{338}/Apl_{338ii} scrapie and G_{338} scrapie (obtained by bioassay in tg338 transgenic mice, VRQ/VRQ), ovine BSE (from ARQ/ARQ hosts), CH1641 scrapie (from an ARQ/AHQ host) and bovine BSE (from bovine hosts). Classical, Apl_{338}/Apl_{338ii}, G_{338} scrapie and ovine BSE were amplified in VRQ/VRQ substrate, CH1641 scapie in AHQ/AHQ substrate and bovine BSE in bovine substrate. rVRQ demonstrated consistent inhibition of prion amplification with each isolate at a concentration of 400 nM. This was independent of strain, disease or genotype with a minimum average percentage inhibition for any individual isolate of 77.4% and a maximum of 90.7%. This further highlights the potential of rVRQ and other rPrP inhibitors to act as broad-spectrum inhibitors of ruminant prion diseases.

The discovery that elution buffer can inhibit amplification was observed in optimising the conditions for bovine BSE amplification. In these experiments, it was observed that bovine BSE treated with elution buffer and 20% (w/v) sucrose did not amplify, indicating that a reaction constituent was inhibiting amplification. Upon testing the different buffer constituents, amplifications were only inhibited in the presence of imidazole in elution buffer. Bovine BSE could, however, be

amplified with conversion buffer. Consequently, rPrPs were dialysed against conversion buffer prior to use. As rPrPs were dialysed in a 1:1000 volume ratio for a minimum of two repeats, it is unlikely that imidazole remaining in rPrP preparations was sufficient to interfere in amplification. Consequently, the results observed utilising dialysed rPrP indicate that they act as strong inhibitors of prion amplification despite the possible presence of very low levels of elution buffer.

The mechanism behind rPrP inhibition remains to be elucidated. It has been previously reported that rPrP proteins can selectively bind to PrP^{Sc}, and can be used to precipitate PrP^{Sc} by NaPTA (Meier et al. 2003; Yuan et al. 2013). It was hypothesised that this interaction was important in the inhibitory mechanism (Yuan et al. 2013). Here it was similarly demonstrated that the protein rVRQ can successfully capture PrP^{Sc} from brain homogenate and seed subsequent PMCA reactions. The amplification efficiency of these reactions were 27-32% of reactions spiked with an equivalent volume of brain homogenate. However, this method could not reveal any interaction of rVRQ with PrP^{C}. In an attempt to ascertain the extent of rVRQ binding to PrP^{Sc} and/or PrP^{C}, an ELISA was devised using rVRQ to capture PrP^{Sc} or PrP^{C} from brain homogenate. This assay gave higher readings for wells treated with biotinylated rVRQ probe only and not containing any brain homogenate, suggesting that the biotinylated rVRQ probe could dimerise with the rVRQ used to coat the plate well. This result means that the assay cannot be used to measure rVRQ binding to PrP^{C} or PrP^{Sc} in brain homogenates. An alternative approach could be the capture of PrP^{Sc} by rPrP coated magnetic beads as reported in previous studies (Yuan et al. 2006; Yuan et al. 2013). This was partially demonstrated by the seeding of PMCA reactions with rVRQ captured PrP^{Sc} in this study. By increasing the scale of the beads/rVRQ used in each experiment, PrP^{Sc} capture could be detected directly by western blotting without the need for additional amplification steps. These data could confirm the findings reported previously, where human recombinant PrP (23-231) captured PrP^{Sc} but not PrP^{C} from brain homogenate (Yuan et al. 2013). Furthermore, the data would enable a comparison between the affinities of different rPrPs for PrP^{Sc}.

(Yuan et al. 2013) proposed that the mechanism of rPrP inhibition may be due to homology between the rPrP sequence and isolate/substrate. Indeed, here rVRQ was observed to inhibit homologous scrapie strains in VRQ/VRQ substrate. However, rVRQ also consistently inhibited amplification of prions of distinct genotypes and in heterologous substrates. Additionally, both rVRQ and rARQ were demonstrated to inhibit bovine BSE amplification in bovine substrate. That rVRQ

remained an effective inhibitor of prion propagation in reactions with homologous and heterologous seed/substrate indicates that the inhibitory mechanism is not completely dependent on sequence identity. The inhibitory mechanism of rPrPs may then be in part due to the lack of secondary modifications. Indeed, different glycosylation states of PrP can selectively affect prion strain amplification. It has been identified that unglycosylated PrP preferentially propagates RML strains while Sc237 prions are inhibited by the same substrate (Nishina et al. 2006). Furthermore, prion peptides and fragments observed to have anti-PrP^{Sc} activity share the lack of secondary modifications (Chabry et al. 1998; Altmeppen et al. 2015; Campbell et al. 2013). This lack of any secondary modifications may enable rPrPs to act as dominant negative inhibitors of prion amplification. This might be achieved by rPrPs acting as less conversion efficient substrates, similar to previous reports of recombinant and heterologous PrP inhibition (Horiuchi et al. 2000; Meier et al. 2003; Geoghegan et al. 2009). Indeed, the inhibition of prion propagation can be affected by the stoichiometric ratio of homologous to heterologous PrP^{C} present. It has been reported that RML-scrapie propagation and symptom onset can be delayed *in vivo* in a dose dependent manner by recombinant hamster PrP (Skinner et al. 2015). Furthermore, the concentration of rPrPs used in these experiments (400 nM in this study, 200 nM by (Yuan et al. 2013) exceeds stoichiometric concentrations of PrP^{C} (~13 nM in 10% brain homogenate, calculated from the values reported by (Moudjou et al. 2001). This higher ratio of homologous conversion efficient PrP^{C} to less conversion efficient rPrP may be an important factor in the inhibitory mechanism, allowing for rPrP inhibitors to out-compete PrP^{C} binding to PrP^{Sc}. However, in this study it was observed that rVRQ has the potential to bind other rVRQ proteins. Indeed, this could be expected as PrP^{C} monomers are known to dimerise (Wang et al. 2015). This could have implications in rVRQ inhibition, where rVRQ self-binding may affect the stoichiometry with PrP^{C} and limit its inhibitory efficacy. Despite these concerns, soluble dimerised rPrP fused to Fc antibodies have been previously reported to delay disease onset in infected mice at substoichiometric amounts (Meier et al. 2003). Therefore, rPrP dimerization may not affect the inhibitory efficacy of these proteins.

The role of rVRQ conformation in inhibition was also investigated in this study. Using heat denatured and non-denatured rVRQ in PMCA elucidated that both can effectively inhibit scrapie amplification, with no statistically significant difference between the two groups. This suggests that the linear primary amino acid sequence is the major contributor to the inhibitory mechanism, rather than the

conformation of rVRQ. This assumes that rVRQ remains in the denatured conformation under the experimental conditions used in this study. This is in contrast to a recent report that the native conformation is key in inhibiting amyloid formation (Honda & Kuwata 2017). In their study, rHum (21-230) inhibited rPrP amyloid formation in a dose dependent manner, inhibitory activity that was lost in increasing concentrations of GdnHCl (Honda & Kuwata 2017). However, it is debatable how representative this inhibition is of prion propagation *in vivo.* Furthermore, linear prion peptides have been previously reported to inhibit prion propagation in *in vitro* cell free assays, as well as in cell culture (Chabry et al. 1998; Chabry et al. 1999) supporting the importance of short peptide structures that are unlikely to form complex conformations compared to rPrP. Indeed, a peptide with residues 119 to 136 of mouse and hamster PrP was observed to cross-inhibit hamster 263K and mouse 87V prion propagation (Chabry et al. 1999). Interestingly, the peptide 119-136 contains the residues that direct susceptibility to prion disease infection, 129 in humans and 136 in sheep (Chabry et al. 1999). Therefore, this sequence may be a contributing factor in the cross-strain and disease inhibition by rVRQ observed in this study. Additionally, the polymorphism at position Q171 has been reported to influence the conversion efficiency of PrP in sheep challenged with SSBP/1 scrapie and BSE, with increased attack rates and shorter incubation periods compared to other genotypes (Houston et al. 2015). The Q171 polymorphism could enhance the affinity of rVRQ for PrP^{Sc} from different disease types while remaining a less efficient conversion substrate. Therefore, although this study has determined that homology between rPrP inhibitors and PrP seed/substrate is not essential for inhibition, the polymorphisms of ovine PrP at positions 136 and 171 may play defining roles. A key means of investigating this would be to explore inhibitory activity of rPrPs with a range of other mutations at ovine residues 136 and 171. Changes in these residues has been shown to affect inhibitory efficacy in this study, with the proteins rARQ and rARR producing lower IC50 values in either classical scrapie or bovine BSE PMCA. By investigating further mutations at these residues inhibitors with greater inhibitory efficacy than rVRQ may be identified.

In conclusion, the work performed in this study has provided new insights into the use of rPrPs as inhibitors of scrapie and BSE PrP^{Sc} amplifications using the *in vitro* PMCA model. It was identified that the ovine protein rVRQ acts a potent inhibitor of prion amplification regardless of prion strain or disease type, possibly by acting as a competitive conversion-resistant substrate. The inhibitory activity of rVRQ implicates this protein and potentially others as having potential to act as broad-

spectrum therapeutic agents for ruminant prion diseases. Whether this inhibition extends to other species can be tested by CJD or CWD PMCA for example, and the use of other recombinant PrPs could be tested to determine whether alternate polymorphic variants or mutants can act as even more efficient inhibitors. That recombinant hamster PrP has been successfully reported to inhibit RML-scrapie propagation *in vivo* also supports the use of rVRQ in a transgenic mouse model of prion infection. Performing such experiments with different prion strains in transgenic mice would elucidate the potential therapeutic application of rVRQ in different disease types *in vivo*.

Chapter 4: rPrP Inhibition of Prion Amplification as a Method of Strain Characterization

4.1. Introduction

The ability of commercial immunoassays to effectively detect PrP^{Sc} in brain tissue has resulted in their widespread use in TSE surveillance in food producing ruminants. These assays utilise protease digestion to selectively detect PrP^{Sc}. However, the sensitivity of atypical scrapie/Nor98 to proteases highlighted the limitation of these diagnostics for detecting and characterising the emergence of new prion strains (Meloni et al. 2012). Therefore, this limitation raises concerns over the capacity for immunoassay techniques to identify the emergence of potentially zoonotic prion strains. Conventionally, the biological identification of prion strains is performed by the serial passage of the prion agent in animals, typically mice (Kübler et al. 2003). In these mouse bioassays prion strains are characterised by their incubation time and neuropathology, which become stable over serial passages (Bruce 2003). However, mouse bioassays require months to years to obtain results. Furthermore, atypical scrapie strains and as many as 20% of classical scrapie strains remain to be non-transmissible to the mouse lines used for strain typing (Thackray et al. 2008). Utilizing transgenic mice expressing PrP^{C} homologous to the infectious prion can shorten incubation periods and increase transmission efficiency, but serial passages are still required in the identification of new strains (Thackray et al. 2008; Thackray et al. 2011). Consequently, rapid tests have been developed that enable the classification of characterised prion strains and may have some capacity for identifying new emerging strains.

Prion strains can be differentiated by their sensitivity to protease digestion, demonstrated by atypical scrapie (Benestad et al. 2008). Additionally, prion strains can be distinguished by the size and ratio of unglycosylated, monoglycosylated or diglycosylated PrP^{res} fragments after protease treatment. For example, BSE (ovine and bovine) and classical scrapie have distinct glycoform ratios and fragment sizes, with BSE exhibiting a predominant lower molecular weight unglycosylated PrP fragment and a relative abundance of diglycosylated PrP^{res} (Hill et al. 1998; Baron et al. 2000; Thuring et al. 2004). These characteristics can also be maintained after propagation *in vitro* by PMCA, removing the need for the long incubation periods in mice (Meyerett et al. 2008). 2010). Although effective at distinguishing between BSE and scrapie, glycoform ratios cannot be used as a definitive characteristic for strain typing in general. This follows from the difficulty in distinguishing between scrapie and CWD glycoforms (Race et al. 2002). Alternatively, some prion strains can be differentiated by the availability of epitopes in denatured and native PrP^{Sc}/PrP^{C} in CDI, or the loss of protease resistance following denaturation in CSA and CSSA (Safar et al. 1998;

Peretz et al. 2001; Safar et al. 2002; Safar et al. 2005; Pirisinu et al. 2010). Prion strains including C-BSE, H-type BSE, L-type BSE, CH1641 and classical scrapie can also be propagated under different PMCA and/or QuiC conditions, such as amplification in substrates with different PrP^C genotypes, and this can be used to differentiate some strains (Taema et al. 2012; Makarava et al. 2013; Gough et al. 2014; Orrú et al. 2015; Masujin et al. 2016; Dassanayake et al. 2016; Murayama et al. 2016; O'Connor et al. 2017). However, most of these studies focused on developing conditions to successfully amplify and detect each individual strain, rather than using these conditions to distinguish between all of them. Therefore, it is uncertain how effective these methods could be to characterise and distinguish a range of prion strains.

These *in vitro* assays offer a more rapid alternative to mouse bioassays for the characterization of prion strains. Combined with mouse bioassays, these methods have identified up to 30 prion strains to date (Safar 2012). However, these methods have often been designed to strain type a strain with certain conditions, e.g. ovine BSE compared to classical scrapie and/or CH1641. None have been demonstrated to be individually applicable for defining a wide range of ruminant strains. This raises concern as to the ability of these methods to identify the emergence of new prion strains in food producing ruminants. Consequently, there is a requirement for *in vitro* methods to characterize and differentiate all known prion strains, as well as the ability to recognise a novel strain.

It has been observed in this study that the recombinant PrP proteins rVRQ, rARR, rARQ and rHam have different inhibitory efficacies against classical scrapie and bovine BSE in PMCA. Therefore, it was hypothesised that their relative inhibitory efficacy may vary between different strains and disease types, allowing for a novel method of strain characterisation. Indeed, it has been previously reported that prion strains can exhibit different sensitivities to inhibitors like quinacrine and swainsonine, raising the question of whether a panel of inhibitors could be used as a method of strain characterisation (Ghaemmaghami et al. 2009; Li et al. 2010). To test this hypothesis, an assay was devised where the rPrP inhibitors were used in PMCA at a set concentration of 400 nM, analysed by one-way ANOVA and post hoc Tukey tests. Optimisations were attempted to make these results more consistent between experiments. It has also been observed that the elution buffer used to store rPrP inhibitors can interfere in the amplification of BSE by PMCA, but not classical scrapie. It was investigated whether this inhibitory activity

may be applied to differentiate prion strains as an alternative assay for strain characterisation.

4.2. Results

4.2.1. Establishing Patterns of rPrP Inhibition in Scrapie PMCA

Data from scrapie (PG1361/05) PMCA reactions treated with 400 nM of rPrP inhibitors (**Chapter 3**, **Section 3.3.**) were compiled (**Figure 4.2.1.**). The purpose of this was to assess whether treating scrapie PMCA reactions at a fixed concentration of rPrPs can generate a pattern of inhibition between experiments. Although the resulting datasets had a high standard deviation, it was observed that at this concentration there is a pattern of inhibition with rVRQ as the strongest inhibitor (**Figure 4.2.1. A**). These data were analysed by one-way ANOVA to compare the effect of each rPrP, which reported a statistically significant difference between groups ($F = 12.56$, $p = <0.01$) (**Figure 4.2.1. A**). Statistically significant differences were reported between the test groups rVRQ/rARR ($p = <0.0001$), rVRQ/rARQ ($p = 0.0247$), rARR/rARQ ($p = 0.0426$) and rARR/rHam ($p = 0.0004$) (**Figure 4.2.1. B**).

In order to investigate the reproducibility of this method between experiments, further PMCA reactions were performed using the rPrP inhibitors at 400 nM, analysed by dot blotting (**Figure 4.2.2.**). The PrP^{Sc} seed used was a scrapie isolate (PG1361/05, ARQ/VRQ) previously identified to amplify efficiently over one round of PMCA. Densitometry values were analysed by one-way ANOVA to compare the mean of each group of rPrP treated reactions, which revealed statistically significant differences between the groups in each experiment (**Figure 4.2.3.**). Statistically significant differences were reported between the groups rVRQ/rARR, rVRQ/rARQ and rVRQ/rHam in all assays, with significant differences between rARR/rHam and rARQ/rHam in one (**Figure 4.2.3.**).

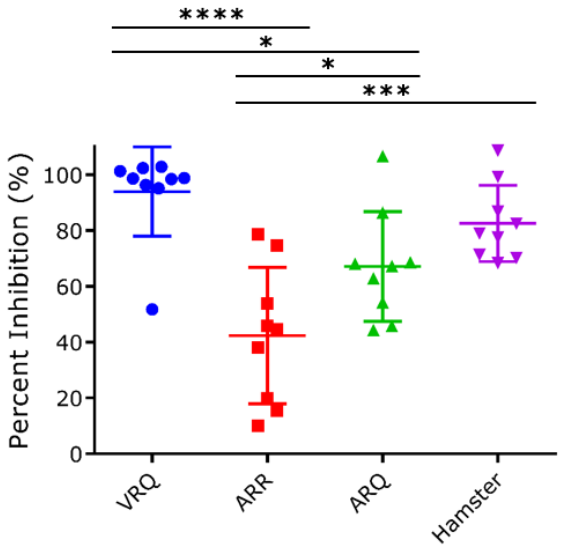

Figure 4.2.1. Comparison of data from scrapie PMCA reactions (PG1361/05) treated with 400 nM of rVRQ, rARQ, rARR or rHam. A plot of the compiled data from three separate experiments, with three replicates per experiment. Each point is the percent inhibition calculated from a single PMCA reaction dot blotted in duplicate, with the average inhibition calculated for each reaction. These data were analysed by one-way ANOVA in Graphpad Prism 7, which reported a statistically significant difference between groups ($F = 12.56$, $p = <0.01$). P values were calculated by a post-hoc Tukey test. Statistically significant differences are reported between the groups rVRQ/rARR, rVRQ/rARQ, rARR/rARQ and rARR/rHam. ****: $p = <0.0001$. ***: $p = <0.001$. **: $p = <0.01$. *: $p = <0.05$.

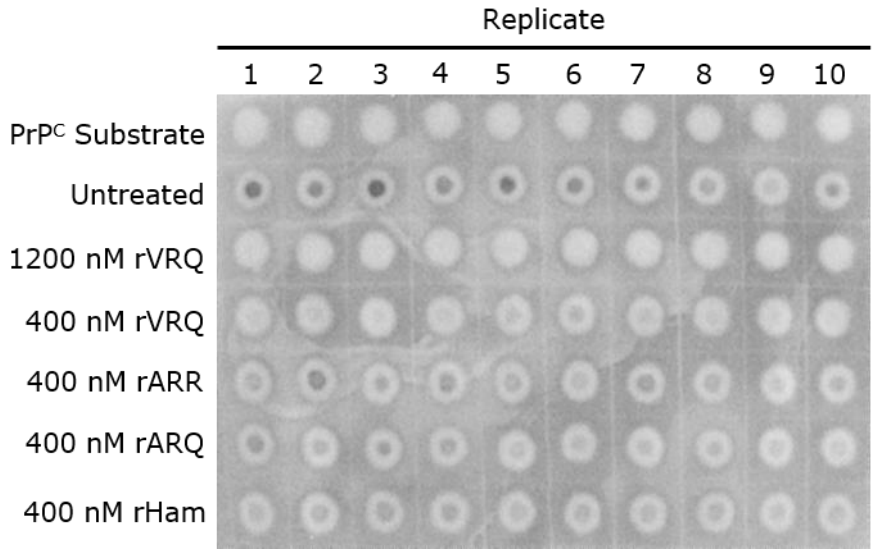

Figure 4.2.2. Representative dot blot of scrapie (PG1361/05) PMCA reactions treated with 400 nM of rVRQ, rARR, rARQ or rHam. Ten reactions were performed per inhibitor, and 0.83 µL of PK digested PMCA product was analysed per reaction. PrP^C substrate, untreated and 1200 nM rVRQ treated (100% inhibition) reaction controls are shown. 1200 nM rVRQ treated reactions were used as background readings and were subtracted from densitometry analysis using ImageJ.

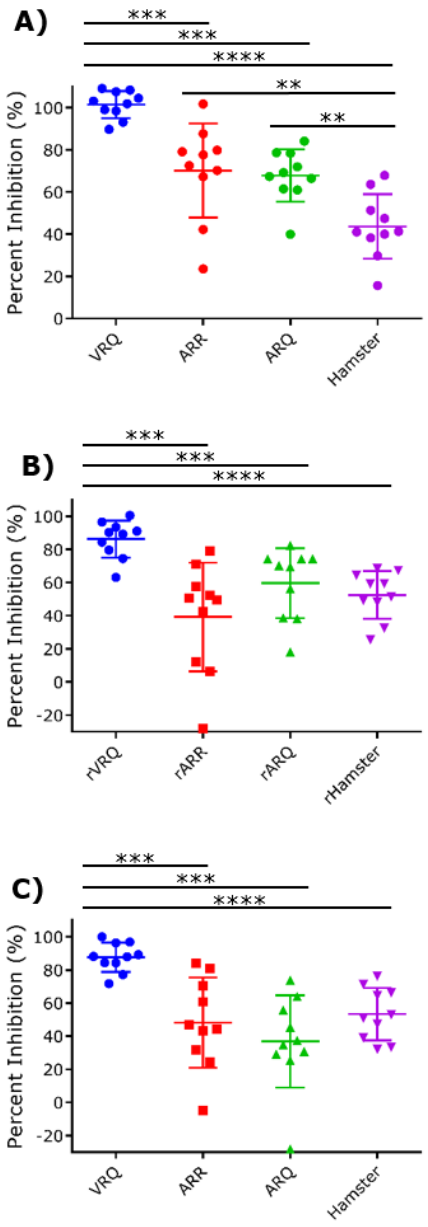

Figure 4.2.3. Plots illustrating the percent inhibition of scrapie amplification caused by the rPrP inhibitors VRQ, ARR, ARQ and Hamster at 400 nM across three separate experiments. Each point represents the percent inhibition calculated from a single PMCA reaction. In each experiment, one-way ANOVA reported statistically significant differences between inhibitors: **A**) F = 7.4, p = <0.01, **B**) F = 8.45, p = <0.01, **C**) F = 10.34, p = <0.01. Tukey post hoc tests revealed significant statistical differences between the groups rVRQ/rARR, rVRQ/rARQ and rVRQ/rHam in each experiment, as well as between rARR/rHam and rARQ/rHam in **A**). ****: p = <0.0001. ***: p = <0.001. **: p = <0.01. *: p = <0.05. All analyses were performed using Graphpad Prism 7.

4.3. Optimisation of Comparative Inhibition Assay Conditions

Experiments using 400 nM of rPrPs rVRQ, rARR, rARQ and rHam revealed that the p values between the inhibitors for each experiment were not always consistent. For instance, when using 10 replicate analyses within an experiment, whilst inhibition by rVRQ was always significantly more effective than the other 3 rPrPs, the differences between rHam and rARQ or rARR were inconsistent. Therefore, attempts to optimise the assay were made to improve the consistency of the statistical analysis between experiments. It was hypothesised that increasing the volume of PrP^{Sc} used in PMCA could increase the differences observed in the mean percent inhibition between the different rPrP inhibitors. Accordingly, the volume of PrP^{Sc} seed used in each reaction was increased from 0.5 µL to 2.5 µL 10% (w/v) scrapie brain homogenate (**Figure 4.3.1.**). Analysis by one-way ANOVA reported statistically significant differences between the inhibitors ($F = 29.77$, $p = <0.01$). Statistically significant differences were reported between the groups rVRQ/rARR, rVRQ/rARQ and rVRQ/rHam, although the due to the efficiency of amplification 1200 nM rVRQ treated control reactions inhibited 70% as effectively (**Figure 4.3.1.**). Alternatively, the length of PMCA reactions was increased from 24 hours to 48 hours in a single round (**Figure 4.3.2.**). Both of these alterations resulted in decreasing the difference between the mean percentage inhibition of each inhibitor and decreased assay efficacy, reflected by statistical analysis (**Figure 4.3.1., 2.**). Following this, three experiments were then run with the original assay conditions but using 200 nM of each rPrP (**Figure 4.3.3.**). Each experiment was analysed by one-way ANOVA, which reported statistically significant differences between groups in each experiment (**Figure 4.3.3.**). In all three experiments, statistically significant differences were reported between rVRQ/rARR, rVRQ/rARQ, rVRQ/rHam, However, there was an additional difference between rARR/rHam in the second repeat (**Figure 4.3.3.**).

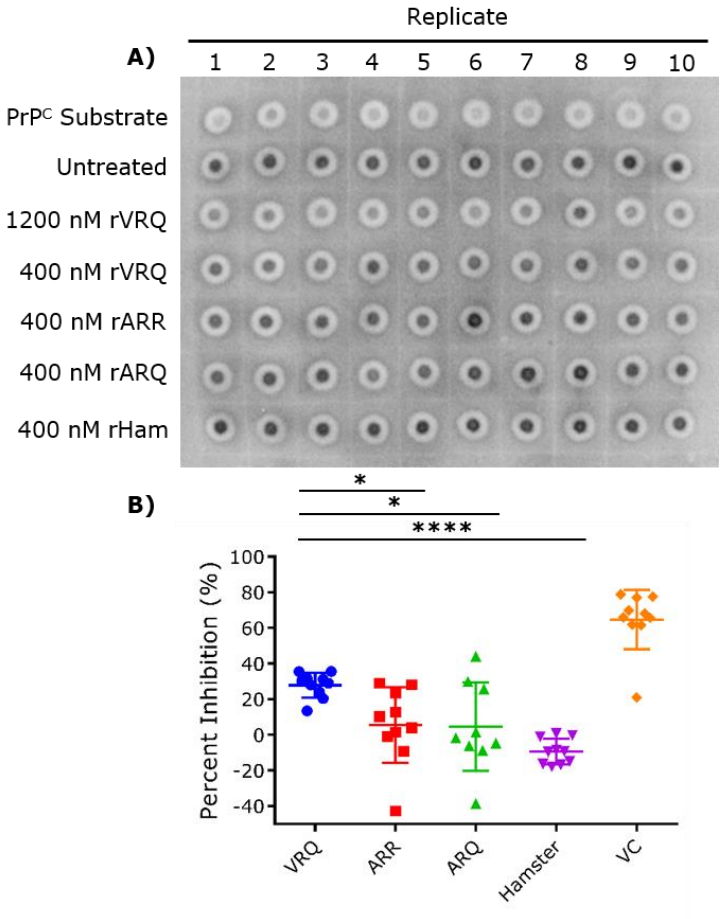

Figure 4.3.1. 10 PMCA reactions were performed per experiment, treated with 400 nM of each inhibitor and using 2.5 µL of PrP^{Sc} (PG1361/05) seed. **A)** PMCA reactions were analysed by dot blot, and 0.83 µL of PK digested PMCA product was analysed per reaction. PrP^{C} substrate, untreated and 1200 nM rVRQ treated reaction controls are shown. **B)** Plot displaying the percent inhibition caused by the rPrP inhibitors VRQ, ARR, ARQ and Hamster at 400 nM. Each point represents the percent inhibition calculated from a single PMCA reaction. Increasing the volume of PrP^{Sc} reduced the effectiveness of the 1200 nM VRQ control (VC) to ~70% inhibition. Consequently, it could not be used as a background control and has been displayed on these graphs as an illustration. Because of this, the PrP^{C} substrate control was used as a background control. Analysis of the data by one-way ANOVA reported a statistically significant difference between the inhibitors ($F = 29.77$, $p = <0.01$), with significant differences between rVRQ/rARR, rVRQ/rARQ and rVRQ/rHam as calculated by a Tukey post hoc test. ****: $p = <0.0001$. ***: $p = <0.001$. **: $p = <0.01$. *: $p = <0.05$. Analysis was performed in Graphpad Prism 7.

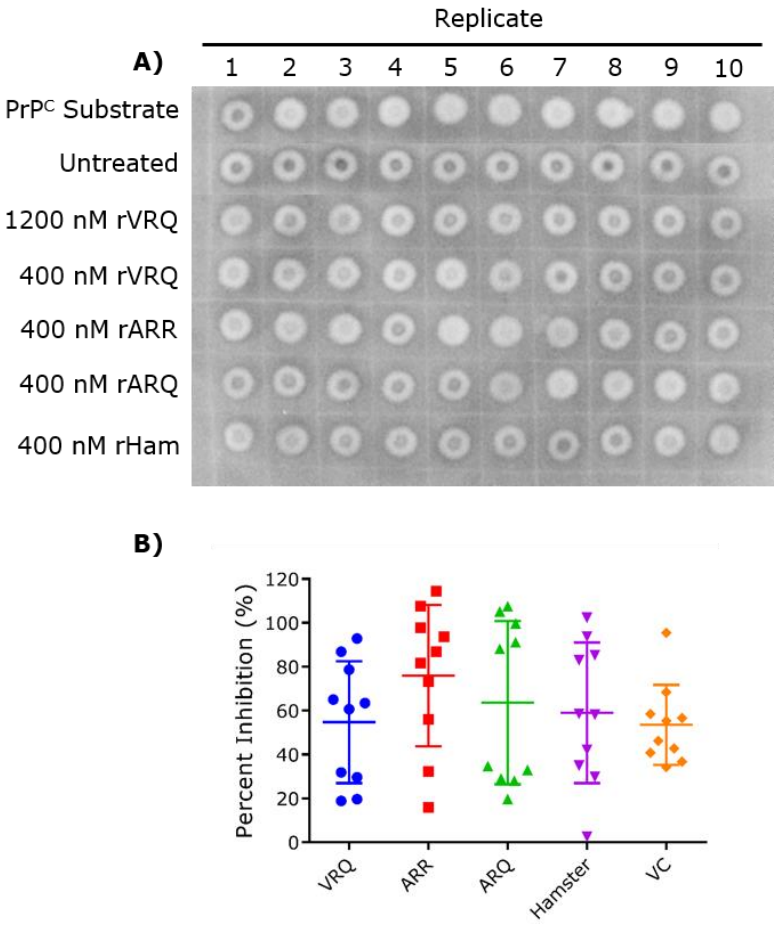

Figure 4.3.2. 10 PMCA reactions were performed per experiment, treated with 400 nM of each inhibitor over 48 hours of PMCA and using 0.5 µL of PrP^{Sc} (PG1361/05) seed. **A)** PMCA reactions were analysed by dot blot, and 0.83 µL of PK digested PMCA product was analysed per reaction. PrP^{C} substrate, untreated and 1200 nM rVRQ treated reaction controls are shown. **B)** Plot displaying the percent inhibition caused by the rPrP inhibitors VRQ, ARR, ARQ and Hamster at 400 nM. Each point represents the percent inhibition calculated from a single PMCA reaction. Increasing the time of PMCA to 48 hours reduced the effectiveness of the 1200 nM VRQ control (VC) to ~50%. Therefore, it could not be used as a background control and has been displayed on these graphs as an illustration. Because of this, the PrP^{C} substrate control was used as a background control. These data were analysed by one-way ANOVA, which reported no significant difference between the inhibitors. Analysis was performed using Graphpad Prism 7.

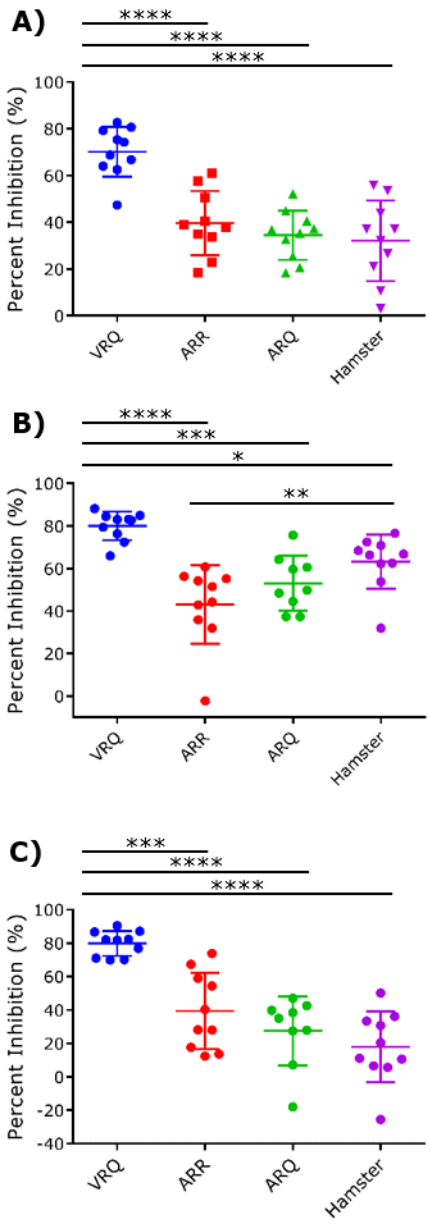

Figure 4.3.3. Plots illustrating the percent inhibition of scrapie amplification caused by the rPrP inhibitors VRQ, ARR, ARQ and Hamster at 200 nM. Each point represents the percent inhibition calculated from a single PMCA reaction. In each experiment, analysis by one-way ANOVA reported statistically significant differences between inhibitors: **A**) F = 7.4, p = <0.01, **B**) F = 8.45, p = <0.01, **C**) F = 10.34, p = <0.01. Tukey post hoc tests revealed significant statistical differences between groups rVRQ/rARR, rVRQ/rARQ and rVRQ/rHam in each experiment, as well as between rARR/rHam in **B**). ****: p = <0.0001. ***: p = <0.001. **: p = <0.01. *: p = <0.05. All analyses were performed in Graphpad Prism 7.

4.4. Differentiating Between Prion Strains Using Inhibition by Imidazole

It was previously identified in this study that the elution buffer used to store rPrP inhibitors could interfere in bovine BSE amplification by PMCA, but not classical scrapie (**Chapter 3, Section 3.4.**). Following these observations, it was hypothesised that this inhibition could be exploited to characterise prion strains. As a predominant ingredient of elution buffer was imidazole, scrapie and ovine BSE PMCA reactions were treated with increasing concentrations of imidazole from 0.5 mM to 40 mM in elution buffer without sucrose or imidazole (300 mM NaCl and 50 mM NaH_2PO_4, pH 7.4) over 5 rounds of sPMCA (**Figure 4.4.1. A**). Inhibition was determined by the decrease in densitometry intensity relative to an untreated control. This elucidated that ovine BSE is more sensitive to imidazole treatment than classical scrapie, and was 100% inhibited by imidazole up to a final concentration in the reaction of 10 mM (**Figure 4.4.1. C**). In contrast, the scrapie isolate was inhibited to ~70% of the control only at 40 mM (**Figure 4.4.1. C**).

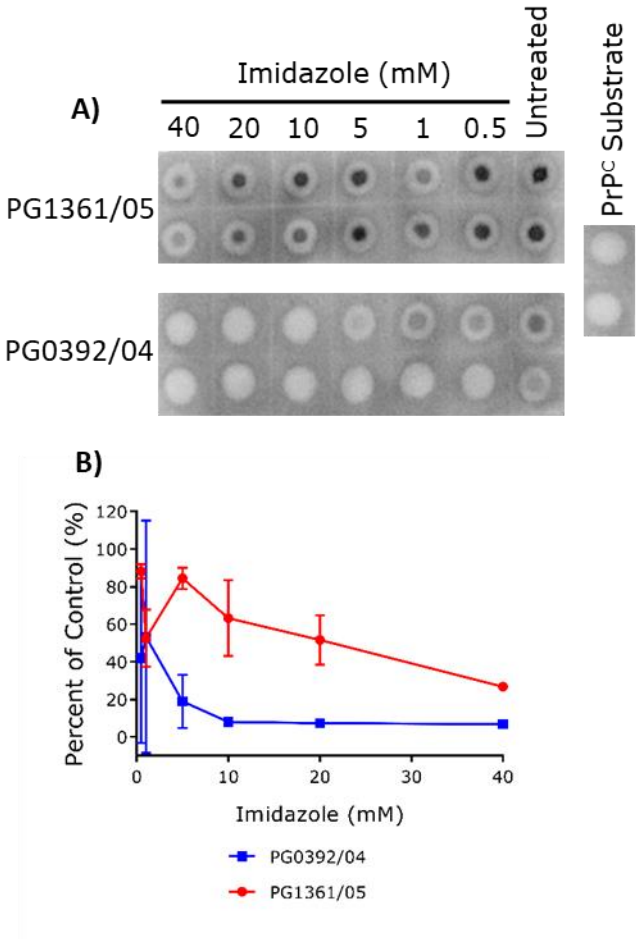

Figure 4.4.1. IMAC elution buffer inhibits prion amplification by PMCA. PMCA reactions were performed using PG1361/05 (ovine scrapie) and PG0392/04 (ovine BSE) as PrP^{Sc} seeds using imidazole diluted in elution buffer without sucrose and imidazole. **A**) Day 5 sPMCA reactions were analysed by dot blotting, with 83 µL of PK digested PMCA product analysed per reaction. The PrP^{C} substrate control acted as a background control. All images shown were from the same blot exposed for the same amount of time. **B)** Plot displaying the percent of control of PG1361/05 and PG0392/04 PMCA reactions calculated by densitometry.

4.5. Discussion

Prion strains are conventionally characterized by their incubation periods and neuropathology in mouse bioassays (Bruce 2003). Although effective at discriminating between strains, not all prion strains are transmissible to mouse lines used for bioassays (Thackray et al. 2008). Mouse bioassays are also time consuming. Furthermore, the sensitivity of current commercial immunoassays used in TSE surveillance can be affected by factors including protease sensitivity, as in the case of atypical scrapie (Benestad et al. 2008). Therefore, both mouse bioassays and commercial immunoassays are limited in their application to rapidly characterize or detect the emergence of novel prion strains in food producing ruminants. This is especially poignant, as prion strains have been observed to adapt and alter their phenotypes under selective pressure by the inhibitors swainsonine and quanicrine *in vitro* and *in vivo* (Ghaemmaghami et al. 2009; Li et al. 2010; Berry et al. 2013). Therefore, there remains a risk of novel prion strain emergence in ruminant livestock which may remain undetected by current surveillance methods.

Other *in vitro* methods for characterizing prion strains have been described. These include sensitivity to protease digestion, glycoform ratios, amplification in different PMCA conditions and conformational stability (Safar et al. 1998; Hill et al. 1998; Safar et al. 2005; Pirisnu et al. 2010; Taema et al. 2012). Although these methods are rapid, they can only distinguish between a limited number of prion strains. Therefore, there is a requirement for new methods that can rapidly characterize a larger range of prion strains. The assay described in this study aimed to reproducibly generate patterns of inhibition caused by ovine and hamster rPrPs in PMCA as a method of strain characterization. It was envisaged that an assay format could include the PMCA/sPMCA amplification of prions strains in a range of substrates and then the inhibition of successful amplification with a range of rPrPs (and potentially other inhibitors). This screening of a panel of substrates and inhibitors may provide a sufficiently detailed 'readout' of amplification properties to allow a comprehensive description of prion strains. As a first step to determine whether rPrP inhibition could provide a reproducible parameter in prion amplification, the amplification of scrapie isolate PG1361/05 (ARQ/VRQ) was performed in a single PMCA round followed by dot blotting and densitometry. Although the results of this assay produced a repeatable pattern of inhibition in classical scrapie PMCA, these differences were not consistently statistically significant in analysis by one-way ANOVA and post-hoc Tukey tests when looking at p values of 0.01 and below. Optimisations were attempted to improve the

consistency between experiments. These included increasing the initial scrapie spike volume and lengthening the amplification period in an attempt to increase the difference in percent inhibition observed between the inhibitors. However, these alterations served to decrease differences between the mean percent inhibition of each group. Decreasing the inhibitor concentration produced an observably clearer pattern of inhibition, reflected by statistical analysis. Despite this, the p values calculated by post hoc Tukey tests for each experiment remained too inconsistent to reliably serve as a statistical output for strain typing.

Further development could potentially include testing additional TSE isolates. Here it was noted that at $p = 0.001$ the inhibition of scrapie isolate PG1361/05 was consistent over three experiments, in that rVRQ inhibited amplification more effectively than the other 3 rPrPs which themselves could not be distinguished. It is possible that other TSE isolates may provide distinct patterns at this level of statistical significance. However, this assay is currently reliant on a single round of PMCA, limiting the assay for use in isolates with higher amplification efficiencies. Therefore, alternative or additional criteria are likely to be required to increase the reproducibility of the assay and expand its applicability to characterise additional prion strains. Further analysis could include using a range of concentrations of each rPrP inhibitor and amplifying prions for up to 5 days of sPMCA. The use of additional rPrP inhibitors may also be explored to increase the panel size in the assay. It has been reported elsewhere that strains can be successfully differentiated by their amplification efficiencies in substrates with different PrP^{C} genotypes. As an example, CH1641 and ovine BSE share identical glycosylation profiles, but only BSE could be successfully amplified in ovine VRQ/VRQ substrate over 5 rounds of sPMCA (Taema et al. 2012). Therefore, the amplification efficiency of strains in PrP^{C} substrates of different genotypes could be used in combination with rPrP inhibition. This can also be included alongside the analysis of PrP^{res} glycoforms by western blotting or other established biochemical criteria for strain typing. An assay using these criteria could include the PMCA/sPMCA amplification of prions strains in a range of substrates and then the inhibition of successful amplification (for example after 5 rounds of sPMCA) with a range of rPrPs (and potentially other inhibitors). This screening of a panel of substrates and inhibitors alongside biochemical analysis of PrP^{Sc} products may provide a sufficiently detailed 'readout' of PrP^{Sc} properties to allow a comprehensive description of prion strains.

It was observed in this study that increasing the volume of PrP^{Sc} seed in PMCA reactions, as well as prolonging the length of the PMCA cycle, reduced the efficacy of the rPrP inhibitors. Indeed, having a single round of PMCA at 48 hours reduced the efficacy of the 1200 nM rVRQ treated control to ~50%, which was not significantly greater than the other inhibitors used at 400 nM. So under these conditions inhibition with rVRQ was not dose dependent, and in addition the inhibition levels were highly variable. These observations may be resultant of replicating PrP^{Sc} overcoming the negative inhibition incurred by rPrPs present in the reaction. If this inhibitory activity is due to rPrPs acting as less efficient conversion substrates as discussed previously (**Chapter 3**), rPrPs will slow the rate of PrP^{Sc} propagation (Hizumi et al. 2009; Honda & Kuwata 2017). Therefore, these observations may be explained by the gradual accumulation of replicating PrP^{Sc}. Alternatively, these observations may be due to populations of PrP^{Sc} able to convert rPrP, and therefore being resistant to its inhibitory effects, becoming more prominent in longer PMCA cycles. Indeed, recombinant PrPs can act as substrates for PMCA under optimised conditions (Atarashi et al. 2008; Faburay et al. 2014). In addition, increasing the amplification time may allow the propagation of minor populations of PrP^{Sc} conformation(s) that do not bind rPrP and are therefore 'resistant' to inhibition. Investigating these findings may reveal more in terms of understanding the mechanism of rPrP inhibition of prion amplification and the mechanism of prion conversion. To do so, experiments could analyse PMCA products obtained over 48 hrs by western blotting. PK digested PrP^{Sc} formed from recombinant PrP in PMCA exhibits unique western blotting patterns due to the absence of secondary modifications (Kim et al. 2010). Therefore, if rPrPs are being used as conversion substrates in these reactions, it may be expected to see a change in the western blot pattern over time as $rPrP^{res}$ is formed. PMCA is known to replicate the biochemical properties of the PrP^{Sc} seed (Castilla et al. 2008). Therefore, by analysing the products of the 48 hr PMCA in the presence and absence of rPrP inhibitor, for instance by CSA, may reveal differences in the dominant PrP^{Sc} product conformation indicating that the presence of rPrP 'selects' for a subset of PrP^{Sc}. Understanding whether rPrP can influence the type of PrP^{Sc} that propagates may have important implications if rPrPs are used as therapeutics *in vivo*.

Increasing the amount of PrP^{Sc} seed also reduced rPrP inhibition efficiency. These conditions could initiate PMCA reactions with a minor population of PrP^{Sc} which are not as effectively inhibited by the rPrP. For uninhibited reactions, there did not appear to be in increase in the total levels of PrP^{res} produced with increased seed

levels, so the decrease in inhibition efficacy of rPrP is unlikely to be a result of a large increase in PrP^{Sc}:rVRQ stoichiometry.

These observations indicate that the efficacy of rPrP inhibition is dependent on the quantity and state of replicating PrP^{Sc}. This may have a potential effect on the efficacy of rPrPs *in vivo*. For instance, in the study by (Skinner et al. 2015), hamsters infected with RML-Chandler scrapie were treated with recombinant hamster PrP at the time of inoculation in high (0.7 mg/mL) and low (0.35 mg/mL) doses. This demonstrably prolonged the onset of disease in the infected hamsters, and reduced the detection of PrP^{Sc} in the brain and spleen (Skinner et al. 2015). However, this result may well be aided by the application of rHam at the time of inoculation, and it was not determined if this treatment would have similar affects at mid or late disease stages (Skinner et al. 2015). Indeed, the observation that increased PrP^{Sc} seed decreases rPrP inhibition in PMCA suggests that the efficacy of rPrP inhibitors as therapeutics may be limited in later stages of disease, where PrP^{Sc} spread and propagation are likely to be more prominent. Further experiments are required to investigate this possibility, potentially through the use of rPrP inhibitors in early, mid and late stages of disease *in vivo*.

It was previously identified that the elution buffer used in IMAC purification of the rPrP proteins interfered in the amplification of BSE by PMCA, but not classical scrapie. As the major component of this buffer was imidazole, it was hypothesised that imidazole was inhibiting prion amplification. Here, increasing concentrations of imidazole were used in sPMCA of classical scrapie and ovine BSE. Out of these strains, ovine BSE was observed to be more sensitive to imidazole, with complete inhibition occurring at concentrations of 10 mM and above. Amplification of classical scrapie was not completely inhibited even at higher concentrations of imidazole. These data indicate that prion strains have different sensitivity to imidazole concentrations in PMCA. The cause of this inhibition is uncertain. Metal chelators including imidazole have been reported to actually increase amplification efficiency by limiting inhibition by metal ions in some instances (Orem et al. 2006; Fujihara et al. 2009). However, the use of imidazole at 250 mM appeared to inhibit the amplification of $PrP^{27\text{-}30}$ (Orem et al. 2006). The authors suggested that these observations could be due to the high ionic strength of imidazole (Orem et al. 2006). To investigate this activity, the sensitivity of different scrapie and BSE strains to imidazole in PMCA could be investigated across a range of imidazole concentrations. This could elucidate the mechanism of imidazole inhibition, and

potentially determine whether prion strains can be distinguished by their sensitivity to imidazole inhibition.

Chapter 5: Identification of Immunoreactive Peptides Specific to Scrapie Autoantibodies by Next Generation Phage Display

5.1. Introduction

The development of ante-mortem diagnostics for prion diseases is a major area of prion research to this day. In humans, the gold standard for disease diagnosis remains to be the detection of PrP^{Sc} in brain tissue obtained post mortem (Lee et al. 2013). Recent years have seen the advancement of rapid diagnostic tests such as RT-QuIC to detect PrP^{Sc} in the aim of developing rapid ante-mortem diagnostics (Orrú et al. 2015; Cramm et al. 2015; McGuire et al. 2016; Fairfoul et al. 2016). However, PrP^{Sc} is typically at very low concentrations in tissues in early stages of disease, limiting assays to those with very high sensitivity (Nicoll & Collinge 2009). Consequently, the detection of biomarkers unrelated to PrP^{Sc} may permit more effective or complementary disease diagnosis at early disease stages.

Alternative surrogate biomarkers include autoantibodies. Indeed, anti-PrP autoantibodies have been reported in patients with prion diseases that could be exploited for diagnosis (Wei et al. 2012). Additionally, autoantibodies immunoreactive to biomarkers have been identified in both humans and animals with prion diseases, such as against axonial neurofilaments, NDMR or GFAP (Sotelo et al. 1980; Tiwana et al. 1999; Nomura et al. 2009; Mackay et al. 2012). Interestingly, autoantibodies present in the cerebrospinal fluid of patients with other neurodegenerative diseases have been proposed as potential biomarkers of disease (Nagele et al. 2011). It has been reported that patients with AD, PD and MS can be distinguished from healthy patients by the mapping of sera and CSF based autoantibodies by protein microarray (Nagele et al. 2011; Han et al. 2012; Ayoglu et al. 2013; DeMarshall et al. 2016). These studies demonstrate that the presence of autoantibodies in the sera of patients with neurodegenerative diseases can potentially be exploited for disease diagnosis. These studies utilised human protein microarrays to identify disease specific autoantibodies. Although a powerful technique, microarrays can be limited by a number of factors including the availability of protein epitopes in the array, lack of secondary modifications, the use of single splice variants to produce protein arrays and disease heterogeneity (Zhu & Snyder 2003; Jaluria et al. 2007; Ramachandran et al. 2008; Chen & Snyder 2010; Ng et al. 2015).

An alternative to protein microarray is NGPD (Dias-Neto et al. 2009). An advantage of phage display over protein microarray is library size. Phage display utilises large libraries of random sequences (10^{7-11}), while the protein microarrays used to distinguish between AD and healthy patients contained up to 10^4 antigens (Nagele et al. 2011). Therefore, NGPD libraries have a larger range of ligands that

could be utilised for epitope mapping. NGPD has been previously reported to identify immunoreactive peptides that can be used in diagnostic assays to recognize sera based antibodies in pigs or chickens infected with *Salmonella enterica* serovar Typhimurium (Naqid et al. 2016). These peptides were then validated in diagnostic ELISAs that could distinguish between infected and healthy animals (Naqid et al. 2016). NGPD has also been applied to map the epitopes of IgG antibodies in the sera of HIV patients (Ryvkin et al. 2012). However, NGPD has not been applied to the discovery of immunoreactive peptides as diagnostic ligands in neurodegenerative diseases.

In this study, NGPD was applied to the sera from scrapie infected and uninfected sheep to map the epitopes of sera based IgG autoantibodies. This was with the aim of identifying immunoreactive peptides that recognise disease specific IgG autoantibodies. Initially, two panning strategies were attempted using two different elution methods – competitive elution or direct infection of TG1 bacteria. The successful method was then applied to screen sera from scrapie infected or uninfected sheep taken at multiple time points, in addition to unrelated controls. Analysis of sub libraries and phage-peptide selection was performed using a two-proportion Z-score analysis as outlined by (Zhang et al. 2011). Variations in the analysis were also attempted in an attempt to further identify discriminatory peptides. 39 peptides identified in analysis were then selected for synthesis and validation by immunoassay.

5.2. Results

5.2.1. A Proof of Principle Screen for Scrapie Specific Immunoreactive Peptides

The sera available for use in this study are displayed in (**Table 5.2.1.** and **Table 5.2.2.**). These consisted of sera obtained from sheep naturally exposed to and infected with the scrapie agent by introduction onto a scrapie affected farm at birth. Blood samples were then taken at multiple time points. In parallel, sera were taken from age matched animals from a scrapie negative flock obtained across similar time points (**Table 5.2.1.**). Sera were also available from sheep unrelated to this time course experiment and were from both scrapie positive and scrapie negative sheep (**Table 5.2.2.**). Each panning experiment utilised a selection of time course or unrelated sera to enrich phage/peptides that recognise autoantibodies specific to scrapie infected sheep. The workflow of each experiment is illustrated in (**Figure 5.2.1.**). Each phage display experiment was performed for just two rounds of biopanning to enrich peptide binders but to also maintain the diversity of possible peptide binders. Sub libraries produced in round 2 panning were sequenced on an Ion Torrent instrument by the University of Pennsylvania's DNA sequencing facility using a PI chip, with 70-90 M reads per chip. The data received was processed to give the frequency of individual peptides in each barcoded sample, using Perl scripts prepared by members of ADAS and ADAC (**Figure 5.2.1.**). The frequency and ratio of peptides between target samples and reference controls were used to generate Z-scores by a two-proportion Z-test (**Figure 5.2.1.**). These Z-scores acted as a selection criteria for peptides found in scrapie positive samples, with higher scores in positive samples being indicative of enrichment/specificity in a given sample while those identified in negative samples were selectively removed.

To identify peptides immunoreactive to autoantibodies in the sera of scrapie infected sheep, two screening strategies were performed. These screens used two methods of elution, direct infection of TG1 culture (screen 1, **Figure 5.2.2.**) and competitive elution with purified IgGs (screen 2, **Figure 5.2.3.**). In competitive elution, IgG antibodies were purified from different scrapie-infected sheep (06-1048 to 06-1053, months 12 and 21, **Table 5.2.1.**). The aim of using purified IgGs from different sheep for elution was to increase the specificity of selection in each biopanning round. In the first round of each screen, the phage libraries were panned against the sera of six sheep at months 12 and 21 of scrapie infection (**Figure 5.2.2**, **5.2.3.**). Phage-peptides bound to IgG antibodies were isolated by

capture with protein G coupled magnetic beads before washing and elution. The enriched phage were pooled to form a sub library that was then used for round 2 biopanning (**Figure 5.2.2.**, **5.2.3.**). Each screen utilised different samples in round 2 biopanning. This was in an attempt to investigate whether scrapie specific peptides can be enriched by panning against unrelated samples in round 2 panning (compared to those used in round 1), or whether using the same samples in rounds 1 and 2 would enrich more specific peptides. Another rationale was whether similar peptides or peptide sequences could be identified between the different round 2 screens. If peptides were identified in both screens using different samples, this would be convincing evidence of scrapie specific enrichment. However, at this time there were 49 barcoded primers available, limiting the total selection of samples for screening. In screen 1 the pooled sub library from round 1 was panned against a selection of unrelated scrapie positive and negative samples (**Figure 5.2.2.**). In screen 2 the pooled library was panned against the same 12 sera as in round 1, as well as 6 unrelated positive sera samples and 7 negative sera samples (**Figure 5.2.3.**). These data were then analysed by a two-proportion Z-test, using reference controls (**Figure 5.2.2.**, **5.2.3.**).

Z-scores were obtained for all peptides over a score of 0, as negative Z-scores are indicative of peptide enrichment in the negative control references. In screen 1, these control references were ARSU Pool 1 and 2 (**Figure 5.2.2.**). In screen 2, these control references were a pool of sera from animals N291, N329, N346, N382, N390 and N393 obtained at 12 and 21 months (**Figure 5.2.3.**). In screen 1, peptides were selected in a training cohort of samples using the criteria 1) Z-scores >2 in positive samples, 2) removal of peptides with Z-scores >2 in negative samples and 3) identified in four or more scrapie positive animals out of the 6 'training' samples tested (**Figure 5.2.2**). Peptides identified that met these criteria were then screened in a test cohort of samples (scrapie infected and uninfected) under the same criteria (**Figure 5.2.2.**). In screen 1, one peptide (RELDLSDAA) met the selection criteria used in Z-score analysis for both the training and test cohorts (**Table 5.2.3.**).

In screen 2, peptides were selected in a training cohort of samples using the criteria 1) Z-scores >2 in positive samples, 2) removal of peptides with Z-scores >2 in negative samples and 3) identified in four or more scrapie positive animals out of the 5 'training' samples tested (**Figure 5.2.3.**) Due to the limited number of negative samples, only the first and third selection criteria could be applied to the 'test' cohort (**Figure 5.2.3.**). 34 peptides were identified in screen 2 that met

the selection criteria (**Tables 5.2.4., 5.2.5.**). However, it was difficult to ascertain their specificity due to the limited number of negative samples on which to perform subtractive screening. To compensate, an alternative method of analysis was employed. In this analysis, three sets of Z-scores were produced for each peptide using three separate reference pools, N269/N270 Month15, G130/G320 or ARSU Month 12/21 Pools (**Figure 5.2.3.**). It was hypothesised that alternating the reference controls would produce different Z-scores for each peptide. Therefore, peptides identified consistently using difference reference controls would appear more convincingly diagnostic. As in the previous analyses, Z-scores were obtained for peptides with scores >0. The selection criteria in the training cohort were 1) Z-scores >2, 2) not seen in any negative sample with Z-scores >2 and 3) identified in four or more scrapie positive animals out of 5. Due to the limited number of negative samples, only the first and third selection criteria could be applied in the test cohort. This resulted in a list of 49 peptides that matched these criteria (**Tables 5.2.6., 5.2.7**). Peptides that were consistently identified by the selection criteria between analyses were ranked higher than those that were not. Fourteen of these peptides matched those in the original analysis (**Table 5.2.8.**).

Table 5.2.1. The sera available from scrapie infected or uninfected sheep, obtained from animals that were 3-24 months old. The sheep samples were obtained from a scrapie infected flock (APHA, Ripley). Blood from scrapie negative sheep was sourced from a New-Zealand-derived, classical scrapie free flock (APHA, ARSU).

Scrapie Positive		Scrapie Negative	
Sample ID	Time Point (Month)	Sample ID	Time Point (Month)
06-1026	3, 6, 9, 12, 15, 16, 17, 18, 19, 20, 21, 22	N269	3, 6, 9, 12, 15, 16, 18, 21, 22, 23, 24
06-1030	3, 6, 9, 12, 15, 16, 17, 18, 19, 20, 21, 22	N270	3, 6, 9, 12, 15, 16, 18, 21, 22, 23, 24
06-1032	3, 6, 9, 12, 15, 16, 17, 18, 19, 20, 21	N277	3, 6, 9, 12, 15, 16, 18, 21, 22, 23, 24
06-1033	3, 6, 9, 12, 15, 16, 17, 18, 19, 20, 21, 22	N283	3, 6, 9, 12, 15, 16, 18, 21, 22, 23, 24
06-1038*	3, 6, 9, 12, 15, 16, 17, 18, 19, 20, 21	N284	3, 6, 9, 12, 15, 16, 18, 21, 22, 23, 24
06-1042*	3, 6, 9, 12, 15, 16, 17, 18, 19, 20, 21	N287	3, 6, 9, 12, 15, 16, 18, 21, 22, 23, 24
06-1048	3, 6, 9, 12, 15, 16, 17, 18, 19, 20, 21, 22	N289	3, 6, 9, 12, 15, 16, 18, 21, 22, 23, 24
06-1049	3, 6, 9, 12, 15, 16, 17, 18, 19, 20, 21, 22	N291	3, 6, 9, 12, 15, 16, 18, 21, 22, 23, 24
06-1050*	3, 6, 9, 12, 15, 16, 17, 18, 19, 20, 21	N329	3, 6, 9, 12, 15, 16, 18, 21, 22, 23, 24
06-1051*	3, 6, 9, 12, 15, 16, 17, 18, 19, 20, 21	N346	3, 6, 9, 12, 15, 16, 18, 21, 22, 23, 24
06-1052*	3, 6, 9, 12, 15, 16, 17, 18, 19, 20, 21	N382	3, 6, 9, 12, 15, 16, 18, 21, 22, 23, 24
06-1053	3, 6, 9, 12, 15, 16, 17, 18, 19, 20, 21, 22	N390	3, 6, 9, 12, 15, 16, 18, 21, 22, 23, 24
		N393	3, 6, 9, 12, 15, 16, 18, 21, 22, 23, 24
		N402	3, 6, 9, 12, 15, 16, 18, 21, 22, 23, 24

* Month 21 sera were obtained post mortem.

Table 5.2.2. Sera from sheep unrelated to the scrapie time course samples. Samples from scrapie positive sheep were obtained from a scrapie infected flock (APHA, Ripley). Blood from scrapie negative sheep was sourced from a New-Zealand-derived, classical scrapie free flock (APHA, ARSU).

Scrapie Positive		Scrapie Negative	
Sample ID	Time Point (age in months)	Sample ID	Time Point (age in months)
PG0326/07	23	PG1409/08	Unknown
PG0333/07	23	PG1410/08	Unknown
PG0334/07	23	PG1418/08	Unknown
PG0335/07	23	PG1432/08	Unknown
PG0336/07	23	PG1433/08	Unknown
PG0350/07	23	G130*	72
		G320*	72
		ARSU Pool 1	Unknown
		ARSU Pool 2	Unknown

*Sera was available from three time points: 01/03/06, 05/04/06 and 04/05/06.

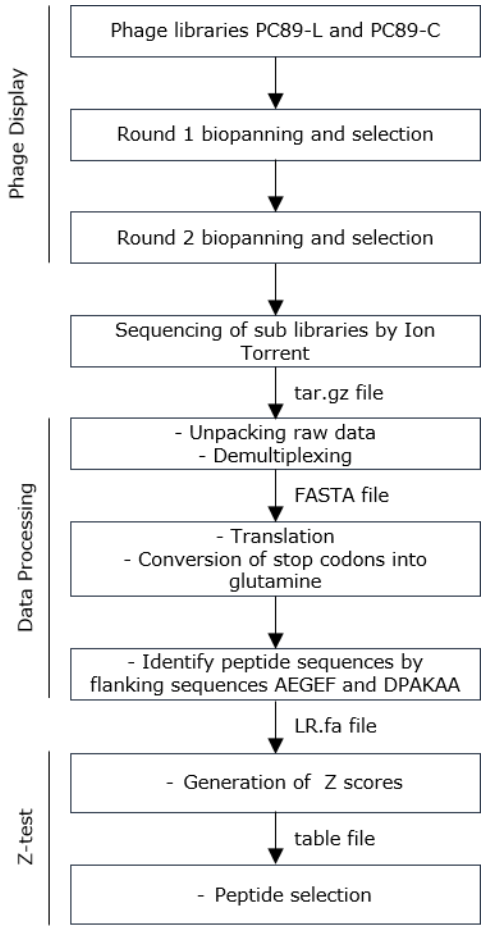

Figure 5.2.1. Workflow of phage display panning, followed by analysis of NGS data. Each step is indicated on the left, with data file types indicated between each stage of analysis. Experiments were performed over two rounds of selection of linear (PC89-L) or constrained (PC89-C) peptides of 9 amino acids. Sub libraries were sequenced by Ion Torrent at the University of Pennsylvania DNA sequencing laboratory. Raw data was received as a tar.gz library file and extracted as FASTQ files. Sequence reads were separated according to peptide length and barcode by demultiplexing to form FASTA files. In translation, unused barcode sequences were excised from the data and stop codons were replaced with glutamine. Peptide sequences were then identified by the flanking motifs AEGEF and DPAKAA. A two-proportion Z-test was performed to produce Z-scores for each peptide sequence, calculated with the frequency and ratio of peptides found in a target sample relative to a reference control. Peptide sequences were then selected for their specificity based on select criteria, including their Z-scores in positive samples relative to negative samples, or the number of positive samples in which they are observed above a defined Z-score.

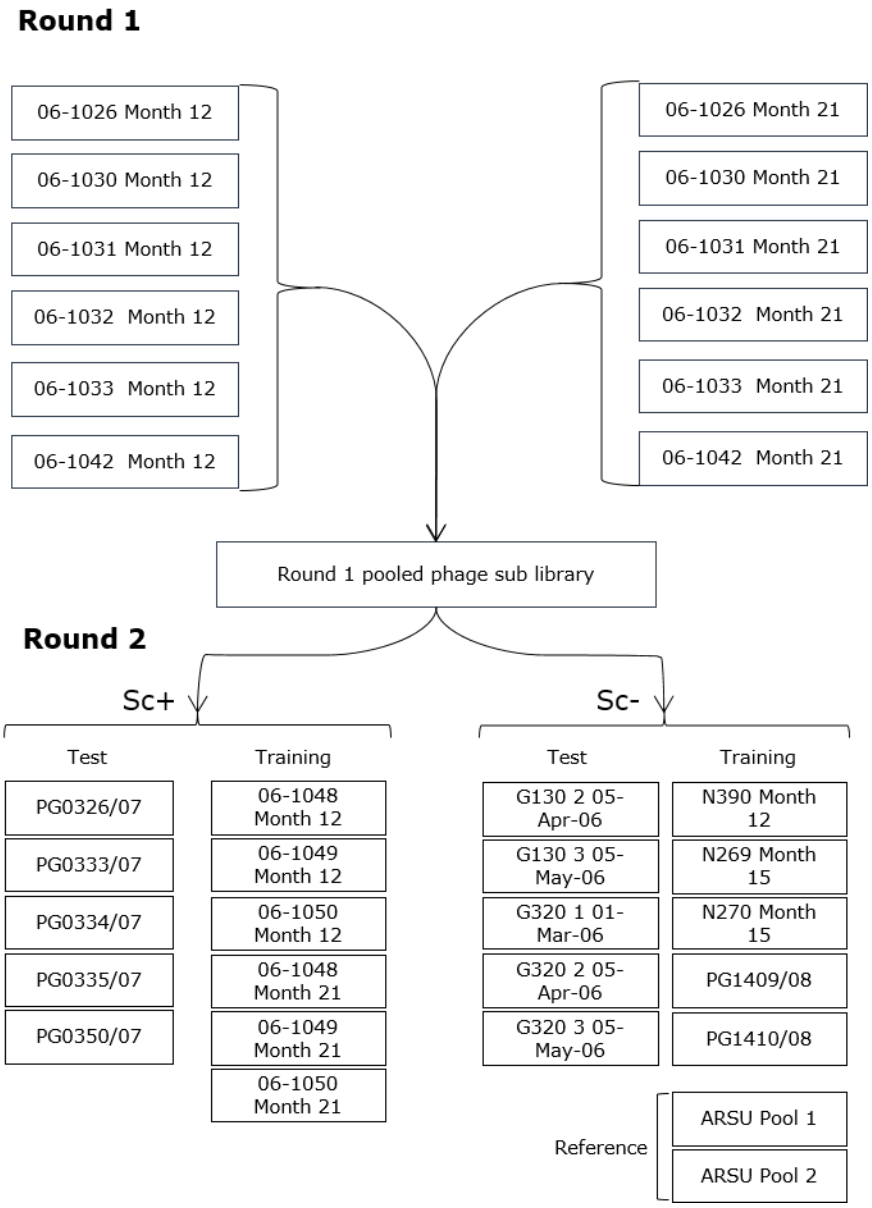

Figure 5.2.2. Panning for peptide mimotopes that bind to scrapie-infection specific autoantibodies - screen 1. Peptide libraries were panned against 6 sera at month 12 scrapie infection or 6 sera at month 21 scrapie infection in round 1. The resulting sub library of phage was pooled and panned against a selection of unrelated sera from scrapie infected or uninfected sheep. Samples used in training and test cohorts for analysis are indicated, as well as the samples used as a negative control reference (data from these two samples were pooled) to calculate Z-scores. This experiment was performed using TG1 elution of phage.

Table 5.2.3. The peptide binder identified in target samples in screen 1. The peptide is displayed as the number of scrapie positive animals in which it was identified in the training cohort, followed by the Z-scores in which they were identified in the test cohort. Blue: Z-scores >2. Orange: Z scores >5. The selection criteria to identify this peptide included 1) Z-scores >2, 2) not seen in any negative sample with Z-scores >2 and 3) identified in four or more scrapie positive animals. From the training cohort, there were 225 peptides that matched the selection criteria of which 1 peptide was identified that matched the criteria in the test cohort - RELDLSDAA.

		Test Cohort (Scrapie Infected, n = 5)				
Peptide	Training Cohort	PG0326	PG0333	PG0334	PG0335	PG0350
RELDLSDAA	5/6	4.58	0	2.45	7.48	9.17

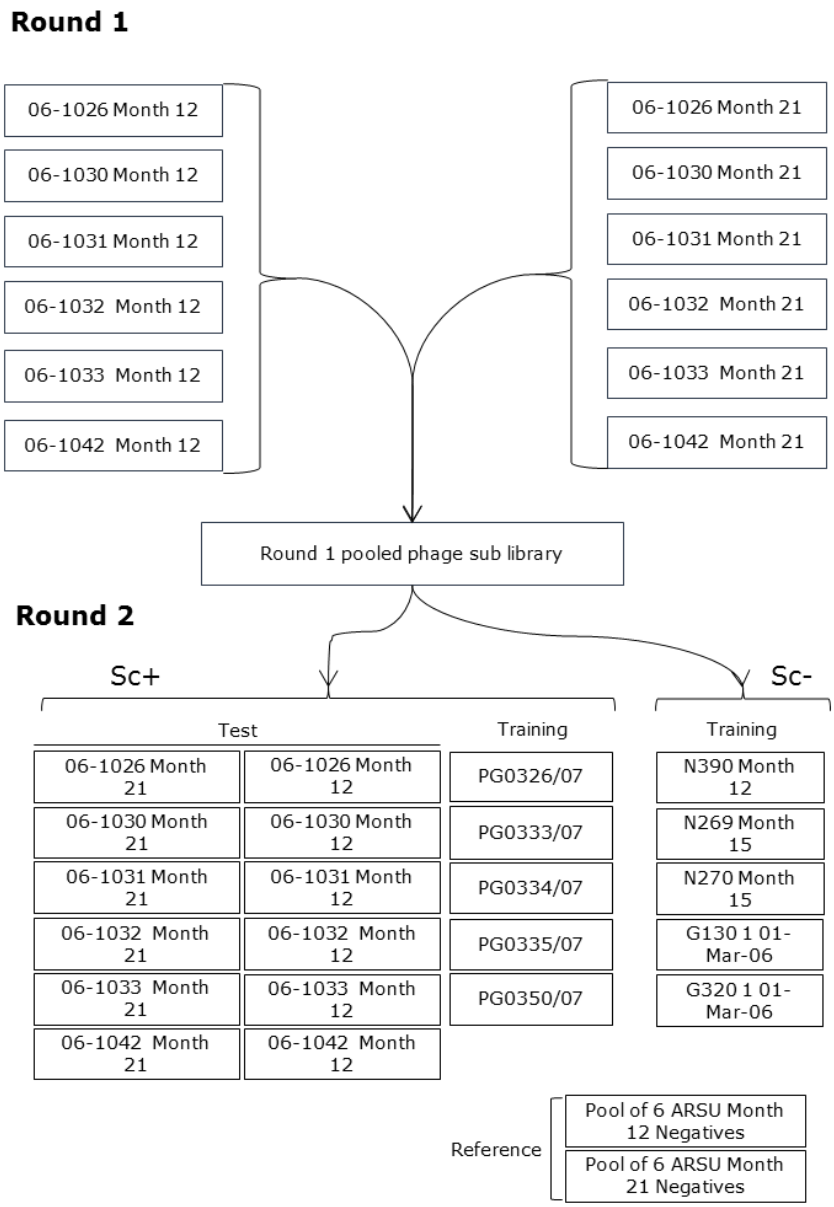

Figure 5.2.3. Panning for peptide mimotopes that bind to scrapie-infection specific autoantibodies - screen 2. Peptide libraries were panned against 6 sera at month 12 scrapie infection (early) or 6 sera at month 21 scrapie infection (late) in round 1. The resulting sub library was pooled and panned against the same sera as in round 1, as well as unrelated scrapie infected or uninfected sera. Samples used in training and test cohorts for analysis are indicated, as well as the samples used as a negative control reference to generate Z-scores (the data from these two samples was pooled). The reference samples constitute equal volumes of sera pooled from N291, N329, N346, N382, N390 and N393 obtained at 12 and 21 months (**Table 5.2.1.**). This experiment was performed using competitive elution with purified IgG antibodies from unrelated positive animals 06-1048 to 06-1053 at months 12 and 21 (**Table 5.2.1.**)

Table 5.2.4. Peptide binders 1-22 identified in target samples in screen 2. Peptides are displayed as the number of scrapie positive animals in which they were identified in the training cohort, followed by the Z-scores in which they were identified in the test cohort. Blue: Z scores >2. Orange: Z scores >5. Red: Z scores >10. Selection criteria included: 1) Z-scores >2, 2) not seen in any negative sample with z-scores >2 and 3) identified in four or more scrapie positive animals.

		Test Cohort											
		Month 12 Infected (n = 6)						Month 21 Infected (n = 6)					
Peptide	Training Cohort	1026	1030	1032	1033	1038	1042	1026	1030	1032	1033	1038	1042
CTAGPTPMSPCG	5/6	5.66	0	0	2.24	5.66	2.24	2.45	5.48	2.83	2	2.45	5.29
CARQFCPLNLCG	4/6	3.16	0	0	3.87	0	3.74	7.94	5.1	7.87	5.74	6.32	3
DYDQEIQPQ	4/6	3	0	0	5.29	3.46	0	7.35	4.47	3.46	2.65	4.36	11
CAALRTRRHSCG	4/6	1.41	0	0	3.32	2.83	3.16	3	0	0	3.46	2.45	6
CSRQPSLPLVCG	5/6	2.65	0	0	3.74	3.74	4.12	0	0	4.69	3.87	2.45	1.41
IRHTVNDSQ	4/6	0	0	0	1.41	3.61	5.2	10.15	0	2.24	7.68	3.61	2.24
KHKQPPGPS	4/6	4	0	31.97	1.73	4	2.65	7.35	0	0	4.9	3.74	2
RPLSVLLLP	5/6	2	13.97	0	4.24	1.73	0	7.14	0	2.83	2.24	4.47	3
CQCPYCLRRQCG	4/6	2.45	0	0	5.2	5.2	1	8.54	0	0	0	3.32	5.2
CQRPSGSPQ	4/6	3.16	0	36.45	2.45	0	0	0	0	3.61	0	2.65	3.74
CQSPAQPS	4/6	1.73	0	0	3.32	4.47	3.46	0	0	0	4	6.56	4.47
DQRTLLESW	4/6	1.41	0	0	3.74	5	4.47	0	0	3.46	0	3.46	3.74
PTIYSYTPQ	5/6	5.39	0	0	3.16	5.57	0	0	0	6.08	2	3.32	3.74
PNWILFQVL	5/6	4.8	0	0	2.65	1	4.24	0	0	4.69	4.47	4.12	1.73
QKQGADKRQ	5/6	2.65	0	0	2.83	3.16	3.87	0	1.41	5	0	0	3.16
RLAKRGSAS	5/6	1	0	0	4.69	4.9	4.36	6.86	0	0	2	3.32	3.46
TTQHAKKRS	4/6	0	1.41	0	3.46	0	2.83	3.46	3.46	0	3.16	1	2.45
VAQLTMRVR	4/6	3	0	0	3.32	4	0	4.12	0	0	4.58	1.41	4
YRSKDSSVP	4/6	1.41	0	0	0	4.24	1	7.07	6.16	0	8.6	3.87	7.68
CAVQARSQRLCG	4/6	2.24	0	0	3	0	3.46	0	0	2.83	1	0	2.65
CGITRALPARCG	4/6	3	0	0	1.73	2	3.74	0	7.55	7	0	1.41	2.24
CQLPRALAFSCG	4/6	3.61	0	0	2.83	0	0	1.73	0	0	2.83	2.45	2.45

Table 5.2.5. Peptide binders 23-34 identified in target samples in screen 2. Peptides are displayed as the number of scrapie positive animals in which they were identified in the training cohort, followed by the Z-scores in which they were identified in the test cohort. Blue: Z scores >2. Orange: Z scores >5. Red: Z scores >10. Selection criteria included: 1) Z-scores >2, 2) not seen in any negative sample with z-scores >2 and 3) identified in four or more scrapie positive animals.

		Test Cohort											
		Month 12 Infected (n = 6)						Month 21 Infected (n = 6)					
Peptide	Training Cohort	1026	1030	1032	1033	1038	1042	1026	1030	1032	1033	1038	1042
FSQNIAAEP	4/6	4.24	0	0	1	0	0	0	5.83	10.49	0	4.9	4.12
IQAAHSTAE	4/6	3	0	0	7.28	0	9.85	0	11.31	4.47	0	2	0
ASSQSNDPL	5/6	0	11.31	29.22	6.16	2	0	0	0	0	5.66	1	0
CLPRHAQRSTCG	4/6	2.83	0	0	2.83	0	2.45	0	1.73	0	2.83	1.41	1.41
CLRNFHGRQVCG	4/6	1.73	0	0	2.24	0	0	1	0	5.57	2.83	1.41	3.46
CRILPPQSKLCG	4/6	2.65	0	0	2.45	1	0	0	0	0	5.57	1.73	11.53
CYPYATPCRQCG	4/6	1.73	0	0	4	2	1.73	7.21	0	1.73	3.32	3.74	0
GIPQTRSKG	4/6	1	0	26.33	0	0	0	0	0	2	2.24	2.45	3
NAPGRHGRQ	4/6	3.61	0	0	0	0	0	0	0	3.61	7.62	1.41	3.46
NVGRAELDS	4/6	3.16	0	0	2.65	0	0	0	0	0	0	2.83	2.24
RGTSSGEFS	4/6	3.32	10.3	0	4.9	4.24	0	0	0	0	0	1.73	0
RIPLPQMAP	4/6	2	0	0	5.48	2.24	2	0	0	3.61	2	1.73	2.83

Table 5.2.6. Peptides 1-31 identified by alternative analysis of screen 2. Z-scores were calculated using three separate reference controls of ARSU Pool1/2, N269/N270 and G130/G320 (**Figure 5.2.3.**). The selection criteria included: 1) Z-scores >2 and 2) not seen in any negative sample with z-scores >2 and 3) identified in four or more scrapie positive animals. Peptides identified consistently between analysis were ranked on the average number of positive samples in which they were seen with Z scores >2 (out of 12). Means were calculated for each peptide to aid presentation. The standard deviation for each was also calculated to indicate peptides more consistently identified with a mean score >4. 49 peptides were identified that met the selection criteria.

Peptide	Score 1	Score 2	Score 3	Mean	SD
QLQMFLSP	10/12	10/12	10/12	10/12	0
CPPWDILTAACG	9/12	9/12	9/12	9/12	0
KHKQPPGPS	8/12	8/12	8/12	8/12	0
RPLSVLLLP	8/12	8/12	8/12	8/12	0
CAQSCLGPPLAG	7/12	7/12	7/12	7/12	0
CHSFQAQHLCG	7/12	7/12	7/12	7/12	0
CLIRPHHAPGCG	7/12	7/12	7/12	7/12	0
CQDDYQHCP	7/12	7/12	7/12	7/12	0
EVVQRTSSM	7/12	7/12	7/12	7/12	0
HTESRPQAQ	7/12	7/12	7/12	7/12	0
IRHTVNDSQ	7/12	7/12	7/12	7/12	0
RLAKRGSAS	7/12	7/12	7/12	7/12	0
CTAGPTPMSPCG	10/12	0/12	10/12	6.67/12	5.77
CTPAQQVSAICG	9/12	0/12	9/12	6/12	5.20
CASQLSHPLVCG	6/12	6/12	6/12	6/12	0
CLSGSDPSQPCG	6/12	6/12	6/12	6/12	0
CQDFHKHLLACG	6/12	6/12	6/12	6/12	0
CTILSAFVLQCG	6/12	6/12	6/12	6/12	0
DQRTLLESW	6/12	6/12	6/12	6/12	0
PNWILFQVL	6/12	6/12	6/12	6/12	0
QKQGADKRQ	6/12	6/12	6/12	6/12	0
CQQACRRHSGCG	6/12	6/12	4/12	5.33/12	1.15
CERIMPAQYQCG	5/12	5/12	5/12	5/12	0
CPARFYEQCWCG	5/12	5/12	5/12	5/12	0
CPQAFLIIACCG	5/12	5/12	5/12	5/12	0
FSQNIAAEP	5/12	5/12	5/12	5/12	0
GIPQTRSKG	5/12	5/12	5/12	5/12	0
PKPQPSKSS	5/12	5/12	5/12	5/12	0
QDKHTRCSS	7/12	0/12	7/12	4.67/12	4.04
CPSSRELTRVCG	5/12	5/12	4/12	4.67/12	0.58
VVLPTLPPQ	6/12	6/12	1/12	4.33/12	2.89

Table 5.2.7. Peptides 32-49 identified by alternative analysis of screen 2. Z-scores were calculated using three separate reference controls of ARSU Pool1/2, N269/N270 and G130/G320 (**Figure 5.2.3.**). The selection criteria included: 1) Z-scores >2 and 2) not seen in any negative sample with z-scores >2 and 3) identified in four or more scrapie positive animals. Peptides identified consistently between analysis were ranked on the average number of positive samples in which they were seen with Z scores >2 (out of 12). Means were calculated for each peptide to aid presentation. The standard deviation for each was also calculated to indicate peptides more consistently identified with a mean score >4. 49 peptides were identified that met the selection criteria.

Peptide	Score 1	Score 2	Score 3	Mean	SD
CIDEPRSQSPCG	6/12	6/12	0/12	4/12	3.46
CQRPSGSPQ	6/12	0/12	6/12	4/12	3.46
CTRQAPFLFGCG	6/12	6/12	0/12	4/12	3.46
GNWHRPPPG	6/12	6/12	0/12	4/12	3.46
AKAQDGSS	4/12	4/12	4/12	4/12	0
CLPRHAQRSTCG	4/12	4/12	4/12	4/12	0
CLPRMQILLSCG	4/12	4/12	4/12	4/12	0
CNRRECSRL	4/12	4/12	4/12	4/12	0
CQTRLTPPAICG	4/12	4/12	4/12	4/12	0
CPASPCPPACG	4/12	4/12	4/12	4/12	0
CPQLLPPSFRCG	4/12	4/12	4/12	4/12	0
CRDSFFSVSQCG	4/12	4/12	4/12	4/12	0
CRILPPQSKLCG	4/12	4/12	4/12	4/12	0
CRQRHRPVRACG	4/12	4/12	4/12	4/12	0
CTCRLGQLITCG	4/12	4/12	4/12	4/12	0
QQPIPFRPT	4/12	4/12	4/12	4/12	0
RGTSSGEFS	4/12	4/12	4/12	4/12	0
YTASFQVPS	4/12	4/12	4/12	4/12	0

Table 5.2.8. Peptides identified between original and multiple analysis of screen 2.

Peptide
CLPRHAQRSTCG
CRILPPQSKLCG
CQRPSGSPQ
CTAGPTPMSPCG
DQRTLLESW
FSQNIAAEP
GIPQTRSKG
IRHTVNDSQ
KHKQPPGPS
PNWILFQVL
QKQGADKRQ
RGTSSGEFS
RLAKRGSAS
RPLSVLLLP

5.3. Panning Against a Time Course of Scrapie Positive and Negative Sheep

The most effective method of elution was determined to be competitive elution with purified IgG antibodies, due to the number of peptides that met the selection criteria in the Z-test analysis of sequencing data. However, screen 2 was limited in its number of negative samples. Therefore, although peptides were identified that met the selection criteria, the specificity of these peptides were undetermined. Another screening strategy (screen 3) was proposed with a larger number of positive and negative samples to provide a comprehensive screen for peptides immunoreactive to scrapie specific autoantibodies (**Figure 5.3.1.**). In this screen, the round 1 sub library from screen 2 was panned against sera taken from scrapie infected sheep or uninfected sheep on a time course of 6, 9, 12, 15, 18 and 21 months (**Figure 5.3.1.**). The sub library was also panned against a range of sera samples from infected and uninfected sheep that were unrelated to the time course experiment (**Figure 5.3.1.**). The round 1 library from screen 2 was used in an attempt to identify peptides in both screen 2 and screen 3. Similar peptides found in both experiments would be indicative of specificity to scrapie specific antibodies. Z-scores were calculated for each peptide using the six pools of additional sera from the time course experiment as non-infected reference controls (**Figure 5.3.1.**). In the analysis of screen 2 it was demonstrated that changing the reference controls used to generate Z-scores altered the selection of peptides, although a number of peptides were identified in both analyses. These differences in the peptides selected is possibly due to the heterogeneity in peptide populations between negative samples. Therefore, the population of peptides in the negative references were insufficient to account for all nonspecific peptides. For these reasons, the number of reference controls were increased to six in the analysis of this screen. Peptides with Z-scores >0 were selected in a training cohort of unrelated samples using the criteria 1) Z-scores >2, 2) not seen in any negative sample with z-scores >2 and 3) identified in four or more scrapie positive animals (**Figure 5.3.**). Peptides identified in the training cohort were screened in a test cohort of time course samples with the same selection criteria. This analysis identified 10 peptides that matched the selection criteria (**Table 5.3.**). Variations in the analysis were attempted with the data from screen 3 to determine whether more effective methods of identifying specific peptides may be discovered, determined by the number of peptides identified by each analysis. These are described in the following sections and each analysis was a variation of the two-proportion Z-score test, using different combinations of samples in training and test cohorts, as well as reference controls.

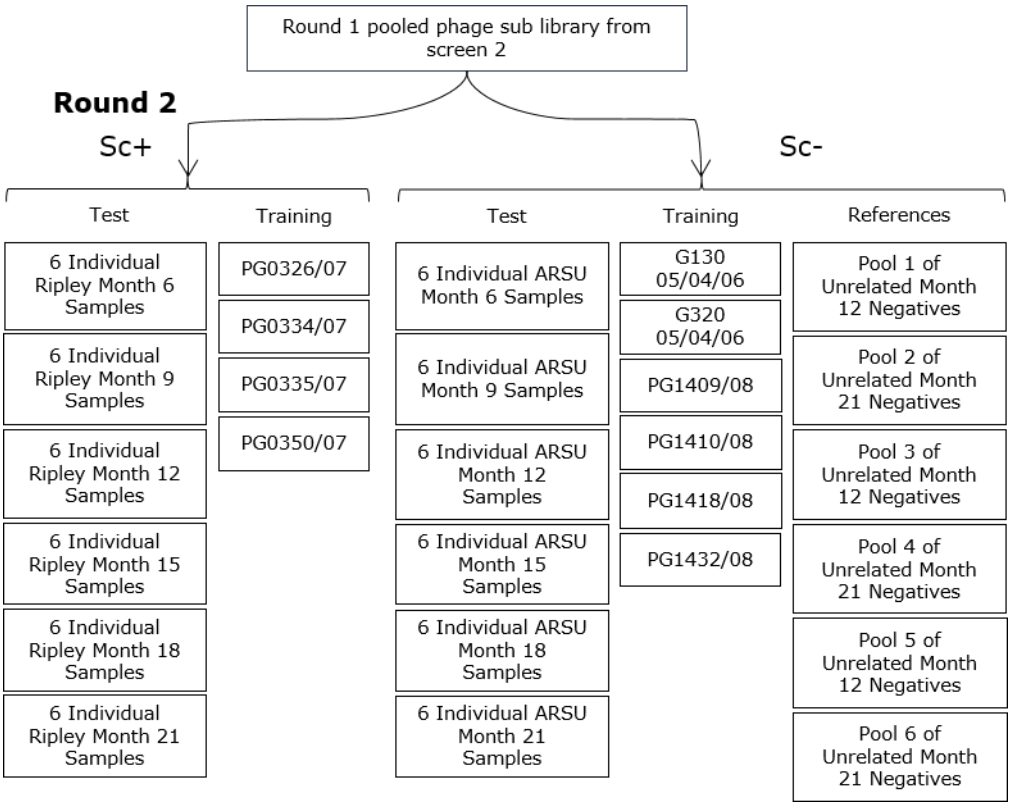

Figure 5.3.1. Panning for peptide mimotopes that bind to scrapie-infection specific autoantibodies **–** screen 3. The round 1 sub library from screen 2 was panned against sera taken over a time course in scrapie infected or uninfected animals, as well as unrelated scrapie positive and negative controls. Ripley groups included sera from the animals 06-1026, 06-1030, 06-1032, 06-1033 and 06-1042 for each time point. ARSU groups included sera from the animals N269, N270, N277, N284, N287 and N289 for each time point. The ARSU samples N291, N329, N346, N382, N390 and N393 from months 12 and 21 of the time course were pooled and used as reference controls (**Table 5.2.1.**). All six samples were pooled for each reference. Each reference control was pooled. This experiment was performed with competitive IgG elution, using IgG antibodies purified from samples 06-1048 to 06-1053 at months 12 and 21 (**Table 5.2.1.**).

Table 5.3. Peptide binders identified in target samples in screen 3. Each time point consisted of 6 samples, and peptides are scored as the number of samples in which the peptide matched the selection criteria in each time point. Peptides are displayed as the number of scrapie positive animals in which they were identified in the training cohort, followed by the number of samples in which they were identified in the test cohort. Selection criteria included 1) Z-scores >2, 2) not seen in any negative sample with z-scores >2 and 3) identified in four or more scrapie positive animals. None of the peptides in this table were observed with Z-scores >2 in any negative sample. Months with Z-scores >2 in samples are highlighted in red.

		Test Cohort					
		Scrapie Infected (n = 36)					
Peptide	Training Cohort	Month 6	Month 9	Month 12	Month 15	Month 18	Month 21
HRTTNTGAK	4/4	2/6	2/6	3/6	2/6	2/6	1/6
RPKLPGRPP	4/4	0/6	0/6	2/6	2/6	3/6	1/6
IARPYPKGL	4/4	1/6	1/6	2/6	0/6	2/6	0/6
LLTPRAQGR	4/4	0/6	0/6	1/6	2/6	2/6	1/6
HKHMSPNFR	4/4	1/6	2/6	0/6	0/6	1/6	1/6
SRRDLKNGA	4/4	2/6	3/6	0/6	0/6	0/6	0/6
AQLVFTSSS	4/4	2/6	2/6	0/6	0/6	0/6	0/6
EKPPIKLTQ	4/4	2/6	2/6	0/6	0/6	0/6	0/6
GGVLRNTKA	4/4	3/6	1/6	0/6	0/6	0/6	0/6
YGSFGRSSA	4/4	1/6	0/6	0/6	1/6	0/6	2/6

5.3.1. Analysis 2: Using Samples to Match Screen 2 Analysis

Screen 3 contained the same positive sera as used in screening strategy 2. It was hypothesised that by using these samples in the same method of analysis as screen 2 peptides could be identified that were enriched in both independent round 2 panning experiments. Identification of the same peptides between experiments would be indicative of enrichment against scrapie specific autoantibodies. Therefore, peptides were selected in the training cohort, followed by screening in Ripley months 12 and 21 only (**Figure 5.3.2.**). In this analysis, peptides with Z-scores >0 were selected in a training cohort of unrelated samples using the criteria 1) Z-scores >2, 2) not seen in any negative sample with z-scores >2 and 3) identified in four or more scrapie positive animals (**Figure 5.3.2.**). Due to the limited number of negative samples, only the first and third selection criteria could be applied in the 'test' cohort (**Figure 5.3.2.**). This analysis identified 29 peptides (**Tables 5.3.1. 5.3.2.**). One peptide, CQCPYCLRRQCG, was identified in both this analysis and screen 2.

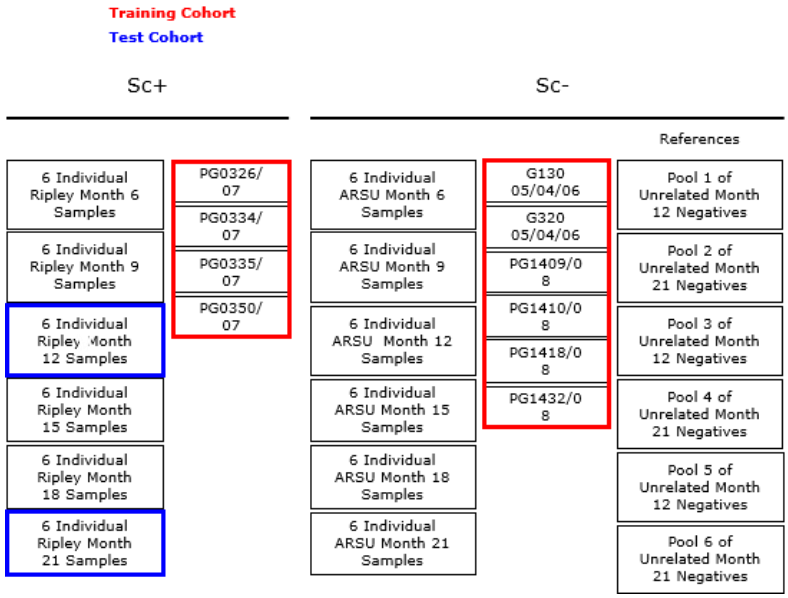

Figure 5.3.2. The samples from screen 3 used for Analysis 2. The same samples that were used in screen 2 were used as the test cohort in this analysis. Samples used for the training cohort are shown in red. Samples used for the test cohort are shown in blue.

Table 5.3.1. Peptides 1-15 identified by using the sera also used in screen 2 to identify peptides in both screens. 29 peptides matched the selection criteria in total. Peptides are displayed as the number of scrapie positive animals in which they were identified in the training cohort, followed by the Z-scores in which they were identified in the test cohort. Blue: Z-scores >2. Orange: Z-scores >5. Red: Z-scores >10. Selection criteria included 1) Z-scores >2, 2) not seen in any negative sample with Z-scores >2 and 3) identified in four or more scrapie positive animals.

		Test Cohort											
		Month 12 Infected (n = 6)						Month 21 Infected (n = 6)					
Peptide	Training Cohort	1026	1030	1032	1033	1038	1042	1026	1030	1032	1033	1038	1042
STRSQSMKQ	4/4	6.53	39.79	9.34	4.23	0	2.19	35.3	9.17	0	0	8.9	0
ANSKLYPRA	4/4	6.77	4.6	24.61	0	27.32	0	0	0	26.04	4.12	22.32	0
GNSKNGVIPP	4/4	0	4.58	0	4.24	0	2.83	0	3.87	5	8.89	0	0
QSSTKAIFT	4/4	2.06	3.3	0	4.15	6.65	0	12.36	0	0	14.62	0	0
RKSPASGPL	4/4	3.27	2.08	0	0	17.64	3.08	0	0	11.63	0	9.32	0
DDLGLKKYS	4/4	2.17	0	0	2.32	5.55	23.5	0	0	0	0	0	18.98
GYASKANPQ	4/4	6.17	0	7.59	0	0	2.94	26.1	0	0	12.7	0	0
HVKPRDQSL	4/4	0	0	6	0	0	15.53	6.08	0	0	3.32	0	10.35
PKKRAFAST	4/4	8.24	0	0	2.26	3.12	10.67	0	0	0	0	0	14.45
QFVEKHDNG	4/4	4.87	3.03	6.36	0	0	0	23.02	0	0	3.55	0	0
SSNKKTSEL	4/4	2.87	0	2.28	0	0	2.05	4.85	0	9.39	0	0	0
ARASSAQIT	4/4	2.13	0	9.25	0	0	0	3.5	3.69	0	0	0	0
ASEFKQSSA	4/4	0	3.03	0	0	0	0	7.17	0	0	0	5.43	19.84
CNQCSAPAPSCG	4/4	5.48	0	2.24	2.65	2.45	0	0	0	0	0	0	0
CQCPYCLRRQCG	4/4	0	0	0	4.38	3.18	3.19	0	0	0	0	4.92	0

Table 5.3.2. Peptides 16-29 identified by using the sera also used in screen 2 to identify peptides in both screens. 29 peptides matched the selection criteria in total. Peptides are displayed as the number of scrapie positive animals in which they were identified in the training cohort, followed by the Z-scores in which they were identified in the test cohort. Blue: Z-scores >2. Orange: Z-scores >5. Red: Z-scores >10. Selection criteria included 1) Z-scores >2, 2) not seen in any negative sample with Z-scores >2 and 3) identified in four or more scrapie positive animals.

		Test Cohort											
		Month 12 Infected (n = 6)						Month 21 Infected (n = 6)					
Peptide	Training Cohort	1026	1030	1032	1033	1038	1042	1026	1030	1032	1033	1038	1042
DPRRKSASL	4/4	0	128.88	0	0	50.55	0	0	152.73	0	0	26.45	0
ETPNIARKL	4/4	0	2.63	0	0	0	16.2	0	0	9.3	0	0	9.19
GYQSSRLNQ	4/4	0	2.45	0	3	0	2	0	0	0	6.93	0	5.75
HRTTNTGAK	4/4	0	48.42	0	0	17.71	5.68	0	62.12	0	0	0	0
KKSAPPQLL	4/4	3.68	0	3.5	0	0	4.9	0	0	0	7.02	0	0
LLTLTNESK	4/4	0	0	0	7.52	0	4.83	0	0	0	22.14	7.51	0
LQETERCPP	4/4	0	3.99	0	4.46	0	0	0	6.61	0	6.57	0	0
RPFKPRGGA	4/4	3.49	4.23	5.85	5.21	0	0	0	0	0	0	0	0
RPKLPGRPP	4/4	7.93	0	0	0	0	3.72	12.51	0	0	0	2.25	0
SERAVAGRP	4/4	0	0	0	0	0	0	0	9.34	2.53	0	3.15	3.04
SNTLFGVAQ	4/4	5.04	0	0	0	0	4.39	0	0	4.27	11	0	0
SPATIGLSW	4/4	0	3.43	0	2.4	2.92	0	0	0	0	7.41	0	0
TKLYAKDLR	4/4	9.04	0	0	0	2.4	6.58	5.47	0	0	0	0	0
YPLKNAQHG	4/4	0	0	5.74	8.73	0	39.85	0	0	0	0	3.25	0

5.3.2. Analysis 3: Identification of Peptides Across the Disease Time Course

It was questioned whether diagnostic peptides could be identified across the course of disease in animals. To do this, the first three samples from each time point were used as the training cohort (18 infected and non-infected samples), with the remaining three samples in each time point and unrelated samples as the test cohort (**Figure 5.3.3.**). To select for peptides enriched in each sample, the test and training cohorts were alternated six times (i.e. 6 analyses were carried out each using a different combination of training and test cohort samples). In each analysis, peptides were identified with Z-scores >0, and selected using the criteria of 1) Z-scores >2, 2) not seen in any negative sample with Z-scores >2 and 3) identified in two or more scrapie positive animals out of 22. The selection criteria were used on both training and test cohorts. Only peptides consistently identified between analyses were selected. This analysis identified six peptides which met the selection criteria (**Table 5.3.3.**).

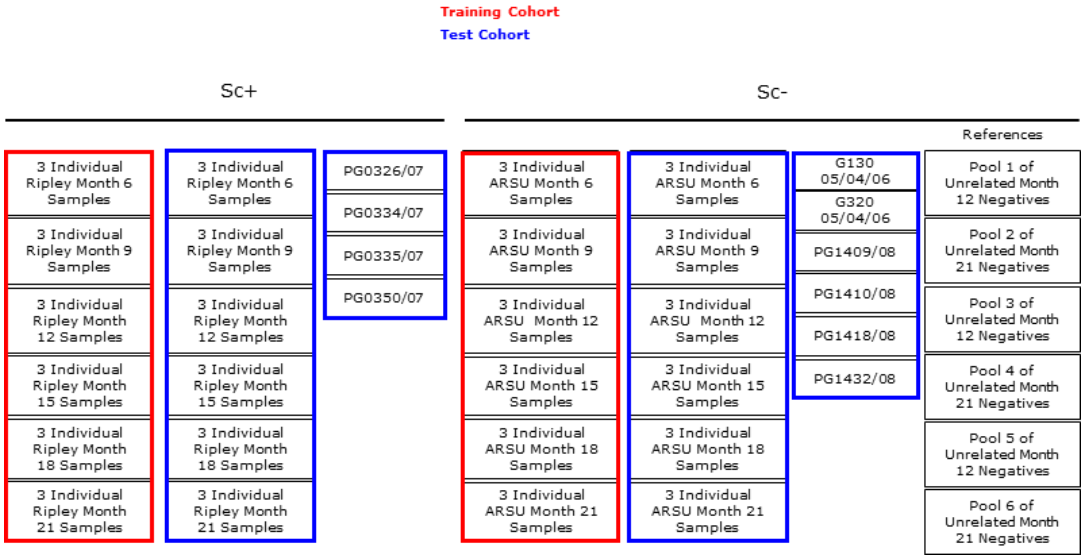

Figure 5.3.3. The samples from screen 3 used for Analysis 3. 3 samples from each time point were either used in the training cohort or test cohort. Unrelated samples were also used in the test cohort. The samples in training and test cohorts were alternated six times to identify peptides enriched in all samples. Samples used for the training cohort are shown in red. Samples used for the test cohort are shown in blue.

Table 5.3.3. Peptide binders identified in target samples in screen 3, Analysis 3. The scrapie/ARSU time courses were used as training and test cohorts, with three samples in each time point randomly assigned to either the training or test cohorts (6 combinations). Selection criteria included 1) Z-scores >2, 2) not seen in any negative sample with Z-scores >2 and 3) identified in two or more scrapie positive animals. None of the peptides in this table were observed with Z-scores >2 in any negative sample. Peptides identified consistently between analysis were ranked on the average number of positive samples in which they were seen with Z-scores >2 (out of 22). Means were calculated for each peptide to aid presentation. None of the peptides in this table were observed with Z-scores >2 in any negative sample.

	Score						
Peptide	1	2	3	4	5	6	Mean
WRALLVNPA	3/22	3/22	3/22	3/22	3/22	3/22	3/22
CTWMPHMSSACG	2/22	2/22	2/22	2/22	2/22	2/22	2/22
RAPSQRLQL	2/22	2/22	2/22	2/22	2/22	2/22	2/22
RKNLANKWQ	2/22	2/22	2/22	2/22	2/22	2/22	2/22
RNIRPRPLQ	2/22	2/22	2/22	2/22	2/22	2/22	2/22
RPNPHGDSG	2/22	2/22	2/22	2/22	2/22	2/22	2/22

5.3.3. Analysis 4: Analysis with Pooled Samples for Each Time Point

The question was raised of whether peptides, although specific, were seen at low frequencies in scrapie positive samples and lost in analysis. Therefore, the data from each time point was pooled (**Figure 5.3.4.**). The purpose of this was to increase overall frequency of a peptide identified in multiple animals. This would allow for the calculation of a higher Z-score value than in the analysis of single samples. In this analysis, the data from all samples at each time point was pooled to make 6 pooled samples for each of the positive and negative time course samples (**Figure 5.3.4.**). These pooled time points were then used as the test cohort (**Figure 5.3.4.**). Peptides were identified with Z-scores >0, and were selected in the training cohort with the criteria of 1) Z-scores >2, 2) seen in all 4 positive animals and 3) in none of the negative samples. Peptides identified in the training cohort were selected in the test cohort with the criteria of 1) Z-scores >2, 2) seen in 2 or more positive time points and 3) in none of the negative samples. The selection criteria in the test cohort was altered due to the lower number of test samples in the cohort compared to previous analyses. Doing so produced a list of 48 peptide candidates (**Table 5.3.4. 1.**). Some of the peptides were identified in both analysis 1 and analysis 5, including HRTTNTGAK. The peptides HRTTNTGAK, LLTPRAQGR, RPKLPGRPP and FPFARSAPA were identified in the later months of the time course (**Table 5.3.4. 1.**). The peptide RPNPHGDSG was also identified in Analysis 3, but not in the other analyses (**Table 5.3.4. 2.**). This analysis was also performed on the data from screen 2 and the data used in Analysis 2, pooling the data for the samples for both month 12 and 21. The data were compared to determine peptides identified in both analyses (**Table 5.3.4. 3.**). Using this method, 9 peptides were selected in both datasets (**Table 5.3.4. 3.**). An analysis was also attempted similar to that performed in screen 2, where Z-scores were calculated from different references. However, this analysis did not identify any different peptides from the analysis performed in **Section 5.3.**

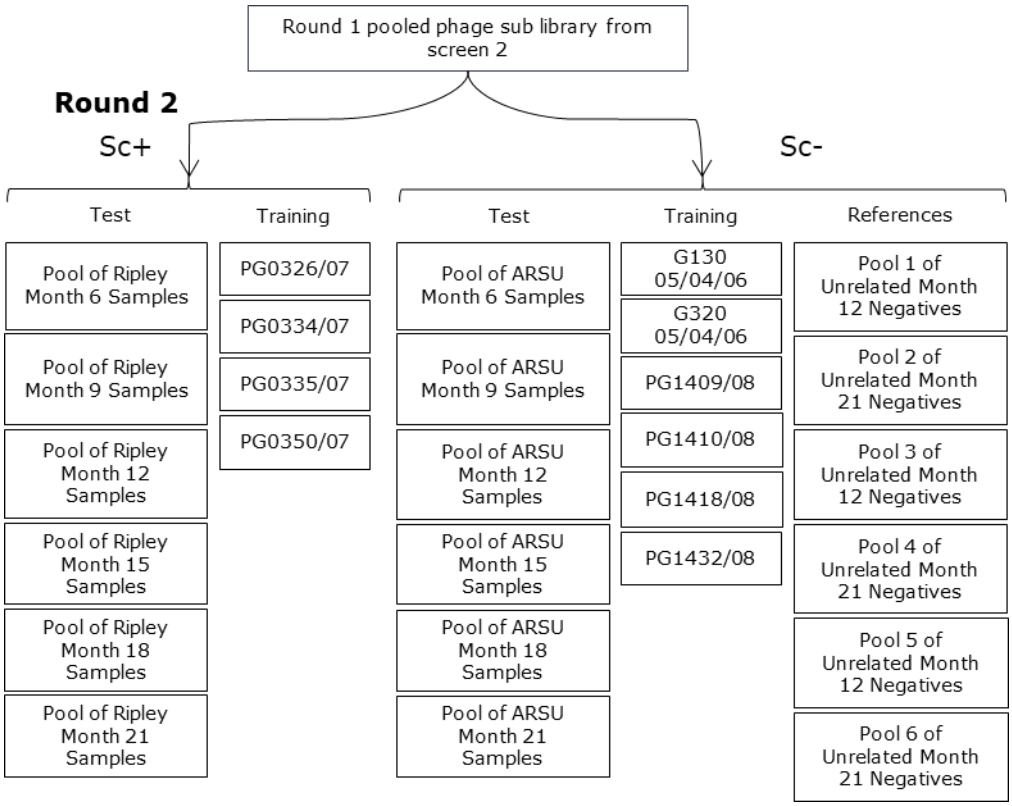

Figure 5.3.4. The samples from screen 3 used for Analysis 4. The data from each sample at each time point were pooled. Pooled samples were used in the test cohort, with unrelated samples used in the training cohort. The samples used in training and test cohorts are indicated.

Table 5.3.4. 1. Peptides 1-35 with Z-scores from screen 3, identified with samples pooled at each time point. Blue: Z-scores >2. Orange: Z-scores >5. Red: Z-scores >10. The data for each sample at each time point was pooled and analysed by two-proportion Z-test. Peptides were selected on the criteria 1) Z-scores >2, 2) seen in 3 or more-time points and 3) seen in none of the negative time points.

		Test Cohort					
		Scrapie Infected (n = 6)					
Peptide	Training Cohort	Month 6	Month 9	Month 12	Month 15	Month 18	Month 21
HRTTNTGAK	4/4	0	62.82	48.66	24.49	55.26	56.19
ARTSSAAPQ	4/4	0	29.02	10.32	24.58	8.2	0
LLTPRAQGR	4/4	0	0	4.24	8.72	18.04	4.47
LWLKGRYYP	4/4	2.82	2.36	5.43	0	3.84	0
RPKLPGRPP	4/4	0	0	7.29	10.15	15.52	10.95
PSLHPAWSK	4/4	2.6	5.4	0	7.87	0	0
APRLGVKSP	4/4	0	5.39	2.24	0	3.61	0
CTQVLPNLRCG	4/4	2.55	2.31	0	0	0	7.89
FPFARSAPA	4/4	0	0	0	2.58	5.31	8.33
GNPKTGHTP	4/4	0	0	2	0	3	2.83
GPGWQRC	4/4	2	0	13.53	0	0	6.63
RILPYKFTA	4/4	4.24	0	3	0	0	2.65
THFREKPSW	4/4	0	2.24	3.46	0	5.1	0
RQWWSVTPP	4/4	0	0	0	7.82	3.39	0
AQAPTDPHA	4/4	0	0	0	0	9.27	2
AQLVFTSSS	4/4	15.1	5.74	0	0	0	0
ASLESIELR	4/4	8.6	5.92	0	0	0	0
CELVQKPVDSCG	4/4	0	2.45	0	0	0	4.24
CQQLKPHPSCG	4/4	0	3.46	2.83	0	0	0
CPRIVATYLHCG	4/4	3	0	2.24	0	0	0
CQRPHPVCKYCG	4/4	0	0	0	3.32	0	2.65
CSPMTGAPNRCG	4/4	0	0	4.03	0	4.59	0
EKPPIKLTQ	4/4	5.65	8.26	0	0	0	0
EQSRKMTSS	4/4	5.6	0	0	2.12	0	0
FAGDTVKVS	4/4	0	4	2.24	0	0	0
GGVLRNTKA	4/4	6.78	3.16	0	0	0	0
GPYNLHKVQ	4/4	5.29	0	0	0	3.24	0
HPKFQNQIL	4/4	2.65	0	3	0	0	0
ILTHTAKFT	4/4	0	4.97	0	0	0	10.06
KNEQSRATM	4/4	2.72	2.85	0	0	0	0
KPARFDRHT	4/4	0	0	2.65	0	8.43	0
KVANSQVNV	4/4	0	2.45	0	0	0	5.2
PTLRVQASG	4/4	0	0	0	6.21	30.68	0
QANRPAHNL	4/4	0	0	5.54	14.65	0	0
QPFYRPSPQ	4/4	0	2.24	2	0	0	0

Table 5.3.4. 2. Peptides 36-48 with Z-scores from screen 3, identified with samples pooled at each time point. Blue: Z-scores >2. Orange: Z-scores >5. Red: Z-scores >10. The data for each sample at each time point was pooled and analysed by two-proportion Z-test. Peptides were selected on the criteria 1) Z-scores >2, 2) seen in 3 or more-time points, 3) no Z-scores <0 and 4) seen in none of the negative time points.

		Scrapie Infected (n = 6)					
Peptide	Training Cohort	Month 6	Month 9	Month 12	Month 15	Month 18	Month 21
RGLSLLYEP	4/4	2.83	2.65	0	0	0	0
RKPDGKAGL	4/4	4	0	0	3.32	0	0
RPLKFSDYP	4/4	5.21	0	0	0	8.78	0
RPNPHGDSG	4/4	2	2.24	0	0	0	0
RRHPFPYEM	4/4	0	0	3.33	0	5.03	0
RRRSAANLV	4/4	2.59	0	0	5.34	0	0
RSNHKYTPQ	4/4	2.93	0	2.32	0	0	0
RSPTPKHGP	4/4	0	0	0	3.74	0	9.54
SQFRPAGGM	4/4	9.41	2.56	0	0	0	0
SRRDLKNGA	4/4	8.03	17.48	0	0	0	0
SVARIRVTK	4/4	0	0	0	8.08	0	9.18
VSRPASLRA	4/4	3.16	4.36	0	0	0	0
YAPSDFPRP	4/4	2.45	3.87	0	0	0	0

Table 5.3.4. 3. Peptides selected in both screen 2 and screen 3 with Z-scores. Blue: Z-scores >2. Orange: Z-scores >5. Red: Z-scores >10. The criteria for this analysis was: 1) Z-scores >2, 2) seen in 3 or more-time points, 3) no Z-scores <0 and 4) not seen in any negative pooled months. These samples are still displayed to illustrate which peptides were identified by both screen 2 and screen 3 (analysis 4) by pooling months 12 and 21.

	Screen 2		Screen 3, Analysis 4	
	Scrapie Infected		Scrapie Infected	
Peptide	Month 12	Month 21	Month 12	Month 21
ARQFIPQPS	0	6.93	2.07	3.32
CGQILNWPSQCG	0	13.6	0	2.82
CPRIVATYLHCG	2.65	0	0	2.24
CRVPSTDRQPCG	0	3.01	3	8.6
CSGCPAQSPTCG	17.89	3.32	0	4.69
CTLQSAQPYTCG	3.24	0	3.38	3.32
QPFYRPSPQ	3.74	0	0	2
RGRPPRSLT	0	6.16	0	3.74
VLSAGPFQR	7.14	4	0	2.45

5.4. Discussion

To date, the confirmatory diagnosis of human prion diseases is the detection of PrP^{Sc} in brain tissue obtained post mortem (Lee et al. 2013). Non-confirmatory diagnosis can be made by the assessment of clinical symptoms, MRI, the detection of 14-3-3 protein and electroencephalography (Zerr et al. 2009; Puoti et al. 2012). Ante-mortem diagnosis of prion diseases in ruminants is possible through the detection of PrP^{Sc} in lymphoid tissue (O'Rourke et al. 2000). However, there are no rapid ante-mortem tests for human prion diseases. Recent years have seen the development of sensitive methods like RT-QuIC which have the potential for rapid ante-mortem diagnosis (Atarashi et al. 2011). These methods rely upon the presence and detection of the pathogenic PrP^{Sc} protein as the disease biomarker. As levels of PrP^{Sc} are low in bodily tissues in early stages of disease, the sensitivity of these methods is required to be very high at these stages (Edgeworth et al. 2011). The identification of surrogate markers of prion diseases could enable the diagnosis of prion diseases in early disease stages, independent of PrP^{Sc} levels. Autoantibodies have been proposed as potential biomarkers in neurodegenerative diseases, following reports that disease and healthy patient cohorts can be distinguished by autoantibody mapping by human protein microarray (Nagele et al. 2011; Han et al. 2012; Ayoglu et al. 2013; DeMarshall et al. 2016). However, protein microarrays are limited by a number of factors including epitope burial or the lack of secondary modifications in protein arrays (Zhu & Snyder 2003; Ramachandran et al. 2008). An alternative method is next generation phage display (NGPD).

In this study NGPD was applied to map the epitopes of sera based antibodies in scrapie infected or uninfected sheep. To do so, three separate screening strategies were employed. The first two of these screens utilized one of two different elution methods – direct infection of TG1 bacteria in screen 1 or competitive elution with purified IgGs in screen 2. IgGs were purified from different scrapie infected animals, so that elution would increase the selection for disease specific epitopes. The frequency and ratio of peptide sequences in each sub library were analysed by a two-proportion Z-test. Out of these two methods, screen 1 reported 1 candidate peptide which fit the selection criteria, while screen 2 reported 34 peptide sequences. Therefore, competitive elution was determined to be the most efficacious for selecting scrapie specific peptides over two rounds of phage display biopanning. That there was such a distinction between these screens could be attributed to the specificity of the elution methods. Direct infection is nonspecific, in that all phage/peptides captured by the protein G magnetic beads have the

potential to be propagated in each sub library. This would lead to the amplification of nonspecific peptide sequences. Indeed, nonspecific elution can result in the enrichment of background binding phage, increasing the difficulty in identifying specific binders (Koide et al. 2009). However, the specificity of peptides identified in screen 2 is uncertain, due to the limited number of negative samples available for subtractive screening. To counter this limitation, the data was analysed using three different pairs of negative samples as reference controls. Using three separate reference controls allowed for the selection of peptides consistently identified between analyses. As each analysis used different reference controls, it could be argued that peptides consistently identified with high Z-scores are consistently enriched against IgGs from scrapie infected sheep. This analysis also identified more peptides that met the selection criteria than in the initial analysis, with 14 peptides that were identified in both analyses. The reason for this could be that each reference control contained different populations of peptide sequences and frequencies. Therefore, the mean scores calculated across multiple analyses selected peptides which would not have been otherwise identified as the peptides were seen in some negative samples but not in others. Ultimately however, there is no definitive way of confirming the specificity of the peptides identified from screen 2 without the use of further negative samples for comparison.

Screen 2 demonstrated the greater efficacy of competitive elution in identifying peptides that met the selection criteria. Consequently, competitive elution was utilized in a larger screen which panned the same sub library from screen 2 against sera from scrapie infected or uninfected sheep at months 6 to 21 of disease onset. Screen 3 consisted of a comprehensive selection of scrapie positive or negatives sera samples, either from a time course or from unrelated infected and non-infected animals. The sub library from round 1 biopanning in screen 2 was used in round 2 biopanning in screen 3 to determine if the same peptides could be identified in both screens. If the same peptides or peptides sharing sequence homology were selected in both screen 2 and 3, it would be convincing of their specificity. The initial analysis of screen 3 identified 10 peptides that matched the selection criteria. The peptide HRTTNTGAK for instance was identified in 12/36 positive samples with Z-scores >2. These peptides did not appear to be enriched towards the later stage of disease, and did not match those identified in screen 2. In an attempt to identify peptides between screens 2 and 3, these data were analysed by the same method as screen 2 using exactly the same samples to identify peptides selected by both screens. The peptide CQCPYCLRRQCG was

identified in both of these analyses, suggesting that it may be successfully binding scrapie specific autoantibodies. However, this peptide was identified in negative samples with a Z-score >2 in some of the other training cohorts of screen 3, indicating that it was also enriched to some extent in negative sera. For this reason, it was not identified in the analyses with a greater number of negative samples.

As sub libraries will be highly diverse in early panning rounds, different Z-scores may be calculated between panning experiments, leading to the selection of different peptides between experiments (Rentero Rebollo et al. 2014). By pooling the data from all the samples at each time point in round 2 selection for both screens, this may make the peptide selection more reproducible as subtle variation between animals will be less influential. As a result, 9 peptides were identified in both screens 2 and 3 in Analysis 4. Pooling the data from each sample at a given time point allows for the analysis of peptide frequencies across multiple animals at once. This could increase the overall frequency of a peptide in the pool if it is present in multiple samples, allowing for the calculation of a higher Z-score value than in the analysis of a single sample. This is demonstrated by the high Z-scores identified for the peptides selected in Analysis 4, where pooling the peptides and frequencies for each time point increased the Z-scores for each peptide selected. A number of these peptides were observed to be enriched in later months of the disease development. Consequently, this analysis could aid the identification of weaker peptide binders or peptides that bind relatively low titre antibodies, which are therefore present only at low frequencies in individual samples. Again, that peptides were identified here between two independent panning experiments is also indicative of their specificity to scrapie-related antibodies. Whether this analysis is allowing for the consistent identification of specific peptides between panning experiments could be investigated through further experimental screens with the same samples. If further panning experiments again select the same peptides, this would help to validate this method in the identification of immunoreactive diagnostic peptides. It may also indicate that the use of phage-peptide binding combined with NGS analysis could be developed as a serological assay.

Here, an alternative method of analysis was also attempted where samples at each point in the time course of scrapie infected and uninfected samples was split into the training or test cohorts, and this was repeated for 6 different combinations. In this analysis peptides were selected with Z scores >2 in both scrapie positive time

course samples and unrelated scrapie positive control samples. However, this analysis only selected for 6 peptides overall. This limited selection suggests that the use of multiple training/test cohorts, in combination with the selection criteria, were too stringent as this will in effect only select for peptides that are enriched over the full time course of disease incubation. However, the peptide RPNPHGDSG was identified by both this method and Analysis 4 but not in the other analyses, suggesting that these methods of analysis could potentially identify peptides at lower frequencies that would otherwise not be selected. Whether the selection of these peptides is representative of peptide/antibody binding *in vivo* remains to be determined. Investigation into this would start with validation by serological ELISA.

The analysis of screen 2 revealed that alternating the reference controls used to calculate Z-scores can affect the peptides identified in selection. A similar strategy was applied to the data from screen 3 to determine whether peptides are consistently identified between three separate analyses. The majority of peptides identified in this analysis were also identified in the other analyses, including LLTPRAQGR, IARPYPKGL, SRRDLKNGA and EKPPIKLTQ, indicating that these peptides are sufficiently enriched in the scrapie positive samples in screen 3. Whether this method of analysis is more efficacious at identifying specific peptides remains to be determined. Validation of these peptides by ELISA would be indicative of this efficacy.

The method of analysis used in this study centred predominantly around the use of a two-proportion Z-test for phage display NGS data analysis as described by (Zhang et al. 2011). Z-tests have been previously described and used in the analysis of microarrays for data normalisation (Cheadle et al. 2003; Comander et al. 2004; Wagner et al. 2011; Yasrebi 2016). Indeed, Z-tests have the advantage over other analysis methods in their simplicity of calculation and interpretation (Cheadle et al. 2003). In the analysis of NGPD data, the Z-test normalises peptides based on their absolute frequency and ratio between target and reference control samples. Therefore, the Z-scores act as a representation of peptide enrichment in target samples through successive panning rounds. Z-tests have been used previously in the analysis of NGPD data to select peptides that are specific to antibodies generated in *Salmonella enterica* serovars Typhimurium infection in chickens and pigs (Naqid et al. 2016). These peptides demonstrated high sensitivity and selectivity in ELISAs (Naqid et al. 2016). This success demonstrated the capacity of NGPD to identify immunoreactive peptides, with the use of Z-test

analysis in the peptide selection. Additionally, Z-tests allow for the effective removal of nonspecific peptides as those identified in negative target samples with high Z-scores can be removed in peptide selection. For these reasons, the two-proportion Z-test analysis method was used in this study. However, Z-tests are limited in that Z-scores are calculated based on the population of peptide frequencies in the control reference. Because of this, using different reference controls can result in the selection of different peptides, as demonstrated in the analysis of screen 2. For this reason, additional control references were included in screen 3 to counteract the heterogeneity between reference controls. It would be beneficial to investigate alternative methods of analysis, and compare the peptide sequences identified between each method.

An alternative method of analysis of NGS peptide library data is by clustering peptides according to frequency and shared motifs (Ngubane et al. 2013; Ravn et al. 2013; Rentero Rebollo et al. 2014; Christiansen et al. 2015; Brinton et al. 2016; Yang et al. 2017). These studies normalised peptides based on their frequency, followed by clustering to identify enriched binding motifs between target samples. (Christiansen et al. 2015) demonstrated the capacity of peptide clustering to identify peptides that recognised the peanut allergen Ara h 1 in sera. Although no diagnostic assay was developed with these peptides, sequences were validated by peptide microarray (Christiansen et al. 2015). This demonstrated that the method of peptide clustering can be applied to map the epitopes of sera based antigens. Peptide clustering by sequence and frequency could be of particular benefit in mapping the epitopes of antibodies in the sera of scrapie infected sheep to find common motifs. Therefore, the application of this method to the data generated in this study could reveal novel peptide sequences and motifs currently unrecognised by Z-test analysis. However, sequence homology is not necessarily a guarantee of target binding. (Yang et al. 2016) identified immunoreactive peptides that specifically identified sera based antibodies to Tuberculosis which were non-homologous. Another possible method of analysis is PHASTpep as described by (Brinton et al. 2016). PHASTpep is a similar analysis to that of the two-proportional Z-test, where peptide data is normalised and sorted by the average ratio of positive to negative read frequencies (Brinton et al. 2016). The efficacy of this method was measured by its capacity to identify peptides containing the HQF motif specific to streptavidin (Brinton et al. 2016). PHASTpep analysis could be applied to the data from this study to determine if the same peptide sequences can be identified between analyses.

The different analyses attempted in this study led to the identification of different peptides that matched the selection criteria. That enriched peptides could be identified according to highly selective screening criteria suggests that this method is capable of identifying peptides immunoreactive to scrapie specific autoantibodies. This is especially the case with the 9 peptides identified in both screen 2 and screen 3, and the peptide CQCPYCLRRQCG separately identified in both screen 2 and 3. However, although peptides that fit specific and highly selective screening criteria can appear to be convincing binders, how representative this is of binding *in vivo* remains to be determined. The only way to validate these analyses is the testing of peptides in serological assays. Any such validation would then provide data to identify the best bioinformatic analysis method(s) for identifying biomarker peptides. Consequently, the first six peptides from each analysis of screen 3 were chosen for screening, as well as the 9 peptides identified between screen 2 and 3 (**Appendix II**).

Chapter 6: The Development of Peptide ELISAs for the Detection of Scrapie Specific Autoantibodies

6.1. Introduction

TSE surveillance in food producing animals is currently performed using commercial immunoassays, based on ELISA and western blotting to detect the presence of PrP^{Sc} after protease digestion (Wang et al. 2015). These methods rely upon the use of brain tissue obtained post mortem. This reliance on brain tissue for diagnosis ultimately limits the application of these diagnostic assays for ante-mortem diagnosis. Additionally, the use of PK digestion as a prerequisite to each immunoassay can affect the sensitivity of these assays to monitor the emergence of novel prion strains, demonstrated by the emergence of atypical scrapie (Benestad et al. 2008). Therefore, alternative biomarkers and tissue sources are sought for sensitive ante-mortem diagnosis of prion diseases. Anti-mortem tests for scrapie in sheep can be performed by the detection of PrP^{Sc} in lymphoid tissue (O'Rourke et al. 2000). In humans, non-confirmatory ante-mortem diagnosis remains based on the analysis of clinical symptoms, MRI, electroencephalography and the detection of 14-3-3 protein in CSF (Zerr et al. 2009; Puoti et al. 2012). Therefore, there remains a continued demand for ante-mortem diagnostics.

Serological surveillance is a powerful method for controlling disease spread in humans and animals, and has significantly contributed to the UK vaccination programme (Osborne et al. 2000). As mentioned in **Chapter 5,** a serology based diagnostic for prion diseases could allow the screening of blood stocks to prevent the transmission of iatrogenic CJD (Lacroux et al. 2014). Furthermore, the availability of a serological diagnostic test could improve the efficacy of TSE surveillance programs in food producing animals. However, to date there remains no commercial serological diagnostic immunoassay for prion diseases in humans or animals. Experimental PrP^{Sc} detection in blood has been reported with RT-QuIC, PMCA and capture with steel beads (Thorne & Terry 2008; Tattum et al. 2010; Edgeworth et al. 2011; Orrú et al. 2011; Lacroux et al. 2014; Jackson et al. 2014). However, these assays remain experimental and have not been applied to surveillance of human or animal prion diseases.

The aim of this study was to develop a serological immunoassay for the ante-mortem diagnosis of scrapie in sheep. In recent years, it has been reported that autoantibodies in the sera of patients with neurodegenerative diseases like AD can be used as biomarkers for disease diagnosis (Nagele et al. 2011; Han et al. 2012; Ayoglu et al. 2013; DeMarshall et al. 2016). These studies highlighted that autoantibodies may act as biomarkers of prion diseases. Following these findings, this study used next generation phage display to map the epitopes of sera based

antibodies from sera infected sheep. Following bioinformatic analysis of NGPD data (**Chapter 5**), 39 peptides were selected that bind IgG antibodies in the sera of scrapie infected sheep. It was hypothesised that these peptides could be utilised in a peptide based immunoassay for scrapie diagnosis.

Peptides or antibodies identified by phage display may be validated *in vitro* assays, including ELISA. Indeed, ELISA based immunoassays are used in the detection of autoantibodies for diagnosis of autoimmune diseases, including vasculitis disease (Tervaert & Damoiseaux 2012). However, there was no optimised ELISA method for screening the phage display derived peptides identified in this study. In previous work by the group, diagnostic peptides had been identified that were immunoreactive to antibodies produced in response to schmallemberg virus (SBV) infection in cattle. These peptides were identified to develop sera based immunoassays that could differentiate infected from vaccinated animals (DIVA). Therefore, the ELISA method used to validate the SBV peptides was further optimised here and then applied to screen the 39 anti-scrapie peptides identified in this study. Further optimisations of the method were attempted to increase assay sensitivity. Other highly sensitive assays were also investigated as an alternative, including real time immuno PCR (RT-IPCR) and fluorescent amplification catalysed by T7 polymerase technique (FACTT).

6.2. Results

6.2.1. Optimisation of Peptide ELISAs with SBV Peptides

39 peptides had been selected by biopanning against antibodies in the sera from scrapie infected sheep or uninfected sheep, as described in **Chapter 5**. However, there was no established or optimised assay with which to validate these peptides. Previous work in the group had identified 15 peptides selected against antibodies in the sera of cattle infected with SBV (**Table 6.2.1.**). Some of these peptides had been previously validated against a selection of sera from SBV infected cattle or vaccinated cattle (**Table 6.2.2.**). This gave the basis for optimising the peptide ELISA method for validation of the scrapie peptides. Firstly, the reactivity of these peptides was tested to corroborate the findings of the previous screen. The peptide ELISA was then further optimised to increase sensitivity.

Table 6.2.1. Peptide numbers and sequences of the SBV peptides used for assay optimisation. These peptides were selected from phage display against sera from SBV infected and vaccinated cattle. These peptides were synthesised with flanking motifs AEGEF and DPAKAA as displayed on bacteriophage.

Peptide Number	Peptide Sequence
SBV Peptide 1	AEGEFAKGGSAASLDPAKAA
SBV Peptide 2	AEGEFSKGGSANEADPAKAA
SBV Peptide 3	AEGEFAKGGSARPLDPAKAA
SBV Peptide 4	AEGEFEKGGSAHNSDPAKAA
SBV Peptide 5	AEGEFEKGGLASPPDPAKAA
SBV Peptide 6	AEGEFGKGGSAAPLDPAKAA
SBV Peptide 7	AEGEFSKGGRSQVADPAKAA
SBV Peptide 8	AEGEFAKGGTSVRPDPAKAA
SBV Peptide 9	AEGEFAKGGSNHYPDPAKAA
SBV Peptide 10	AEGEFGKGGSSHIWDPAKAA
SBV Peptide 11	AEGEFLKRIPTHTGDPAKAA
SBV Peptide 12	AEGEFSKLTSLGYKDPAKAA
SBV Peptide 13	AEGEFLRRIPISSRDPAKAA
SBV Peptide 14	AEGEFSKLTVKSYSDPAKAA
SBV Peptide 15	AEGEFLVAPTRSTPDPAKAA

Table 6.2.2. Sera from cattle experimentally infected with SBV, field infected with SBV or vaccinated available for assay optimisation and screening in this study.

Sera ID		
Vaccinated	Experimentally Infected	Field Infected
C10	C31	726
C11	C34	198
C12	C35	739
C13	C36	745
C14	C37	422
C15		739
C16		744
C17		213
C18		210
C20		733
C22		731
C23		

6.2.2. Testing Peptides Selected Against Anti-SBV Antibodies

It was previously identified that the SBV peptides 7, 8 and 15 reacted to the sera 422 and 726 to give positive absorption values (data not shown). Therefore, these combinations of peptides and sera were used to confirm the efficacy of the peptide ELISA method. In these assays, higher concentrations of sera (1 in 25) and secondary antibody (1:7500) were used than in the original method described by (Naqid et al. 2016) (1 in 50 sera, with 1:7500 secondary antibody) to increase the generation of positive signals. However, in the two assays performed, neither peptide produced absorbance signals greater than the nonspecific binding control PIF (data not shown).

6.2.3. Optimisation of Assay Temperature

Performing the peptide ELISA using the existing protocol was unsuccessful in producing positive absorbance signals. It was hypothesised that these observations may be due to the ambient room temperature. In the original method, each incubation step was performed at room temperature. However, the previous screen was performed at ambient temperatures higher (~25°C) than in this study (16-18°C) due to seasonal changes. To test the effect of temperature on assay performance, two peptide ELISAs were performed at 25°C and 22°C (**Figure 6.2.3.**). At each temperature, the SBV peptide 15 generated signals above the nonspecific control with sera diluted 1 in 25 (**Figure 6.2.3. A/B**). At 25°C, peptide 15 produced observably higher signals than the nonspecific control at each sera dilution (**Figure 6.2.3. B**).

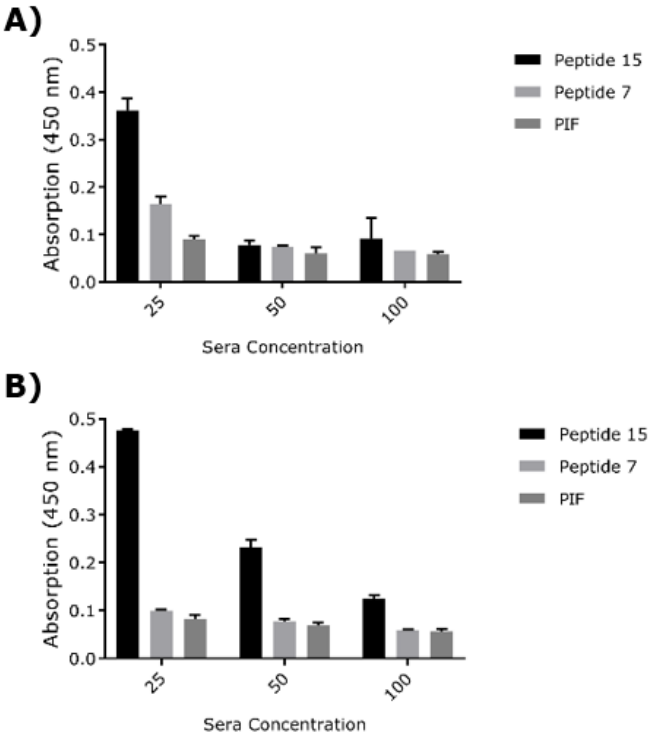

Figure 6.2.3. Optimisation of peptide ELISA temperature. Assays were performed at **A**) 22°C and **B)** 25°C at each incubation step. Each assay tested the SBV peptides 15 and 7 against the sera 726 at dilutions of 1 in 25, 1 in 50 and 1 in 100 in triplicate. PIF acted as a nonspecific binding control. Each assay was performed using Nunc-Immuno Maxisorp plates, coated with 100 µg/mL of each peptide. Bound antibodies were detected with an anti-bovine IgG secondary antibody (HRP-conjugate) at a concentration of 1:7500. Wells treated with carbonate buffer (pH 9.6.) were used as a background control and were subtracted.

6.2.4. Optimisation of Secondary Antibodies

It was determined that increasing the temperature in each incubation step to 25°C increased the absorbance produced in ELISA. It was then questioned whether optimising the choice of secondary antibody could increase assay these signals. An additional anti-bovine IgG secondary antibody was sourced from Sigma Aldrich with an alkaline phosphatase (AP) reporter enzyme conjugate. The secondary antibody used in assay optimisation to this point utilized a horseradish peroxidase (HRP) conjugated enzyme. The efficacy of each antibody was determined in a short dilution series of either antibody (**Figure 6.2.4.**). Each assay used SBV peptide 15, probed with sera 726. The optimal dilution for the AP conjugate was 1:15000, and 1:5000 for the HRP conjugate (**Figure 6.2.4.**). In these and subsequent assays sera were used at a dilution of 1 in 50, rather than 1 in 25, due to the limited volume of sera available. Out of the two antibodies, the AP conjugated secondary produced a higher signal at each dilution relative to the HRP conjugate, although both gave similar noise to signal ratios (**Figure 6.2.4.**). The AP conjugate was chosen as the optimal secondary antibody, as signal production can be allowed to develop over a prolonged time to increase assay sensitivity.

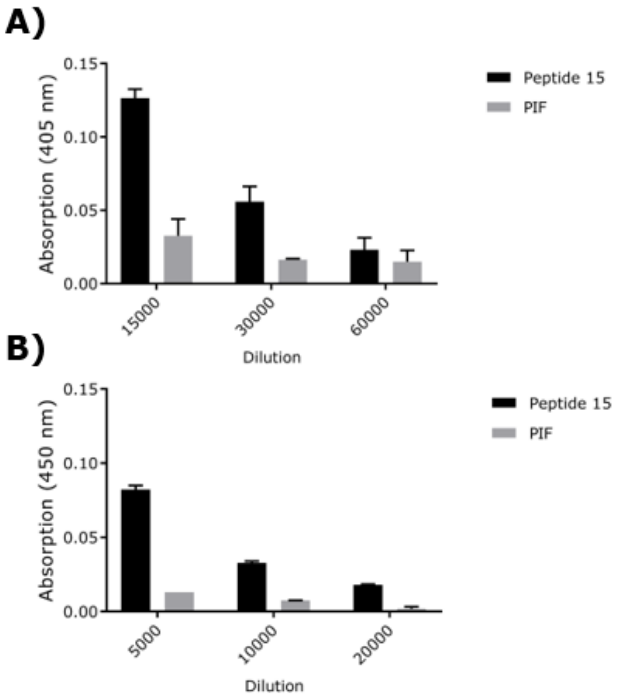

Figure 6.2.4. Secondary antibody optimisation. Secondary anti-bovine IgG antibodies were sourced from Sigma Aldrich as **A)** AP conjugate, diluted 1:15000 to 1:60000 or **B)** HRP conjugate, diluted 1:5000 to 1:20000. PIF acted as a nonspecific binding control. All samples were added to the ELISA plate in triplicate. Each assay was performed using Nunc-Immuno Maxisorp plates, coated with 100 µg/mL of SBV peptide 15. Peptide 15 was probed with sera 726 diluted 1 in 50. Absorbance was measured after 3 hours with the AP conjugate, and after 30 minutes with the HRP conjugate. Wells treated with carbonate buffer (pH 9.6.) were used as a background control and were subtracted.

6.2.5. Optimisation of Plate Agitation During Incubation

It was questioned what effect plate agitation has on assay sensitivity. Two peptide ELISAs were performed in parallel, with or without plate agitation during each incubation step (**Figure 6.2.5.**). Both SBV peptides 15 and 8 were used to probe sera 726. Out of the two peptides, only peptide 15 produced positive signals in the assay with agitation, due to the high SD of the nonspecific PIF control in the still assay (**Figure 6.2.5**.).

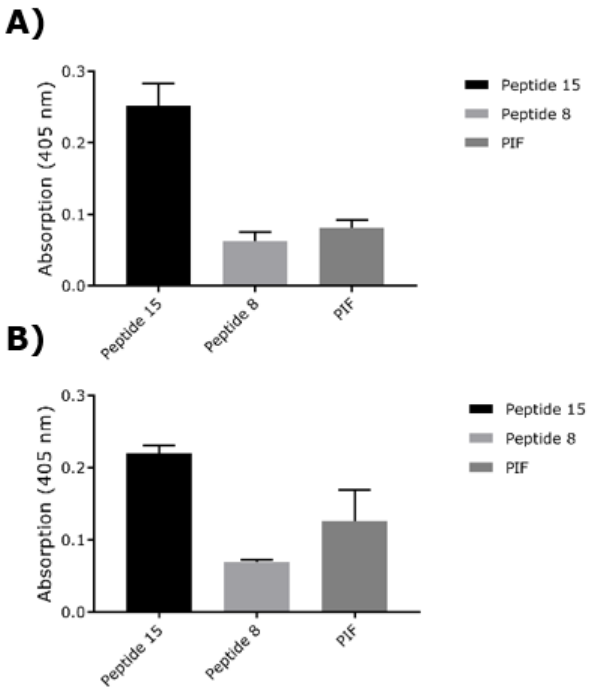

Figure 6.2.5. Peptide ELISAs were performed with **A)** agitation in incubation steps or **B)** no agitation. Each assay was performed using Nunc-Immuno Maxisorp plates, coated with 100 µg/mL of SBV peptide 15 or 8. PIF acted as a nonspecific binding control. Peptides were probed with sera 726 diluted 1 in 50. Absorbance was read after 3 hours.

6.2.6. Testing Optimised Conditions Across Multiple Peptides and Sera

The optimised method was then applied to the SBV peptides 2, 3, 4, 7, 8, and 15 to probe the sera 726, 422 and C12 (**Figure 6.2.6.**). Prior to this study, these peptides had been demonstrated to be immunoreactive to the sera 726 and 422. Therefore, positive signals were expected with this selection of peptides/sera. Sera C12 in this experiment was used as a negative control. Out of the peptides tested, only peptide 15 produced positive signals greater than the nonspecific binding control PIF in both sera 726 and 422 (**Figure 6.2.6.**). None of the peptides were observed to produce signals higher than the nonspecific control PIF in the negative sera C12.

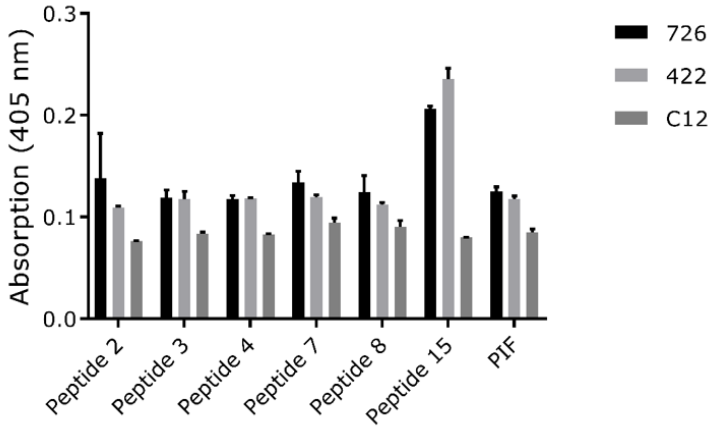

Figure 6.2.6. Testing optimised conditions on multiple peptides and sera. The assay was performed using a Nunc-Immuno Maxisorp plate, coated with 100 µg/mL of each SBV peptide. PIF acted as a nonspecific binding control. Peptides were probed with sera 726, 422 and C12 diluted 1 in 50. Absorbance was read after 3 hours.

6.2.7. Confirmation of Peptide 15 Immunoreactivity

In the optimised tests, only SBV peptide 15 had displayed observable positive signals for the sera 422 and 726. To determine whether these observations are due to peptide 15 binding SBV specific antibodies, two peptide ELISAs were performed. In the first, peptide 15 was included in a dilution series from 200 µg/mL to 0 µg/mL during sera incubation to compete with antibody binding (**Figure 6.2.7. A**). If peptide 15 was binding to SBV specific antibodies in sera, free peptide would compete for antibody binding and reduce the signals observed in the assay. The addition of free peptide at each concentration effectively inhibited signal production, with signals observed to be lower than that of the nonspecific PIF control (**Figure 6.2.7. A**). In the second ELISA, peptide 15 was probed with a dilution series of sera 726 in negative sera C12 from 100% (1 in 50 sera 726) to 0% (1 in 50 sera C12) (**Figure 6.2.7. B**). Signals produced from this assay would determine the extent of specific antibody binding by peptide 15. Absorbance at 405 nm dropped With increasing dilutions of sera 726 (**Figure 6.2.7. B**).

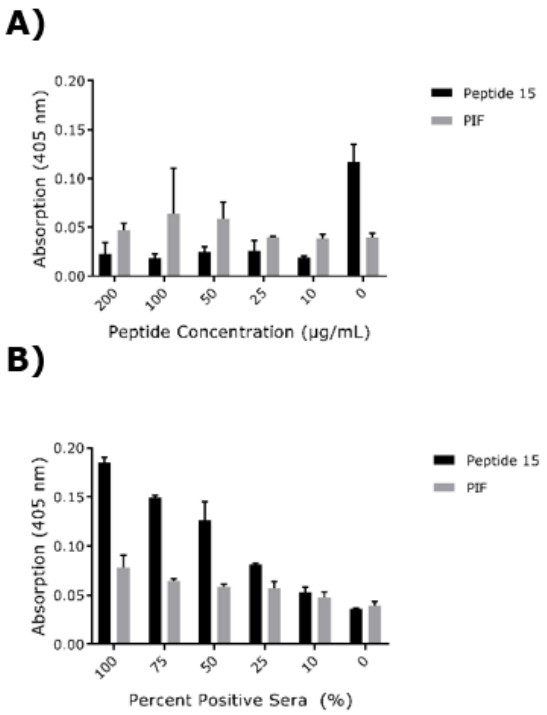

Figure 6.2.7. Confirmation of SBV peptide 15 immunoreactivity. Two peptide assays were performed with **A)** a dilution series of free peptide 15 included during incubation with sera 726. **B)** a dilution series of sera 726 in C12 from 100% to 0%. Sera were used at a dilution of 1 in 50 in each assay. Assays were performed using a Nunc-Immuno Maxisorp plate, coated with 100 µg/mL of peptide 15. PIF acted as a nonspecific binding control. Absorbance was read after 3 hours.

6.3. Screening Scrapie Sera with Optimised ELISA Conditions

With the peptide ELISA method optimised and the specific peptide 15/SBV-positive sera interaction confirmed, this method was applied to validate the scrapie (Sc) peptides identified in **Chapter 5**. Firstly, two anti-ovine IgG secondary antibodies (AP conjugate) from Invitrogen and Sigma Aldrich were tested in a dilution series against sheep sera. The secondary antibody from Sigma Aldrich was determined to be the most efficacious, with an optimal dilution between 1:5000 and 1:10000 (data not shown). The 39 Sc peptides were then screened against a selection of 12 scrapie positive sera (**Table 6.3.1.**) and 12 scrapie negative sera (**Table 6.3.2.**). For each assay, the nonspecific binding control PIF was used as a background measurement and subtracted. Absorbance values of up to 0.2 405 nm and over were considered as positive values. A number of peptides were immunoreactive in scrapie positive sera only including Sc peptide 2, 4, 5 and 12 (**Table 6.3.1.**, **2**). The ELISA data was then evaluated by receiver operating characteristic (ROC) analysis using Graphpad Prism 7. This analysis generates a ROC curve, which represents the trade-off of sensitivity versus specificity. The area under the curve (AUC) value generated with the ROC curve indicates the capacity of the test/peptide to discriminate between positive and negative samples, with values closer to 1 being indicative of greater efficacy. Each AUC value is accompanied by a calculated p value to answer the hypothesis of whether the observed difference between the cohorts is statistically significant. ROC analysis of each Sc peptide reported no statistically significant p value, with the exception of peptide 9 ($p = 0.0056$) and peptide 11 ($p = 0.0153$) (**Table 6.3.3.**). However, these values are not reflected in the absorbance values from the ELISA tests (**Table 6.3.1.**, **6.3.2.**).

Table 6.3.1. A heat map matrix generated using conditional formatting in Microsoft Excel for the Sc peptides tested against scrapie positive sera from months 21 and 18 of disease, or from animals unrelated to the time course. The nonspecific binding control PIF was used as background reading and subtracted.

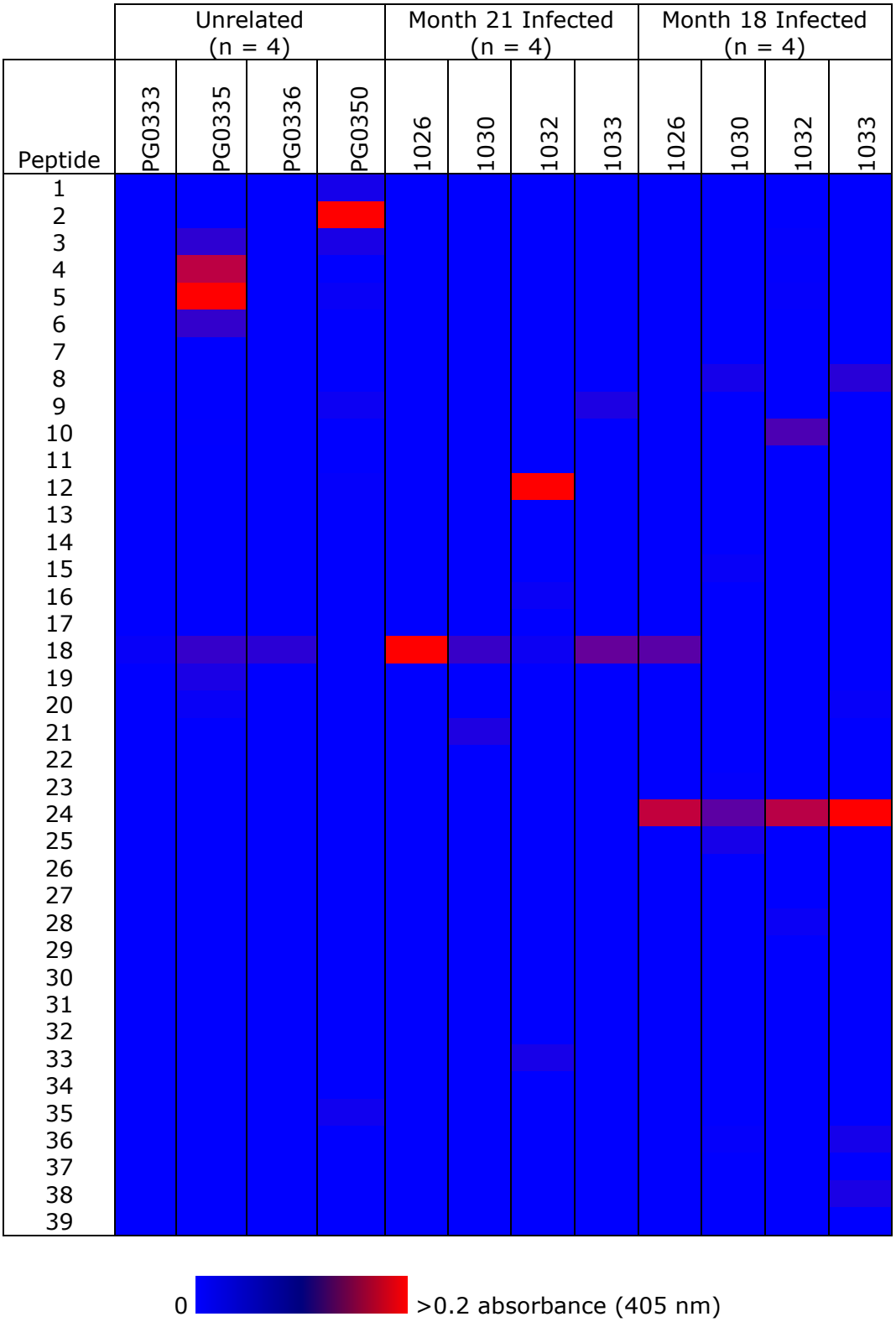

Table 6.3.2. A heat map matrix generated using conditional formatting in Microsoft Excel for the peptides tested against scrapie negative sera from unrelated animals, or from months 21 and 18. The nonspecific binding control PIF was used as background reading and subtracted.

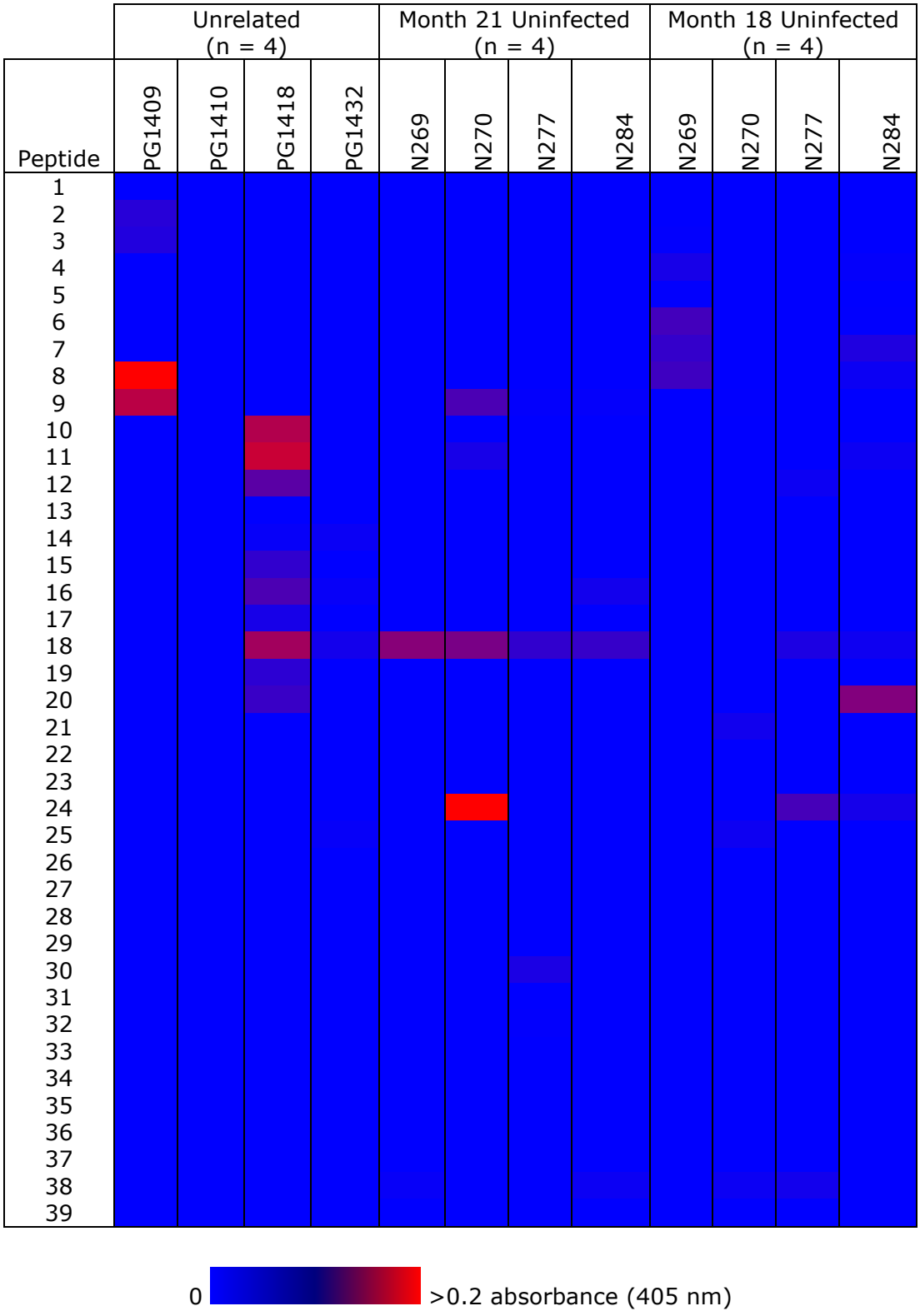

Table 6.3.3. ROC curves were produced for the recognition of peptides by IgG antibodies from the sera of scrapie infected (n = 12) and uninfected (n = 12) samples. AUC and p values are listed.

Sc Peptide	Peptide Sequence	AUC of ROC	P Value
1	AEGEFHRTTNTGAKDPAKAA	0.5278	0.8174
2	AEGEFRPKLPGRPPDPAKAA	0.5208	0.8625
3	AEGEFLLTPRAQGRDPAKAA	0.5417	0.7290
4	AEGEFSRRDLKNGADPAKAA	0.5278	0.8174
5	AEGEFAQLVFTSSSDPAKAA	0.5486	0.6861
6	AEGEFEKPPIKLTQDPAKAA	0.6041	0.3865
7	AEGEFSTRSQSMKQDPAKAA	0.5486	0.6861
8	AEGEFANSKLYPRADPAKAA	0.6111	0.3556
9	AEGEFGNSKNGVIPPDPAKAA	0.8333	0.0056
10	AEGEFQSSTKAIFTDPAKAA	0.6806	0.1333
11	AEGEFRKSPASGPLDPAKAA	0.7917	0.0153
12	AEGEFDDLGLKKYSDPAKAA	0.6736	0.1489
13	AEGEFWRALLVNPADPAKAA	0.6875	0.1190
14	AEGEFCTWMPHMSSACGDPAKAA	0.7292	0.0567
15	AEGEFRAPSQRLQLDPAKAA	0.6319	0.2727
16	AEGEFRKNLANKWDPAKAA	0.6736	0.1489
17	AEGEFRNIRPRPLQDPAKAA	0.5417	0.7290
18	AEGEFRPNPHGDSGDPAKAA	0.5903	0.4529
19	AEGEFIARPYPKGLDPAKAA	0.5556	0.6442
20	AEGEFHKHMSPNFRDPAKAA	0.5278	0.8174
21	AEGEFDKIKQFDSTDPAKAA	0.6736	0.1489
22	AEGEFEKPPIKLTDPAKAA	0.5764	0.5254
23	AEGEFGGVLRNTKADPAKAA	0.5833	0.4884
24	AEGEFLQPSLDFVDPAKAA	0.5208	0.8625
25	AEGEFARTSSAAPQDPAKAA	0.6042	0.3865
26	AEGEFLWLKGRYYPDPAKAA	0.6111	0.3556
27	AEGEFPSLHPAWSKDPAKAA	0.5764	0.5254
28	AEGEFAPRLGVKSPDPAKAA	0.5278	0.8174
29	AEGEFCTVLPNLRCGDPAKAA	0.5903	0.4529
30	AEGEFFPFARSAPADPAKAA	0.6597	0.1842
31	AEGEFARQFIPQPSDPAKAA	0.5972	0.4189
32	AEGEFCGQILNWPSQCGDPAKAA	0.6458	0.2253
33	AEGEFCPRIVATYLHCGDPAKAA	0.5486	0.6861
34	AEGEFCRVPSTDRQPCGDPAKAA	0.5417	0.7290
35	AEGEFCSGCPAQSPTCGDPAKAA	0.5903	0.4529
36	AEGEFCTLQSAQPYTCGDPAKAA	0.5833	0.4884
37	AEGEFQPFYRPSPQDPAKAA	0.7153	0.0735
38	AEGEFRGRPPRSLTDPAKAA	0.7083	0.0833
39	AEGEFVLSAGPFQRDPAKAA	0.6667	0.1659

6.4. Further Peptide ELISA Optimisation

The optimised peptide ELISA was able to identify a number of positive signals in scrapie positive sera using the Sc peptides. However, ROC analysis of these peptides revealed only 2 peptides with any possible discriminatory ability, and these produced very low ELISA signals. Therefore, it was determined to conduct further optimisations of the method to increase assay sensitivity. These conditions could then be applied to the peptide ELISA to reassess the scrapie peptides.

6.4.1. Confirmation of Peptide 2 Immunoreactivity

During screening of the scrapie peptides, it was observed that Sc peptide 2 was immunoreactive with the sera PG0350/07. If this is representative of peptide 2 immunoreactivity, the combination of peptide 2 and PG0350/07 could then be utilised in further assay optimisation. To confirm the immunoreactivity of peptide 2, two peptide ELISAs were performed (**Figure 6.4.1.**). In the first assay, free peptide 2 was included in a dilution series from 200 µg/mL to 0 µg/mL during sera incubation to compete with antibody binding (**Figure 6.4.1. A**). At each concentration, free peptide 2 reduced absorbance to that of the nonspecific binding control PIF (**Figure 6.4.1. A**). In the second ELISA, peptide 2 was probed with a dilution series of sera PG0350/07 in negative sera PG1409/08 from 100% to 0% (**Figure 6.2.6. B**). Absorbance at 405 nm dropped with increasing dilutions of sera PG0350/07 (**Figure 6.4.1. B**).

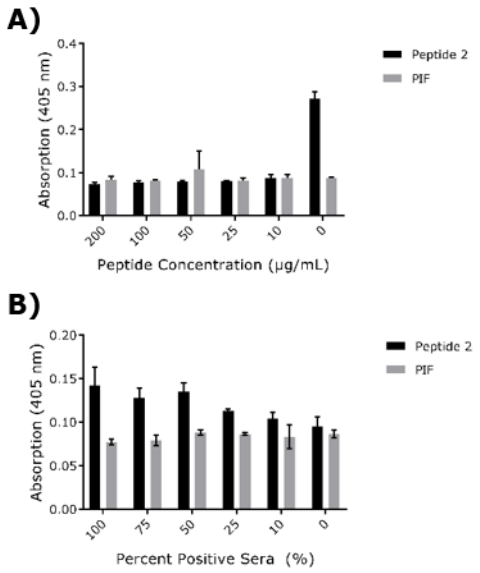

Figure 6.4.1. Confirmation of Sc Peptide 2 immunoreactivity. Two peptide assays were performed with **A**) a dilution series of free peptide 2 included during sera incubation. Peptide 2 was probed with sera PG0350/07 at a dilution of 1 in 50. **B**) a dilution series of scrapie positive sera PG0350/07 in scrapie negative sera PG1409/08 from 100%-0%. Sera were used at a dilution of 1 in 50 in the assay. Assays were performed using a Nunc-Immuno Maxisorp plate, coated with 100 µg/mL of peptide 2 or PIF. PIF acted as a nonspecific binding control. Absorbance was read after incubation overnight at room temperature.

6.4.2. Optimising Coating Temperatures with Maxisorp Plates

Nun-Immuno Maxisorp plates were typically coated with peptide at a temperature of 4°C overnight. To determine whether increasing temperature during plate coating affects assay sensitivity, plates were coated at 4°C, 25°C or 37°C with Sc peptide 2 or PIF. Bound peptide was probed with a dilution series of PG0350/07 in PG1409 from 50%-0%. Bound antibody was detected with an anti-ovine IgG secondary antibody, AP conjugate. Each temperature did not observably increase the sensitivity of the assay (data not shown).

6.4.3. Selection and Optimisation of Plate Type

Each peptide ELISA used in the study so far used Nunc-Immuno Maxisorp plates. These plates bind a combination of hydrophilic and hydrophobic molecules. To determine whether the use of alternative plate types can increase assay sensitivity, peptide assays were initially performed with Nunci-Immuno Maxisorp plates, Nunc-Immuno Polysorp Immobilizer plates or streptavidin coated plates (**Figure 6.4.3. A**). Each assay was performed using the SBV peptide 15, with SBV sera 726 diluted in sera C12. Peptide 15 was chosen for this optimisation as it was also available with a biotin modification (for use with the Streptavidin plates). Assays performed on Polysorp Immobilizer and streptavidin coated plates observably increased assay sensitivity, with streptavidin coated plates being the most sensitive format, detecting up to 1% of positive sera above the limit of detection (LOD) (**Figure 6.4.3. A**). The LOD was calculated as the mean absorption at 0% positive sera, plus three times the standard deviation. The Polysorp Immobilizer plates were the second most sensitive, detection up to 10% of positive sera above the LOD. However, the use of either Polysorp Immobilizer plates or streptavidin coated plates for large scale screening was limited due to availability from the supplier or expense of producing panels of biotinylated peptides. As an alternative, peptide ELISAs were performed on Maxisorp or maleic anhydride coated plates coated withSc peptide 2 (**Figure 6.4.3. B**). The use of maleic anhydride plates detected up to 25% positive sera, compared to 50% with Maxisorp plates (**Figure 6.4.3. B**).

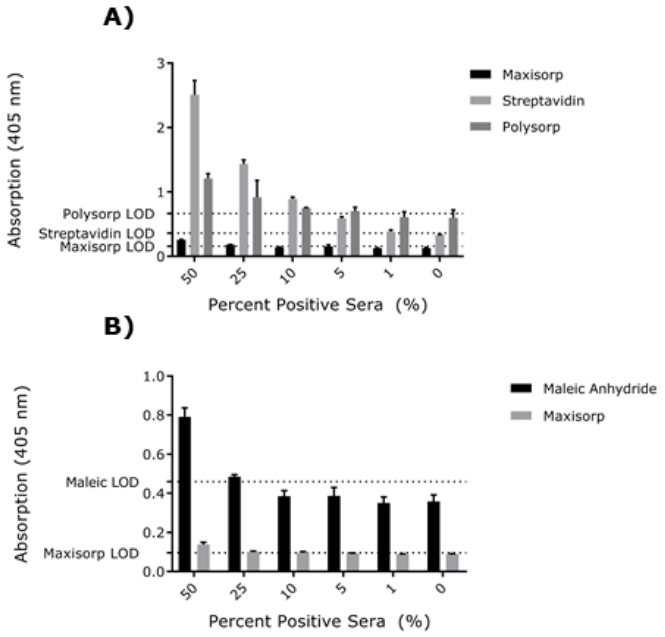

Figure 6.4.3. Comparison and optimisation of plate types used in peptide ELISAs. **A**) SBV peptide 15 was coated at a concentration of 100 µg/mL on Maxisorp, PolySorp or streptavidin coated plates. Bound peptide was probed with a dilution series of sera 726 in sera C12 from 50% to 0%. Biotinylated peptide 15 was used to coat streptavidin coated plates. **B**) Sc peptide 2 was coated at a concentration of 100 µg/mL on Maxisorp or maleic anhydride coated plates. Bound peptide was probed with a dilution series of sera PG0360/07 in PG1409/08 from 50% to 0%. peptide 2 was probed with sera PG0350/07 diluted in sera PG1409/08 from 100%-0%. Sera were used at a dilution of 1 in 50 in each assay. Absorbance was read after incubation overnight at room temperature. The LOD for each plate are shown. The LOD was calculated as the mean absorption at 0% positive sera plus three times the standard deviation.

6.4.4. Optimisation of Sera Blocking

Due to the higher signals produced using maleic anhydride coated plates, these plates were used for all future assays. Although the use of these plates allowed for greater signal generation, there remained background signal which limited assay sensitivity. It was hypothesised that this could be resultant of the binding of nonspecific antibodies in sera. It was investigated whether pre-blocking sera in blocking buffer increases the sensitivity (**Figure 6.4.4.**). Sera were pre-incubated in blocking buffer (3% (w/v) Marvel in TBS) for one hour with rotation prior to use in the assay. Pre-blocking sera observably enabled the differentiation of greater dilutions of sera to 10-5% (PG350/07) (**Figure 6.4.4.**).

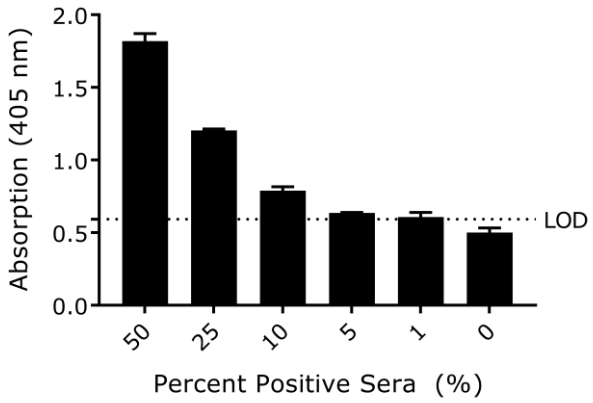

Figure 6.4.4. A peptide ELISA performed with pre-incubated sera. Sc peptide 2 or PIF was used to coat a maleic anhydride coated plate at a concentration of 100 µg/mL. PIF acted as a nonspecific binding control. Peptides were probed with a dilution series of sera PG0350/07 diluted in sera PG1409/08 from 100%-0%. Sera were used at a dilution of 1 in 50. Absorbance was read after incubation over 2 hours at room temperature. The LOD is shown, calculated as the mean absorption at 0% positive sera plus three times the standard deviation.

6.4.5. Testing Sera Against Purified IgGs

Pre-blocking sera was observed to reduce assay background signals and increase assay sensitivity. In an attempt to further reduce assay background signals, IgG antibodies were purified from the sera of PG0350/07 by capture with protein G coupled magnetic beads or melon gel, analysed by SDS-PAGE (**Figure 6.4.5. A**). Purified antibodies were used in a peptide ELISA with Sc peptide 2 in a dilution series from 50 µg/mL to 1 µg/mL (**Figure 6.4.5. B**). This was run in parallel to a peptide ELISA with sera PG0350/07 in a dilution series from 100%-2% in sera PG1409/08 (**Figure 6.4.5. C**). The normal range of IgG antibodies in sheep sera is between 18-24 mg/mL (Sigma Aldrich). Therefore, a dilution series of 100% positive sera to 2% diluted 1 in 50 is the equivalent of 360/420 µg/mL to 7.2/9.6 µg/mL of sheep IgG. 10% diluted sera would contain a concentration of IgGs approximate to 50 µg/mL of purified antibody (**Figure 6.4.5 B/C**). At this concentration both protein G purified IgGs and sera gave signals above the LOD, although wells probed with sera had a higher SD (**Figure 6.4.5. B**/**C**).

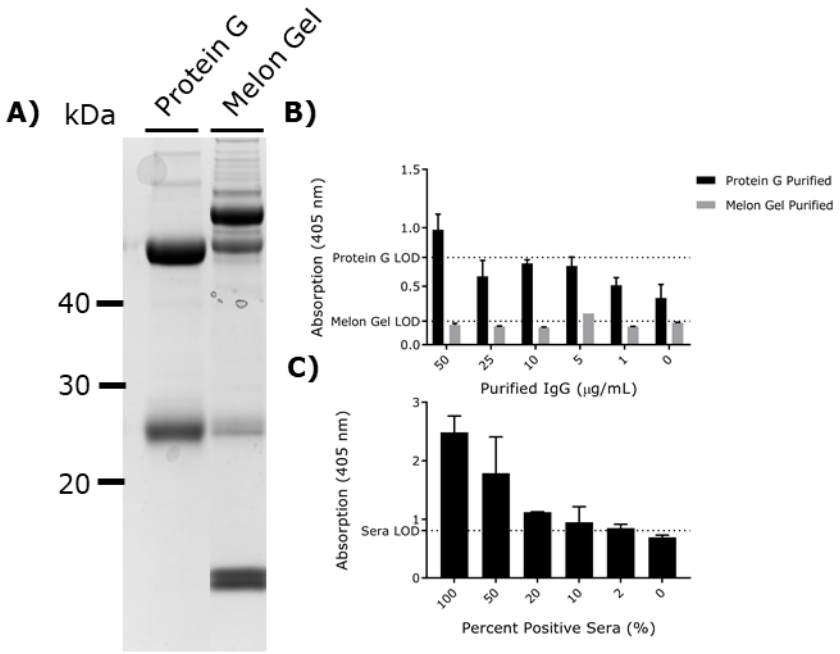

Figure 6.4.5. Comparing the use of purified IgGs with sera in peptide ELISAs. IgG antibodies were purified from the sera of PG0350/07 by protein G capture or melon gel. **A**) 20 µg of protein was analysed for purity by SDS-PAGE. Molecular weight markers are shown. The purified/partially purified IgGs were used in a peptide ELISAs with a maleic anhydride plate coated with Sc peptide 2 or PIF at a concentration of 100 µg/mL. PIF acted as a nonspecific binding control. Peptides were probed with a dilution series of **B**) IgG antibodies purified by protein G capture or melon gel, or **C**) peptide 2 was probed with sera PG0350/07 diluted in sera PG1409/08 from 100%-0%. Sera were used at a dilution of 1 in 50. Absorbance was read after incubation over 2 hours at room temperature. LODs are shown, calculated as the mean absorption at 0% positive sera plus three times the standard deviation.

6.5. The Development of RT-IPCR as an Alternative Diagnostic Assay

Further optimisations of the peptide ELISA had increased the sensitivity to detect scrapie positive sera to dilutions below 10%. Other diagnostics assays were investigated as more sensitive alternatives to the peptide ELISA method. One such method is immuno PCR (IPCR) or real time immuno PCR (RT-IPCR). IPCR is a similar method to that of an ELISA, with the exception that bound antibody is detected by a reporter enzyme is replaced with the amplification and detection of a DNA probe conjugated to the secondary antibody. In IPCR, the bound DNA probe is digested with a restriction enzyme and used as a template in PCR, analysed by gel electrophoresis. In RT-IPCR the digested probe is used as a template in RT-PCR for more sensitive quantification (Niemeyer et al. 2007). RT-IPCR is reported to be a highly sensitive method that can detect antigens with a 100-1000-fold greater sensitivity than conventional ELISAs (He and Patfield 2015). Indeed, RT-IPCR has been reported to detect measles-specific IgG antibodies in sera, demonstrating its potential use for detecting sera based antibodies as biomarkers (Mckie et al. 2002). Furthermore, RT-IPCR has been demonstrated to detect the scrapie prion protein with 1000-fold greater sensitivity than the Bio-Rad TeSeE ELISA (Reuter et al. 2009). Due to the high sensitivity of this assay, the RT-IPCR method was adopted and developed for use in this study.

6.5.1. Development of IPCR and RT-IPCR as a Functional Assay

Anti-ovine and anti-bovine IgG secondary antibodies (biotin conjugated) were optimised at concentrations of 1:4000 to 1:20000/30000 against a dilution series of bovine or ovine sera coated to a Nunc-Immuno Maxisorp plate (data not shown). The optimal dilution of each antibody was determined to be 1:4000. To first establish RT-IPCR as a functional assay, a conventional IPCR assay was performed. In this assay, SBV peptide 15 was used to coat the wells of a Nunc-Immuno Maxisorp plate at a concentration of 100 µg/mL. Maxisorp plates were used for initial assay development. This method was also developed prior to assay optimisation with pre-blocking sera. Peptide 15 was probed with a dilution series of sera 726 diluted in sera C12, and bound antibodies were detected with anti-bovine IgG secondary antibody (biotin conjugate). The secondary antibody was incubated with streptavidin at a molar ratio of 2:1 for 1-hour prior to use. Bound secondary/streptavidin was incubated with 250 ng/mL of biotinylated DNA probe containing BamHI restriction sites at the 5’ terminus. Bound probe was digested with BamHI, and products were used as the template in PCR. PCR products were analysed by agarose gel electrophoresis (**Figure 6.5.1. A**). For further analysis, the gel was analysed by densitometry using Image J software (**Figure 6.5.1. B**).

The secondary binding control consisted of wells treated with secondary antibody/streptavidin and biotinylated DNA probe only. This was used as a background reading and subtracted. Reactions treated with 100%, 50% and 25% positive sera were statistically significantly different from each reaction with 0% positive sera as determined by by one-way ANOVA ($F = 9.334$, $p = <0.01$). P values were calculated by a post-hoc Dunnett's test (100%: $p = 0.0112$, 50%: $p = 0.0015$, 25%: $p = 0.0012$). The digest products were also used for amplification by RT-PCR (**Figure 6.5.2.**). The quantification cycle (ΔCq) values from RT-IPCR represent the PCR cycle at which a sample produces fluorescent signal that overcomes the threshold value. ΔCq values are inversely proportional to the detection of target antigen, as the greater amount of DNA probe bound to the target, the fewer cycles of PCR are required to exceed the threshold. Consequently, ΔCq values were used as a value of assay efficacy. ΔCq values were plotted as a factor of sera dilution (**Figure 6.5.2. B**). A peptide ELISA was run in parallel to RT-IPCR to compare sensitivity of both assays (**Figure 6.5.2. C**). This ELISA used the same secondary antibody as RT-IPCR, detected with a streptavidin-HRP conjugate to allow for a direct comparison between methods. Both methods detected sera 726 at dilutions down to the lowest level of positive sera used, 25% (**Figure 6.5.2. B/C**).

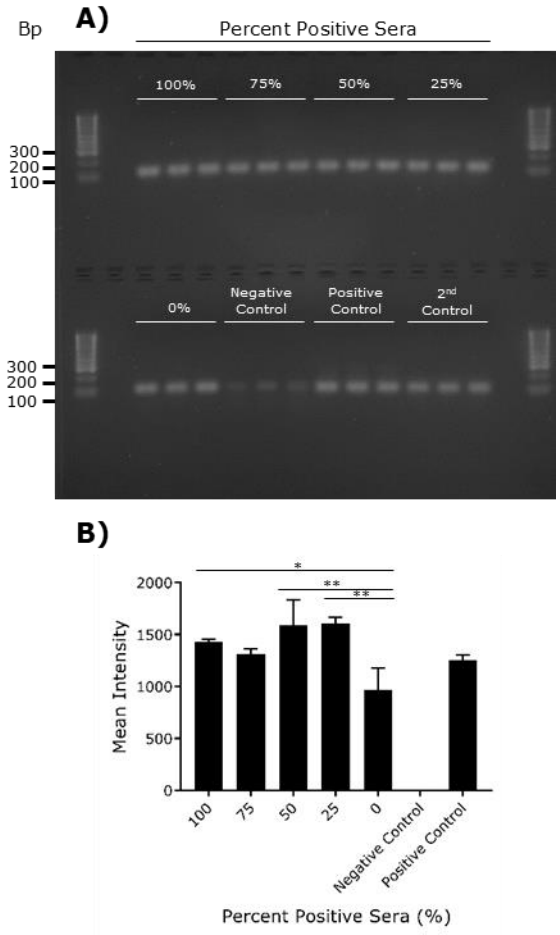

Figure 6.5.1. Analysis of IPCR by gel electrophoresis and densitometry. A Nunc-Immuno Maxisorp plate was coated with 100 µg/mL of SBV peptide 15. Peptide 15 was probed with sera 726 diluted in C12 from 100-0%. Sera were used at a dilution of 1 in 50 in the assay. Bound antibody was detected with an anti-bovine IgG secondary antibody conjugated to biotin/streptavidin. Bound secondary antibody was probed with biotinylated DNA. The bound DNA was then digested with BamHI and used as a template in PCR. 10 µL of PCR products were analysed by **A**) agarose gel electrophoresis and **B**) densitometry. Molecular weight markers are shown. P values are represented as: * = <0.05, ** = <0.01. Negative Controls were reactions using dH_2O instead of template. Positive Controls were reactions using 2.5 µL of 0.5 ng/mL biotinylated DNA probe as template. 2nd Controls were wells treated with secondary antibody/streptavidin and biotinylated DNA probe only. These values acted as a background reading and were subtracted.

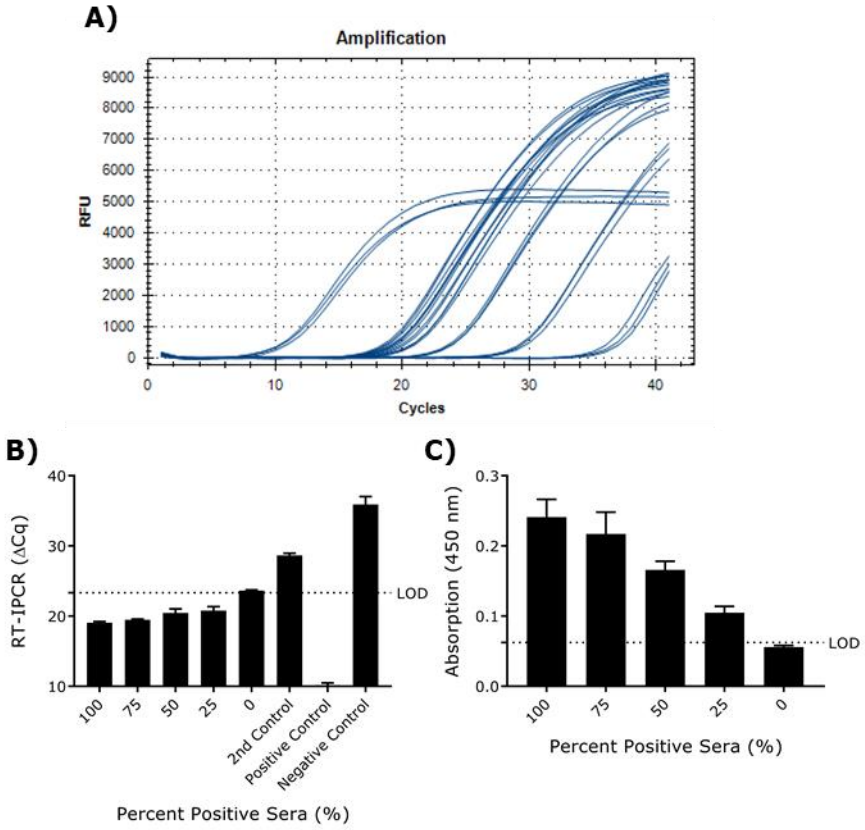

Figure 6.5.2. The detection of antibody capture by SBV peptide 15 using RT-IPCR. The digest products from the IPCR immunoassay were used as a template in RT-PCR. **A**) RT-PCR read out with fluorescence (RFU) over PCR cycles. **B**) Bar graph illustrating mean ΔCq values for each set of reactions. Reactions were run in triplicate. Negative Controls were reactions using dH_2O instead of template. Positive Controls were reactions using 2.5 µL of 0.5 ng/mL biotinylated DNA probe as template. 2^{nd} Controls were wells treated with secondary antibody/streptavidin and biotinylated DNA probe only. **C**) A peptide ELISA was run in parallel to RT-IPCR using the same biotinylated anti-bovine IgG secondary antibody, detected with a streptavidin-HRP conjugate diluted 1:500. LODs are shown, calculated as the mean absorption at 0% positive sera plus three times the standard deviation.

6.5.2. Optimisation of RT-IPCR Using Direct, Modular or Sequential Methods

IPCR and RT-IPCR had been successfully developed for use in detecting antibody capture by SBV peptide 15. However, IPCR or RT-IPCR displayed no greater sensitivity when run in parallel with a peptide ELISA. RT-IPCR can be performed in three formats to increase sensitivity: direct, modular or sequential (Niemeyer et al. 2007). In the direct method, secondary antibody, streptavidin and biotinylated DNA probe are pre-incubated prior to use in the assay to form a single detection conjugate. In the modular method streptavidin and secondary antibody are pre-incubated prior to use. The conjugate is then detected using the biotinylated DNA probe. In the sequential method the secondary antibody, streptavidin and DNA probe are added in sequential steps, interspersed with washes. Increased washes could potentially improve assay sensitivity, depending on the affinity of the capture peptides (Niemeyer et al. 2007). Each method was applied to RT-IPCR. These assays used Sc peptide 2, probed with sera PG0350/07 in a dilutions series from 50%-1% in sera PG1409/08. Each assay was compared by the ΔCq values generated by each experiment (**Figure 6.5.3.**). Neither method appeared to increase assay sensitivity (**Figure 6.5.3.**).

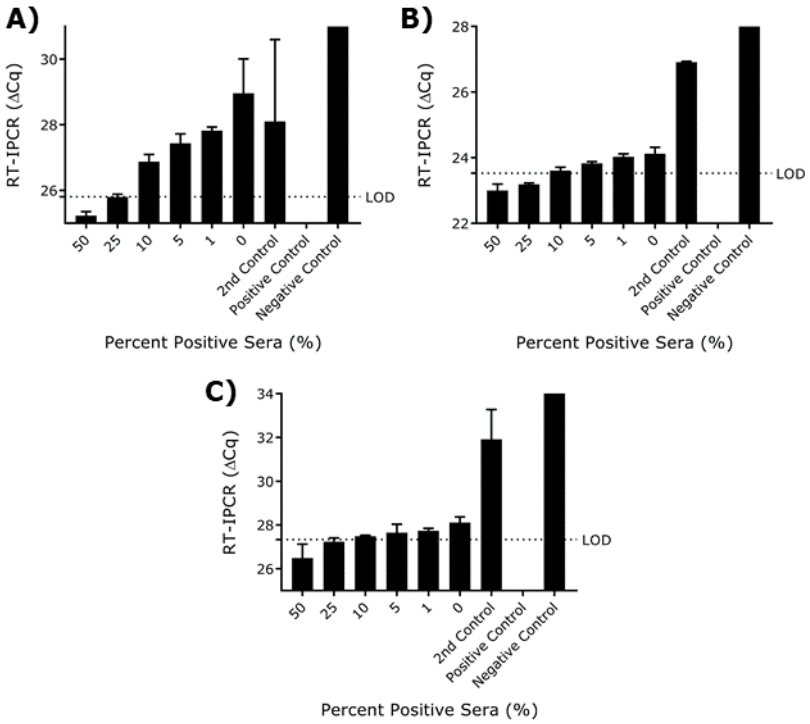

Figure 6.5.3. Modular, direct or sequential methods of RT-IPCR. Each assay was performed with Sc peptide 2 coated on maleic anhydride plates at a concentration of 100 µg/mL. Peptide 2 was probed with a dilution series of sera PG0350/07 in PG1409/08 from 50% to 1%. Sera were used at a concentration of 1 in 50 in each assay. Bound antibodies were detected with **A**) modular **B**) direct or **C**) sequential RT-IPCR methods. In the modular method bound antibody is probed with a secondary antibody/streptavidin conjugate, followed by detection with the biotinylated DNA probe. In direct RT-IPCR the secondary/streptavidin/DNA are pre-incubated to form a single detection conjugate prior to use. In sequential RT-IPCR secondary, streptavidin and DNA are bound in sequential steps interspersed with washing. Positive Controls were reactions using 2.5 µL of 0.5 ng/mL biotinylated DNA probe as template. 2nd controls were wells treated with secondary antibody/streptavidin and biotinylated DNA probe only. LODs are shown, calculated as the mean absorption at 0% positive sera plus three times the standard deviation. A shortened X-axis is displayed to demonstrate the differences between dilutions. Positive and negative controls were either too low or too large to be visualised on the shortened axis.

6.5.3. Optimising the Choice of Secondary Antibody.

The modular method of RT-IPCR was used in further experiments as it is less labour intensive, and limits the use of biotinylated DNA probe. A factor that can affect the sensitivity of RT-IPCR is the specificity and affinity of the antibodies used in the assay (Niemeyer et al. 2007; He and Patfield 2015). Consequently, the use of anti-ovine IgG secondary antibody was compared to protein G in RT-IPCR. Two serial dilution assays were performed using Sc peptide 2, probed with sera PG0350/07 diluted 50-1% in sera PG1409/08. These assays were performed either as peptide ELISAs, or by RT-IPCR using biotinylated anti-ovine IgG antibody or protein G (**Figure 6.5.4.**). The use of protein G did not detect scrapie positive sera below the LOD, while the anti-ovine IgG antibody was able to detect positive sera diluted 50% (**Figure 6.5.4. A/C**). However, in the parallel ELISA the protein G-HRP conjugate was observed to detect down to 25-10% positive sera, while the anti-ovine IgG antibody detected 50% (**Figure 6.5.4. B/D**).

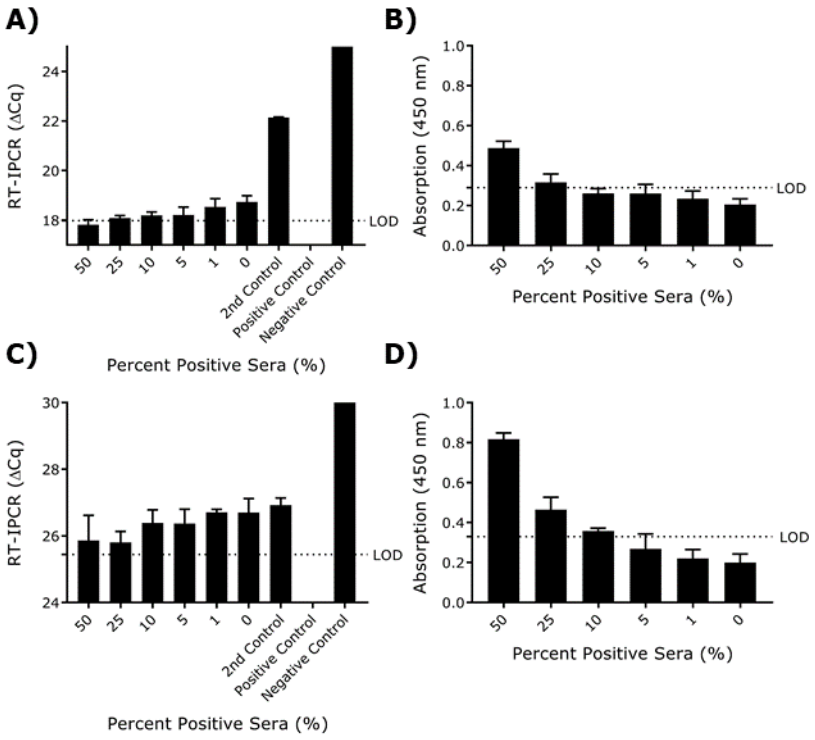

Figure 6.5.4. RT-IPCR and peptide ELISAs using biotinylated anti-ovine IgG secondary antibody or protein G as detection agents. **A**) RT-IPCR and **B**) ELISA with biotinylated anti-ovine IgG secondary antibody. **C**) RT-IPCR and **D**) ELISA with protein G. In ELISAs, bound antibody was detected with a streptavidin-HRP conjugate or protein G-HRP conjugate. Signals were measured after 30 minutes. Each assay was performed with Sc peptide 2 coated on maleic anhydride plates at a concentration of 100 µg/mL. Peptide 2 was probed with a dilution series of sera PG0350/07 in PG1409/08 from 50% to 1%. Sera were used at a dilution of 1 in 50 in each assay. In RT-IPCR Positive Controls were reactions using 2.5 µL of 0.5 ng/mL biotinylated DNA probe as template. 2nd Controls were wells treated with secondary antibody/streptavidin and biotinylated DNA probe only. For RT-IPCR reactions, positive and negative controls were either too low or too large to be visualised on the shortened axis. LODs are shown, calculated as the mean absorption at 0% positive sera plus three times the standard deviation. A shortened X-axis is displayed to demonstrate the differences between dilutions. Positive and negative controls were either too low or too large to be visualised on the shortened axis.

6.5.4. Determining the Limit of Detection of RT-IPCR Compared to Peptide ELISAs

Although protein G-HRP displayed greater sensitivity in the peptide ELISA, it did not improve the sensitivity of RT-IPCR. Consequently, the anti-ovine IgG secondary antibody continued to be used in each RT-IPCR method. Given that the RT-IPCR did not show improvements over the conventional ELISA, it was then questioned whether the RT-IPCR could detect ovine IgG antibodies at higher dilutions than ELISA. In this assay, sera PG1409/08 was used to coat a Nunc-Immuno Maxisorp plate at dilutions of 1:2500 to 1:15000 in carbonate buffer (pH 9.6.) (**Figure 6.5.5.**). The RT-IPCR method was run in parallel with peptide ELISAs to detect increasing dilutions of sera antibodies bound to the maxisorp plate (**Figure 6.5.5. A/B**). At these dilutions, RT-IPCR was no more sensitive than either ELISA using AP or HRP conjugated secondary antibodies, each detecting no lower than sera diluted 1:2500 (**Figure 6.5.5.**).

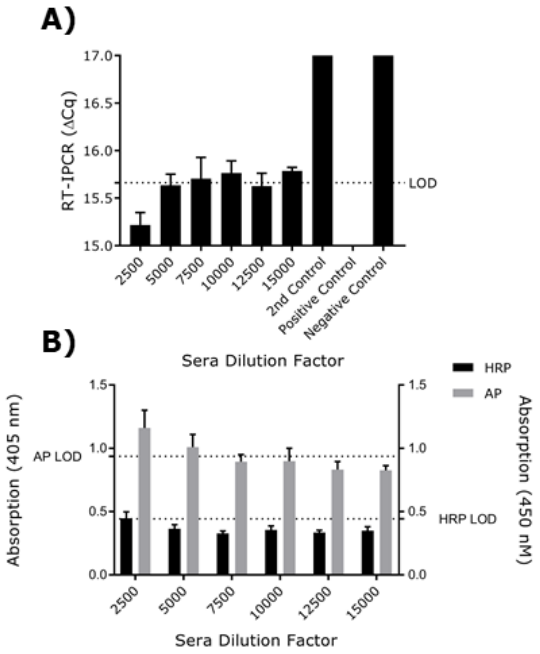

Figure 6.5.5. Detection of ovine IgGs in increasing dilutions of ovine sera with RT-IPCR or peptide ELISA. A dilution series of PG1409/08 was prepared in carbonate buffer (pH 9.6) from 1:2500 to 1:15000. This dilution series was used to coat the wells of a Nunc-Immuno Maxisorp plate in triplicate. Bound sera antibodies were detected with anti-ovine IgG antibodies, biotin conjugated for detection by RT-IPCR or strepativin-HRP conjugate, or AP conjugated. LODs are shown, calculated as the mean absorption at 0% positive sera plus three times the standard deviation. For RT-IPCR reactions a shortened X-axis is displayed to demonstrate the differences between dilutions. 2nd, positive and negative controls were either too low or too large to be visualised on the shortened axis.

6.6. Investigation into FACTT as an Alternative Diagnostic Assay

Although RT-IPCR had been developed as a functional assay, it was not more sensitive than ELISA. Therefore, another possible immunoassay was investigated which may have greater sensitivity than the optimised peptide ELISAs. FACTT is a similar method to that of IPCR, and uses a detection module consisting of secondary antibody/streptavidin/DNA. However, instead of PCR, detection is performed by incubating T7 Polymerase with the bound DNA template. In the presence of rNTPs, T7 Polymerase produces RNA oligomers over time that can be detected with a fluorescent dye (Zhang et al. 2006; Chang et al. 2007). FACTT has been previously reported to detect prion aggregates in the blood of infected mice (Chang et al. 2007). Therefore, this study attempted to adopt and optimise FACTT as a more sensitive method to serological ELISA.

6.6.1. RNA Polymerase Test

To ascertain the concentration of DNA required for detection in an assay plate format, 60 U of T7 RNA Polymerase was incubated with a dilution series of biotinylated DNA template from 250-0 ng/mL over the course of 3 hours at 37°C. RNA oligomers were quantified by the addition of Ribogreen fluorescent dye, followed by the measurement of fluorescence (ex 480 nm, em 520 nm) (**Figure 6.6.1.**). This produced a curve of fluorescence proportional to DNA concentration (**Figure 6.6.1.**). The limit of detection was determined to be between 50-25 ng/mL of DNA template (**Figure 6.6.1.**).

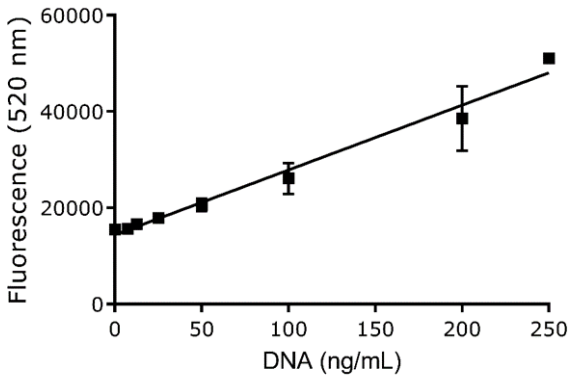

Figure 6.6.1. Determining the concentration of DNA probe required for detection by FACTT. 60 U of T7 RNA polymerase was incubated with a dilution series of DNA template over 3 hours in a Nunc-Immuno Maxisorp plate. RNA production was quantified using Ribogreen fluorescent dye, with fluorescence measured at ex 480 nm, em 520 nm. This generated a linear dilution curve. R^2 value: 0.98.

6.6.2. Testing the FACTT Detection Module

To test the efficacy of the detection module, biotinylated anti-ovine IgG secondary antibody was used to coat a Nunc-Immuno Maxisorp plate at a concentration of 1:4000. Bound antibody was conjugated with streptavidin and probed with a dilution series of 250-25 ng/mL biotinylated DNA template. Bound template was incubated with 60 U T7 RNA Polymerase for either 3 hours or overnight. RNA products were detected with Ribogreen fluorescent dye. No fluorescence signals were detected at either 3 hour or overnight time points (data not shown). This indicated that in our hands the assay format was not functional.

6.7. Screening SBV Peptides in Sera Using the Optimised Peptide ELISA.

Out of the methods investigated and optimised in this study, the optimised peptide ELISA was determined to be the most sensitive method for validating peptides identified by phage display. The optimised assay used maleic anhydride plates, with all incubation steps carried out at 25°C. Additionally, sera was pre-blocked in blocking buffer for 1 hour prior to use. The standard method used Maxisorp plates with all incubation steps performed at room temperature (Naqid et al. 2016). To test the optimised assay, the SBV peptides 1-15 were screened against the range of available sera from SBV infected or vaccinated cattle (**Table 6.7.1.**). In these assays, the nonspecific peptide control PIF acted as a background reading and was subtracted. This identified positive signals for each peptide, where the original method did not result in any signals in this study prior to optimisation. The ELISA data was then evaluated by ROC analysis using Graphpad Prism 7

(**Table 6.7.2.**). ROC analysis of each SBV peptide reported statistically significant AUC values for peptides 1, 2, 3, 5, 8, 9, 10, 11, 12, 13 and 15 (**Table 6.7.2.**).

Table 6.7.1. Peptide ELISA data using the optimised ELISA protocol with SBV peptides 1-15 against sera from infected and vaccinated cattle. There was sufficient sera 191 to permit screening with peptides 2, 3, 4, 9, 10 and 15 only. Blue: 0.1-0.2. Red: >0.2. The nonspecific peptide control PIF was used as a background control and subtracted.

	Field Infected (n = 13-14)													Experimentally Infected (n = 5)					Vaccinated (n = 10)									
SBV Peptide	191	198	210	213	367	422	424	726	731	739	744	745	749	C31	C34	C35	C36	C37	C12	C13	C14	C15	C16	C17	C18	C20	C22	C23
1		0.7	0.0	0.4	0.2	0.7	0.5	0.0	-0.2	0.0	0.1	0.3	1.6	0.0	0.4	0.4	0.3	0.0	0.1	0.0	0.0	0.0	0.0	0.0	0.0	0.0	0.0	0.1
2	0.4	0.1	0.1	0.1	0.0	0.1	0.3	0.2	0.1	0.1	0.2	0.3	0.6	0.1	0.4	0.9	0.2	0.1	0.1	0.2	0.1	0.1	0.1	0.1	0.1	0.1	0.0	0.0
3	0.9	0.0	0.1	0.4	0.1	0.2	0.6	0.0	-0.1	-0.1	0.0	0.6	0.8	0.0	0.6	0.4	0.2	0.1	0.0	0.0	0.0	0.0	0.1	0.0	0.0	0.0	0.0	0.0
4	0.8	0.0	0.1	0.4	0.1	0.2	0.6	0.1	0.0	0.0	0.1	0.6	0.7	0.1	0.6	0.7	0.3	0.1	0.1	0.2	0.1	0.0	0.0	0.0	0.0	0.1	0.0	0.0
5		0.6	0.1	0.4	0.2	0.7	0.6	0.0	-0.1	0.1	0.1	0.2	1.5	0.0	0.4	0.5	0.3	0.1	0.1	0.1	0.0	0.0	0.0	0.0	0.0	0.0	0.0	0.0
6		0.5	0.0	0.1	0.1	0.5	0.2	-0.1	-0.2	0.0	0.0	0.1	0.9	-0.1	0.2	0.2	0.2	0.0	0.1	0.0	0.0	0.0	0.0	0.0	-0.1	0.0	0.0	0.0
7		0.0	0.0	0.0	0.0	0.0	0.9	0.0	-0.1	0.0	0.0	0.1	0.7	0.0	0.1	0.6	0.0	0.0	0.0	0.0	0.0	0.0	0.0	0.0	0.0	0.0	0.0	0.0
8		0.0	0.1	0.2	0.0	0.1	0.9	0.0	-0.1	0.0	0.1	0.4	0.9	0.0	0.2	0.3	0.3	0.1	0.0	0.0	0.0	0.0	0.0	0.1	0.0	0.0	0.0	0.0
9	0.3	0.7	0.0	0.5	0.1	0.8	0.5	0.0	-0.1	0.0	0.1	0.3	1.3	0.0	0.2	0.2	0.3	0.1	0.1	0.0	0.1	0.1	0.0	0.0	0.0	0.0	0.0	0.0
10	0.9	0.6	0.1	0.3	0.3	0.8	0.5	0.2	0.0	0.1	0.1	0.2	2.1	0.1	0.4	0.4	0.2	0.1	0.1	0.0	0.5	0.1	0.1	0.0	0.0	0.0	0.0	0.0
11		0.7	0.0	0.0	0.1	0.4	0.3	-0.1	-0.2	0.2	0.0	0.1	0.3	0.9	0.3	0.0	0.1	0.0	0.1	-0.1	0.0	0.0	0.0	0.0	-0.1	0.0	0.0	0.1
12		0.1	0.8	0.0	0.4	1.1	0.4	0.0	-0.1	0.0	0.1	0.1	0.2	0.1	0.1	0.0	0.5	0.0	0.1	-0.1	0.0	0.0	0.0	0.0	0.0	0.0	0.0	0.0
13		1.1	0.0	0.1	0.2	0.5	1.2	0.0	0.1	0.5	0.1	0.3	0.3	2.1	0.7	0.1	0.3	0.0	0.1	0.0	0.1	0.0	0.0	0.1	0.0	0.0	0.0	0.0
14		0.1	0.6	0.0	0.1	0.9	0.2	0.0	-0.1	0.0	0.0	0.0	0.1	0.0	0.1	0.0	0.3	0.0	0.0	-0.1	0.1	0.1	0.1	0.1	0.1	0.1	0.1	0.1
15	0.9	0.0	0.0	1.1	0.1	1.1	0.0	1.1	1.0	0.0	0.0	0.6	1.2	0.1	0.7	1.0	1.2	0.2	0.0	0.0	0.0	0.0	0.0	0.0	0.0	0.0	0.0	0.0

Table 6.7.2. ROC curves were produced for the recognition of peptides by antibodies from the sera of SBV field infected (n = 12-13), experimentally infected (n = 5) and vaccinated (n = 10) samples. AUC and p values are listed.

SBV Peptide	Peptide Sequence	AUC of ROC	P Value
1	AEGEFAKGGSAASLDPAKAA	0.7382	0.042
2	AEGEFSKGGSANEADPAKAA	0.8278	0.0047
3	AEGEFAKGGSARPLDPAKAA	0.8139	0.0067
4	AEGEFEKGGSAHNSDPAKAA	0.8833	0.0647
5	AEGEFEKGGLASPPDPAKAA	0.8	0.0104
6	AEGEFGKGGSAAPLDPAKAA	0.7059	0.0789
7	AEGEFSKGGRSQVADPAKAA	0.6676	0.1524
8	AEGEFAKGGTSVRPDPAKAA	0.8618	0.002
9	AEGEFAKGGSNHYPDPAKAA	0.8333	0.004
10	AEGEFGKGGSSHIWDPAKAA	0.8278	0.0047
11	AEGEFLKRIPTHTGDPAKAA	0.75	0.0329
12	AEGEFSKLTSLGYKDPAKAA	0.8294	0.049
13	AEGEFLRRIPISSRDPAKAA	0.8706	0.0016
14	AEGEFSKLTVKSYSDPAKAA	0.5029	0.98
15	AEGEFLVAPTRSTPDPAKAA	0.9222	0.0003

6.8. Screening Scrapie Peptides in Sera Using Optimised Methods.

The 39 Sc peptides were re-screened using the optimised ELISA method (**Table 6.8.1.** and **Table 6.8.2.**). ELISA data was then analysed by ROC analysis in Graphpad Prism 7 (**Table 6.8.3.**). The peptides 9 (p = 0.01), 20 (p = 0.01), 31 (p = 0.01) and 38 (p = 0.03) were reported with significant AUC values, but these values were not reflected by relatively high ELISA signals or they produced higher signals in the healthy controls, and may be considered as false positives (**Table 6.8.1.** and **6.8.2.**). To account for inter plate variation in absorbance signals, an average reading of the nonspecific peptide control PIF were taken from each plate. This value plus one standard deviation acted as a threshold value. Assay values were considered as abnormal if signals for the PIF control exceeded the threshold and the plate was repeated. For each assay, the nonspecific control PIF was also used as a background reading.

Table 6.8.1. A heat map matrix generated using conditional formatting in Microsoft Excel for the Sc peptides tested against scrapie positive sera from months 21 and 18 of disease, or from animals unrelated to the time course. The nonspecific binding control PIF was used as background reading and subtracted.

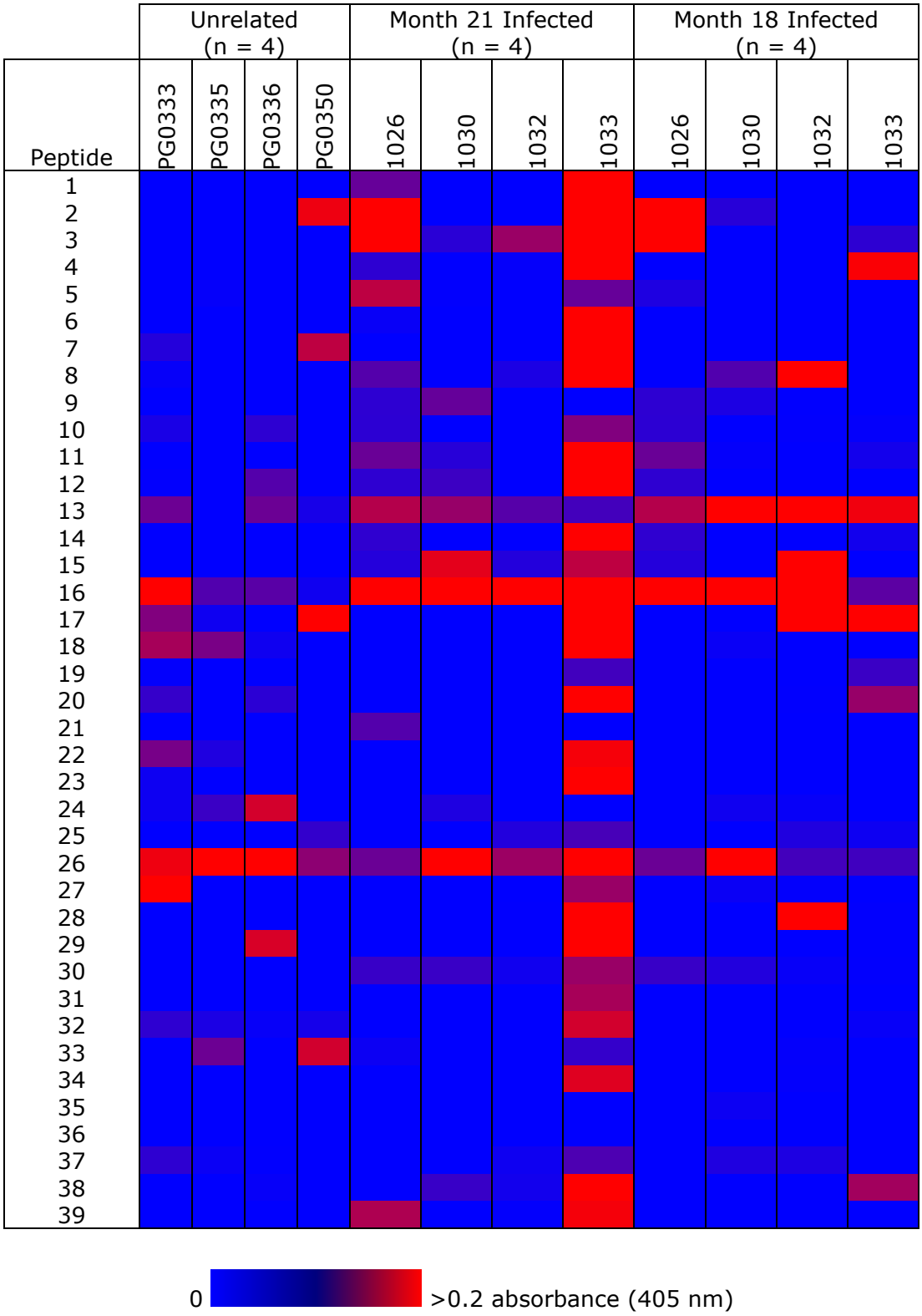

Table 6.8.2. A heat map matrix generated using conditional formatting in Microsoft Excel for the peptides tested against scrapie negative sera from unrelated animals, or from months 21 and 18. The nonspecific binding control PIF was used as background reading and subtracted.

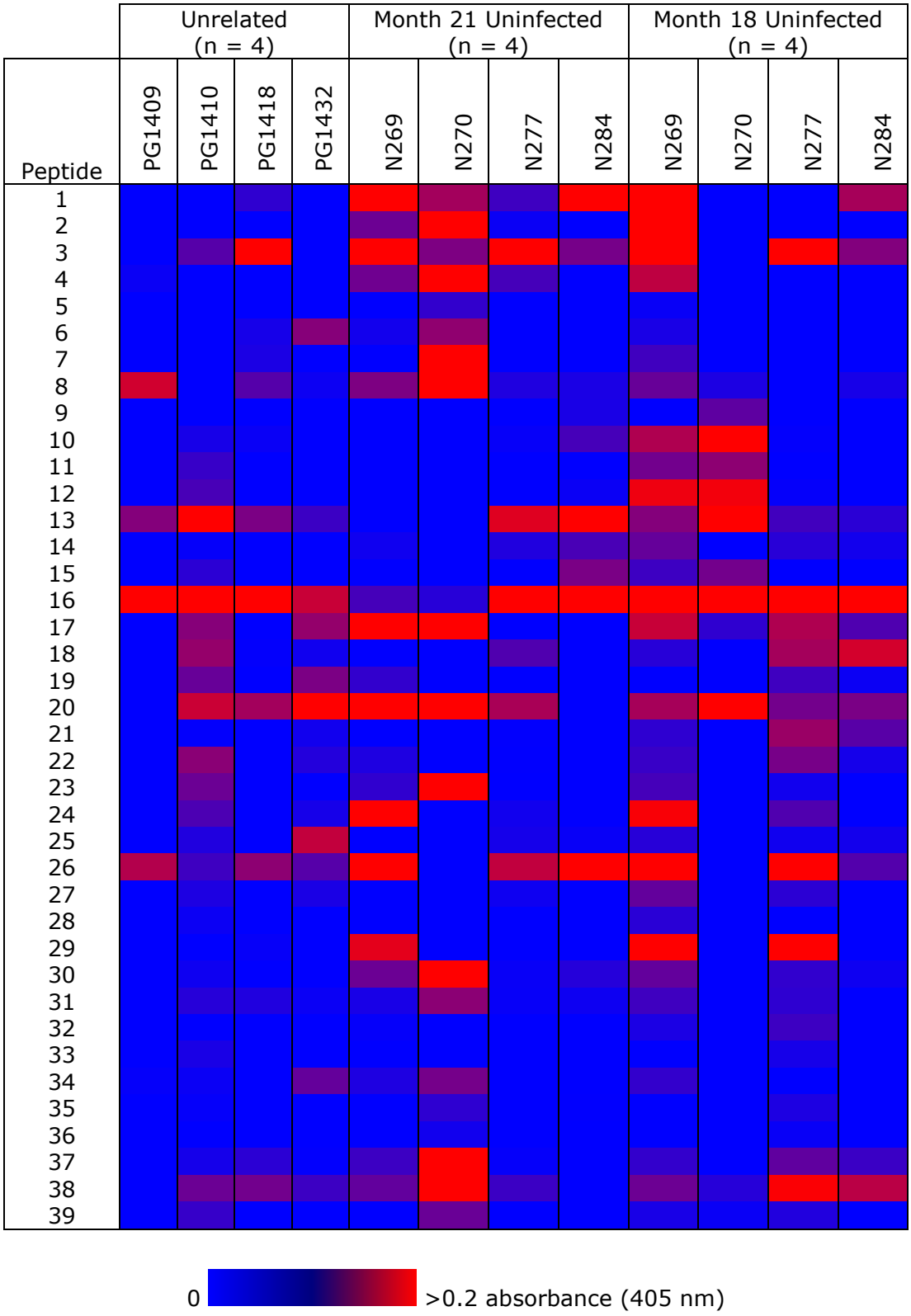

Table 6.8.3. ROC curves were produced for the recognition of peptides by IgG antibodies from the sera of scrapie infected (n = 12) and uninfected (n = 12) samples. AUC and p values are listed.

Sc Peptide	Peptide Sequence	AUC of ROC	P Value
1	AEGEFHRTTNTGAKDPAKAA	0.7014	0.0941
2	AEGEFRPKLPGRPPDPAKAA	0.5347	0.7728
3	AEGEFLLTPRAQGRDPAKAA	0.6181	0.3263
4	AEGEFSRRDLKNGADPAKAA	0.5347	0.7728
5	AEGEFAQLVFTSSSDPAKAA	0.7014	0.0941
6	AEGEFEKPPIKLTQDPAKAA	0.5417	0.7290
7	AEGEFSTRSQSMKQDPAKAA	0.5764	0.5254
8	AEGEFANSKLYPRADPAKAA	0.6597	0.1842
9	AEGEFGNSKNGVIPPDPAKAA	0.7361	0.0496
10	AEGEFQSSTKAIFTDPAKAA	0.5139	0.9081
11	AEGEFRKSPASGPLDPAKAA	0.6042	0.3865
12	AEGEFDDLGLKKYSDPAKAA	0.5451	0.7075
13	AEGEFWRALLVNPADPAKAA	0.5625	0.6033
14	AEGEFCTWMPHMSSACGDPAKAA	0.5139	0.9081
15	AEGEFRAPSQRLQLDPAKAA	0.5417	0.7290
16	AEGEFRKNLANKWDPAKAA	0.5833	0.4884
17	AEGEFRNIRPRPLQDPAKAA	0.625	0.2987
18	AEGEFRPNPHGDSGDPAKAA	0.5625	0.6033
19	AEGEFIARPYPKGLDPAKAA	0.6597	0.1842
20	AEGEFHKHMSPNFRDPAKAA	0.8264	0.0067
21	AEGEFDKIKQFDSTDPAKAA	0.6528	0.2040
22	AEGEFEKPPIKLTDPAKAA	0.5833	0.4884
23	AEGEFGGVLRNTKADPAKAA	0.6667	0.1659
24	AEGEFLQPSLDFVDPAKAA	0.5417	0.7290
25	AEGEFARTSSAAPQDPAKAA	0.5417	0.7290
26	AEGEFLWLKGRYYPDPAKAA	0.6597	0.1842
27	AEGEFPSLHPAWSKDPAKAA	0.5208	0.8625
28	AEGEFAPRLGVKSPDPAKAA	0.5833	0.4884
29	AEGEFCTVLPNLRCGDPAKAA	0.5694	0.5637
30	AEGEFFPFARSAPADPAKAA	0.5347	0.7728
31	AEGEFARQFIPQPSDPAKAA	0.7986	0.0130
32	AEGEFCGQILNWPSQCGDPAKAA	0.6111	0.3556
33	AEGEFCPRIVATYLHCGDPAKAA	0.6319	0.2727
34	AEGEFCRVPSTDRQPCGDPAKAA	0.7222	0.0647
35	AEGEFCSGCPAQSPTCGDPAKAA	0.6736	0.1489
36	AEGEFCTLQSAQPYTCGDPAKAA	0.5556	0.6442
37	AEGEFQPFYRPSPQDPAKAA	0.6458	0.2253
38	AEGEFRGRPPRSLTDPAKAA	0.7639	0.0282
39	AEGEFVLSAGPFQRDPAKAA	0.5833	0.4884

6.9. Discussion

To date, TSE surveillance in food producing animals is performed using commercial immunoassays to detect PrP^{Sc} as a surrogate biomarker. However, the reliance of these assays on brain derived tissue, as well as the detection of protease digested PrP^{Sc}, limits their capacity for sensitive ante-mortem diagnosis (Lee et al. 2013). Additionally, accumulation of PrP^{Sc} in the CNS occurs in later stages of disease, necessitating the use of an alternative tissue source for ante-mortem diagnosis (Gough et al. 2010). Methods like RT-QuIC, PMCA or capture with steel beads can be used to enrich or amplify PrP^{Sc} from tissue sources including milk, urine, buccal swabs, faeces, CSF and blood (Maddison et al. 2007; Castilla et al. 2008; Maddison et al. 2009; Gough et al. 2009; Maddison et al. 2010; Atarashi et al. 2011; Edgeworth et al. 2011; Terry et al. 2011; Gough et al. 2012; Moda et al. 2014; Jackson et al. 2014; Orrú et al. 2015). However, these methods remain experimental and are not currently employed in TSE surveillance. Out of these tissue sources, a serological based diagnostic test would be beneficial in its simplicity, rapidity and applicability to both human patients and livestock. It could also be used to screen blood stocks to detect and reduce the risk of iatrogenic CJD (Lacroux et al. 2014). However, the low levels of PrP^{Sc} in blood during prion disease onset limits it as a reliable ante-mortem biomarker for disease diagnosis (Edgeworth et al. 2011). Alternative blood based biomarkers of disease have been investigated, including autoantibodies. Autoantibodies can be used to selectively distinguish between healthy and diseased patients with AD, PD or MS (Nagele et al. 2011; Han et al. 2012, Ayoglu et al. 2013, DeMarshall et al. 2016).

In this study, NGPD was used to map the epitopes of autoantibodies in the sera of scrapie infected sheep. Analysis of the resulting phage display sub libraries led to the selection of 39 peptides for validation by peptide ELISA. In previous work by the group, NGPD had been used to identify peptides immunoreactive to antibodies in the sera of cattle infected with SBV. These peptides had been screened, and some were demonstrated to be reactive specifically to SBV-infected sera. These peptide/sera combinations formed the basis for optimising the peptide ELISA method for screening the anti-scrapie peptides. However, the optimised assay was not sensitive enough to reliably detect antibody binding in the sera tested. However, Sc peptide 2 was observed to consistently react with scrapie positive sera PG0350/07. Therefore, this combination of peptide/phage was used in further ELISA optimisation. The immunoreactivity of both SBV peptide 15 and Sc peptide 2 to sera samples from animals infected with SBV and scrapie, respectively, was confirmed by competitive peptide ELISA, which reduced the reactivity of each

peptide in a dose dependent manner. Reactivity was also reduced in a dose dependent manner by diluting positive sera into negative sera. These observations confirmed that the peptides can mimic antibody epitopes present in these sera.

Because of the low sensitivity observed in peptide ELISAs, further optimisations of the assay were attempted that increased the limit of detection from 50-25% sera to 10% sera. Using this optimised assay format, the SBV peptides were screened against the entire set of available sera from SBV infected or vaccinated cattle. The optimised method was more sensitive, and 9/15 peptides were reported with statistically significantly high AUC values. However, when this method was applied to screen the Sc peptides, none were found that were specific for the scrapie infected animals. These data indicate that although mapping antibodies in the sera of scrapie infected sheep by NGPD can identify panels of peptides by bioinformatic analysis of phage-peptide binding, these peptides lacked specificity for the disease state itself when tested by peptide ELISA. Assay sensitivity and specificity can be limited by the buffer systems used in serological ELISAs, due to poor blocking of nonspecific binding (Terato et al. 2014). This can be countered by using buffered heterologous sera as blocking and sample dilution buffer, but this is limited for use in screening sera samples due to competitive inhibition by sera based antibodies (Terato et al. 1990; Terato et al. 1996). Recently the development of the ELISA buffer ChonBlock™ was reported, which aided the detection and quantification of IgG responses to autoimmune diseases and bacterial infection in human sera (Terato et al. 2014). Therefore, investigating alternative buffer systems with the ELISA method developed in this study could decrease the nonspecific binding and background noise observed. ELISA specificity may have also been affected by the difference in conditions between phage display panning and ELISA. Indeed, the epitopes of peptides as they are displayed on bacteriophage may not be faithfully reproduced in an ELISA format, resulting in antibody binding with lower affinity. Indeed, that streptavidin coated plates increased assay sensitivity compared to other plates suggests that bound peptides are mimicking their presentation on bacteriophage. It would be beneficial to further investigate the use of streptavidin coated plates in peptide ELISAs, coupled with the use of biotinylated peptides. Another possible avenue of investigation is to use phage ELISAs to screen phage display derived peptides. In recent years, peptide phage ELISAs have been successfully applied as a serological diagnostic assay for the detection of IgG antibodies produced in Strongyloidiasis and neurocysticercosis (da Silva Ribeiro et al. 2010; Feliciano et al. 2014). Additionally, a dual-display phage ELISA was developed for the detection of rheumatoid arthritis autoantibodies specific to the

biomarker UH-RA.21, although no serological ELISA was produced (Rajaram et al. 2014). To determine the efficacy of phage ELISAs compared to peptide ELISAs, each method could be performed in parallel using a selection of 'scrapie peptides' and sera. If the phage ELISA method demonstrates greater specificity and sensitivity, it could be used to re-evaluate the anti-scrapie peptides identified in this study.

The heterogeneity of antigen specific and nonspecific antibodies present in sera may also have affected assay specificity. Indeed, the peptide mimitopes identified from panning experiments may not represent all epitopes of target sera antibodies across multiple animals. Therefore, peptides identified by phage display may not react with sera from all sheep infected with scrapie. Indeed, this is represented by the reactivity of the anti-scrapie peptides to different animals. For instance, 24 of the 39 anti-scrapie peptides displayed positive reactivity in sera 06-1033 at month 21, while few peptides were reactive with more than 3 of the 12 scrapie infected sera. This was an issue similarly encountered with studies using phage display to map epitopes of tuberculosis specific antibodies in human sera (Yang et al. 2011; Yang et al. 2013). This was overcome by alternative phage display panning strategies. (Yang et al. 2017) reported the identification of eight immunoreactive peptides, of which three were specific to sera from tuberculosis infected patients. To achieve this, they selected peptides by screening phage libraries against sera from healthy patients in biopanning, followed by screening the non-binding peptides against sera from infected patients (Yang et al. 2017). For comparison, they also attempted subtractive screening similar to this study that identified 12 immunoreactive peptides, with one that was specific (Yang et al. 2017). Therefore, alternating panning strategies can result in the identification of different diagnostic peptides. It could be beneficial to compare different phage display panning strategies on identifying peptides immmunoreactive to scrapie specific autoantibodies. These panning strategies could be performed in parallel, assessed by peptide selection and validation in serological peptide/phage peptide ELISAs. Alternatively, the use of a panel of peptides can be used to identify infected animals. This has been demonstrated previously, where a panel of peptides could be used to identify infected animals (Naqid et al. 2016; Naqid et al. 2016).

Another option could be the utilisation of protein microarrays to identify scrapie specific autoantibodies. Indeed, the use of protein microarrays was previously reported to identify and differentiate between healthy patients and those with AD, PD and MS (Nagele et al. 2011; Han et al. 2012; Ayoglu et al. 2013; DeMarshall

et al. 2016). Recently protein microarray was reported to identify AD patients with MCI with a sensitivity and specificity of 100% (DeMarshall et al. 2016). Therefore, the application of protein microarrays could be applied to map the epitopes of autoantibodies produced in scrapie infection. This would also serve as a comparison between the efficacies of protein microarrays and phage display at identifying diagnostic ligands. If successful, this method could be a powerful alternative method for the ante-mortem diagnosis of prion diseases.

Due to the limited sensitivity of peptide ELISAs, alternative high sensitivity assays were investigated. Among these were IPCR and RT-IPCR. RT-IPCR is a reportedly highly sensitive assay, which can detect antigens with up to 100-1000 times greater sensitivity than standard ELISAs (He & Patfield 2015). Indeed, RT-IPCR has been reported for the detection of IgG and IgE antibodies produced in measles infection or Bermuda allergen (McKie et al. 2002; Rahmatpour et al. 2017). In these studies, it was reported that IPCR increased the sensitivity of Bermuda allergen detection by 100-fold over conventional ELISA (Rahmatpour et al. 2017). Because of this reported sensitivity, IPCR and RT-IPCR was developed in this study as a more sensitive alternative to peptide ELISA. Despite the high sensitivity of RT-IPCR reported in other studies, this method did not demonstrate superior sensitivity than the peptide ELISA. A common factor determining the sensitivity of IPCR and RT-IPCR is the affinity of the capture antibody or peptide used for the assay (Niemeyer et al. 2007). Therefore, the sensitivity of RT-IPCR in this study is ultimately limited by the affinity of antibodies that recognise the epitope presented by each peptide. If this affinity is low, then the sensitivity of RT-IPCR can be affected (He and Patfield 2015). This may also have been affected by the affinity of the secondary antibodies. If these antibodies had a poor affinity for target IgG antibodies, this would also reduce assay sensitivity. Therefore, to improve RT-IPCR sensitivity peptides with greater affinity to target antibodies are required. This could be achieved through further phage display panning experiments using different screening strategies. If peptides are identified through these screens with a higher affinity for target antibodies, this could increase assay sensitivity. Additionally, further secondary antibodies can be tested to determine if antibodies with a greater affinity can increase assay sensitivity. Alternatively, different assay formats could be attempted. The conventional assay format was used in this study, where bound secondary antibody is detected with a streptavidin-biotinylated DNA probe conjugate. An alternative format includes detecting peptide-captured antibodies by microbeads coated with secondary antibody and DNA probe (Khan & Sadroddiny 2016). Investigating these

alternatives could improve the sensitivity of RT-IPCR to challenge that of the peptide ELISA developed in this study.

Another assay investigated was that of FACTT. FACTT has been reported to detect Her2 in the sera of human patients and PrP^{Sc} in the blood of infected mice (Zhang et al. 2006; Chang et al. 2007). However, in this study it proved difficult to generate detectable levels of RNA using the detection conjugate binding to secondary antibodies coated on the ELISA plate. It could be that with further optimisation, this method could be developed and for use. However, that this method has not been further developed and utilised in recent years raises questions as to its original efficacy (Zhang et al. 2006, Chang et al. 2007, Freudenberg 2008). Indeed, here it was observed that at least 50-25 ng/mL DNA probe is required to produce a fluorescence signal greater than background readings, in contrast to 1 ng/mL reported previously (Zhang et al. 2006). That wells coated with secondary antibody were insufficient to capture enough DNA probe for detection implies that the sensitivity of the assay is too low for the purposes of this study. Furthermore, that the similar methods RT-IPCR and IPCR were not more sensitive than the peptide ELISA raises the question as to whether FACTT would be more sensitive.

In this study, NGPD was used to map the epitopes of autoantibodies in the sera of scrapie infected sheep. Analysis of the resulting phage display sub libraries led to the selection of 39 peptides for validation by peptide ELISA. As there was no method previously established to screen these peptides, the peptide ELISA method was optimised using peptides selected against antibodies produced in the sera of cattle infected with SBV. This allowed for the development of a peptide ELISA method. However, the method was not sensitive enough to identify Sc peptides that reacted with specific sera. Sc peptide 2 was identified to react consistently to sera PG0350/07, which was used for further optimisations. The optimised ELISA was used to screen the SBV peptides, which demonstrated higher specificity and sensitivity.

Both SBV and Sc peptides were identified by analogous biopanning and analysis strategies. In both phage display experiments, round 1 biopanning phage libraries were selected against infected animals. This was followed by selection against the same infected animals as well as additional infected and uninfected animals in round 2 biopanning. Therefore, that the SBV peptides identified could differentiate between infected and vaccinated cohorts with the optimised peptide ELISA

demonstrates that NGPD can be successfully used to identify diagnostic peptides for use in serological peptide ELISAs. However, none of the Sc peptides were found to specifically distinguish between scrapie infected and uninfected animals. This could be due to a low titre of disease specific antibodies in the sera of infected sheep. As these low titres could have been affecting assay sensitivity, alternative sensitive assay formats were attempted, including IPCR and RT-IPCR, and FACTT. Although developed into a functional assay, IPCR and RT-IPCR were not more sensitive than the optimised ELISA method. Attempts to establish FACTT as a functional assay were unsuccessful. The results from this study potentially implicate that autoantibodies, if present, in the sera of scrapie infected sheep are at too low a level for sensitive detection by peptide ELISA or RT-IPCR. Additionally, the complexity and heterogeneity of antibody epitopes present in the sera could increase the difficulty in identifying disease specific peptides. Nevertheless, this work produced a peptide ELISA method that can be used to validate peptides identified in future phage display experiments. By performing phage display experiments with different panning strategies, and with the use of protein or peptide microarrays, a diagnostic assay may be developed to distinguish between scrapie infected and uninfected sheep. If successful, this would act as proof of principle for the development of ante-mortem serological diagnostic tests for prion diseases in humans and animals.

Chapter 7: General Discussion, Conclusions and Future Perspectives

7.1. Introduction

This study focused on two prominent areas of prion disease research: therapeutics and diagnostics. Here, novel findings are reported that can further advance research into these areas. This work included the use of recombinant PrP proteins as inhibitors of prion propagation *in vitro* by PMCA. These inhibitors were also used in an attempt to characterize prion strains. Alternatively, next generation phage display was employed to map the epitopes of autoantibodies in the sera of scrapie infected sheep. The peptides identified from this work were then used to attempt to develop a serological peptide ELISA as a diagnostic assay.

7.2. Recombinant PrPs as Therapeutic Ligands: Potential Therapeutics and Tools for Understanding Prion Propagation

This study reports novel insights into the action of rPrPs as inhibitors of prion propagation *in vitro*. Here, it was demonstrated that the ovine and hamster rPrPs can act as dose dependent inhibitors of prion amplification in PMCA. Although human, mouse, bovine, bank vole and hamster rPrPs have been reported previously to inhibit prion amplification in PMCA (Yuan et al. 2013; Skinner et al. 2015). This study was the first to demonstrate ovine rPrPs as inhibitors in a range of natural and experimental ruminant strains/isolates. Importantly, the ovine protein rVRQ can act as a potent inhibitor of prion amplification by PMCA, independent of host genotype or prion disease or strain type. This is contrary to the hypothesis proposed by (Yuan et al. 2013), who suggested that rPrP inhibition is species specific. That rPrP inhibition was consistently demonstrated across a range of different genotypes as well as strains and disease types in this study suggests otherwise. This has important implications for the use of rVRQ as a therapeutic ligand, where rVRQ could possibly be utilized as a broad-spectrum inhibitor of prion propagation. Coupled with the recent report that rPrP can prolong disease onset *in vivo*, rPrP proteins could even eventually be considered for use as therapeutics in human prion diseases (Skinner et al. 2015; Seelig et al. 2015). Therefore, it is recommended that the protein rVRQ be investigated as a potential therapeutic for prion diseases. This can be pursued with additional *in vitro* studies in PMCA and cell culture, as well as in *in vivo* mouse models of prion infection. However, in the previous report of rHam prolonging disease onset *in vivo*, RML-Chandler scrapie was inoculated at the same time as rPrP treatment rather than after prolonged incubation (Skinner et al. 2015). In this study, it was demonstrated that increasing the amount of PrP^{Sc} seed in PMCA decreases the inhibition efficiency of rPrPs. Therefore, the efficacy of rPrPs as therapeutics may be limited by the stage of disease and state/presence of replicating PrP^{Sc} at the

time of treatment. Whether this is the case can be elucidated by treating infected mouse models at increasing incubation periods with a range of rPrP doses.

This study also presents insights into the mechanism of rPrP inhibition. Previously it was reported that rPrPs bound to magnetic beads can selectively capture PrP^{Sc}, indicating that rPrPs binding PrP^{Sc} is a key part of the inhibitory mechanism (Yuan et al. 2013). These results are corroborated here, where rVRQ coated magnetic beads were demonstrated to capture PrP^{Sc} that could seed subsequent PMCA reactions. It was also demonstrated that the 3D structure of rPrP is not essential to the inhibitory mechanism, indicating that the primary amino acid sequence is involved in the inhibitory mechanism. In addition, here it was demonstrated that polymorphisms at residues 136 and 171 of ovine rPrP can affect inhibition efficacy, with the proteins rVRQ and rARQ displaying stronger inhibition that the protein rARR. rVRQ was also observed to be the more potent inhibitor of bovine BSE. These findings are corroborated by studies investigating the use of linear prion peptides (Chabry et al. 1998; Chabry et al. 1999). Therefore, the primary sequence, as well as key residues are critical to prion propagation and rPrP inhibition. Investigating rPrPs with different mutations at residues 136 and 171 could identify inhibitors with greater efficacy than rVRQ. Once identified, these inhibitors could be validated in PMCA and cell culture models, as well as *in vivo* mouse models of prion amplification.

It is hypothesised here that rPrPs are competitive inhibitors of prion propagation by acting as conversion-inefficient substrates that compete with PrP^{C} for binding to PrP^{Sc}, similar to heterologous PrP^{C} (Scott et al. 1993; Priola et al. 1994; Horiuchi et al. 2000; Geoghegan et al. 2009; Hizumi et al. 2009; Kobayoshi et al. 2009; Kobayoshi et al. 2015; Asante et al. 2015; Skinner et al. 2015; Seelig et al. 2015). This was observed previously when incubating rPrPs in PMCA and ScN2a cell culture, as well as in PMCA (Yuan et al. 2013). That rPrPs may act as competitive, conversion-inefficient inhibitors is also supported by studies investigating the conversion of rPrPs into PrP^{res}. Indeed, rPrPs can be converted into infectious PrP^{res} that causes disease in mice, indicating that rPrPs can act as a conversion substrate (Atarashi et al. 2008; Kim et al. 2010; Faburay et al. 2014). Therefore, although rPrPs may act as substrates in PMCA, the low efficiency of conversion would prolong prion propagation when rPrPs are present and can compete with PrP^{C} for binding to PrP^{Sc}. Indeed, by performing PMCA over 48 hours instead of 24 hours reduced the efficacy of rPrP inhibitors. These observations may represent PrP^{Sc} propagation at a slower rate due to the competition between rPrP and PrP^{C} for

binding to PrP^{Sc}, or the propagation of small populations of PrP^{Sc} able to convert rPrP with greater efficacy or that do not bind rPrP and in either case are 'resistant' to inhibition. This can be investigated further by performing PMCA reactions over increasing periods of time in the presence or absence of inhibitors, and analysing products by western blotting or CSA to investigate the potential differences in PrP^{Sc} product conformations. Another route of investigation is to elucidate the characteristics which define rPrPs as conversion-inefficient substrates. A means of doing this could be to selectively remove of secondary modifications by using unglycosylated PrP^{C}, as well as the removal of GPI anchors by cathespin D (Nishina et al. 2006; Lewis et al. 2006). The capacity of these proteins to act as substrates in PMCA can be characterised to establish the post translational modifications that may contribute to conversion efficacy. The findings from these experiments could in turn aid the development of novel therapeutics or strategies to inhibit prion propagation.

7.2. The Use of Recombinant PrPs for Prion Strain Characterisation

This study demonstrates that when used at a specific concentration in PMCA, rPrPs can generate a repeatable pattern of inhibition. Initially it was hypothesised that this could serve as the basis for a novel prion strain characterisation assay. However, this pattern of inhibition was ultimately limited by the efficacy of prion propagation, in that one round of PMCA was required for the assay readout. However, it was not tested here whether once a strain has been amplified over several rounds of sPMCA, the inhibition using rPrPs is consistent over a single subsequent round of amplification. Such an approach could be tested and may open the method to a wide range of strains that amplify by sPMCA. The pattern of inhibition observed here could be utilized as part of a more comprehensive assay that identifies prion strains based on multiple characteristics. For example, different prion strains and disease types are known to amplify in substrates with specific PrP^{C} genotypes, and can be characterized by distinct glycosylation ratios in western blotting (Hill et al. 1998; Taema et al. 2012) or by PrP^{Sc} stability by CSA (Safar et al. 1998; Peretz et al. 2001). An assay using a combination of these methods could be developed to differentiate strains based on different characteristics, including the amplification efficiency in sPMCA in substrates with different genotypes, followed by inhibition of successful amplification with a panel of rPrP inhibitors, as well as glycosylation ratios and PrP^{Sc} stability. If developed, this assay would require validation by characterising multiple strain types. This assay could then be of importance to aid the identification of novel prion strains in food producing animals.

It was also identified that the imidazole present in elution buffer can inhibit prion amplification in a dose dependent manner. This inhibition was shown to be strain specific, were ovine BSE was completely inhibited at concentrations of imidazole above 10 mM while classical scrapie remained uninhibited. Interestingly, studies have previously reported that imidazole can enhance amplification efficiency by sequestering copper ions (Orem et al. 2006; Fujihara et al. 2009). However, at higher concentrations imidazole inhibited prion replication, indicating that imidazole may inhibit prion amplification under specific conditions (Orem et al. 2006). With further investigation using different prion strains and isolates, inhibition with imidazole could serve as an independent strain characterisation assay. Alternatively, it could be used in combination with the assay described above as a comprehensive, multi-faceted strain characterisation assay.

7.3. Next Generation Phage Display to Map the Epitopes of Autoantibodies in the Sera of Scrapie Infected Sheep

This study demonstrated the capacity of NGPD to map the epitopes of autoantibodies in the sera of sheep infected with scrapie. Here, peptide binders were identified over two rounds of biopanning. This demonstrates that NGPD can be used to selectively identify peptides that bind polyclonal IgG antibodies. To validate these peptides, a peptide ELISA was optimised using peptides selected against antibodies in SBV infected cattle. Although the optimised peptide ELISA was demonstrated to have greater sensitivity when screening peptides selected against antibodies to SBV, none of the peptides identified against antibodies from scrapie infected sheep demonstrated specificity. These observations demonstrate that either NGPD did not isolate specific peptides, or that the conditions used in the ELISAs were not sensitive enough to detect low affinity peptide/antibody binding. It is possible that scrapie specific antibodies are present at too low titres in sera to accurately quantify in a plate based immunoassay format. For this reason, alternative assays were also investigated, including RT-IPCR, reported to be a highly sensitive immunoassay (Niemeyer et al. 2007). However, although RT-IPCR was successfully developed as an assay, it did not demonstrate greater sensitivity than that of the peptide ELISA. A key factor in determining the sensitivity of RT-IPCR is the affinity of the antibody for the target antigen (Niemeyer et al. 2007). Therefore, the observation that RT-IPCR was not more sensitive than peptide ELISA indicates that both methods may be limited by the affinity of peptides for their target antibodies. This may also be affected by the affinity of the secondary antibodies utilized in the study, as secondary antibodies with lower affinities would decrease assay sensitivity.

Factors affecting this affinity could include the environment in which peptides are displayed in phage display biopanning and immunoassays. The conditions in these immunoassays are different from those during biopanning itself. Because of these differences in conditions, epitopes presented by peptides may be displayed differently between biopanning and immunoassay. Ultimately, this may decrease the efficacy of immunoassays in validating peptides identified by phage display. Phage-peptide ELISAs can also be combined with RT-IPCR to enhance assay sensitivity (Lo et al. 2007). These methods could be developed in an attempt to increase the sensitivity and specificity of the peptides identified in this study. Alternatively, NGPD could be exploited as the diagnostic test itself. Indeed, that peptides were identified across two experiments is convincing of their reactivity to scrapie specific antibodies. Performing a third phage display experiment with the same samples could help to determine whether these peptides identified in biopanning can be used as a diagnostic biomarker of the disease state. If the same peptides are identified in a third panning experiment, it would be convincing that using such a specific sub-library of phage to bind polyclonal antibodies followed by NGS analysis may represent a sensitive serodiagnostic assay format. It could also be beneficial to investigate the potential of peptide or protein microarrays for identifying scrapie specific autoantibodies. Indeed, that autoantibodies have been used as a diagnostic biomarker in the sera of patients with AD, PD and MS with protein microarrays strongly suggests that this method could be applied to detect scrapie specific autoantibodies (Nagele et al. 2011; Han et al. 2012; Ayoglu et al. 2013; DeMarshall et al.2016).

The complexity of the target can also affect the success of phage display in identifying target specific peptides. For example, complex targets such as cells may require additional rounds of biopanning to select for specific binders (Brinton et al. 2016). Therefore, due to the complexity of sera the two rounds of biopanning used in this study may have resulted in specific peptides being at too low a frequency to be identified by the two-proportion Z-test used for analysis. Two rounds of biopanning were reported to be sufficient for the identification of peptides that recognize antibodies produced in response to *Salmonella enterica* serovars Typhimurium in chickens (Naqid et al. 2016). However, it is likely that autoantibodies produced in response to prion disease would be at a lower titre. Therefore, in future panning experiments it could be beneficial to extend the number of biopanning rounds. The sub library of each round could then be analysed for the enrichment of target-specific peptides. The enrichment of peptides over increasing rounds of biopanning could be indicative of their

specificity, although there could be a risk of enriching target unrelated peptides ('T Hoen et al. 2012). Alternatively, a similar approach could be employed as described above, identifying peptides enriched consistently over three independent phage display experiments. If peptides are consistently identified over a triplicate of experiments that match the selection criteria, it would be convincing of their specificity. It could also be beneficial to attempt different panning strategies. For instance, (Yang et al. 2016) performed biopanning where peptides which did not bind negative sera were then further screened. This was performed in parallel to another experiment using comparative screening, similar to that performed in this study (Yang et al. 2016). Out of these two strategies, the first strategy identified three specific peptides, while comparative screening identified one (Yang et al. 2016). Therefore, further panning experiments could attempt to use this method in parallel to comparative screening, to determine if either method has a greater efficacy in identifying specific peptides. These strategies can be accompanied by alternative methods of analysis to identify enriched peptides, including peptide clustering and PHASTpep as a comparison to the two-proportion Z-test used in this study (Ravn et al. 2013; Brinton et al. 2016). The observations from these experiments could highlight panning strategies and analysis methods with greater efficacy at identifying immunoreactive peptides by NGPD.

Professional Internships for PhD Students
Reflection Form

Name of Organization

The Oxford Protein Production Facility UK (OPPF-UK)

Details of Placement

Please describe your main activities during the placement.

From October-December 2015 I undertook a placement at the OPPF-UK at the Harwell Research Institute, Oxfordshire. This placement at the OPPF-UK focused on developing a system for expressing the membrane protein Tok-1 from the yeast *Candida albicans*, a major cause of fungal infection in humans. Tok-1 is a potassium ion channel, and a potential therapeutic target.

The aim the project was to clone the gene for Tok-1 from *Candida albicans* with different purification tags, and to express these clones in the yeast *Saccharomyces cerevisiae*. The objective was to make as much progress possible towards the expression and purification of Tok-1 for X-ray crystallography. This involved the use of techniques including cloning, yeast and bacterial cell culture, chromatography and confocal microscopy.

Benefits to the group included developing a protein expression system in yeast, which was unavailable to the group until the time of the project. The methods developed would also enable the group to express and purify membrane proteins in future years.

Placement Achievements

Please detail all outcomes from the placement, including any publications, presentations given and reports written etc.

By the end of the project each of the seven Tok-1 clones had been successfully expressed, with two of these clones used to test potential purification methods. To assess the functionality of the clones, the expression of clones fused with yeast-Enhanced Green Fluorescent Protein (yEGFP) were visualized using confocal microscopy to confirm expression and correct cellular localization. This suggested that the system developed in the placement could successfully express functional Tok-1 proteins. Therefore, X-ray crystallography structures created with these proteins would be biologically relevant.

As part of the placement I participated in a Researcher Poster Presentation day, where students from each department and organization presented their research. Additionally, I presented the data and methodology developed during the placement in a leaving presentation. The work from this placement has the potential to be published. However, further work is required to purify further Tok-1 protein for X-ray crystallography.

Skill development

Has this Placement helped you developed any new skills or enhanced your previous skill set?

The environment at the OPPF-UK and Harwell Research Institute is highly stimulating, with many research groups available with which to collaborate and learn new techniques from. These included confocal microscopy and X-ray crystallography. The placement greatly enhanced my skills in cloning and protein expression, as well as in problem solving and working autonomously.

Future Work

Has this Placement influenced your future career aspirations? If so, in what way?

The placement confirmed my enthusiasm for scientific research and my willingness to pursue a research career. As such, protein expression and purification is a potential research area that I may consider in future years.

Appendices

Appendix I

The unique barcode sequences used in barcoded primers 1-50. Each unique barcode sequence was flanked by the sequences:

CCATCTCATCCCTGCGTGTCTCCGACTCAG and GTAATCCTTGTGGTATCG.

Barcode	Sequence	Barcode	Sequence
1	CTAAGGTAAC	26	TTACAACCTC
2	TAAGGAGAAC	27	AACCATCCGC
3	AAGAGGATTC	28	ATCCGGAATC
4	TACCAAGATC	29	TCGACCACTC
5	CAGAAGGAAC	30	CGAGGTTATC
6	CTGCAAGTTC	31	TCCAAGCTGC
7	TTCGTGATTC	32	TCTTACACAC
8	TTCCGATAAC	33	TTCTCATTGAAC
9	TGAGCGGAAC	34	TCGCATCGTTC
10	CTGACCGAAC	35	TAAGCCATTGTC
11	TCCTCGAATC	36	AAGGAATCGTC
12	TAGGTGGTTC	37	CTTGAGAATGTC
13	TCTAACGGAC	38	TGGAGGACGGAC
14	TTGGAGTGTC	39	TAACAATCGGC
15	TCTAGAGGTC	40	CTGACATAATC
16	TCTGGATGAC	41	TTCCACTTCGC
17	TCTATTCGTC	42	AGCACGAATC
18	AGGCAATTGC	43	CTTGACACCGC
19	TTAGTCGGAC	44	TTGGAGGCCAGC
20	CAGATCCATC	45	TGGAGCTTCCTC
21	TCGCAATTAC	46	TCAGTCCGAAC
22	TTCGAGACGC	47	TAAGGCAACCAC
23	TGCCACGAAC	48	TTCTAAGAGAC
24	AACCTCATTC	49	TCCTAACATAAC
25	CCTGAGATAC	50	CGGACAATGGC

The unique barcode sequences used in barcoded primers 51-96. Each unique barcode sequence was flanked by the sequences:
CCATCTCATCCCTGCGTGTCTCCGACTCAG and GTAATCCTTGTGGTATCG.

Barcode	Sequence	Barcode	Sequence
51	TTGAGCCTATTC	74	CGATCGGTTC
52	CCGCATGGAAC	75	TCAGGAATAC
53	CTGGCAATCCTC	76	CGGAAGAACCTC
54	CCGGAGAATCGC	77	CGAAGCGATTC
55	TCCACCTCCTC	78	CAGCCAATTCTC
56	CAGCATTAATTC	79	CCTGGTTGTC
57	TCTGGCAACGGC	80	TCGAAGGCAGGC
58	TCCTAGAACAC	81	CCTGCCATTCGC
59	TCCTTGATGTTC	82	TTGGCATCTC
60	TCTAGCTCTTC	83	CTAGGACATTC
61	TCACTCGGATC	84	CTTCCATAAC
62	TTCCTGCTTCAC	85	CCAGCCTCAAC
63	CCTTAGAGTTC	86	CTTGGTTATTC
64	CTGAGTTCCGAC	87	TTGGCTGGAC
65	TCCTGGCACATC	88	CCGAACACTTC
66	CCGCAATCATC	89	TCCTGAATCTC
67	TTCCTACCAGTC	90	CTAACCACGGC
68	TCAAGAAGTTC	91	CGGAAGGATGC
69	TTCAATTGGC	92	CTAGGAACCGC
70	CCTACTGGTC	93	CTTGTCCAATC
71	TGAGGCTCCGAC	94	TCCGACAAGC
72	CGAAGGCCACAC	95	CGGACAGATC
73	TCTGCCTGTC	96	TTAAGCGGTC

Appendix II

Peptides selected for synthesis and validation by screening. Peptides were synthesised with flanking motifs AEGEF and DPAKAA as displayed on bacteriophage.

Peptide Number	Peptide Sequence
1	AEGEFHRTTNTGAKDPAKAA
2	AEGEFRPKLPGRPPDPAKAA
3	AEGEFLLTPRAQGRDPAKAA
4	AEGEFSRRDLKNGADPAKAA
5	AEGEFAQLVFTSSSDPAKAA
6	AEGEFEKPPIKLTQDPAKAA
7	AEGEFSTRSQSMKQDPAKAA
8	AEGEFANSKLYPRADPAKAA
9	AEGEFGNSKNGVIPPDPAKAA
10	AEGEFQSSTKAIFTDPAKAA
11	AEGEFRKSPASGPLDPAKAA
12	AEGEFDDLGLKKYSDPAKAA
13	AEGEFWRALLVNPADPAKAA
14	AEGEFCTWMPHMSSACGDPAKAA
15	AEGEFRAPSQRLQLDPAKAA
16	AEGEFRKNLANKWDPAKAA
17	AEGEFRNIRPRPLQDPAKAA
18	AEGEFRPNPHGDSGDPAKAA
19	AEGEFIARPYPKGLDPAKAA
20	AEGEFHKHMSPNFRDPAKAA
21	AEGEFDKIKQFDSTDPAKAA
22	AEGEFEKPPIKLTDPAKAA
23	AEGEFGGVLRNTKADPAKAA
24	AEGEFLQPSLDFVDPAKAA
25	AEGEFARTSSAAPQDPAKAA
26	AEGEFLWLKGRYYPDPAKAA
27	AEGEFPSLHPAWSKDPAKAA
28	AEGEFAPRLGVKSPDPAKAA
29	AEGEFCTVLPNLRCGDPAKAA
30	AEGEFFPFARSAPADPAKAA
31	AEGEFARQFIPQPSDPAKAA
32	AEGEFCGQILNWPSQCGDPAKAA
33	AEGEFCPRIVATYLHCGDPAKAA
34	AEGEFCRVPSTDRQPCGDPAKAA
35	AEGEFCSGCPAQSPTCGDPAKAA
36	AEGEFCTLQSAQPYTCGDPAKAA
37	AEGEFQPFYRPSPQDPAKAA
38	AEGEFRGRPPRSLTDPAKAA
39	AEGEFVLSAGPFQRDPAKAA

References

Acevedo-Morantes, C.Y. & Wille, H., 2014. The structure of human prions: From biology to structural models - considerations and pitfalls. *Viruses*, 6(10), pp.3875–3892.

Adamson, C.S. et al., 2007. Novel single chain antibodies to the prion protein identified by phage display. *Virology*, 358(1), pp.166–77.

Aguzzi, A., Montrasio, M. & Kaeser P.S., 2001. Prions: health scare and biological challenge. *Nature Reviews Molecular Cell Biology*, 2, pp.118-126.

Aguzzi, A. & Calella, A.M., 2009. Prions: protein aggregation and infectious diseases. *Physiological reviews*, 89(4), pp.1105–52.

Aguzzi, A. & Falsig, J., 2012. Prion propagation, toxicity and degradation. *Nature Neuroscience*, 15(7), pp.936–939.

Aguzzi, A., Heikenwalder, M. & Polymenidou, M., 2007. Insights into prion strains and neurotoxicity. *Nature reviews. Molecular cell biology*, 8(7), pp.552–61.

Aguzzi, A. & Rajendran, L., 2009. The Transcellular Spread of Cytosolic Amyloids, Prions, and Prionoids. *Neuron*, 64(6), pp.783–790.

Allroggen, H. et al., 2000. New variant Creutzfeldt-Jakob disease: three case reports from Leicestershire. *J.Neurol.Neurosurg.Psychiatry*, 68(0022–3050), pp.375–378.

Altmeppen, H.C. et al., 2015. The sheddase ADAM10 is a potent modulator of prion disease. *eLife*, 4, pp.1–50.

Anderson, K.S. et al., 2011. A Protein Microaaray Signature of Autoantibody Biomarkers for the Early Detection of Breast Cancer. *Journal of proteome research*, 10(1), pp.617–632.

The Animal and Plant Health Agency, United Kingdom.

Apetri, A.C. et al., 2006. Early Intermediate in Human Prion Protein Folding as Evidenced by Ultrarapid Mixing Experiments. *Journal of the American Chemical Society,* 128(35), pp.11673-11678.

Asante, A.A. et al., 2015. A naturally occuring variant of the human prion protein completely prevents prion disease. *Nature*, 522(7557), pp.478-481.

Atarashi, R. et al., 2011. Real-time quaking-induced conversion: a highly sensitive assay for prion detection. *Prion*, 5(3), pp.150–3.

Atarashi, R. et al., 2008. Simplified ultrasensitive prion detection by recombinant PrP conversion with shaking. *Nature methods*, 5(3), pp.211–212.

Ayoglu, B. et al., 2013. Autoantibody profiling in multiple sclerosis using arrays of human protein fragments. *Molecular & cellular proteomics : MCP*, 12(9), pp.2657–72.

Baker, H.F. et al., 1994. Induction of beta (A4)-amyloid in priomates by injection of Alzheimer's disease brain homogenate. Comparison with transmission of

spongiform encephalopathy. *Molecular Neurobiology*, 8(1), pp.25-39.

Barletta, J.M. et al., 2005. Detection of ultra-low levels of pathologic prion protein in scrapie infected hamster brain homogenates using real-time immuno-PCR. *Journal of Virological Methods*, 127(2), pp.154–164.

Barnard, G. et al., 2007. Direct detection of disease associated prions in brain and lymphoid tissue using antibodies recognizing the extreme N terminus of PrPC. *Prion*, 1(2), pp.121–7.

Barnard, G. et al., 2000. The measurement of prion protein in bovine brain tissue using differential extraction and DELFIA as a diagnostic test for BSE. *Luminescence : the journal of biological and chemical luminescence*, 15(6), pp.357–62.

Baron, T.G.M. et al., 2000. Comparison of French natural scrapie isolates with bovine spongiform encephalopathy and experimental scrapie infected sheep. *Neuroscience Letters*, 284(3), pp.175–178.

Barret, A. et al., 2003. Evaluation of quinacrine treatment for prion diseases. *Journal of virology*, 77(15), pp.8462–8469.

Barry, D.N. et al., 1986. A microplate enzyme-linked immunosorbent assay for measuring antibody to *anaplasma marginale* in cattle serum. *Australian Veterinary Journal*, Volume 64, pp.76-79.

Bartos, A. et al., 2012. Patients with Alzheimer disease have elevated intrathecal synthesis of antibodies against tau protein and heavy neurofilament. *Journal of Neuroimmunology*, 252(1–2), pp.100–105.

Bartz, J.C. et al., 2007. Prion interference is due to a reduction in strain-specific PrP^{Sc} levels. *Journal of virology*, 81(2), pp.689–697.

Baskakov, I. V, 2014. The many shades of prion strain adaptation. *Prion*, 8(2), pp.169–172.

Bateman, D.A. & Wickner, R.B., 2013. The [PSI+] Prion Exists as a Dynamic Cloud of Variants. *PLoS Genetics*, 9(1), pp.1–13.

Baylis, M. et al., 2004. Risk of scrapie in British sheep of different prion protein genotype. *Journal of General Virology*, 85(9), pp.2735–2740.

Bellon, A. et al., 2003. Improved conformation-dependent immunoassay: Suitability for human prion detection with enhanced sensitivity. *Journal of General Virology*, 84(7), pp.1921–1925.

Bellon, A., 2003. Improved conformation-dependent immunoassay: suitability for human prion detection with enhanced sensitivity. *Journal of General Virology*, 84(7), pp.1921–1925.

Benestad, S.L. et al., 2008. Atypical/Nor98 scrapie: Properties of the agent, genetics, and epidemiology. *Veterinary Research*, 39(4), pp.1–14.

Benestad, S.L. et al., 2003. Cases of scrapie with unusual features in Norway and designation of a new type, Nor98. *The Veterinary record*, 153(7), pp.202–208.

Benestad, S.L. et al., 2016. First case of chronic wasting disease in Europe in a Norwegian free-ranging reindeer. *Veterinary Research*, 47(1), pp.1–7.

Beringue, V. & Andreoletti, O., 2014. Classical and atypical TSE in small ruminants. *Animal Frontiers*, 4(1), pp.33–43.

Berry, D.B. et al., 2013. Drug resistance confounding prion therapeutics. *Proceedings of the National Academy of Sciences of the United States of America*, 110(44), pp.E4160-9.

Berry, D.B. et al., 2015. Use of a 2-aminothiazole to Treat Chronic Wasting Disease in Transgenic Mice. *Journal of Infectious Diseases*, 212(S1), S17-25.

Bian, J., Kang, H.-E. & Telling, G.C., 2014. Quinacrine promotes replication and conformational mutation of chronic wasting disease prions. *Proceedings of the National Academy of Sciences of the United States of America*, 111(16), pp.6028–33.

Bone, I. et al., 2008. Intraventricular pentosan polysulphate in human prion diseases: An observational study in the UK. *European Journal of Neurology*, 15(5), pp.458–464.

Bossers, a et al., 1996. PrP genotype contributes to determining survival times of sheep with natural scrapie. *The Journal of General Virology*, 77 (Pt 10, pp.2669–73.

Bougard, D. et al., 2016. Detection of prions in the plasma of presymptomatic and symptomatic patients with variant Creutzfeldt-Jakob disease. *Science Translational Medicine*, 8(370), pp.370ra182.

Bousset, L. et al., 2013. Structural and functional characterization of two alpha-synuclein strains. *Nature communications*, 4, p.2575.

Bradford, B.M. & Mabbott, N.A., 2012. Prion disease and the innate immune system. *Viruses*, 4(12), pp.3389–3419.

Brammer, L.A. et al., 2008. A target-unrelated peptide in an M13 phage display library traced to an advantageous mutation in the gene II ribosome-binding site. *Analytical Biochemistry*, 373(1), pp.88–98.

Brinton, L.T. et al., 2016. PHASTpep: Analysis Software for Discovery of Cell-Selective Peptides via Phage Display and Next-Generation Sequencing. *PLoS ONE*, 11(5), pp.1–22.

Brown, P. et al., 2012. Iatrogenic creutzfeldt-Jakob disease, final assessment. *Emerging Infectious Diseases*, 18(6), pp.901–907.

Bruce, M.E., 2003. TSE strain variation. *British Medical Bulletin*, 66, pp.99–108.

Budka, H. & Will, R.G., 2015. The end of the BSE saga: Do we still need surveillance for human prion diseases? *Swiss Medical Weekly*, 145, pp.1–8.

Büeler, H. et al. 1992. Normal development and behavious of mice lacking the neuronal cell-surface PrP protein. *Nature*, 356, pp. 577-582.

Büeler, H. et al., 1993. Mice devoid of PrP are resistant to scrapie. *Cell*, 73(7), pp.1339–1347.

Canadian Food Inspection Agency.

Campbell, L. et al., 2013. The PrPC C1 fragment derived from the ovine A136R154R171 PRNP allele is highly abundant in sheep brain and inhibits fibrillisation of full-length PrPC protein in vitro. *Biochimica et Biophysica Acta - Molecular Basis of Disease*, 1832(6), pp.826–836.

Cardinale, A. & Biocca, S., 2008. The potential of intracellular antibodies for therapeutic targeting of protein-misfolding diseases. *Trends in Molecular Medicine*, 14(9), pp.373–380.

Castilla, J., Morales, R., et al., 2008. Cell-free propagation of prion strains. *The EMBO journal*, 27(19), pp.2557–66.

Castilla, J. et al., 2008. Crossing the species barrier by PrP(Sc) replication in vitro generates unique infectious prions. *Cell*, 134(5), pp.757–68.

Castilla, J. et al., 2005. In vitro generation of infectious scrapie prions. *Cell*, 121(2), pp.195–206.

Caughey, B. et al., 1991. Secondary structure analysis od the scrapie-associated protein PrP 27-30 in water by infrared spectroscopy. *Biochemistry*, 30(31), pp.7672-80.

Caughey, B., 2001. Interactions between prion protein isoforms : the kiss of death ? PrP isoforms : normal versus abnormal. *TRENDS in Biochemical Sciences*, 26(4), pp.235–242.

Caughey, B., 2003. Probing for prions: recognizing misfolded PrP. *Nature medicine*, 9(7), pp.819–20.

Centres for Disease Control and Prevention.

Chabry, J. et al., 1999. Species-Independent Inhibition of Abnormal Prion Protein (PrP) Formation by a Peptide Containing a Conserved PrP Sequence Species-Independent Inhibition of Abnormal Prion Protein (PrP) Formation by a Peptide Containing a Conserved PrP Sequence. *Journal of Virology*, 73(8), pp.6245-6250.

Chabry, J., Caughey, B. & Chesebro, B., 1998. Specific inhibition of in vitro formation of protease-resistant prion protein by synthetic peptides. *J Biol Chem*, 273(21), pp.13203–13207.

Chan, C.E.Z. et al., 2014. The role of phage display in therapeutic antibody

discovery. *International immunology*, 26(12), pp.649–657.

Chang, B. et al., 2007. Test for detection of disease-associated prion aggregate in the blood of infected but asymptomatic animals. *Clinical and Vaccine Immunology*, 14(1), pp.36–43.

Cheadle, C. et al., 2003. Analysis of microarray data using Z score transformation. *The Journal of molecular diagnostics : JMD*, 5(2), pp.73–81.

Chen, R. & Snyder, M., 2010. Yeast Proteomics and Protein Microarrays. *Journal of Proteomics*, 73(11), pp.2147-2157.

Chi, E.Y. et al., 2008. Lipid membrane templates the ordering and induces the fibrillogenesis of Alzheimer's disease amyloid-β peptide. *Proteins: Structure, Function and Genetics*, 72(1), pp.1–24.

Cho-Chung, Y.S., 2006. Autoantibody biomarkers in the detection of cancer. *Biochimica et Biophysica Acta - Molecular Basis of Disease*, 1762(6), pp.587–591.

Christiansen, A. et al., 2015. High-throughput sequencing enhanced phage display enables the identification of patient- specific epitope motifs in serum. *Scientific Reports*, 5:12913, pp.1–13.

Clewley, J.P. et al., 2009. Prevalence of disease related prion protein in anonymous tonsil specimens in Britain: cross sectional opportunistic survey. *BMJ (Clinical research ed.)*, 338, p.1442.

Cobb, N.J. et al., 2007. Molecular architecture of human prion protein amyloid: a parallel, in-register beta-structure. *Proc Natl Acad Sci U S A*, 104(48), pp.18946–18951.

Colby, D.W. & Prusiner, S.B., 2011. Prions. *Cold Spring Harbor Perspectives in Biology*, pp.1–22.

Collinge, J. et al., 2006. Kuru in the 21st century-an acquired human prion disease with very long incubation periods. *Lancet*, 367(9528), pp.2068–2074.

Collinge, J. et al., 1994. Prion protein is necessary for normal synaptic function. *Nature*, 370(6487), pp.295–297.

Collinge, J. et al., 2009. Safety and efficacy of quinacrine in human prion disease (PRION-1 study): a patient-preference trial. *The Lancet Neurology*, 8(4), pp.334–344.

Comander, J. et al., 2004. Improving the statistical detection of regulated genes from microarray data using intensity-based variance estimation. *BMC genomics*, 5(1), p.17.

Come, J.H., Fraser, P.E. & Lansbury, P.T., 1993. A kinetic model for amyloid formation in the prion diseases: importance of seeding. *Proceedings of the National Academy of Sciences*, 90(13), pp.5959–5963.

Comoy, E.E. et al., 2015. Transmission of scrapie prions to primate after an extended silent incubation period. *Scientific reports*, 5, p.11573.

Concha-Marambio, L. et al., 2016. Detection of prions in blood from patients with varient Creutzfelt-Jakob disease. *Science Translational Medicine*, 8(370), pp. 370ra183.

Cortese, I., 1996. Identification of peptides specific for cerebrospinal fluid antibodies in multiple sclerosis by using phage libraries. *Proceedings of the National Academy of Sciences of the United States of America,* 93, pp.11063–11067.

Cramm, M. et al., 2014. Characteristic CSF Prion Seeding Efficiency in Humans with Prion Diseases. *Molecular Neurobiology*, 51(1), pp.396–405.

D'Angelo, S. et al., 2014. From deep sequencing to actual clones. *Protein Engineering Design and Selection*, 27(10), pp.301–307.

Dabaghian, R.H. et al., 2006. An immunoassay for the pathological form of the prion protein based on denaturation and time resolved fluorometry. *Journal of Virological Methods*, 132(1–2), pp.85–91.

Dassanayake, R.P. et al., 2016. Sensitive and specific detection of classical scrapie prions in the brains of goats by real-time quaking-induced conversion. *Journal of General Virology*, 97(3), pp.803–812.

Deleault, N.R. et al., 2012. Cofactor molecules maintain infectious conformation and restrict strain properties in puri fi ed prions. *PNAS*, 109(28), E1938-E1946.

Deleault, N.R. et al., 2007. Formation of native prions from minimal components in vitro. *Proceedings of the National Academy of Sciences of the United States of America*, 104(23), pp.9741–6.

DeMarco, M.L. & Daggett, V., 2004. From conversion to aggregation: protofibril formation of the prion protein. *Proceedings of the National Academy of Sciences of the United States of America*, 101(8), pp.2293–2298.

DeMarshall, C.A. et al., 2016. Detection of Alzheimer's disease at mild cognitive impairment and disease progression using autoantibodies as blood-based biomarkers. *Alzheimer's and Dementia: Diagnosis, Assessment and Disease Monitoring*, 3, pp.51–62.

Derda, R. et al., 2011. Diversity of phage-displayed libraries of peptides during panning and amplification. *Molecules*, 16(2), pp.1776–1803.

Diack, A.B. et al., 2014. Variant CJD: 18 years of research and surveillance. *Prion*, 8(3), pp.0–1.

Dias-Neto, E. et al., 2009. Next-generation phage display: Integrating and comparing available molecular tools to enable costeffective high-throughput

analysis. *PLoS ONE*, 4(12).

Diaz-Espinoza, R. & Soto, C., 2012. High-resolution structure of infectious prion protein: the final frontier. *Nature structural & molecular biology*, 19(4), pp.370–7.

Díez, P. et al., 2015. High-throughgput phage-display screening in array format. *Enzyme and Microbial Technology*, 79–80, pp.34–41.

Dikiy, I. & Eliezer, D., 2012. Folding and misfolding of alpha-synuclein on membranes. *Biochimica et Biophysica Acta - Biomembranes*, 1818(4), pp.1013–1018.

Doh-ura, K. et al., 2004. Treatment of Transmissible Spongiform Encephalopathy by Intraventricular Drug Infusion in Animal Models. *Journal of Virology*, 78(10), pp.4999–5006.

Edgeworth, J.A. et al., 2011. Detection of prion infection in variant Creutzfeldt-Jakob disease: a blood-based assay. *Lancet*, 377(9764), pp.487–93.

Edgeworth, J.A. et al., 2010. Spontaneous generation of mammalian prions. *Proceedings of the National Academy of Sciences of the United States of America*, 107(32), pp.14402–14406.

Enari, M., Flechsig, E. & Weissmann, C., 2001. Scrapie prion protein accumulation by scrapie-infected neuroblastoma cells abrogated by exposure to a prion protein antibody. *Proceedings of the National Academy of Sciences of the United States of America*, 98(16), pp.9295–9299.

Faburay, B. et al., 2014. In vitro amplification of scrapie and chronic wasting disease PrP(res) using baculovirus-expressed recombinant PrP as substrate. *Prion*, 8(6), pp.393–403.

Fairfoul, G. et al., 2016. Alpha-synuclein RT-QuIC in the CSF of patients with alpha-synucleinopathies. *Annals of clinical and translational neurology*, 3(10), pp.812–818.

Feliciano, N.D., et al., 2014. Bacteriophage-Fused Peptides for Serodiagnosis of Human Strongyloidiasis. *PLoS Neglected Tropical Diseases*, 8(5), p.e2792.

Féraudet, C. et al., 2005. Screening of 145 anti-PrP monoclonal antibodies for their capacity to inhibit PrPSc replication in infected cells. *Journal of Biological Chemistry*, 280(12), pp.11247–11258.

Ferreira, N.C. et al., 2014. Anti-prion activity of a panel of aromatic chemical compounds: In Vitro and In Silico approaches. *PLoS ONE*, 9(1), pp.1–11.

Flego, M. et al., 2007. Generation of human scFvs antibodies recognizing a prion protein epitope expressed on the surface of human lymphoblastoid cells. *BMC biotechnology*, 7, p.38.

Florent-Béchard, S. et al., 2009. The essential role of lipids in Alzheimer's disease.

Biochimie, 91(6), pp.804–809.

Fluharty, B.R. et al., 2013. An N-terminal fragment of the prion protein binds to amyloid-β oligomers and inhibits their neurotoxicity in vivo. *Journal of Biological Chemistry*, 288(11), pp.7857–7866.

Forloni, G. et al., 2015. Preventive study in subjects at risk of fatal familial insomnia: Innovative approach to rare diseases. *Prion*, 9(2), pp.75–79.

Forloni, G. et al., 2002. Tetracyclines affect prion infectivity. *Proceedings of the National Academy of Sciences of the United States of America*, 99(16), pp.10849–54.

De Franceschi, G. et al., 2011. Structural and morphological characterization of aggregated species of α-synuclein induced by docosahexaenoic acid. *Journal of Biological Chemistry*, 286(25), pp.22262–22274.

Freir, D.B. et al., 2011. Interaction between prion protein and toxic amyloid β assemblies can be therapeutically targeted at multiple sites. *Nature communications*, 2, p.336.

Freudenberg, J.A. et al., 2008. Non-invasive, ultra-sensitive, high-throughput assays to quantify rare biomarkers in the blood. *Methods*, 46(1), pp.33-38.

Friedhoff, P. et al., 2000. Structure of tau protein and assembly into paired helical filaments. *Biochimica et biophysica acta*, 1502(1), pp.122–132.

Frosh, A. et al., 2004. Analysis of 2000 consecutive UK tonsillectomy specimens for disease-related prion protein. *Lancet*, 364(9441), pp.1260–1262.

Fujihara, A. et al., 2009. Hyperefficient PrPSc amplification of mouse-adapted BSE and scrapie strain by protein misfolding cyclic amplification technique. *FEBS Journal*, 276(10), pp.2841–2848.

Gambetti, P. et al., 2008. A Novel Human Disease with Abnormal Prion Protein Sensitive to Protease. *Annals of Neurology*, 63(6), pp.697-708.

Garza, M.C. et al., 2014. Distribution of peripheral PrPScin sheep with naturally acquired scrapie. *PLoS ONE*, 9(5).

Geoghegan, J.C. et al., 2009. Trans-dominant inhibition of prion propagation in vitro is not mediated by an accessory cofactor. *PLoS Pathogens*, 5(7).

Georgsson, G., Sigurdarson, S. & Brown, P., 2006. Infectious agent of sheep scrapie may persist in the environment for at least 16 years. *Journal of General Virology*, 87(12), pp.3737–3740.

Gerber, R. et al., 2007. Oligomerization of the human prion protein proceeds via a molten globule intermediate. *Journal of Biological Chemistry*, 282(9), pp.6300–6307.

Geschwind, M.D. et al., 2013. Quinacrine treatment trial for sporadic creutzfeldt-Jakob disease. *Neurology*, 81(23), pp.2015–2023.

Ghaemmaghami, S. et al., 2009. Continuous quinacrine treatment results in the formation of drug-resistant prions. *PLoS Pathogens*, 5(11).

Ghoshal, S. et al., 2016. Phage display for identification of serum biomarkers of traumatic brain injury. *Journal of Neuroscience Methods*, 272, pp.33–37.

Gilch, S. et al., 2003. Polyclonal anti-PrP auto-antibodies induced with dimeric PrP interfere efficiently with PrP^{Sc} propagation in prion-infected cells. *Journal of Biological Chemistry*, 278(20), pp.18524–18531.

Gilch, S. & Schätzl, H.M., 2009. Aptamers against prion proteins and prions. *Cellular and Molecular Life Sciences*, 66(15), pp.2445–2455.

Giles, K. et al., 2011. Human prion strain selection in transgenic mice. *Annals of Neurology*, 68(2), pp.151–161.

Gill, O.N. et al., 2013. Prevalent abnormal prion protein in human appendixes after bovine spongiform encephalopathy epizootic: large scale survey. *British Medical Journal*, 347, p.f5675.

Gnanasekar, M. et al., 2004. Novel phage display-based subtractive screening to identify vaccine candidates of Brugia malayi. *Infection and Immunity*, 72(8), pp.4707–4715.

Gonzalez-Montalban, N. et al., 2011. Highly efficient protein misfolding cyclic amplification. *PLoS Pathogens*, 7(2).

Gonzalez-Montalban, N. et al., 2013. Changes in prion replication environment cause prion strain mutation. *FASEB Journal*, 27(9), pp.3702–3710.

Gough, K.C., Bishop, K. & Maddison, B.C., 2014. Highly sensitive detection of small ruminant bovine spongiform encephalopathy within transmissible spongiform encephalopathy mixes by serial protein misfolding cyclic amplification. *Journal of Clinical Microbiology*, 52(11), pp.3863–3868.

Gough, K.C. et al., 2015. Methods for Differentiating Prion Types in Food-Producing Animals. *Biology*, 4(4), pp.785–813.

Gough, K.C. et al., 2009. In vitro amplification of prions from milk in the detection of subclinical infections. *Prion*, 3(4), pp.236–239.

Gough, K.C. et al., 2012. The Oral Secretion of Infectious Scrapie Prions Occurs in Preclinical Sheep with a Range of *PRNP* Genotypes. *Journal of Virology*, 86(1), pp.566–571.

Gough, K.C., Bishop, K. & Maddison, B.C., 2014. Highly sensitive detection of small ruminant bovine spongiform encephalopathy within transmissible spongiform encephalopathy mixes by serial protein misfolding cyclic amplification. *Journal of Clinical Microbiology*, 52(11), pp.3863–3868.

Gough, K.C. & Maddison, B.C., 2010. Prion transmission. *Prion*, 4(4), pp.275–282.

Govaerts, C. et al., 2004. Evidence for assembly of prions with left-handed beta-

helices into trimers. *Proceedings of the National Academy of Sciences of the United States of America*, 101(22), pp.8342–8347.

Govarts, C. et al., 2007. Exploring cDNA phage display for autoantibody profiling in the serum of multiple sclerosis patients: Optimization of the selection procedure. *Annals of the New York Academy of Sciences*, 1109, pp.372–384.

Grassi, J. et al., 2008. Progress and limits of TSE diagnostic tools. *Veterinary Research*, 39(4).

Groschup, M.H. et al., 2007. Classic scrapie in sheep with the ARR/ARR prion genotype in Germany and France. *Emerging Infectious Diseases*, 13(8), pp.1201–1207.

Groveman, B.R. et al., 2014. Parallel in-register intermolecular β-sheet architectures for prion-seeded prion protein (PrP) amyloids. *Journal of Biological Chemistry*, 289(35), pp.24129–24142.

Haïk, S. et al., 2014. Doxycycline in Creutzfeldt-Jakob disease: A phase 2, randomised, double-blind, placebo-controlled trial. *The Lancet Neurology*, 13(2), pp.150–158.

Hadlow, W.J., Kennedy, R.C. & Race, R.E., 1982. Natural infection of Suffolk sheep with scrapie virus. *The Journal of infectious diseases*, 146(5), pp.657–64.

Haley, N.J. et al., 2016. Antemortem detection of chronic wasting disease prions in nasal brush collections and rectal biopsy specimens from white-tailed deer by real-time quaking-induced conversion. *Journal of Clinical Microbiology*, 54(4), pp.1108–1116.

Hall, V. et al., 2014. Managing the risk of iatrogenic transmission of Creutzfeldt-Jakob disease in the UK. *Journal of Hospital Infection*, 88(1), pp.22–27.

Han, M. et al., 2012. Diagnosis of parkinson's disease based on disease-specific autoantibody profiles in human sera. *PLoS ONE*, 7(2).

Hawkins, S. a C. et al., 2014. Persistence of ovine scrapie infectivity in a farm environment following cleaning and decontamination. *The Veterinary record*, pp.1–5.

He, B. et al., 2016. BDB: Biopanning data bank. *Nucleic Acids Research*, 44(D1), pp.D1127–D1132.

He, X. & Patfield, S.A., 2015. Immuno-PCR Assay for Sensitive Detection of Proteins in Real Time. *ELISA: Methods and Protocols, Methods in Molecular Biology*, 1318(c), pp.139–148.

Heilbronner, G. et al., 2013. Seeded strain-like transmission of β-amyloid morphotypes in APP transgenic mice. *EMBO reports*, 14(11), pp.1017–22.

Heinzel, S. et al., 2014. Naturally occurring alpha-synuclein autoantibodies in Parkinson's disease: Sources of variance in biomarker assays. *PLoS ONE*,

9(12), pp.1–16.

Herva, M.E. et al., 2014. Anti-amyloid Compounds Inhibit α-Synuclein Aggregation Induced by Protein Misfolding Cyclic Amplification (PMCA). *Journal of Biological Chemistry*, 289(17), pp.11897–11905.

Hill, A. et al., 1997. The same prion strain causes vCJD and BSE. *Nature*, 389(6650), pp.448–450, 526.

Hill, A.F. et al., 1998. Molecular screening of sheep for bovine spongiform encephalopathy. *Neurosci Lett*, 255(3), pp.159–162.

Hill, A.F. et al., 1999. Investigation of variant Creutzfeldt-Jakob disease and other huan prion diseases with tonsil biopsy samples. *The Lancet*, 353(9148), pp.183-189.

Hilton, D.A. et al., 2004. Prevalence of lymphoreticular prion protein accumulation in UK tissue samples. *Journal of Pathology*, 203(3), pp.733–739.

Hizume, M. et al., 2009. Human prion protein (PrP) 219K is converted to PrPSc but shows heterozygous inhibition in variant Creutzfeldt-Jakob disease infection. *Journal of Biological Chemistry*, 284(6), pp.3603–3609.

Honda, R.P. & Kuwata, K., 2017. The native state of prion protein (PrP) directly inhibits formation of PrP-amyloid fibrils in vitro. *Scientific reports*, 7(1), p.562.

Horiuchi, M. et al., 2000. Interactions between heterologous forms of prion protein: Binding, inhibition of conversion, and species barriers. *Proceedings of the National Academy of Sciences*, 97(11), pp.5836–5841.

Hosszu, L.L.P. et al., 2005. Definable equilibrium states in the folding of human prion protein. *Biochemistry*, 44(50), pp.16649–16657.

Houston, F. et al., 2015. Comparative susceptibility of sheep of different origins, breeds and PRNP genotypes to challenge with bovine spongiform encephalopathy and scrapie. *PLoS ONE*, 10(11), pp.1–17.

Huang, J., Ru, B. & Dai, P., 2011. Bioinformatics resources and tools for phage display. *Molecules*, 16(1), pp.694–709.

Hunter, N., 1997. PrP genetics in sheep and the implications for scrapie and BSE. *Trends in Microbiology*, 5(8), pp.331–334.

Hwang, S., Greenlee, J.J. & Nicholson, E.M., 2017. Use of bovine recombinant prion protein and real-time quaking-induced conversion to detect cattle transmissible mink encephalopathy prions and discriminate classical and atypical L- and H-Type bovine spongiform encephalopathy. *PLoS ONE*, 12(2), pp.1–14.

Imamura, M. et al., 2016. Heparan sulfate and heparin promote faithful prion replication in vitro by binding to normal and abnormal prion proteins in protein

misfolding cyclic amplification. *Journal of Biological Chemistry*, 291(51), pp.26478–26486.

Ironside, J.W., 2012. Variant Creuzfelt-Jakob disease: an update. *Folia Neuropathology*, 50(1), pp.50-56.

Jackson, G.S. et al., 2014. Population screening for variant Creutzfeldt-Jakob disease using a novel blood test: diagnostic accuracy and feasibility study. *JAMA neurology*, 71(4), pp.421–8.

Jaluria, P. et al., 2007. A perspective on microarrays: current applications, pitfalls, and potential uses. *Microbial cell factories*, 6, p.4.

Jaunmuktane, Z. et al., 2015. Evidence for human transmission of amyloid-β pathology and cerebral amyloid angiopathy. *Nature*, 525(7568), pp.247–50.

Jenkins, D.C., Sylvester, I.D. & Pinheiro, T.J.T., 2008. The elusive intermediate on the folding pathway of the prion protein. *FEBS Journal*, 275(6), pp.1323–1335.

Joiner, S. et al., 2002. Irregular presence of abnormal prion protein in appendix in variant Creutzfeldt-Jakob disease. *Journal of Neurology, Neurosurgery, and Psychiatry*, 73, pp.597-603.

Jucker, M. & Walker, L.C., 2013. Self-propagation of pathogenic protein aggregates in neurodegenerative diseases. *Nature*, 501(7465), pp.45–51.

Kaneko, K. et al., 1997. Evidence for protein X binding to a discontinuous epitope on the cellular prion protein during scrapie prion propagation. *Proceedings of the National Academy of Sciences of the United States of America*, 94(19), pp.10069–10074.

van Keulen, L.J.M., Vromans, M.E.W. & van Zijderveld, F.G., 2002. Early and late pathogenesis of natural scrapie infection in sheep. *APMIS : acta pathologica, microbiologica, et immunologica Scandinavica*, 110(1), pp.23–32.

Khan, A.H. & Sadroddiny, E., 2016. Application of immuno-PCR for the detection of early stage cancer. *Molecular and Cellular Probes*, 30(2), pp.106–112.

Kim, J. Il et al., 2010. Mammalian prions generated from bacterially expressed prion protein in the absence of any mammalian cofactors. *Journal of Biological Chemistry*, 285(19), pp.14083–14087.

Kittelberger, R. et al., 2010. Atypical scrapie/Nor98 in a sheep from New Zealand. *J Vet Diagn Invest*, 22(6), pp.863–875.

Klyubin, I. et al., 2014. Peripheral administration of a humanized anti-PrP antibody blocks Alzheimer's disease Abeta synaptotoxicity. *J Neurosci*, 34(18), pp.6140–6145.

Kobayashi, A. et al., 2009. Heterozygous inhibition in prion infection: the stone fence model. *Prion*, 3(1), pp.27–30.

Kobayashi, A. et al., 2015. The influence of PRNP polymorphisms on human prion disease susceptibility: an update. *Acta Neuropathologica*, 130(2), pp.159–170.

Kocisko, D.A. et al., 2004. Evaluation of new cell culture inhibitors of protease-resistant prion protein against scrapie infection in mice. *Journal of General Virology*, 85(8), pp.2479–2483.

Kocisko, D.A. et al., 2003. New inhibitors of scrapie-associated prion protein formation in a library of 2000 drugs and natural products. *Journal of virology*, 77(19), pp.10288–94.

Koide, A. et al., 2009. Accelerating phage-display library selection by reversible and site-specific biotinylation. *Protein Engineering, Design and Selection*, 22(11), pp.685–690.

Kolb, G. & Boiziau, C., 2005. Selection by phage display of peptides targeting the HIV-1 TAR element. *RNA biology*, 2(1), pp.28–33.

Kong, Q. et al., 2013. Thermodynamic stabilization of the folded domain of prion protein inhibits prion infection in vivo. *Cell Reports*, 4(2), pp.248–254.

Korth, C. et al., 1997. Prion (PrPSc)-specific epitope defined by a monoclonal antibody. *Nature*, 390(6655), pp.74–77.

Kramer, M.L. & Bartz, J.C., 2009. Rapid, high-throughput detection of PrPSc by 96-well immunoassay. *Prion*, 3(1), pp.44–8.

Kübler, E., Oesch, B. & Raeber, A.J., 2003. Diagnosis of prion diseases. *British Medical Bulletin*, 66, pp.267–279.

Kurt, T.D. & Sigurdson, C.J., 2016. Cross-species transmission of CWD prions. *Prion*, 10(83), pp.83-91.

Lacroux, C. et al., 2014. Preclinical Detection of Variant CJD and BSE Prions in Blood. *PLoS Pathogens*, 10(6), 1-10.

Lau, A.L. et al., 2007. Characterization of prion protein (PrP)-derived peptides that discriminate full-length PrP Sc from PrP C. *Proceedings of the National Academy of Sciences*, 104(28), pp.11551–11556.

Lee, C.I. et al., 2007. The dominant-negative effect of the Q218K variant of the prion protein does not require protein X. *Protein science : a publication of the Protein Society*, 16(2166), pp.2166–2173.

Lee, J. et al., 2013. Prion Diseases as Transmissible Zoonotic Diseases. *Osong Public Health and Research Perspectives*, 4(1), pp.57–66.

Lewis, P. a et al., 2006. Removal of the glycosylphosphatidylinositol anchor from PrP(Sc) by cathepsin D does not reduce prion infectivity. *The Biochemical journal*, 395, pp.443–448.

Li, A. et al., 2000. Physiological Expression of the Gene for PrP-Like Protein,

PrPLP/Dpl, by Brain Endothelial Cells and its Ectopic Expression in Neurons of PrP-Deficient Mice Ataxic Due to Purkinje Cell Degeneration. *The American Journal of Pathology*, 157(5), pp.1447–1452.

Li, J. et al., 2010. Darwinian Evolution of Prions in Cell Culture. Science, 327, pp.869–873.

Liu, G.W. et al., 2015. Efficient Identification of Murine M2 Macrophage Peptide Targeting Ligands by Phage Display and Next-Generation Sequencing. *Bioconjugate Chemistry*, 26(8), pp.1811–1817.

Lo, R.Y.Y. et al., 2007. New molecular insights into cellular survival and stress responses: Neuroprotective role of cellular prion protein (PrPC). *Molecular Neurobiology*, 35(3), pp.236–244.

Lomakin, A. et al., 1996. On the nucleation and growth of amyloid beta-protein fibrils: detection of nuclei and quantitation of rate constants. *Proceedings of the National Academy of Sciences of the United States of America*, 93(3), pp.1125–1129.

De Luigi, A. et al., 2008. The efficacy of tetracyclines in peripheral and intracerebral prion infection. *PLoS ONE*, 3(3).

Lukan, A., Vranac, T. & Čurin Šerbec, V., 2013. TSE diagnostics: Recent advances in immunoassaying prions. *Clinical and Developmental Immunology*, 2013.

Ma, J., 2012. The role of cofactors in Prion propagation and infectivity. *PLoS Pathogens*, 8(4), pp.8–10.

Mackay, G. et al., 2012. NMDA receptor autoantibodies in sporadic Creutzfeldt-Jakob disease. *Journal of Neurology*, 259(9), pp.1979–1981.

Maddison, B.C. et al., 2015. Incubation of ovine scrapie with environmental matrix results in biological and biochemical changes of PrP^{Sc} over time. *Veterinary Research,* 46(46), pp. 1-6.

Maddison, B.C. et al., 2009. Prions are secreted in milk from clinically normal scrapie-exposed sheep. *Journal of virology*, 83(16), pp.8293–8296.

Maddison, B.C. et al., 2010. Prions are secreted into the oral cavity in sheep with preclinical scrapie. *The Journal of infectious diseases*, 201(11), pp.1672–1676.

Maddison, B.C., Whitelam, G.C. & Gough, K.C., 2007. Cellular prion protein in ovine milk. *Biochemical and Biophysical Research Communications*, 353(1), pp.195–199.

Maftei, M. et al., 2012. Antigen-Bound and Free??-Amyloid Autoantibodies in Serum of Healthy Adults. *PLoS ONE*, 7(9), pp.3–10.

Makarava, N. et al., 2016. New molecular insight into mechanism of evolution of mammalian synthetic prions. *American Journal of Pathology*, 186(4),

pp.1006–1014.

Makarava, N. & Baskakov, I. V., 2012. Genesis of tramsmissible protein states via deformed templating. *Prion*, 6(3), pp.252–255.

Makarava, N., Savtchenko, R. & Baskakov, I. V., 2013. Selective amplification of classical and atypical prions using modified protein misfolding cyclic amplification. *Journal of Biological Chemistry*, 288(1), pp.33–41.

Makarava, N. & Baskakov, I. V., 2013. The Evolution of Transmissible Prions: The Role of Deformed Templating. *PLoS Pathogens*, 9(12), pp.1–3.

Mandelkow, E.-M.M. and E., 2012. Biochemistry and cell biology of tau protein in neurofibrillart degeneration. *Cold Spring Harb Perspect Med*, 2(5), p.a006247.

Manson, J.C. et al., 1994. 129/Ola mice carrying a null mutation in PrP that abolishes mRNA production are developmentally normal. *Molecular Neurobiology*, 8(2-3), pp. 121-127.

De Marco, M.F. et al., 2010. Large-scale immunohistochemical examination for lymphoreticular prion protein in tonsil specimens collected in Britain. *Journal of Pathology*, 222(4), pp.380–387.

Masel, J., Genoud, N. & Aguzzi, A., 2005. Efficient inhibition of prion replication by PrP-Fc 2 suggests that the prion is a PrP Sc oligomer. *Journal of Molecular Biology*, 345(5), pp.1243–1251.

Masujin, K. et al., 2016. Detection of Atypical H-Type Bovine Spongiform Encephalopathy and Discrimination of Bovine Prion Strains by Real-Time Quaking-Induced Conversion. *Journal of Clinical Microbiology*, 54(3), pp.676–686.

Masujin, K. et al., 2013. The N-terminal sequence of prion protein consists an epitope specific to the abnormal isoform of prion protein (PrP(Sc)). *PloS one*, 8(2), p.e58013.

Matochko, W.L. et al., 2012. Deep sequencing analysis of phage libraries using Illumina platform. *Methods*, 58(1), pp.47–55.

Matochko, W.L. et al., 2014. Prospective identification of parasitic sequences in phage display screens. *Nucleic acids research*, 42(3), pp.1784–98.

Mccarthy, J.M. et al., 2013. Anti-Prion Drug mPPIg5 Inhibits PrP^{C} Conversion to PrP^{Sc}. *PLoS ONE* , 8(1), e55282.

McGuire, L.I. et al., 2012. RT-QuIC analysis of cerebrospinal fluid in sporadic Creutzfeldt-Jakob disease. *Annals of Neurology*, 72(2), pp.278-285.

McGuire, L.I. et al., 2016. Cerebrospinal fluid real-time quaking-induced conversion is a robust and reliable test for sporadic creutzfeldt–jakob disease: An international study. *Annals of Neurology*, 80(1), pp.160–165.

McKie, A. et al., 2002. A quantitative immuno-PCR assay for the detection of mumps-specific IgG. *Journal of Immunological Methods*, 270(1), pp.135–141.

McKinley, M.P., Bolton, D.C. & Prusiner, S.B., 1983. A protease-resistant protein is a structural component of the Scrapie prion. *Cell*, 35(1), pp.57–62.

Mead, S. et al., 2009. A novel protective prion protein variant that colocalizes with kuru exposure. *The New England journal of medicine*, 361(21), pp.2056–2065.

Meier, P. et al., 2003. Soluble dimeric prion protein binds PrPSc in vivo and antagonizes prion disease. *Cell*, 113(1), pp.49–60.

Melchior, M.B. et al., 2010. Eradication of scrapie with selective breeding: are we nearly there? *BMC veterinary research*, 6, p.24.

Meloni, D. et al., 2012. EU-Approved Rapid Tests for Bovine Spongiform Encephalopathy Detect Atypical Forms: A Study for Their Sensitivities. *PLoS ONE*, 7(9), pp.1-8.

Merz, P.A. et al., 1981. Abnormal fibrils from scrapie-infected brain. *Acta neuropathologica*, 54, pp.474-476.

Meyer, V. et al., 2014. Amplification of Tau Fibrils from Minute Quantities of Seeds. *Biochemistry*, 53(36), pp.5804–5809.

Meyerett, C. et al., 2008. In vitro strain adaptation of CWD prions by serial protein misfolding cyclic amplification. *Virology*, 382(2), pp.267–276.

Miller, M.W. & Fischer, J.R., 2016. The First Five (or More) Decades of Chronic Wasting Disease: Lessons for the Five Decades to Come. *Transactions of the North American Wildlife and National Resources Conference,* 81, pp.1–12.

Moda, F. et al., 2014. Prions in the Urine of Patients with Variant Creutzfeldt–Jakob Disease. *New England Journal of Medicine*, 371(6), pp.530–539.

Mok, T. & Jaunmuktane, Z., 2017. Variant Creuztfelt-Jakob Disease in a Patient with Heterozygosity at *PRNP* Codon 129. *The New England Journal of Medicine*, 376(3), pp.292-294.

Molek, P., Strukelj, B. & Bratkovic, T., 2011. Peptide phage display as a tool for drug discovery: Targeting membrane receptors. *Molecules*, 16(1), pp.857–887.

Moore, R.C. et al., 1999. Ataxia in prion protein (PrP)-deficient mice is associated with upregulation of the novel PrP-like protein doppel. *Journal of Molecular Biology*, 292(4), pp.797–817.

Morel, N. et al., 2004. Selective and efficient immunoprecipitation of the disease-associated form of the prion protein can be mediated by nonspecific interactions between monoclonal antibodies and scrapie-associated fibrils.

Journal of Biological Chemistry, 279(29), pp.30143–30149.

Moudjou, M. et al., 2001. Cellular prion protein status in sheep: tissue-specific biochemical signatures. *J. Gen. Virol*, 82(2001), pp.2017–2024.

Moudjou, M., Sibille, P. & Fichet, G., 2014. Highly Infectious Prions Generated by a Single Round of Microplate-. *mBio*, 5(1), pp.1–10.

Müller, W.E.G. et al. 1997. Protection of Flurpirtine on β-Amyloid-Induced Apoptosis in Neuronal Cells In Vitro: Prevention of Amyloid-Induced Glutathione Depletion. *Journal of Neurochemistry*, 68(6), pp.2371-2377.

Murayama, Y. et al., 2016. L-Arginine ethylester enhances in vitro amplification of PrPSc in macaques with atypical L-type bovine spongiform encephalopathy and enables presymptomatic detection of PrPSc in the bodily fluids. *Biochemical and Biophysical Research Communications*, 470(3), pp.563–568.

Nagele, E. et al., 2011. Diagnosis of Alzheimer's disease based on disease-specific autoantibody profiles in human sera. *PLoS ONE*, 6(8), pp.1–7.

Naqid, I.A. et al., 2016. Mapping B-cell responses to Salmonella enterica serovars Typhimurium and Enteritidis in chickens for the discrimination of infected from vaccinated animals. *Scientific reports*, 6, p.31186.

Naqid, I.A, et al., 2016. Mapping polyclonal antibody responses to bacterial infection using next generation phage display. *Scientific reports*, 6(24232), pp.1-11.

Nath, A. et al., 2003. Autoantibodies to amyloid β-peptide (Abeta) are increased in Alzheimer's disease patients and Abeta antibodies can enhance Abeta neurotoxicity: implications for disease pathogenesis and vaccine development. *Neuromolecular Med*, 3(1), pp.29–39.

Necula, M., Chirita, C.N. & Kuret, J., 2003. Rapid Anionic Micelle-mediated α-Synuclein Fibrillization in Vitro. *Journal of Biological Chemistry*, 278(47), pp.46674–46680.

Ng, C.K.Y. et al., 2015. Breast cancer genomics from microarrays to massively parallel sequencing: paradigms and new insights. *Journal of the National Cancer Institute*, 107(5), p.p.1-18.

Ngubane, N.A.C. et al., 2013. High-throughput sequencing enhanced phage display identifies peptides that bind mycobacteria. *PLoS ONE*, 8(11), pp.1-11.

Nicoll, A.J. & Collinge, J., 2009. Preventing prion pathogenicity by targeting the cellular prion protein. *Infectious disorders drug targets*, 9(1), pp.48–57.

Niemeyer, C.M., Adler, M. & Wacker, R., 2007. Detecting antigens by quantitative immuno-PCR. *Nature protocols*, 2(8Niemeyer, C. M., Adler, M., Wacker, R. (2007). Detecting antigens by quantitative immuno–PCR. *Nature Protocols*, 2(8), 1918–1930.

Nikles, D. et al., 2005. Circumventing tolerance to the prion protein (PrP): vaccination with PrP-displaying retrovirus particles induces humoral immune responses against the native form of cellular PrP. *Journal of virology*, 79(7), pp.4033–42.

Nishina, K. a et al., 2006. The Stoichiometry of Host PrP^{C} Glycoforms Modulates the Efficiency of PrP^{Sc} Formation in Vitro. *Biochemistry*, (1), pp.14129–14139.

Nomura, S. et al., 2009. Autoantibody to glial fibrillary acidic protein in the sera of cattle with bovine spongiform encephalopathy. *Proteomics*, 9(16), pp.4029–4035.

Nurmi, M.H. et al., 2003. The normal population distribution of PRNP codon 129 polymorphism. *Acta neurologica Scandinavica*, 108(5), pp.374–8.

O'Connor, M.J. et al., 2017. *In vitro* amplification of H-type atypical bovine spongiform encephalopathy by protein misfolding cyclic amplification. *Prion*, 11(1), pp.54–64.

Orem, N.R. et al., 2006. Copper (II) ions potently inhibit purified PrPres amplification. *Journal of Neurochemistry*, 96(5), pp.1409–1415.

O'Rourke, K.I. et al., 2000. Preclinical diagnosis of scrapie by immunohistochemistry of third eyelid lymphoid tissue. *Journal of Clinical Microbiology*, 38(9), pp.3254–3259.

Orrú, C.D. et al., 2014. A test for Creutzfeldt-Jakob disease using nasal brushings. *The New England journal of medicine*, 371(6), pp.519–29.

Orrú, C.D. et al., 2015. Bank Vole Prion Protein As an Apparently Universal Substrate for RT-QuIC-Based Detection and Discrimination of Prion Strains. *PLoS Pathogens*, 11(6), pp.1–20.

Orrú, C.D. et al., 2016. Factors that improve RT-QuIC detection of prion seeding activity. *Viruses*, 8(5).

Orrú, C.D. et al., 2015. Rapid and Sensitive RT-QuIC Detection of Human Creutzfeldt-Jakob Disease Using Cerebrospinal Fluid. *Folia Neuropathologica*, 6(1), pp.1–7.

Orrú, C.D., Wilham, J.M. & Raymond, L.D., 2011. Prion Disease Blood Test Using Immunoprecipitation and Improved. *mBio*, 2(3), pp.1–9.

Ortiz-Pelaez, a, Thompson, C.E. & Dawson, M., 2014. The impact of the National Scrapie Plan on the PRNP genotype distribution of the British national flock, 2002-2012. *The Veterinary record*, 174(21), p.530.

Osborne, K. et al., 2000. Ten years of serological surveillance in England and Wales: methods, results, implications and action. *International journal of epidemiology*, 29(2), pp.362–8.

Otto, M. et al., 2004. Efficacy of fluirtine on cognitive function in patients with

CJD: A double-blind study. *Neurology*, 62(5), pp.714-718.

Owen, J.P. et al., 2007. Diagnosis of Prion Diseases With Thermolysin Use of Thermolysin in the Diagnosis of Prion Diseases. , 35.

Owen, J.P. et al., 2007. Use of thermolysin in the diagnosis of prion diseases. *Molecular Biotechnology*, 35(2), pp.161–170.

Palmer, M.S. et al., 1991. Homozygous prion protein genotype predisposes to sporadic Creutzfeldt-Jakob disease. *Nature*, 352, pp.340-342.

Pan, K.M. et al. 1993. Conversion of alpha-helices into beta-sheets features in the formation of the scrapie prion proteins. *Proceeedings of the National Academy of Sciences of the United States of America*, 90(23), pp.10962-10966.

Pan, T. et al., 2005. An aggregation-specific enzyme-linked immunosorbent assay: detection of conformational differences between recombinant PrP protein dimers and PrP(Sc) aggregates. *Journal of virology*, 79(19), pp.12355–12364.

Pande, J., Szewczyk, M.M. & Grover, A.K., 2010. Phage display: Concept, innovations, applications and future. *Biotechnology Advances*, 28(6), pp.849–858.

Panegyres, P.K. & Armari, E., 2013. Therapies for human prion diseases. *American journal of neurodegenerative disease*, 2(3), pp.176–86.

Peden, A.H. et al., 2012. Sensitive and specific detection of sporadic Creutzfeldt-Jakob disease brain prion protein using real-time quaking-induced conversion. *The Journal of general virology*, 93(Pt 2), pp.438–49.

Peretz, D., Williamson, R. a, et al., 2001. Antibodies inhibit prion propagation and clear cell cultures of prion infectivity. *Nature*, 412(6848), pp.739–43.

Peretz, D., Scott, M.R., et al., 2001. Strain-specified relative conformational stability of the scrapie prion protein. *Protein science : a publication of the Protein Society*, 10(4), pp.854–863.

Perrier, V. et al., 2000. Mimicking dominant negative inhibition of prion replication through structure-based drug design. *Proceedings of the National Academy of Sciences*, 97(11), pp.6073–6078.

Phizicky, E. et al., 2003. Protein analysis on a proteomic scale. *Nature*, 422(6928), pp.208–215.

Piccardo, P. et al., 1998. An Antibody Raised Against a Conserved Sequence of the Prion Protein Recognizes Pathological Isoforms in Human and Animal Prion Diseases, Including Creutzfeldt-Jakob Disease and Bovine Spongiform Encephalopathy. *American Journal of Pathology*, 152(6), pp.1415–1420.

Pirisinu, L. et al., 2010. A new method for the characterization of strain-specific conformational stability of protease-sensitive and protease-resistant PrPSc.

PLoS ONE, 5(9), pp.1–13.

Pirisinu, L. et al., 2013. Biochemical Characterization of Prion Strains in Bank Voles. *Pathogens*, 2(3), pp.446–456.

Pirisinu, L. et al., 2011. Molecular discrimination of sheep bovine spongiform encephalopathy from scrapie. *Emerging Infectious Diseases*, 17(4), pp.695–698.

Priola, S.A. et al., 1994. Heterologous PrP molecules interfere with accumulation of protease-resistant PrP in scrapie-infected murine neuroblastoma cells. *Journal of virology*, 68(8), pp.4873–8.

Priola, S. A., 1999. Prion protein and species barriers in the transmissible spongiform encephalopathies. *Biomedicine and Pharmacotherapy*, 53(1), pp.27–33.

Prionics® - Check PrioSTRIP, Prionics AG, Schlieren-Zurich, Switzerland.

Properzi, F. & Pocchiari, M., 2013. Identification of misfolded proteins in body fluids for the diagnosis of prion diseases. *International Journal of Cell Biology*, 2013.

Prusiner, S.B., 1982. Novel Proteinaceous Infectious Particles Cause Scrapie. *Science*, 216, pp.136-144.

Prusiner, S.B., 1998. Prions. *Proc. Natl. Acad. Sci*, 11, pp.13363-13383.

Puoti, G. et al., 2012. Sporadic human prion diseases: Molecular insights and diagnosis. *The Lancet Neurology*, 11(7), pp.618–628.

Rahmatpour, S. et al., 2017. Application of immuno-PCR assay for the detection of serum IgE specific to Bermuda allergen. *Molecular and Cellular Probes*, 32, pp.1–4.

Rajaram, K. et al., 2014. Construction of helper plasmid-mediated dual-display phage for autoantibody screening in serum. *Applied Microbiology and Biotechnology*, 98(14), pp.6365–6373.

Ramachandran, N., Srivastava, S. & LaBaer, J., 2008. Applications of protein microarrays for biomarker discovery. *Proteomics - Clinical Applications*, 2(10–11), pp.1444–1459.

Rambold, A.S. et al., 2008. Stress-protective signalling of prion protein is corrupted by scrapie prions. *The EMBO journal*, 27(14), pp.1974–84.

Ran, Y. et al., 2008. Profiling tumor-associated autoantibodies for the detection of colon cancer. *Clinical Cancer Research*, 14(9), pp.2696–2700.

Ravn, U. et al., 2013. Deep sequencing of phage display libraries to support antibody discovery. *Methods*, 60(1), pp.99–110.

Rentero Rebollo, I. et al., 2014. Identification of target-binding peptide motifs by high-throughput sequencing of phage-selected peptides. *Nucleic acids research*, 42(22), p.e169.

Reuter, T. et al., 2009. Prion protein detection via direct immuno-quantitative real-time PCR. *Journal of Microbiological Methods*, 78(3), pp.307–311.

Ricci, A. et al., 2017. Chronic wasting disease (CWD) in cervids. *EFSA Journal*, 15(1).

Riek, R. et al., 1996. NMR structure of the mouse prion protein domain PrP(121-231). *Nature*, 382, pp.180–2.

Rigter, A. et al., 2009. Prion protein self-peptides modulate prion interactions and conversion. *BMC biochemistry*, 10, p.29.

Rigter, A. et al., 2010. Prion protein self-interactions: A gateway to novel therapeutic strategies? *Vaccine*, 28(49), pp.7810–7823.

Rivera-milla, E. et al., 2005. Disparate evolution of prion protein domains and the distinct origin of Doppel- and prion-related loci revealed by fish-to-mammal comparisons. , 19, pp.1–19.

Roettger, Y. et al., 2013. Prion Peptide Uptake in Microglial Cells - The Effect of Naturally Occurring Autoantibodies against Prion Protein. *PLoS ONE*, 8(6).

Roucou, X., 2014. Regulation of PrPC signaling and processing by dimerization. *Frontiers in Cell and Developmental Biology*, 2, pp.1–6.

Rovis, T.L. & Legname, G., 2014. Prion protein-specific antibodies-development, modes of action and therapeutics application. *Viruses*, 6(10), pp.3719–3737.

Ryvkin, A. et al., 2012. Deep panning: Steps towards probing the IgOme. *PLoS ONE*, 7(8), pp.1–11.

Saa, P. et al., 2012. Strain-Specific Role of RNAs in Prion Replication. *Journal of Virology*, 86(19), pp.10494–10504.

Saá, P. & Cervenakova, L., 2015. Protein misfolding cyclic amplification (PMCA): Current status and future directions. *Virus Research*, 207, pp.47–61.

Saborio, G.P., Permanne, B. & Soto, C., 2001. Sensitive detection of pathological prion protein by cyclic amplification of protein misfolding. *Nature*, 411(6839), pp.810–813.

Safar, J. et al. 1993. Conformational transitions, dissociation, and unfolding of scrapie amyloid (prion) protein. *Journal of Biological Chemistry*, 268(27), pp.20276-84.

Safar, J. et al., 1998. Eight prion strains have PrP(Sc) molecules with different conformations. *Nature medicine*, 4(10), pp.1157–1165.

Safar, J.G. et al., 2005. Diagnosis of human prion disease. *Proc Natl Acad Sci U S A*, 102(9), pp.3501–3506.

Safar, J.G. et al., 2002. Measuring prions causing bovine spongiform encephalopathy or chronic wasting disease by immunoassays and transgenic mice. *Nature biotechnology*, 20, pp.1147–1150.

Safar, J.G., 2012. Molecular pathogenesis of sporadic prion diseases in man. *Prion*, 6(2), pp.108–115.

Sanders, D.W. et al., 2014. Distinct tau prion strains propagate in cells and mice and define different tauopathies. *Neuron*, 82(6), pp.1271–88.

Sano, K., Atarashi, R. & Nishida, N., 2015. Structural conservation of prion strain specificities in recombinant prion protein fibrils in real-time quaking-induced conversion. *Prion*, 9(4), pp.237–43.

Satoh, J. et al., 2009. Protein microarray analysis identifies human cellular prion protein interactors. *Neuropathology and Applied Neurobiology*, 35(1), pp.16–35.

Saunders, S.E., Bartelt-Hunt, S.L. & Bartz, J.C., 2012. Occurrence, transmission, and zoonotic potential of chronic wasting disease. *Emerging Infectious Diseases*, 18(3), pp.369–376.

Schmitz, M. et al., 2016. Application of an in vitro-amplification assay as a novel pre-screening test for compounds inhibiting the aggregation of prion protein scrapie. *Scientific Reports*, 6(1), p.28711.

Schmitz, M. et al., 2014. Behavioral abnormalities in prion protein knockout mice and the potential relevance of PrP^{C} for the cytoskeleton. *Prion*, 8(6), pp.381–386.

Scott, M. et al., 1993. Propagation of prions with artificial properties in transgenic mice expressing chimeric PrP genes. *Cell*, 73(5), pp.979–988.

Seelig, D.M., Goodman, P.A. & Skinner, P.J., 2015. Potential Approaches for Heterologous Prion Protein Treatment of Prion Diseases. *Prion*, 10, pp.18-24.

Seuberlich, T. et al., 2007. Atypical scrapie in a Swiss goat and implications for transmissible spongiform encephalopathy surveillance. *Journal of veterinary diagnostic investigation : official publication of the American Association of Veterinary Laboratory Diagnosticians, Inc*, 19(1), pp.2–8.

Schneider, C. a, Rasband, W. S., & Eliceiri, K. W. (2012). NIH Image to ImageJ: 25 years of image analysis. *Nature Methods*, *9*(7), 671–675.

Sigurdsson, E.M. et al., 2002. Immunization Delays the Onset of Prion Disease in Mice. *American Journal of Pathology*, 161(1), pp.13–17.

Silva, C.J. et al., 2015. Proteinase K and the structure of PrP^{Sc}: The good, the bad and the ugly. *Virus Research*, 207, pp.120–126.

da Silva Ribeiro, V. et al., 2010. Selection of high affinity peptide ligands for detection of circulating antibodies in neurocysticercosis. *Immunology Letters*, 129(2), pp.94–99.

Simon, S. et al., 2008. Rapid typing of transmissible spongiform encephalopathy strains with differential ELISA. *Emerging Infectious Diseases*, 14(4), pp.608–

616.

Skinner, P.J. et al., 2015. Treatment of prion disease with heterologous prion proteins. *PLoS ONE*, 10(7), pp.1–17.

Somers, K. et al., 2011. Novel autoantibody markers for early and seronegative rheumatoid arthritis. *Journal of Autoimmunity*, 36(1), pp.33–46.

Sotelo, J., Gibbs Jr., C.J. & Gajdusek, D.C., 1980. Autoantibodies against axonal neurofilaments in patients with Kuru and Creutzfeldt-Jakob disease. *Science*, 210(4466), pp.190–193.

Soto, C. et al., 1998. Beta-sheet breaker peptides inhibit fibrillogenesis in a rat brain model of amyloidosis: implications for Alzheimer's therapy. *Nature medicine*, 4(7), pp.822-826.

Soto, C. et al., 2000. Early report Reversion of prion protein conformational changes by synthetic b -sheet breaker peptides. *THE LANCET*, 355, pp.192–197.

Soto, C., 2003. Unfolding the role of protein misfolding in neurodegenerative diseases. *Nature reviews. Neuroscience*, 4(1), pp.49–60.

Stanker, L.H. et al., 2010. Conformation-dependent high-affinity monoclonal antibodies to prion proteins. *Journal of immunology (Baltimore, Md. : 1950)*, 185(1), pp.729–37.

Steele, A.D., Lindquist, S. & Aguzzi, A., 2007. The prion protein knockout mouse: a phenotype under challenge. *Prion*, 1(2), pp.83–93.

Stein, K.C. & True, H.L., 2014. Extensive Diversity of Prion Strains Is Defined by Differential Chaperone Interactions and Distinct Amyloidogenic Regions. *PLoS Genetics*, 10(5), pp.6300-6307.

Stewart, C.E. et al., 2012. Evaluation of differentiated human bronchial epithelial cell culture systems for asthma research. *Journal of allergy*, 2012, p.943982.

Stohr, J. et al., 2012. Purified and synthetic Alzheimer's amyloid beta (A) prions. *Proceedings of the National Academy of Sciences*, 109(27), pp.11025–11030.

Taema, M.M. et al., 2012. Differentiating ovine BSE from CH1641 scrapie by serial protein misfolding cyclic amplification. *Molecular Biotechnology*, 51(3), pp.233–239.

Taema, M.M. 2012. The *In Vitro* Characterisation of Prion Diseases of Sheep. PhD Thesis. University of Nottingham.

Tagliavini, F. et al., 2000. Tetracycline affects abnormal properties of synthetic PrP peptides and PrP(Sc) in vitro. *Journal of molecular biology*, 300(5), pp.1309–1322.

Tagliavini, F., 2008. Prion Therapy: Tetracyclic Compounds in Animal Models and Patients with Creutzfelt-Jakob Disease. *Symposia S3-01: Other Dementias*,

T149-T150.

Tan, E.M., 2001. Autoantibodies as reporters identifying aberrant cellular mechanisms in tumorigenesis. *Journal of Clinical Investigation*, 108(10), pp.1411–1415.

Tattum, M.H. et al., 2010. Discrimination between prion-infected and normal blood samples by protein misfolding cyclic amplification. *Transfusion*, 50(5), pp.996–1002.

Telling, G.C. et al., 1996. Evidence for the conformation of the pathologic isoform of the prion protein enciphering and propagating prion diversity. *Science*, 274(5295), pp.2079–2082.

Telling, G.C. et al., 1995. Prion propagation in mice expressing human and chimeric PrP transgenes implicates the interaction of cellular PrP with another protein. *Cell*, 83, pp.79–90.

Terato, K. et al., 2014. Preventing intense false positive and negative reactions attributed to the principle of ELISA to re-investigate antibody studies in autoimmune diseases. *Journal of Immunological Methods*, 407, pp.15–25.

Terato, K. et al., 1990. Specificity of Antibodies to Type II Collagen in Rheumatoid Arthritis. *Arthritis and Rheumatism*, 33(10), pp.1493-1500.

Terato, K. et al., 1996. The mechanism of autoantibody formation to cartilage in rheumatoid arthritis: possible cross-reaction of antibodies to dietary collagens with autologous type II collagen. *Clinical immunology and immunopathology*, 79(2), pp.142–54.

Terry, L.A. et al., 2011. Detection of prions in the faeces of sheep naturally infected with classical scrapie. *Veterinary Research*, 42(1), p.65.

Tervaert, J.W.C. & Damoiseaux, J., 2012. Antineutrophil cytoplasmic autoantibodies: How are they detected and what is their use for diagnosis, classification and follow-up? *Clinical Reviews in Allergy and Immunology*, 43(3), pp.211–219.

Terzi, E., Hölzemann, G. & Seelig, J., 1997. Interaction of Alzheimer beta-amyloid peptide(1-40) with lipid membranes. *Biochemistry*, 36(48), pp.14845–14852.

Thackray, A.M. et al., 2011. Emergence of multiple prion strains from single isolates of ovine scrapie. *Journal of General Virology*, 92(6), pp.1482–1491.

Thackray, A.M. et al., 2008. Molecular and transmission characteristics of primary-passaged ovine scrapie isolates in conventional and ovine PrP transgenic mice. *Journal of virology*, 82(22), pp.11197–207.

Thackray, A.M., Hopkins, L. & Bujdoso, R., 2007. Proteinase K-sensitive disease-associated ovine prion protein revealed by conformation-dependent

immunoassay. *The Biochemical journal*, 401(2), pp.475–83.

The National CJD Research and Surveillance Unit

'T Hoen, P.A.C. et al., 2012. Phage display screening without repetitious selection rounds. *Analytical Biochemistry*, 421(2), pp.622–631.

Thompson, A.G.B. et al., 2013. The medical research council prion disease rating scale: A new outcome measure for prion disease therapeutic trials developed and validated using systematic observational studies. *Brain*, 136(4), pp.1116–1127.

Thorne, L. et al., 2012. In vitro amplification of ovine prions from scrapie-infected sheep from Great Britain reveals distinct patterns of propagation. *BMC veterinary research*, 8(1), p.223.

Thorne, L. & Terry, L.A., 2008. In vitro amplification of PrPSc derived from the brain and blood of sheep infected with scrapie. *Journal of General Virology*, 89(12), pp.3177–3184.

Thuring, C.M.A. et al., 2004. Discrimination between Scrapie and Bovine Spongiform Encephalopathy in Sheep by Molecular Size , Immunoreactivity , and Glycoprofile of Prion Protein Discrimination between Scrapie and Bovine Spongiform Encephalopathy in Sheep by Molecular Size , Immunore. , 42(3), pp.972–980.

Tiwana, H. et al., 1999. Autoantibodies to Brain Components and Antibodies to Acinetobacter calcoaceticus Are Present in Bovine Spongiform Encephalopathy Autoantibodies to Brain Components and Antibodies to Acinetobacter calcoaceticus Are Present in Bovine Spongiform Encephalopathy. *Society*, 67(12), pp.6591–6595.

Todd, N. V et al., 2005. Cerebroventricular infusion of pentosan polysulphate in human variant Creutzfeldt – Jakob disease. , pp.394–396.

Tong, Y.Q. et al., 2008. Autoantibodies as potential biomarkers for nasopharyngeal carcinoma. *Proteomics*, 8(15), pp.3185–3193.

Tranulis, M.A., 2002. Influence of the prion protein gene, Prnp, on scrapie susceptibility in sheep. *APMIS : acta pathologica, microbiologica, et immunologica Scandinavica*, 110(1), pp.33–43.

Trevitt, C.R. & Collinge, J., 2006. A systematic review of prion therapeutics in experimental models. *Brain*, 129(9), pp.2241–2265.

Truscott, J.E. & Ferguson, N.M., 2009. Control of scrapie in the UK sheep population. *Epidemiology and infection*, 137(6), pp.775–86.

TSE Surveillance and Research Unit

Tsuboi, Y., Doh-Ura, K. & Yamada, T., 2009. Continuous intraventricular infusion of pentosan polysulfate: Clinical trial against prion diseases: Symposium:

Prion diseases - Updated. *Neuropathology*, 29(5), pp.632–636.

Tzaban, S. et al., 2002. Protease-sensitive scrapie prion protein in aggregates of heterogeneous sizes. *Biochemistry*, 41(42), pp.12868–12875.

Ugnon-Café, S. et al., 2011. Rapid screening and confirmatory methods for biochemical diagnosis of human prion disease. *Journal of Virological Methods*, 175(2), pp.216–223.

Vázquez-Fernández, E. et al., 2016. The Structural Architecture of an Infectious Mammalian Prion Using Electron Cryomicroscopy. *PLoS Pathogens,* 12(9), pp.1-21.

Wadia, J.S. et al., 2008. Pathologic prion protein infects cells by lipid-raft dependent macropinocytosis. *PLoS ONE*, 3(10), pp.1–8.

Wagner, B.D., Robertson, C.E. & Harris, J.K., 2011. Application of two-part statistics for comparison of sequence variant counts. *PLoS ONE*, 6(5), pp.1–8.

Wan, W. et al., 2012. Degradation of Fungal Prion HET-s(218-289) Induces Formation of a Generic Amyloid Fold. *Biophysical Journal*, 102(10), pp.2339.2344.

Wang, F. et al., 2010. Generating a Prion with Bacterially Expressed Recombinant Prion Protein. *Science*, 327(5969), pp.1132-1135.

Wang, G., Wang, M. & Li, C., 2015. The Unexposed Secrets of Prion Protein Oligomers. *Journal of Molecular Neuroscience*, 56(4), pp.932–937.

Wang, J. et al., 2015. Prion Diseases and their Prpsc-Based Molecular Diagnostics History of Prion Disease Discovery. *iMedPub Journals*, pp.1–11.

Weber, P. et al., 2007. Generation of genuine prion infectivity by serial PMCA. *Veterinary Microbiology*, 123(4), pp.346–357.

Webster, K. et al., 2009. Determination of analytical sensitivity for currently approved TSE rapid tests. Veterinary Laboratories Agency Weybridge , United Kingdom.

Wei, X. et al., 2012. Human anti-prion antibodies block prion peptide fibril formation and neurotoxicity. *Journal of Biological Chemistry*, 287(16), pp.12858–12866.

White, A.R. et al., 2003. Monoclonal antibodies inhibit prion replication and delay the development of prion disease. *Nature*, 422(March), pp.18–21.

Wickner, R.B. et al., 2010. Prion amyloid structure explains templating: how proteins can be genes. *FEMS Yeast Research*, 10(8), pp.980–991.

Wilham, J.M. et al., 2010. Rapid end-point quantitation of prion seeding activity with sensitivity comparable to bioassays. *PLoS Pathogens*, 6(12).

Will, R.G et al., 1996. A new variant of Creutzfeldt-Jakob disease in the UK. *The*

Lancet, 347(9006), pp.921-925.

Wille, H. et al., et al., 2009. Natural and synthetic prion structure from X-ray fiber diffraction. *Proceedings of the National Academy of Science of the United States of America*, 106(40, pp.16990-16995.

Williamson, R. a et al., 1996. Circumventing tolerance to generate autologous monoclonal antibodies to the prion protein. *Proceedings of the National Academy of Sciences of the United States of America*, 93(14), pp.7279–7282.

Wong, P.T. et al., 2009. Amyloid-β Membrane Binding and Permeabilization are Distinct Processes Influenced Separately by Membrane Charge and Fluidity. *Journal of Molecular Biology*, 386(1), pp.81–96.

Wu, X. et al., 2012. Science. *Science (New York, N.Y.)*, 333(6049), pp.1593–1602.

Wuertzer, C.A. et al., 2008. CNS Delivery of Vectored Prion-specific Single-chain Antibodies Delays Disease Onset. *Molecular Therapy*, 16(3), pp.481–486.

Yam, A.Y. et al., 2010. The octarepeat region of the prion protein is conformationally altered in PrPSc. *PLoS ONE*, 5(2).

Yang, H. et al., 2013. A Novel B-Cell Epitope Identified within Mycobacterium tuberculosis CFP10/ESAT-6 Protein. *PLoS ONE*, 8(1).

Yang, H. et al., 2016. Screening and identification of immunoactive peptide mimotopes for the enhanced serodiagnosis of tuberculosis. *Applied Microbiology and Biotechnology*, 100(5), pp.2279–2287.

Yang, H. et al., 2011. Selection and application of peptide mimotopes of MPT64 protein in Mycobacterium tuberculosis. *Journal of Medical Microbiology*, 60(1), pp.69–74.

Yang, W. et al., 2017. Next-generation sequencing enables the discovery of more diverse positive clones from a phage-displayed antibody library. *Experimental & Molecular Medicine*, 49(3), p.e308.

Yao, Y. et al., 2012. Potential application of non-small cell lung cancer-associated autoantibodies to early cancer diagnosis. *Biochemical and Biophysical Research Communications*, 423(3), pp.613–619.

Yasrebi, H., 2016. Comparative study of joint analysis of microarray gene expression data in survival prediction and risk assessment of breast cancer patients. *Briefings in Bioinformatics*, 17(5), pp.771–785.

Ydens, E. et al., 2017. The Next Generation of Biomarker Research in Spinal Cord Injury. *Molecular Neurobiology*, 54(2), pp.1482–1499.

Yip, C.M., Darabie, A.A. & McLaurin, J., 2002. A??42-peptide assembly on lipid bilayers. *Journal of Molecular Biology*, 318(1), pp.97–107.

Yu, X. et al., 2013. Molecular interactions of Alzheimer amyloid-β oligomers with neutral and negatively charged lipid bilayers. *Physical chemistry chemical*

physics : PCCP, 15(23), pp.8878–89.

Yuan, J. et al., 2006. Insoluble aggregates and protease-resistant conformers of prion protein in uninfected human brains. *Journal of Biological Chemistry*, 281(46), pp.34848–34858.

Yuan, J. et al., 2013. Recombinant Human Prion Protein Inhibits Prion Propagation in vitro. *Scientific Reports*, 3(1), p.2911.

Zerr, I., 2013. Human prion diseases: Progress in clinical trials. *Brain*, 136(4), pp.996–997.

Zerr, I. et al., 2009. Updated clinical diagnostic criteria for sporadic Creutzfeldt-Jakob disease. *Brain*, 132(10), pp.2659–2668.

Zhang, H. et al., 2006. A sensitive and high-throughput assay to detect low-abundance proteins in serum. *Nat Med*, 12(4), pp.473–477.

Zhang, H. et al., 2011. Phenotype-information-phenotype cycle for deconvolution of combinatorial antibody libraries selected against complex systems. *Proceedings of the National Academy of Sciences of the United States of America*, 108(33), pp.13456–13461.

Zhang, H. et al., 1997. Physical Studies of Conformational Plasticity in a Recombinant Prion Protein. *Biochemistry*, 36(12), pp.3543-3553.

Zhang, Z. et al., 2013. De novo generation of infectious prions with bacterially expressed recombinant prion protein. *FASEB Journal*, 27(12), pp.4768–4775.

Zhao, H., Tuominen, E.K.J. & Kinnunen, P.K.J., 2004. Formation of amyloid fibers triggered by phosphatidylserine-containing membranes. *Biochemistry*, 43(32), pp.10302–10307.

Zhou, S. et al., 2016. Protective V127 prion variant prevents prion disease by interrupting the formation of dimer and fibril from molecular dynamics simulations. *Sci Rep*, 6, p.21804.

Zhu, F. et al., 2008. Raman Optical Activity and Circular Dichroism Reveal Dramatic Differences in the Influence of Divalent Copper and Manganese Ions on Prion Protein Folding. *Biochemistry*, 47(8), pp.2510–2517.

Zhu, H. & Snyder, M. Protein chip technology. *Current Opinion in Chemical Biology,* 7(1), pp.55-63.

Zou, W.Q. & Gambetti, P., 2005. From microbes to prions: The final proof of the prion hypothesis. *Cell*, 121(2), pp.155–157.

Zuber, C. et al., 2008. Single chain Fv antibodies directed against the 37 kDa/67 kDa laminin receptor as therapeutic tools in prion diseases. *Molecular Immunology*, 45(1), pp.144–151.

Zurawel, A. et al., 2014. Prion Nucleation Site Unmasked by transient Interaction with Phospholipid Cofactor. *Biochemistry*, 53(1), pp.68-76.